DEPARTMENT OF ECOLOGY
State of Washington

Mapping Bluffs and Beaches of Puget Sound to Quantify Sediment Supply

Estuary and Salmon Restoration Program Learning Project: Final Report

September 2018

Publication 18-06-008

Publication and Contact Information

This document is available on the Department of Ecology's website at:
https://fortress.wa.gov/ecy/publications/summarypages/1806008.html

For more information contact:

Heather Weiner, MS
Coastal Geomatics Scientist
heather.weiner@ecy.wa.gov

George Kaminsky, PhD, PE
Coastal Engineer
george.kaminsky@ecy.wa.gov

Coastal Monitoring & Analysis Program
Shorelands and Environmental Assistance Program
P.O. Box 47600
Olympia, WA 98504-7600
Phone: 360-407-6600

Washington State Department of Ecology — www.ecology.wa.gov

- Headquarters, Olympia 360-407-6000
- Northwest Regional Office, Bellevue 425-649-7000
- Southwest Regional Office, Olympia 360-407-6300
- Central Regional Office, Union Gap 509-575-2490
- Eastern Regional Office, Spokane 509-329-3400

Recommended citation:

Weiner, H.M., G.M. Kaminsky, A. Hacking, D. McCandless, K. Bolles, M. Gostic, J. Liljegren, and H. Drummond, 2018. Mapping Bluffs and Beaches of Puget Sound to Quantify Sediment Supply, Estuary and Salmon Restoration Program Learning Project Final Report. Shorelands and Environmental Assistance Program, Washington State Department of Ecology, Olympia, WA. Publication #18-06-008. Available at: https://fortress.wa.gov/ecy/publications/summarypages/1806008.html

Mapping Bluffs and Beaches of Puget Sound to Quantify Sediment Supply

Estuary and Salmon Restoration Program Learning Project: Final Report

Prepared for:

Estuary and Salmon Restoration Program
Washington Department of Fish & Wildlife
Olympia, Washington

Prepared by:

Heather M. Weiner, George M. Kaminsky, Amanda Hacking, Diana McCandless, Kasey Bolles, Michelle Gostic, Jaime Liljegren, and Hannah Drummond
Coastal Monitoring & Analysis Program
Washington State Department of Ecology
Olympia, Washington

This page is purposely left blank

Table of Contents

List of Figures and Tables

Page

Figures

Tables

Acknowledgements

The authors of this report would like to thank the following people and organizations for their contribution to this study:

- The Washington Department of Fish & Wildlife's Estuary and Salmon Restoration Program (ESRP) who funded this project (PRISM Record Number 13-1556)
- Paul Cereghino (NOAA), Betsy Lyons (WDFW), and Hugh Shipman (Ecology) who provided key input to the site-selection process
- Ginny Broadhurst (Northwest Straits Commission) who assisted with identifying MRC and other stakeholder interests and priority sites
- Many individuals and groups who assisted with site access for land-based survey operations, including:
    - Island County and Camano Island Beach Watchers (now Sound Water Stewards)
    - Beach Cottages at Marrowstone
    - Washington State Parks
    - Washington Department of Natural Resources
    - Naval Air Station Whidbey Island
    - Northwest Watershed Institute
    - Taylor Shellfish
    - South Puget Sound Salmon Enhancement Group
    - Cherry Point Citizen Stewardship Committee
    - Phillips 66
    - Alcoa Intalco Works
    - Cape San Juan Home Owners Association
    - Cattle Point Estates Owners Association
    - Friends of the San Juans
    - San Juan County Public Works
    - San Juan Island National Historical Park
    - San Juan Islands National Monument
    - Dungeness National Wildlife Refuge

This page is purposely left blank

Executive Summary

In an effort to collect high-resolution baseline coastal topographic data of beaches and bluffs around the Puget Sound and Strait of Juan de Fuca, the Washington State Department of Ecology Coastal Monitoring & Analysis Program (CMAP) conducted a series of boat-based lidar surveys in October 2013, May through September 2015, and May 2016 at a total of 16 sites spanning 220 km of shoreline and over two dozen drift cells. The drift cells were selected based on a rigorous and systematic geospatial analysis of bluff-backed beaches for their potential for significant bluff sediment supply to intact shorelines identified as having a relative abundance of habitat for forage fish, eelgrass, herring, shellfish, and geoduck, as well as having previous investments in beach restoration projects and potential for future shoreline armoring and habitat loss based on population growth scenarios. As such, the surveyed drift cells are top candidates for implementing drift cell-scale protection and restoration strategies.

The boat-based topographic lidar data were complemented by the concurrent collection of (1) shoreline photographs taken from the boat during the survey to document the shoreline conditions and help with point cloud interpretation, (2) ground-based GPS surveys to ground-truth the lidar data and fill in minor gaps and shadows, and (3) beach sediment grain size data to characterize spatial variations in beach texture at each survey site. The photos taken from the boat provide images of the coast from the viewpoint of the laser scanner as the boat navigated along the shoreline. For each site, a series of digital photographs were merged to create photomosaics that span a few hundred meters of shoreline to provide a reach-scale image of the landscape. During the ground-based GPS surveys, a photogrammetric technique known as "cobble cam" was used to obtain sediment grain size data at 13 of the 16 sites. Photographs of the beach surface sediment were collected at 0.5-m elevation intervals along 108 cross-shore transects spaced approximately 1-km apart. These photographs were processed to obtain grain size information to assess the alongshore and cross-shore variability in sediment texture. Sediments with larger grain sizes were often found near feeder bluffs while finer sediments were observed toward the distal end of the drift cells, indicating the dispersal and sorting of beach sediment with distance from its origin.

The boat-based lidar and GPS topography data were used to produce 0.5-m digital elevation models (DEMs) for the beaches and bluffs at each of the survey sites. The accuracy of the lidar data was assessed by comparing independently surveyed ground control targets with lidar points; on average, the lidar data were within 9 cm horizontally and 2 cm vertically, after adjustment (12 cm vertically, prior to adjustment). These DEMs provide the opportunity to inventory and characterize the shoreline landscape that affects nearshore ecosystem services such as feeder bluff activity, beach slope and width, and the position, length, and elevation of armoring relative to the backshore. Compared to airborne lidar, boat-based lidar provides a more advantageous point of view of the bluff face, resulting in much higher resolution data which is needed to gain insight into bluff failure and erosion mechanisms and corresponding sediment transport processes. In addition, the near-horizontal look angle of the laser successfully collects data under overhanging vegetation and overwater structures. Repeat surveys in the future would enable change analyses for quantifying bluff sediment supply, changes in marine riparian vegetation, and a better understanding of the linkages between physical and ecological processes.

This page is purposely left blank

Introduction

Bluff erosion is the principal method of sediment delivery to Puget Sound beaches and governs their structure and ecological function. Rates and patterns of bluff erosion are influenced by geologic structure, geomorphic setting, water levels, exposure variables (waves, wind, precipitation, surface water run-off, ground-water pressure, vegetation), and corresponding human factors such as shoreline armoring, upland development, and land-use practices. The state of the knowledge of these processes can only be expressed by simplistic conceptual models; we lack quantitative documentation and understanding about the methods, rates, and patterns of sediment supply to beaches and how these processes affect their physical structure and ecological function. Our inability to predict sediment supply and transport processes undermines our ability to answer critical questions about how much sediment supply is necessary to maintain beach structure and function.

Nearshore habitats, including forage fish spawning beaches, fringing eelgrass beds, shellfish beds, and shorebird feeding sites, depend on nearshore processes in order to actively create the proper conditions to successfully function. Beach sediment texture affects the type and abundance of prey, the suitability of habitat substrate for marine vegetation, and the amount of suitable habitat for feeding and avoiding predators. In order to address critical uncertainties associated with diminished biological function, it is essential to first understand sediment supply and transport because these physical processes govern the structure of the nearshore ecosystem.

Under present shoreline development trends and rising sea levels, sediment supply is among the most at-risk service, while intact beaches and the connectivity of nearshore habitats are among the most difficult to restore. The most apparent change to a beach occurs when structures (e.g., shoreline armoring) cut off or isolate bluffs that are sediment sources. As the delivery of sediment to a beach declines, some of the physical characteristics of the beach can be altered (Pilkey and Wright, 1988). For example, beaches in the vicinity of structures can disappear and beach width can decline (Macdonald et al., 1994; Griggs, 2005). In drift cells with insufficient sediment supply from local rivers, streams, or bluffs, beaches will erode or become submerged, diminishing their recreational value and causing critical beach and nearshore habitats to degrade or be eliminated entirely. The ability of beaches, associated nearshore ecosystems, and beach restoration projects to remain viable in the future and successfully respond to sea-level rise will depend on the supply of sediment to the beach.

While land-use planners and coastal managers are in need of long-term erosion rates for prudent resource management, property owners experience localized erosion and tend to be most interested and concerned with the magnitude of bluff recession occurring in relatively small increments of space along their bluff-top property boundary. Using boat-based lidar provides the ability to deliver high-resolution, spatially explicit data products that reveal detailed topographic relief and, through repeat monitoring, depictions of bluff recession over relevant time scales for highly localized parcel-by-parcel decision-making. This type of data enables property owners and coastal managers alike to take a more refined approach in assessing bluff erosion as well as the consequences of attempting to mitigate bluff erosion. Moreover, the high-resolution, 3D coastal topography collected using boat-based lidar allows for quantitative metrics to be extracted, such as bluff height, bluff slope, bluff toe elevation, beach slope, surficial sediment

texture, and quantities of beach wrack, overhanging vegetation, and large woody debris. These metrics are useful as indicators of beach quality and function, and can help provide feedback about whether beach restoration and regional recovery efforts are working.

In addition to topography, an understanding of the sediment grain size distribution of a beach provides important information about its physical properties and ecological functions. Sediment grain size data provides information related to shoreline armoring impacts, feeder bluff activity, and the sediment budget of a littoral drift cell, which can help to inform land-use and resource management decisions. Likewise, the ability of forage fish to produce viable spawn is highly dependent on the grain size present; therefore, grain size information can help to identify viable forage fish habitat.

This report presents the process developed for objectively ranking Puget Sound drift cells and selecting priority sites for baseline mapping followed by a description of the methods and results of the boat-based lidar, GPS topography, and sediment grain size data collected for this project. The topographic data from these surveys will serve as baseline digital elevation models (DEMs) that can be used to analyze bluff recession and beach change over time as more surveys are conducted, while repeat surveys of the sediment grain size will provide insight to sediment supply and transport processes through changes in beach texture. Appendices to this report include: Appendix A, which discusses lessons learned from the site-selection process, and the collection and processing of boat-based lidar and cobble cam data; Appendix B, which provides a selection of images, including shoreline photos and photomosaics, sediment grain size photos, and photos of survey equipment and data collection operations; Appendix C, which describes and illustrates the DEMs produced for each of the survey sites; Appendix D, which presents the collected beach sediment grain-size data; and Appendix E, which presents a multitude of examples of features, metrics, and attributes extracted from the lidar point clouds for detailed mapping and quantification of shoreline morphology, armoring, and habitat characteristics with applications to change analyses and restoration assessment.

Site Selection

While baseline mapping of bluff-backed beaches is the priority goal of this project, the long term objective is to understand the relationship between sediment supply and its transport and distribution alongshore. It is therefore important to first inventory shoreline characteristics at the drift-cell scale. Starting with almost 900 unique drift cells in the Salish Sea, a GIS-based, multi-criteria site-selection process was developed to identify highest-priority drift cells with feeder bluffs that actively provide sediment to the nearshore and sustain an unusually high level of ecosystem services. The goal of the process was to implement an objective, systematic, and data-based approach to identifying and prioritizing intact shorelines (contiguous drift cells with minimal modifications) that offer a high potential for learning, protection, and restoration, where stakeholder interest and institutional capacity for collaborative nearshore ecosystem management converge. As part of this process, a suitability model was developed for geospatial analysis and drift cell prioritization, with sensitivity analyses performed and incorporated into the final classification scheme (Figure 1).

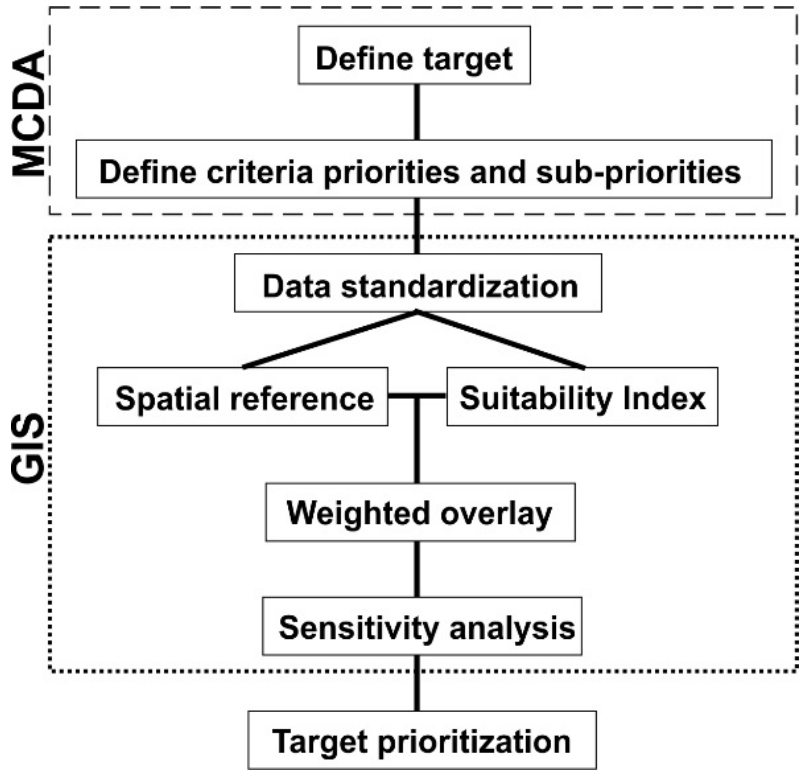

Figure 1: Diagrammatic workflow of the site-selection scheme, starting with Multi-Criteria Decision Analysis (MCDA) followed by a GIS-based, spatial analysis of the weighted criteria

The first step of the site-selection process involves identifying and gathering priority criteria for which to evaluate all potential sites. Multi-criteria decision analysis (MCDA) allows for empirical data to be integrated with and weighted against stakeholder and expert opinion. Practitioners and project proponents who represent the interest of local restoration projects were consulted to identify input criteria (priorities and sub-priorities) to be included in the suitability

model (Figure 2), as well as the weighting of the parameters, and to recommend drift cells or study sites of high priority. Using drift cell units delineated in the Washington State Coastal Atlas (Ecology, 2003), and extending their areas on- and offshore, the Salish Sea shoreline was divided into 1,652 polygon segments[1]. Data for each priority and sub-priority were obtained from various sources and transformed into a standardized numerical, spatially-referenced format corresponding to one value for each criteria per shoreline segment. Using the transformed data as input, the suitability model was run with four different weighting schemes.

The first model run was based on three main criteria: shoretype, stakeholder interest, and natural resources, in order to focus on locations that have an intersection between sediment supply (feeder bluffs) and nearshore habitats and resources in valued locations. Given that a high percentage of feeder bluffs contained within an individual drift cell increases the potential for sediment to be supplied to the littoral system within a relatively short timeframe, criteria for site selection required 30% or more of a drift cell be designated as a feeder bluff (the higher the percentage, the higher the ranking). Locations of feeder bluffs, including rapidly eroding feeder bluffs ("Feeder Bluff Exceptional" or FBE) and more slowly eroding rocky cliffs and slopes ("Feeder Bluff - Talus" or FB-T), were extracted from Ecology's Puget Sound Feeder Bluff Mapping project dataset carried out by Coastal Geologic Services (MacLennan et al., 2013).

Second, a drift cell must be near potential stakeholders. This variable was evaluated based on a drift cell's proximity to other ESRP-funded projects or ongoing work by local Marine Resource Committees (MRCs). The closer a drift cell was to one of these projects, the more desirable a feeder bluff study site becomes, and the higher the drift cell is ranked. Third, a drift cell must have a presence of natural resources which may be affected by changes to beach sediment input and transport processes. Data on natural resources considered in the analysis include: forage fish spawning sites from Washington Department of Fish and Wildlife; recreational shellfish beaches, commercial shellfish areas, documented geoduck areas, and areas of observed herring spawning from the Puget Sound Nearshore Ecosystem Restoration Project's sub-basin geodatabases (downloaded from the Washington State Geospatial Data Archive at http://wagda.lib.washington.edu/data/geography/wa_state/#PSNERP); and presence of eelgrass from the Washington Department of Natural Resources Submerged Vegetation Monitoring Program (Gaeckle et al., 2011).

The other three model runs were focused more on physical variables contributing to sediment supply, both current and future, prioritizing shorelines threatened by development. Each of these three runs use similar criteria but different weightings, which include: shoretype, presence of feeder bluffs, presence of armoring, erosion potential due to physical factors (e.g., slope stability), and the potential for future ecological or geomorphological change due to armoring (e.g., erosion, loss of eelgrass or forage fish spawning habitat).

Like the first model, 30% or more of a drift cell must be designated as a feeder bluff (the higher the percentage, the higher the ranking). The percentage of a drift cell's shoreline designated as feeder bluff (including FBE and FB-T) and shoreline armoring was also considered; drift cells with a higher percentage of feeder bluff and low percentage of armoring were ranked higher.

[1]The delineation of drift cell units in the Coastal Atlas is comprised of linear segments for drift cells and their convergence and divergence zones, and separate polygons were made for each component.

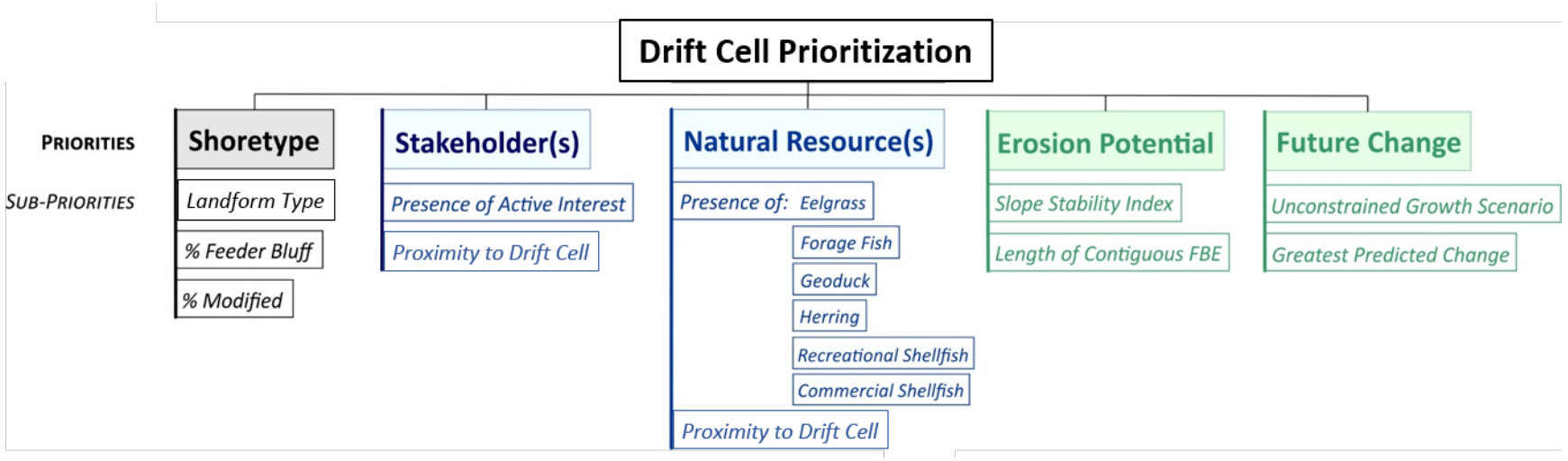

Figure 2: Priority and sub-priority criteria defined for prioritizing drift cells in the site-selection process. Shoretype parameters (gray) were included in all suitability model runs, as these relate directly to project learning goals. Stakeholder interests and natural resources (blue) are included in model run 1, while erosion potential and future change (green) are included in model runs 2 through 4

Slope stability data was acquired from the Washington Coastal Atlas (Ecology, 2004); the more unstable a slope or the more recent a slide had occurred, the higher the weighting. The future potential effects of armoring were quantified by the Beach Armoring Index (BAI) obtained from the U.S. Geological Survey (USGS) Puget Sound Ecosystem Portfolio Model (Byrd et al., 2011). The BAI correlates population growth scenarios with future shoreline armoring potential to assess which shorelines are at a greater risk of beach erosion and habitat loss through the year 2060; the greater the risk of future change, the higher the BAI score, and the higher ranking a stretch of shoreline received. The third and fourth model runs also rank the length of contiguous FBE, a metric that is assumed would lead to higher sediment supply to the adjacent beaches; the longer the FBE, the higher the ranking. In Figure 3, maps from Useless Bay and Dabob Bay illustrate the graphical overlay of each variable in ArcGIS.

Shoreline characteristics describing the length of various shoretypes present and evidence of or likeliness of erosion, as well as the proximity to natural resources and potential stakeholders, are shown in Table 1 and Table 2. Attributes for each criteria were converted to a standardized index on a scale from 1 to 9, giving the most desirable attributes a greater preference (Table 3). For example, FBE shoretypes were assigned a rank of 9 out of 9, while FB and FB-T were ranked a 7 out of 9, and all other shoretypes (stable, modified, and barrier beaches) were ranked a 1 out of 9. For the proximity criteria, the shorter the distance to a project site or resource, the higher the assigned ranking; a site over 10 km away was given a zero ranking. A weighted overlay of the transformed data was performed in ESRI ArcGIS for each weighting scheme using various percentages (Table 4). The results from the model runs were averaged together to assign one mean value to each shoreline segment (Table 2).

Only 17% of the sites received a mean rating of 4.5 or greater out of 9. Three sites earned the highest mean rating of an 8 out of 9, followed by 14 sites earning a 7 out of 9. These sites were combined to form the top-tier (“Tier 1”) of the ranking process, encompassing 163 km of shoreline within the Puget Sound and Strait of Juan de Fuca, which would be prioritized for baseline surveying. Closely following, 123 sites earned a mean rating of 6 out of 9 from the suitability model, comprising 491 km of shoreline. From these, a second tier (“Tier 2”) was selected, subjectively chosen based on their proximity to Tier 1 sites or other ESRP projects, as well as a few hand-selected sites by key stakeholders that had a model rating of less than 6, so that additional high-interest sites could be included in the surveys where logistically feasible. The 26 sites chosen for Tier 2 encompass 149 km of shoreline, while the remaining 106 sites with a rating of 6, spanning 400 km of shoreline, were classified as “Tier 3.”

The 17 sites within Tier 1 (16 drift cells) are predominantly located in north Puget Sound; only one site (Maury Island) is located in south central or south Puget Sound sub-basins, whereas 8 of the 26 Tier 2 sites (7 drift cells) are located in these southern basins (Figure 4). The Tier 1 sites selected include a total 75 km of feeder bluff with 29 km designated as FBE. The longest FBE in Tier 1 is part of the Dungeness Bluffs in Clallam County along the Strait of Juan de Fuca, with a length of 11.5 km, followed by a 4 km-long FBE on the west side of Whidbey Island.

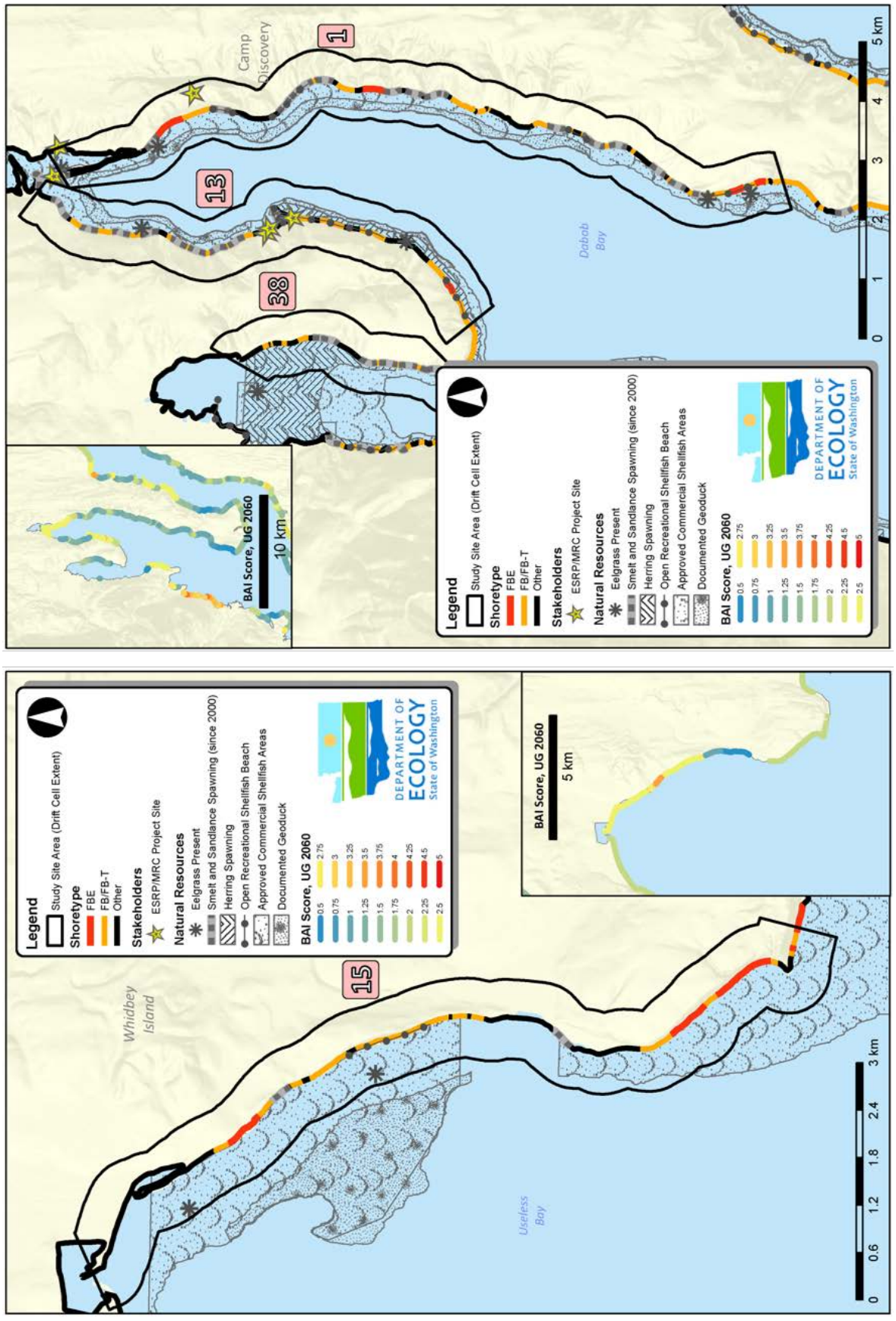

Figure 3: Maps showing the spatial overlay of various parameters used in site selection; left—Useless Bay, right—Dabob Bay

Table 1: Parameters describing physical shoreline characteristics for each Tier 1-ranked site, including the designated drift cell and shoreline process unit (SPU), overall site length, length of feeder bluff (FB), feeder bluff exceptional (FBE), and armored (modified) shoreline (MOD) present within the site, the ratio of FB and MOD to overall site length, the number of landslides recorded in each site, the slope stability (*provided as transformed indices (0-9) related to the degree of stability; the more unstable the slope, the higher the value), and the beach armoring index (BAI) score (0-4), which characterizes the potential for future morphological and ecological change out to 2060 (higher BAI scores reflect greater potential change)

Site Identifiers				Shoreline Characteristics									
FID	Drift Cell	SPU	Location	Site Length (m)	FB Length (km)	FBE Length (km)	MOD Length (km)	FB:Site Length	MOD:Site Length	Land-slides	Slope Stability*		BAI Score
											Max	Mean	
30	JE-16	2062	Toandos Peninsula/Dabob Bay	19.4	11.4	1.6	2.0	58.8	10.2	84	6	5	3
46	JF-16-1	1025	Dungeness Bluffs	30.2	12.9	11.5	0.1	42.8	0.4	56	6	4	3
1	GUE-11	7137	Guemes Island/W Shore Rd.	1.3	1.0	0.9	0.1	79.1	10.4	3	4	3	2.25
23	IS-4	5034	Whidbey Island/Useless Bay	10.4	5.9	2.0	0.1	57.3	0.6	16	6	3	3.5
135	WHID-27/ WHID-28	5029	Whidbey Island/Ledgewood Beach	2.8	1.8	0.9	0.0	63.0	1.7	2	5	4	4
131	WHID-25	8057	Whidbey Island/Deception Pass SP to Fort Ebey SP	22.6	9.0	4.0	0.5	39.6	2.1	23	4	2	1.5
133	WHID-26	8058	Whidbey Island/Fort Ebey SP to Fort Casey SP	11.3	5.1	1.5	0.0	45.5	0.0	23	4	2	3.5
12	CAM-5	6043	Whidbey Island/Elger Bay to Dallman Rd.	8.0	3.2	1.1	3.0	40.4	37.1	17	4	2	4
32	JE-17	2059	Dabob Bay/W Side	9.4	5.1	0.3	0.8	54.3	8.5	45	6	5	3.5
43	JEF-3	5008	Marrowstone Island/Fort Flagler SP to Robbins Rd.	10.0	7.6	1.5	0.1	76.2	0.7	20	6	5	3
53	KI-14-2	4099	Maury Island/Maury to Summerhurst	8.5	3.6	1.4	3.4	42.3	39.8	22	6	2	4.5
83	SJ-9	7028	San Juan Island/ Cattle Point	0.6	0.1	0.0	0.0	18.7	0.0	0	0	0	0
109	SJ-10	7028	San Juan Island/SJI National Historical Park	4.0	1.6	1.5	0.0	39.4	0.0	7	4	3	2
110	SJ-9/SJ-10	7028	San Juan Island/Cattle Point	1.3	0.0	0.0	0.0	0.0	0.0	2	4	4	0
122	WH-1-1	7138	Point Roberts	7.8	1.2	0.0	0.6	15.8	8.1	6	6	4	3.5
125	WH-3-8	7146	Whatcom/Point Whitehorn MP to Semiahmoo Spit	13.5	5.0	0.4	0.8	37.1	6.3	34	6	4	3
132	WHID-25/ WHID-26	8057	Whidbey Island/Fort Ebey SP	1.8	0.5	0.5	0.0	25.8	0.0	3	4	3	4.25

Table 2: Distance of each Tier 1-ranked site to documented natural resource variables of interest and restoration project sites from the Estuary and Salmon Restoration Program (ESRP) or Marine Resource Committees (MRC) as well as output from each run of the suitability model and final mean rating used in the site-selection process

Site Identifiers				Proximity to Natural Resources/Stakeholders Distance (km) to documented							Rating				
FID	Drift Cell	SPU	Location	Eel-grass	Forage Fish Spawning	Herring Spawning	Rec. Shellfish	Comm. Shellfish	Geo-duck	ESRP/ MRC Project	RUN 1	RUN 2	RUN 3	RUN 4	Mean Rating
30	JE-16	2062	Toandos Peninsula/Dabob Bay	0.1	0.1	1	0.1	0.1	0.1	0.1	9	8	8	8	8.3
46	JF-16-1	1025	Dungeness Bluffs	0	0.1	0	0	0.1	0.1	0.1	8	8	7	8	7.8
1	GUE-11	7137	Guemes Island/W Shore Rd.	2	1	10	2	0	0	10	6	8	8	8	7.5
23	IS-4	5034	Whidbey Island/Useless Bay	0.1	0.1	0	0.1	0.1	0.5	10	7	8	7	7	7.3
135	WHID-27/ WHID-28	5029	Whidbey Island/Ledgewood Beach	0.5	5	5	0.1	5	0.1	20	7	8	7	7	7.0
131	WHID-25	8057	Whidbey Island/Deception Pass SP to Fort Ebey SP	0.1	0.1	0	0.1	0.1	0	1	7	7	7	7	7.0
133	WHID-26	8058	Whidbey Island/Fort Ebey SP to Fort Casey SP	5	0.1	0	0.1	5	5	10	6	8	7	7	6.8
12	CAM-5	6043	Whidbey Island/Elger Bay to Dallman Rd.	0.1	0.1	1	0.1	0.1	5	5	7	7	7	6	6.8
32	JE-17	2059	Dabob Bay/W Side	0.1	0.1	0.1	0.1	0.1	0.1	0.1	7	7	7	6	6.8
43	JEF-3	5008	Marrowstone Island/Fort Flagler SP to Robbins Rd.	0.1	0.1	0.5	0.1	0.5	2	10	7	7	6	7	6.8
53	KI-14-2	4099	Maury Island/Maury to Summerhurst	0.1	0.1	0.1	0	0.1	0.1	0.1	7	7	7	6	6.8
83	SJ-9	7028	San Juan Island/ Cattle Point	2	0.5	10	0	10	0	10	6	7	7	7	6.8
109	SJ-10	7028	San Juan Island/SJI National Historical Park	0.1	0.5	0	0	10	0	10	6	7	7	7	6.8
110	SJ-9/SJ-10	7028	San Juan Island/Cattle Point	1	0.1	10	0	10	0	10	6	7	7	7	6.8
122	WH-1-1	7138	Point Roberts	0.1	0.1	0.1	0	0	0	0.5	8	7	6	6	6.8
125	WH-3-8	7146	Whatcom/Point Whitehorn MP to Semiahmoo Spit	0.1	0.1	0.1	0	0.5	0	20	6	8	7	6	6.8
132	WHID-25/ WHID-26	8057	Whidbey Island/Fort Ebey SP	2	5	0	0.1	10	10	10	6	7	7	7	6.8

Table 3: Criteria standardization scheme, listing the numerical index (1-9) assigned to each attribute (*Continued on next page*)

Priority	Sub-Priority	Attribute	Suitability Index
Shoretype	Landform Type	FBE	9
		FB/FB-T	7
		OTHER	1
	% Feeder Bluff	≥ 70	9
		60-70	8
		50-60	7
		40-50	6
		30-40	5
		25-30	4
		15-25	3
		5-15	2
		≤ 5	1
	% Modified	≤ 5	9
		5-15	8
		15-25	7
		25-30	6
		30-40	5
		40-50	4
		50-60	3
		60-70	2
		≥ 70	1
Stakeholders	Presence of Active Interest	Y	9
		N	1
	Proximity to Drift Cell (km)	≤ 0.1	9
		≤ 0.5	7
		≤ 1	5
		≤ 2	3
		≤ 5	2
		≤ 10	1
Natural Resources	Proximity to Drift Cell (km)	≤ 0.1	9
		≤ 0.5	7
		≤ 1	5
		≤ 2	3
		≤ 5	2
		≤ 10	1
	# of Resources in Proximity to Drift Cell	6	9
		5	7
		4	5
		3	3
		2	2
		1	1

Table 3: Continued from previous page

Priority	Sub-Priority	Attribute	Suitability Index
Erosion Potential	Slope Stability	Unstable - Recent Slide	9
		Unstable - Old Slide	8
		Unstable	7
		Intermediate Slope	5
		Stable Slope	3
		Modified	2
		OTHER	1
	Length of Contiguous FBE (km)	≥ 2.5	9
		1.5-2.5	8
		1.0-1.5	7
		0.8-0.9	6
		0.7-0.8	5
		0.5-0.7	4
		0.25-0.5	3
		0.05-0.25	2
		≤ 0.05	1
Future Change	Unconstrained Growth Scenario (out to 2060)	≥ 4	9
		3.5-3.75	8
		3-3.25	7
		2.5-2.75	6
		2-2.25	5
		1.75	4
		1.5	3
		1-1.25	2
		≤ 0.75	1
	Proximity to areas of greatest predicted change	≤ 0.1	9
		≤ 0.5	7
		≤ 1	5
		≤ 2	3
		≤ 5	2
		≤ 10	1

Table 4: Site-selection criteria weighting used for each model run

Criteria	RUN 1	RUN 2	RUN 3	RUN 4
Shoretype	50%	20%	15%	17%
Proximity to stakeholders	25%	---	---	---
Proximity to natural resources	25%	---	---	---
Presence of feeder bluffs	---	20%	15%	16%
Presence of armoring	---	20%	15%	16%
Slope stability	---	20%	15%	17%
Beach Armoring Index	---	20%	15%	17%
Contiguous FBE	---	---	25%	17%

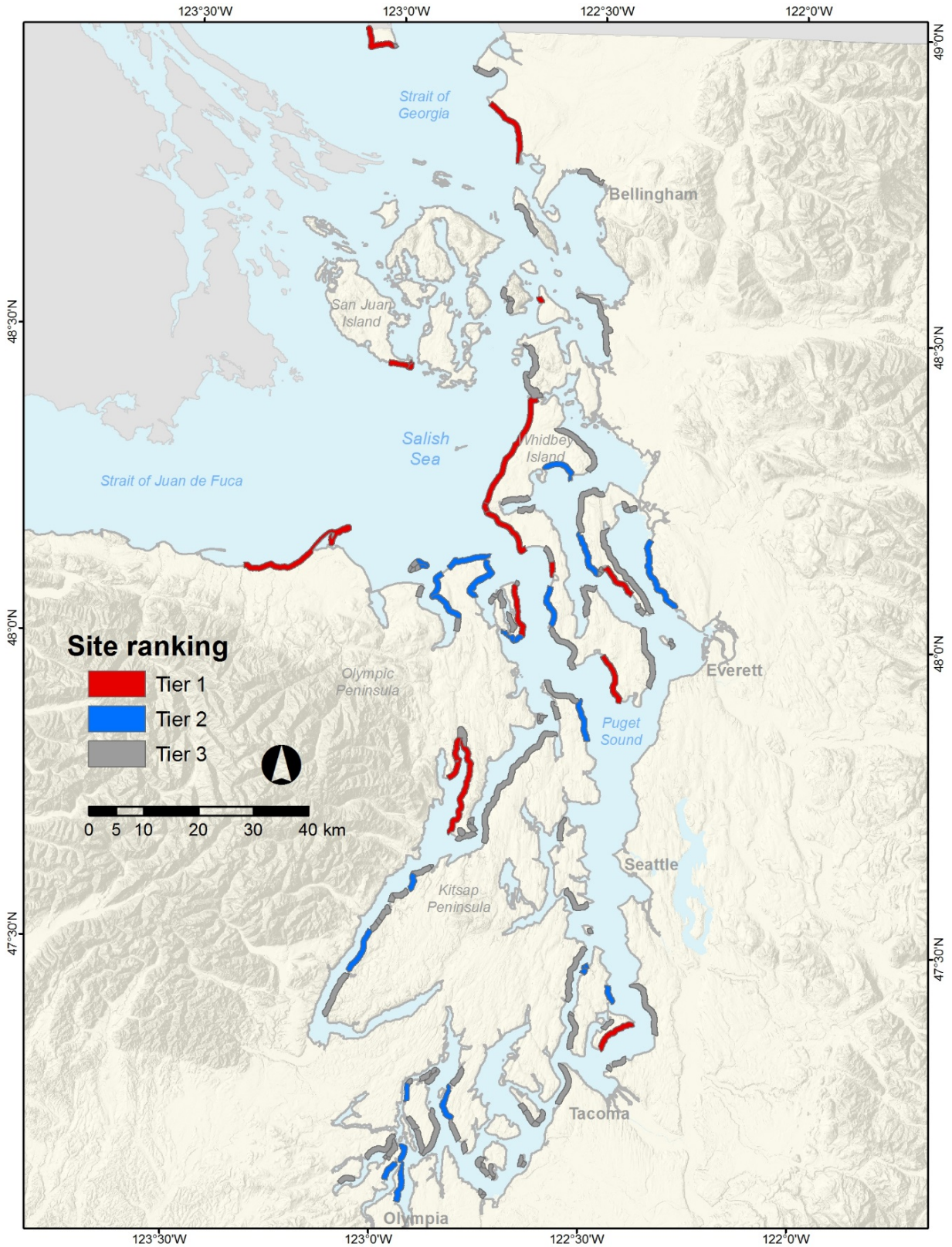

Figure 4: Map showing top-tier drift cells identified within the Puget Sound and Strait of Juan de Fuca through the site-selection process; these survey sites were prioritized for mapping and monitoring using boat-based lidar

This page is purposely left blank

Survey Planning

While one survey of an un-ranked drift cell was completed in fall 2013 (Seahurst Park[2]), surveys of all the Tier 1 sites identified during the site-selection process were planned to occur within one extended survey season (spring-fall 2015). This scope of planning required bringing several factors together, including an estimate of the time needed to survey each site (based on the shoreline length), maximizing data acquisition per mobilization of personnel and equipment to the field, and duration of tidal windows.

Each Tier 1 site was examined for adjacent prioritized drift cells. Neighboring Tier 1 sites were combined as one planned survey site (e.g., the west side of Whidbey Island was composed of three top-tier sites spanning two adjacent drift cells and surveyed in one mobilization). Adjacent Tier 2 or Tier 3 sites were then evaluated for the feasibility, efficiency, and relative value of including them in the survey; they were more likely to be included in the planned survey site if they had exposed or lightly vegetated feeder bluffs, and less likely to be included if they consisted of densely vegetated bluffs or had no backing bluff, determined from aerial and oblique shoreline photos. An assessment of previous boat-based lidar surveys by CMAP indicated that, on average, 1 hour of data collection was needed for each kilometer of shoreline. Based on this average, estimates were made of the time required to survey each site plus the additional time it would take to survey any neighboring sites.

Efficiency of mobilization and data acquisition increases as survey time increases; a 5-day survey requires the same amount of planning, preparation, and mobilization as a 1-day survey. Therefore, it is prudent to maximize data acquisition for each deployment, especially for sites a long distance from Ecology headquarters in Olympia. To the extent possible, planned survey sites were grouped based on whether they could be surveyed during the same mobilization, depending on survey time required, available survey windows based on tides, daylight, and weather, spatial proximity to each other, distance from Olympia, availability of marine facilities, and transportation logistics over both land and sea.

With 163 km of Tier 1 shoreline to be surveyed, plus an interest in surveying additional sites, the timing of deployments required optimizing tidal windows for data acquisition. Due to the spatial extent and estuarine morphology of Puget Sound, tides vary significantly in the region. Puget Sound was divided into eight tidal regions that corresponded with at least one survey site and could be characterized by a harmonic tidal station. For each station, the predicted tidal height at 15-minute increments was compared with the time of sunrise and sunset on that day to determine the number of daylight hours that the tide was below 50% of mean tide level at that location, which ranged from 2.1 to 4.2 ft MLLW (NOAA, 2013; Table 5). The 50% threshold provided enough potential survey days between May and October with at least 2-3 hours on either side of a daylight lower low tide. Days with 4+ hours below the tidal threshold and no previously scheduled surveys or other logistical conflicts were considered for data acquisition.

[2]Seahurst Park, located in South Central Puget Sound, was surveyed in advance because of an ESRP-funded bulkhead removal project taking place in fall 2013. This drift cell, however, was not ranked as a top-tier site during the site-selection process.

Table 5: Mean tide level (MTL) and 50% MTL threshold for each tide station used during survey planning

Location	Water Body	Station ID	Latitude	Longitude	MTL (ft)	50% MTL (ft)
Bangor Wharf	Hood Canal	9445133	47.7483	-122.7270	6.53	3.26
Budd Inlet	South Puget Sound	9446807	47.0983	-122.8950	8.29	4.15
Cherry Point	Strait of Georgia	9449424	48.8633	-122.7580	5.45	2.73
Everett	Possession Sound	9447659	47.9800	-122.2230	6.49	3.24
Port Angeles	Strait of Juan de Fuca	9444090	48.1250	-123.4400	4.25	2.13
Port Townsend	Admiralty Inlet	9444900	48.1117	-122.7580	5.17	2.58
Richardson	San Juan Channel	9449982	48.4467	-122.9000	4.38	2.19
Tacoma	Commencement Bay	9446484	47.2667	-122.4133	6.94	3.47

Once available dates were chosen, individual surveys were planned out. Each mobilization required a nearby boat launch and mooring facility, nearby lodging for boat and shore crews (which were sometimes in different locations depending on the survey site), a survey monument for the GPS base station, beach access points, and suitable locations to place at least three ground control targets.

Existing geodetic benchmarks were explored for use as base station monuments, but many were found to be unusable due to distance from the shoreline, proximity of trees obstructing line-of-sight, inconvenience of location, or lack of a precise coordinate for recovery. As a result, extra time was required for finding a suitable location for, and installing a new survey monument at, most survey sites.

Ground control targets are used to check the lidar point cloud positioning and must be set up prior to the boat-based lidar survey. Ideally, the targets are set up at various ranges from the laser scanner with no more than 1-km spacing alongshore. They must be visible from the water (i.e., not obscured by vegetation or rocks) and not too low on the beach if left over a tide cycle. Many target locations were chosen based on public access points to bluff tops and beaches, but some survey sites required coordinating with homeowners for access or permission to set up a ground control target. A smaller, more portable ground control target was also occasionally set up by a land surveyor as they walked along the beach in coordination with the boat team to obtain multiple target scans along the length of the site during the lidar survey.

Transportation logistics for both the boat and shore crews were based on time of tide, distance and transit time between lodging or mooring and the survey site, and access to the site, sometimes including ferry service schedules (e.g., Ledgewood, Guemes Island, Cattle Point, south Whidbey Island, and Maury Island). When possible, public beach access points were utilized. When public access was not available, additional allowance had to be made for coordinating with local landowners or performing boat beach landings to move the shore crew to a survey site.

Data Collection

Boat-based lidar and GPS topography data were collected at 16 sites around the Puget Sound and Strait of Juan de Fuca (Figure 5), with sediment grain size data collected at 13 of the 16 sites (no data for Dungeness, Dabob Bay, or Agate Beach). Each site took 1-5 days to survey, depending on the shoreline length, which varied between 0.9-36 km, for a total of 220 km surveyed in 31 days (Table 6). In most cases, more than the prioritized Tier 1 area was surveyed, extending to at least the natural extents of the complete drift cell (as noted in the field) plus any feasible Tier 2 or 3 sites. Data collection was focused around low tide ± 2-4 hours, depending on the tide level, such that the beach was as exposed as possible. In some places where wide, shallow regions were exposed or unnavigable at the lowest tides, boat-based lidar data were collected at a higher or mid-tide in order to achieve higher resolution and density of coverage on the sub-aerial beach and bluff.

Geodetic control

For the majority of the surveys, a local GPS base station (Trimble R7) was set up near the survey site on a known location and Real-Time Kinematic (RTK) corrections were transmitted to the vessel for centimeter-level positional accuracy relative to the North American Datum of 1983 (NAD83) in the horizontal and the North American Vertical Datum of 1988 (NAVD88) in vertical (Figure 6A). When possible, existing benchmarks were used for setting up the GPS base station. If no existing, usable benchmarks were available for a survey site, a monument was created using a 5-cm diameter spherical cap of epoxy with a small center divot placed on a stable surface in an open, easily accessible location that would remain relatively undisturbed to provide a repeatable accurate position for future surveys (Figure 6B). Based on previous surveys, the placement of a small patch of epoxy on stable surface has proven to be a quick, durable method for making a survey mark that provides accurate repeatability. At some survey sites, additional geodetic control was set up around the survey site as quality control.

In addition to providing RTK corrections, the base station logged its position at 1-second intervals during occupation of the monument for use in post-processing the data when the RTK signal to the GPS rovers was not maintained. For surveys performed at Guemes Island and one day of surveying at Maury Island, a local base station (Trimble R8-3 or R10) was set up and its position was logged each second, but there was no radio available for transmitting RTK corrections during acquisition due to a logistical conflict with needing the equipment for another survey. At Seahurst Park, the base station was set up with RTK transmission; however, it was not ready in time for the boat crew to utilize the corrections during the boat-based lidar data collection.

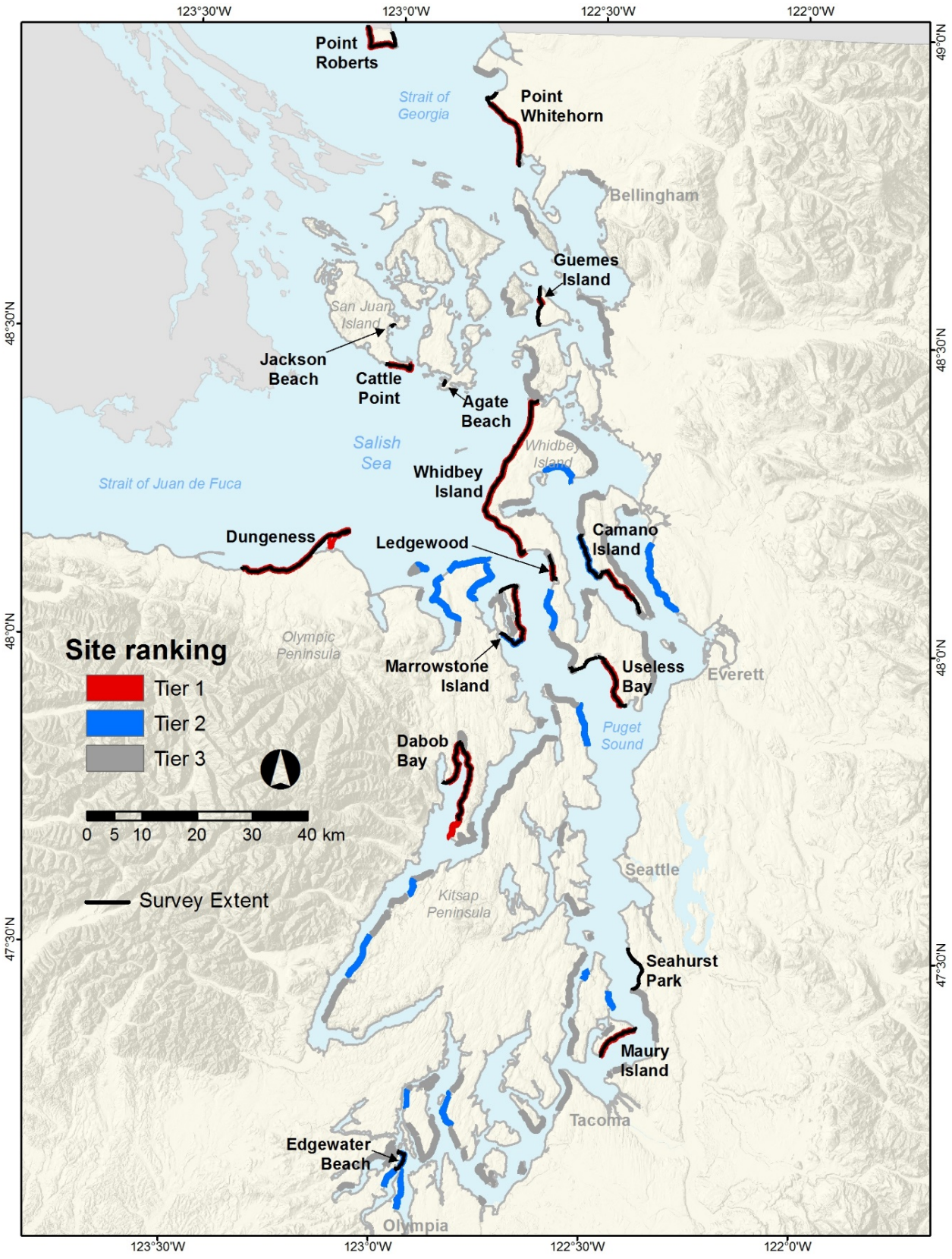

Figure 5. Map showing 16 sites surveyed using boat-based lidar for this project

Table 6: List describing location, extent, and data collection dates for boat-based lidar surveys (*Continued on next page)*

Survey site	County	Local Integrating Organization (LIO)	Survey extent	Shoreline Length (km)	Tier	Lidar Survey Dates	Additional on-site setup dates
Agate Beach, Lopez Island	San Juan	San Juan Action Agenda Oversight Group	All of Agate Beach, bounded by rocky headlands to the north and south	1.1	n/a	5/24/2016	n/a
Camano Island	Island	Island (WRIA 6)	Spit north of Onamac Point to small point south of Pebble Beach	21.9	1, 2, 3	9/9-9/10/2015	n/a
Cattle Point, San Juan Island	San Juan	San Juan Action Agenda Oversight Group	Grandma's Cove to shoreline immediately west of the north tip of Goose Island	5.9	1	5/24/2016	5/23/2016
Dabob Bay	Jefferson	Hood Canal Coordinating Council	Fishermans Point to south side of point north of Zelatched Point	25.9	1	7/6-7/10/2015	n/a
Dungeness Bluffs & Spit	Clallam	Strait Ecosystem Recovery Network	Morse Creek to small spit on inside of Dungeness Spit just west of lighthouse	25.5	1	6/29-7/2/2015	n/a
Edgewater Beach, Olympia	Thurston	Alliance for a Healthy South Sound	Inlet south of Edgewater Beach to just south of Carlyon Beach	5.2	2	9/24/2015	n/a
Guemes Island	Skagit	Skagit-Samish Watersheds**	Clark Point to Kellys Point on west side	7.6	1	6/5/2015	6/4/2015
Jackson Beach, San Juan Island	San Juan	San Juan Action Agenda Oversight Group	All of Jackson Beach, bounded by Little Island to east and rocky upland to west	0.9	n/a	5/24/2016	n/a
Ledgewood, Whidbey Island	Island	Island (WRIA 6)	Creek south of the Admirals Cove Beach Club to Lake Hancock	4.8	1, 3*	5/22/2015	n/a
Marrowstone Island	Jefferson	Hood Canal Coordinating Council	South end of Portage Canal to Rat Island (south, east, and north sides)	19.0	1, 2, 3	5/19-5/21/2015	5/17-5/18/2015
Maury Island	King	South Central Action Area Caucus Group	Piner Point to Point Robinson	9.2	1	6/2-6/3/2015	6/1/2015

*Only a portion of the Tier 3 site was surveyed
**An LIO has not yet been formed in the Skagit-Samish Watersheds, though this region has been identified as an Action Agenda Area by the Puget Sound Partnership

Table 6: Continued from previous page

Survey site	County	Local Integrating Organization (LIO)	Survey extent	Shoreline Length (km)	Tier	Lidar Survey Dates	Additional on-site setup dates
Point Roberts	Whatcom	Whatcom (WRIA 1)	US Border on the west side at Monument Park to Maple Beach on the east side	11.4	1, 3	8/15-8/16/2015	n/a
Point Whitehorn	Whatcom	Whatcom (WRIA 1)	Birch Bay SP to Sandy Point	17.3	1	8/13-8/14/2015	n/a
Seahurst Park	King	South Central Action Area Caucus Group	Brace Point to Three Tree Point	9.8	n/a	10/31/2013	n/a
Useless Bay, Whidbey Island	Island	Island (WRIA 6)	Double Bluff to Scatchet Head	18.6	1, 3*	9/11-9/12/2015	n/a
Whidbey Island	Island	Island (WRIA 6)	Deception Pass to Fort Casey on the west side	36.0	1	7/27-7/28/2015 & 8/1-8/2/2015	7/26/2015

*Only a portion of the Tier 3 site was surveyed

Figure 6: Photos of GPS base station setup: (A) GPS and radio tripods used for RTK surveying at Cattle Point; (B) epoxy monument installed on concrete slab for base station setup during Marrowstone Island surveys

Boat-based lidar

An Optech ILRIS HD-ER laser scanner with motion compensation mounted to the cabin top of CMAP's research vessel, the R/V *George Davidson*, was used for lidar data collection (Figure 7). The laser scanner has a maximum range of over 1,000 m, with range accuracies of 7 mm at a distance of 100 m and a ping rate of up to 10,000 Hz. The maximum point spacing is 1.3 cm at 1,000-m distance; the beam diameter of the laser is approximately 19 mm at a distance of 100 m. The Class 1 infrared laser has a wavelength of 1,535 nm and is eye-safe throughout all operating ranges – essential when scanning populated coastlines. This wavelength is absorbed by water, so returns on wet beaches were sparse. However, this generally provides a more distinct waterline, except where breaking waves and swash generate air bubbles, sea foam, and suspended sediment which obscures the shoreline.

The laser scanner is coupled with an inertial navigation system, the Applanix Position and Orientation System for Marine Vessels (POS MV 320 V5 RTK), used for georeferencing and motion compensation to obtain accurate, real-time positioning of the lidar data. The POS MV consists of a GNSS-aided Inertial Measurement Unit (IMU; mounted next to the scanner) that measures the survey vessel's motion (roll, pitch, and heave), and two GNSS antennas, mounted 1.85 m (~6 ft) apart, that provide the vessel's heading and position (Figure 7). Data from the POS MV were logged at 10 Hz and integrated with the lidar data in real-time in QINSy 8.10, hydrographic survey software by QPS (Quality Positioning Services), which was also used for navigation.

Figure 7: Photo of equipment used for mobile lidar surveys (Optech ILRIS-HD-ER laser scanner and POS MV V5 320 RTK system) mounted to a cabin-top platform

During acquisition, the laser continuously scans in a vertical line pattern with a fixed angular interval of 0.09° such that nearer objects give closer spaced returns than far objects (1.6 cm at 10-m distance vs. 32 cm at 200-m distance). An object's range is determined by measuring the last returned laser pulse[3]. While laser scanning, the boat operator navigates as close to shore as possible and transits slowly alongshore, rotating the vessel occasionally to acquire data from different angles and from behind objects such as large rocks (Figure 8).

During the surveys, the distance of the scanner to the shoreline typically varied between 20-200 m, depending on water depth and breaking waves. Alongshore point spacing depends on the speed of the vessel, so the objective is to drive as slow as possible (1-3 knots) while monitoring the incoming data density in real time. Some shoreline segments were scanned multiple times to increase data coverage during more favorable conditions (e.g., lower tide, lifted fog, less people or birds). Data were set to populate a 0.5-m grid that was viewed by "hit count" (the number of data points within one grid cell), standard deviation, and elevation to assist the boat and survey equipment operators in acquiring sufficient coverage and perform an initial quality check of the data. High-resolution digital photographs of the shoreline were taken simultaneously to aid in data processing and qualitative assessment of shoreline morphology.

Figure 8: Photo of R/V *George Davidson* navigating close to shore while performing mobile lidar survey (photo taken at Cattle Point, San Juan Island)

[3]The last return was used for 13 of the 16 survey sites; however, the first three sites (Seahurst Park, Marrowstone Island, and Ledgewood) were surveyed using the first pulse return. The final DEM for these sites is much sparser on vegetated bluffs and hillsides because the laser returned more often from the vegetation than the ground surface. Switching to the last return helped discern a ground surface in more cases, but was still difficult in areas of dense vegetation. The last return is also better in conditions of fog or rain.

Ground control targets (1 m^2 sheet metal, spray-painted flat white or covered with a checkerboard pattern of alternating engineer-grade reflective material and either black vinyl or flat black paint) were set up on the beach for checking positional alignment of the laser point cloud with independently surveyed GPS points (Figure 9A). After a target was set up and checked to be level and plumb, surveyors on land measured the target's center and upper corners using RTK-GPS for a several-second occupation. A light-weight ground control target was also used when the shore-based crew was working in the same area as the boat and there were no larger targets in the vicinity. This target was a thin sheet metal sign, 0.77 m wide x 0.61 m high and spray-painted flat white, that a surveyor could easily carry while walking on the beach, set up quickly, survey its position before or after being scanned by the laser, then recover it and continue down the beach (Figure 9B). These portable targets allowed for ground control to be placed close to the water's edge where they are easily seen by the laser scanner, ensuring dense returns on the target's surface, and not in danger of being submerged by a rising tide.

Figure 9: Photos of ground control targets used during boat-based lidar survey: (A) 1 m^2 sheet metal, spray-painted flat white; (B) smaller, light-weight sheet metal (0.77 x 0.61 m)

Beach topography

Beach topography data were collected on foot with Trimble GNSS/GPS receivers mounted to a backpack to supplement the lidar data in places where small data gaps or shadows were likely due to the oblique look-angle of the laser scanner, such as behind large rocks, logs, and on backshore platforms, and also to define features such as a scarp top or toe, especially if dense vegetation was present (Figure 10). Data collected on the beach face where laser returns are dense were used to ground-truth the lidar data.

In most locations, data were collected using RTK-GPS, receiving real-time corrections from the local base station to the GPS rover. In places where RTK positioning was unavailable (e.g., line-of-sight obstructed due to morphology of coastline or dense trees, or no radio was set up for the survey), surveyors collected data in "autonomous" mode in which real-time positions were accurate to a few meters, rather than centimeters, and raw GPS data were logged at 1 Hz. These data required post-processing in the office and had no impact on the quality of the final data.

Figure 10: Photo of surveyor collecting beach topography data using a GNSS receiver mounted to a backpack

Sediment grain size

Rather than collecting physical sediment samples at each survey site, photographs of the beach surface sediment were taken as part of an in-situ technique known as "cobble cam." This photogrammetric approach to sediment grain size analysis obviates the need to collect physical samples for processing in the lab, which not only significantly reduces processing time, but it allows for large cobbles to be accounted for in sediment grain size characterization. Due to their size and weight, traditional sieving methods cannot physically handle large gravel and cobbles, which are found on many beaches throughout Puget Sound.

Sediment grain size data were collected along 108 cross-shore transects at approximately 1-km intervals at 13 of the 16 survey sites (no data for Dungeness, Dabob Bay, or Agate Beach; Figure 11). Photographs were captured at 0.5-m elevation intervals along each transect or more frequently where there were significant changes in substrate (roughly 4-7 samples per transect).

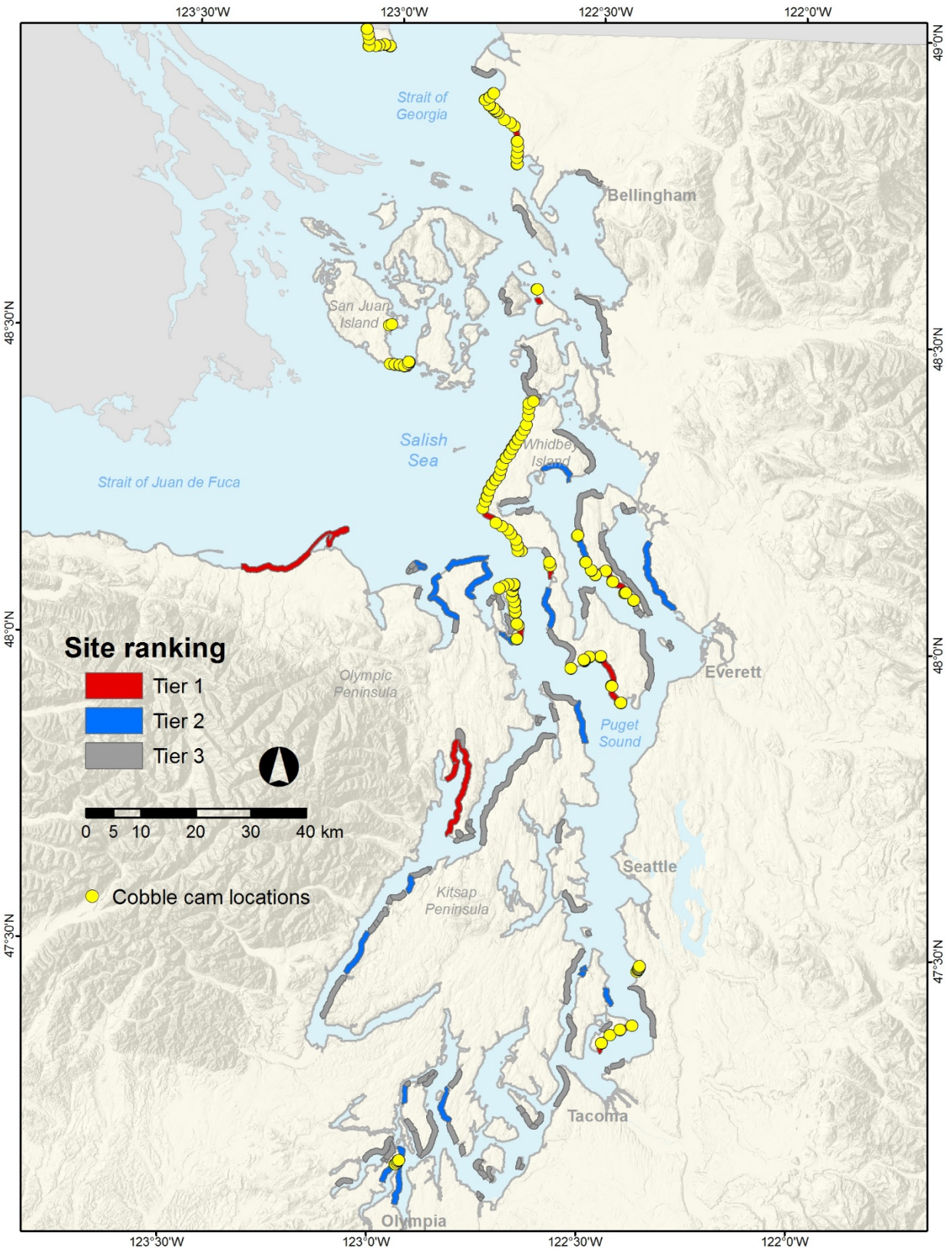

Figure 11: Map showing 108 cobble cam transect locations where sediment grain size photos were collected at 13 of the 16 boat-based lidar survey sites

A reference scale was included in each photograph to provide the means of determining the mm-to-pixel ratio of each picture (Figure 12). The distance of the camera from the substrate was dependent on the size of the sediment, set to include approximately 100 particles along the horizontal (long) axis of each photograph. RTK-GPS (or logging data for post-processing when RTK was not available), was used to collect the position and elevation of each sample location, as well as the cross-shore profile of the entire cobble cam transect.

Figure 12: Cobble cam photograph taken at 1.2-m elevation along Transect 6 for the Cattle Point, San Juan Island survey

This page is purposely left blank

Data Processing

Geodetic control

The static GPS data logged during each 2+ hour occupation of a monument were processed through the National Geodetic Survey's Online Positioning User Service (OPUS) to obtain high-accuracy coordinates using precise satellite orbits (Table 7). For survey locations where a monument was occupied more than once, the OPUS solutions were averaged to obtain a more robust and accurate position. These coordinates were used during post-processing of both boat-based lidar and ground-based GPS data to ensure all data are identically georeferenced, allowing for comparisons between each data type.

Boat-based lidar

Data logged by the base station during the survey, along with the final coordinates from OPUS, were used to post-process the vessel's position in Applanix POSPac Mobile Mapping Suite software (POSPac MMS v7.26) using Applanix IN-Fusion Single Base Station Processing to correct for RTK dropouts experienced in the field or establish accurate vessel positioning for surveys without RTK. For Seahurst Park, where there was no local base station set up during the boat-based lidar survey, the Applanix IN-Fusion SmartBase Processing was used, which utilizes a network of GNSS reference stations to generate accurate positioning. The resultant Smoothed Best Estimate of Trajectory (SBET) file was applied to the lidar data in QINSy v8.1 Processing Manager to adjust the point cloud position.

Preparation for interpreting and cleaning the lidar point cloud began with generation of photomosaics by stitching overlapping photographs together using Autopano Giga Pro v3.0.3 (Figure 13). An initial cleaning of the post-processed point cloud was done in Qloud v2.3, to remove high-fliers, reflections, and other noise due to sun glare or debris on the water surface. Final cleaning was done in the QPS 3D Editor (available in both Qimera v1.3 and Fledermaus v7.5) by examining cross-sections of the point cloud in 3D to remove all vegetation, buildings, overwater structures (e.g., docks, piers), large woody debris, and to define a clear waterline, resulting in a "bare earth" surface (Figure 14). Backshore protection structures (i.e., armoring) were left in the point cloud as a contiguous part of the ground surface. Data upland of the bluff top or landward of the vegetation line were removed.

Beach topography

Ground-based beach topography ("topo") data were processed in Trimble Business Center v3.70 using the final coordinates computed for each base station location. Data collected without fixed RTK were post-processed using the raw GPS data logged by the base station and GPS rover. Where two or more GPS rovers were used at the same site, data between surveyors within a 30-cm radius were compared, and each topo data set was adjusted for vertical agreement based on the average of individual comparisons to produce the combined final XYZ coordinates.

Table 7: List of monuments used as base station or control points and their positions; latitude/longitude are provided in Degree Minute Second format, NAVD88 elevation uses GEOID12B. The number of occupations performed on a monument increases the accuracy of its position (*Continued on next page)*

Survey site	Monument Name	Date est. or first used	Type	Purpose	No. of occup	NAD83 (2011) State Plane			NAD83 (2011) Geog.		Ellip Ht (m)	NAVD88 Elev (m)
						Easting (m)	Northing (m)	Zone	Latitude	Longitude		
Camano Island	Cam Park Hill	9/9/2015	Wood stake (not reusable)	Base	2	376850.96	126002.06	WA North	48 07 16.99095	122 29 15.61505	14.20	37.17
Cattle Point	Cattle Light	5/23/2016	Epoxy	Base	2	342462.48	163451.50	WA North	48 27 01.75718	122 57 48.04107	-2.18	19.19
Cattle Point	Fort Reset	5/23/2016	Existing BM	Control	1	338631.82	164965.19	WA North	48 27 47.27032	123 00 56.48597	41.80	63.00
Dabob Bay	Gatchet	7/6/2015	Epoxy	Base	5	351001.48	89866.38	WA North	47 47 27.47377	122 49 20.05691	-18.29	3.34
Dungeness	Dungeness	6/29/2015	Epoxy	Base	2	323963.95	129167.43	WA North	48 08 14.72450	123 11 56.62163	19.78	40.52
Edgewater Beach	Connie	9/24/2015	Metal pipe	Base	2	315682.90	205051.23	WA South	47 09 09.15282	122 55 51.01776	1.00	22.89
Guemes Island	Edens	6/4/2015	Epoxy	Base	2	365722.14	173925.51	WA North	48 33 00.06378	122 39 08.39672	-18.43	3.47
Ledgewood	Teronda	5/22/2015	Epoxy	Base	1	368451.73	126909.70	WA North	48 07 40.32596	122 36 02.68044	-19.49	3.16
Marrowstone Island	Cottage	5/17/2015	Epoxy	Base	3	360851.42	114620.40	WA North	48 00 56.72128	122 41 55.74313	-19.02	3.03
Marrowstone Island	East Beach Park	5/17/2015	Epoxy	Base	1	362080.16	119132.60	WA North	48 03 23.73771	122 41 01.69893	-18.63	3.58
Marrowstone Island	Flag	5/17/2015	Existing BM	Base	1	361511.77	123300.63	WA North	48 05 38.20868	122 41 34.00530	-5.96	16.32
Marrowstone Island	Rawlins	5/18/2015	Existing BM	Control	2	361312.91	124226.62	WA North	48 06 08.02632	122 41 44.69707	18.17	40.46
Maury Island	Gold	6/1/2015	Epoxy	Base	3	379531.12	42384.71	WA North	47 22 11.95507	122 25 42.09188	-18.81	3.81
Point Roberts	Lighthouse	8/15/2015	Epoxy	Base	2	335206.19	221861.30	WA North	48 58 25.20076	123 05 04.18415	-17.37	3.87
Point Whitehorn	Gulf	8/13/2015	Epoxy	Base	2	360859.60	208066.38	WA North	48 51 21.18759	122 43 46.45439	-17.90	3.67
Seahurst Park	Bulkhead	10/31/2013	Concrete bulkhead	Base	1	384723.97	54360.80	WA North	47 28 43.06854	122 21 46.12416	-17.69	5.30

Table 7: Continued from previous page

Survey site	Monument Name	Date est. or first used	Type	Purpose	No. of occup	NAD83 (2011) State Plane			NAD83 (2011) Geog.		Ellip Ht (m)	NAVD88 Elev (m)
						Easting (m)	Northing (m)	Zone	Latitude	Longitude		
Useless Bay	Double Bluff	9/11/2015	Epoxy	Base	2	374546.42	110531.74	WA North	47 58 54.58656	122 30 50.69280	-18.79	4.01
Whidbey Island	Ebeys Landing	7/26/2015	Epoxy	Base	3	360719.11	134141.10	WA North	48 11 27.48559	122 42 25.05941	-19.03	3.36
Whidbey Island	Joseph	8/1/2015	Epoxy	Base	2	360365.18	147147.73	WA North	48 18 29.19006	122 42 57.59901	-18.60	3.59

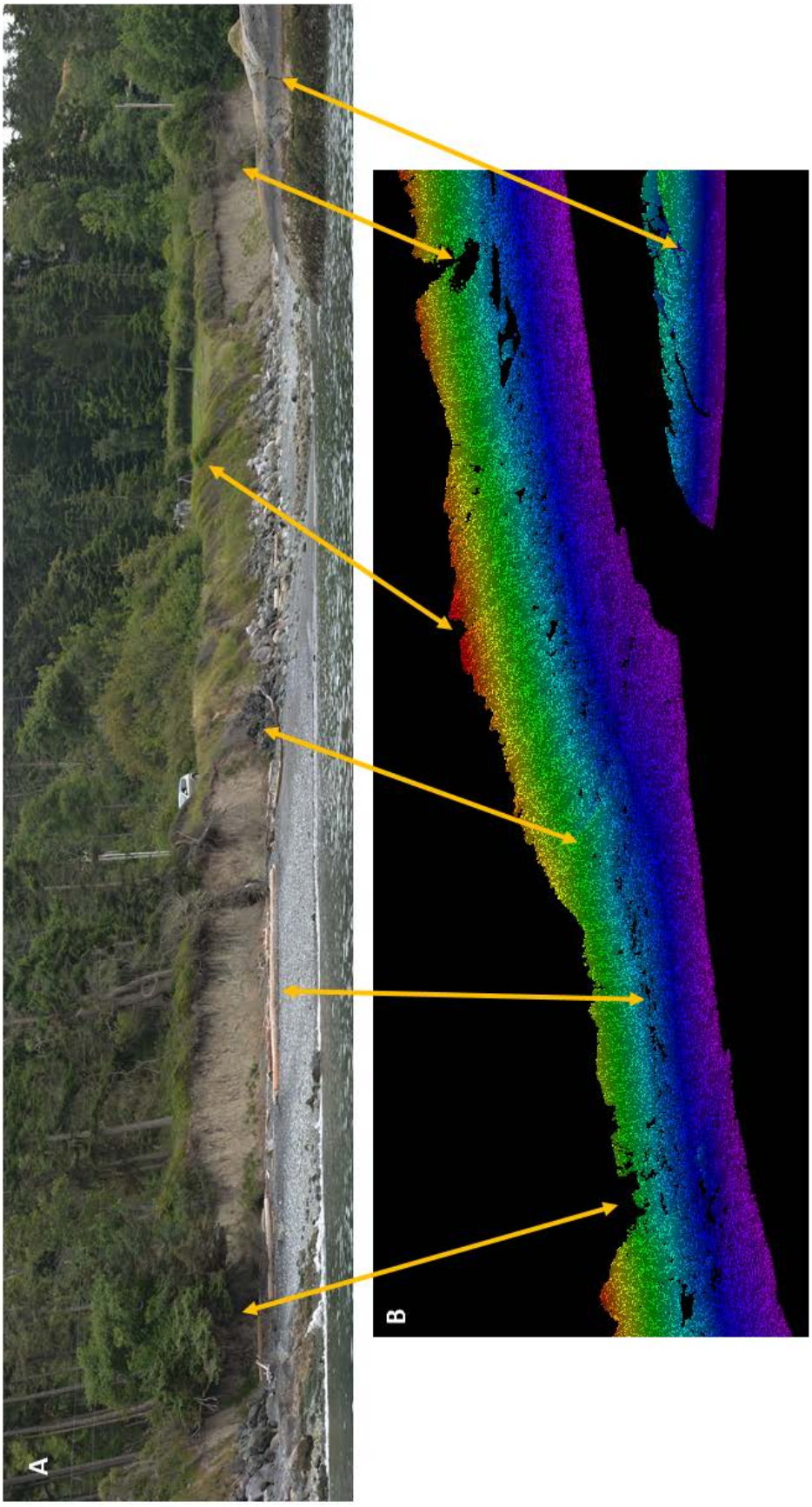

Figure 13: Example of (A) digital photomosaic used to aid in interpretation of (B) boat-based lidar point cloud; the point cloud has already been cleaned, therefore vegetation is shown as an absence of data

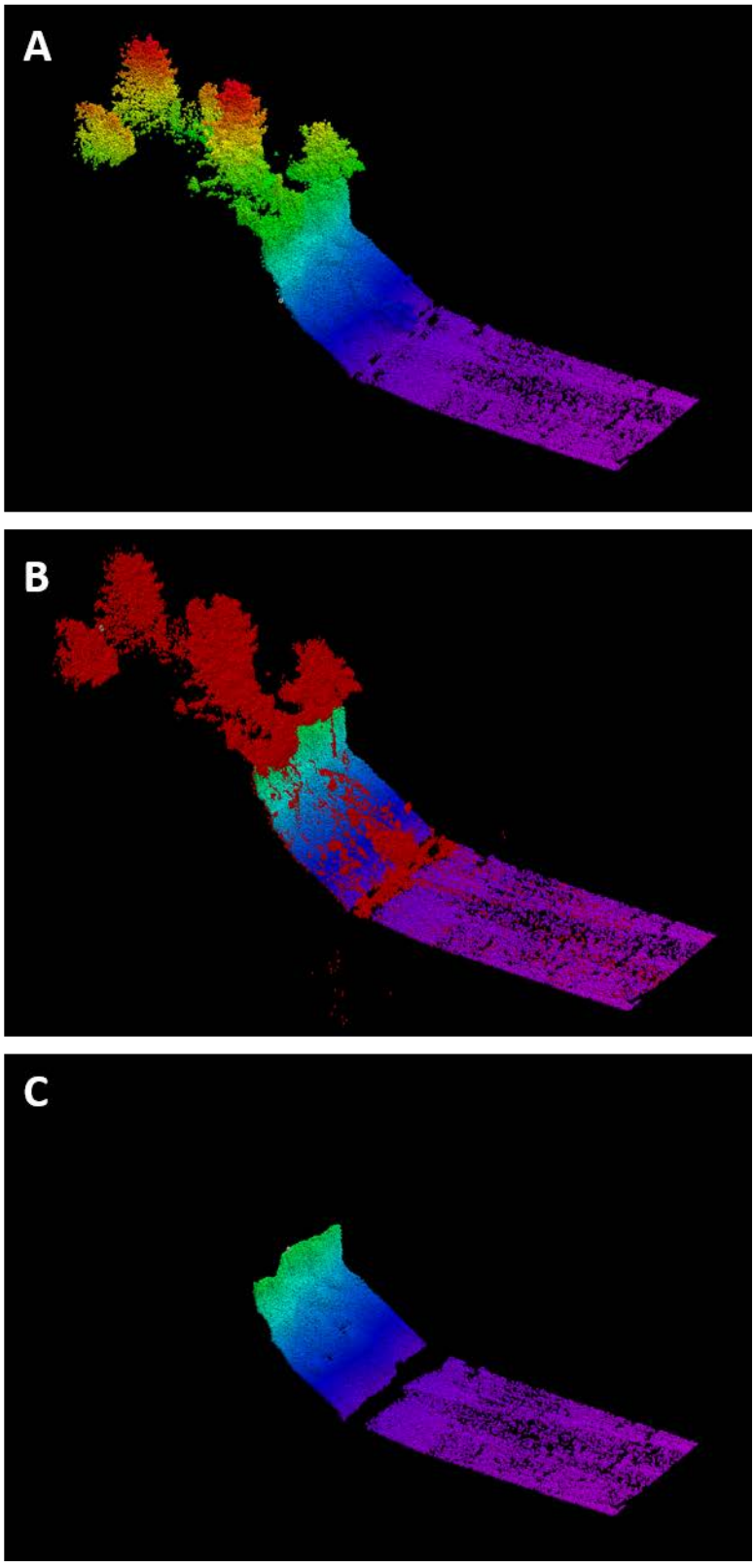

Figure 14: Illustration of point cloud cleaning by removing vegetation from bluff; (A) uncleaned point cloud, (B) rejected points highlighted in red, and (C) clean point cloud with only beach and bluff ground surface remaining

Digital elevation model

A section of beach from the lidar point cloud free of drift logs and vegetation with a relatively uniform slope and gravel-sized or finer texture was extracted for comparison with the ground-based GPS data. Each GPS topo point was compared to the surrounding lidar points within a 30-cm radius to check for discrepancies between the datasets. The average offset was calculated based on the population of comparisons, and the lidar point cloud was adjusted vertically to match. Extraneous topo data outside of the lidar coverage were removed. The remaining topo points and clean, adjusted lidar point cloud were combined in Qimera and gridded at 0.5 m using the average elevation within a grid cell. A "bare earth" digital elevation model (DEM) with 0.5-m resolution of the beach and bluffs for each survey site was created in ArcGIS v10.2 by interpolating the gridded data using a Triangulated Irregular Network (TIN).

Sediment grain size

Sediment grain size photos were processed using a MATLAB-based point-count algorithm developed by Ian Miller at the Washington Sea Grant. The algorithm randomly places 100 dots on the photograph, and the user traces the intermediate diameter of each particle that is overlaid with a dot. For small grain sizes, the photo is divided into subsections so the user can zoom in and more effectively trace each particle. Once 100 diameters have been traced, the algorithm uses the millimeter-to-pixel conversion factor to calculate the millimeter length of each traced diameter.

Various parameters can be determined from the 100 diameter lengths, such as mean, median, and range. For this study, the median grain size (D_{50}) was calculated for each transect. D_{50} is the diameter that splits a grain size distribution in half, with half of a sample's mass being larger and half of the sample's mass being smaller. D_{50} accurately describes the size of a sediment sample because, unlike the mean grain size, the median grain size is not heavily skewed by the presence of a few outliers.

Results

The selected survey sites consisted of a variety of shoretypes: vegetated and bare/exposed (active feeder) bluffs interspersed with armored and natural beaches, bluff-backed lagoons, residential-backed beaches, and barrier spits. Overall, active feeder bluffs (FBEs) make up a small percentage of the Puget Sound shoreline, and the beaches at several of the Tier 1 survey sites were backed by densely vegetated bluffs or hillsides. While these settings do not provide as much sediment to the nearshore, the areas included good habitat for natural resources, such as ample overhanging vegetation, large woody debris, and submerged aquatic vegetation.

Ground-based GPS data collected at each site showed good agreement between surveyors. Antenna height adjustments ranged from -2.2 to +2.7 cm, with 61% being smaller than ± 1 cm and 95% being smaller than ± 2 cm. Inconsistencies between measured elevations may be due to precision of field-measured antenna heights, change in surveyor posture while walking, or uneven compression of sediment between surveyors. Where control points were collected, the surveyed positions agreed closely with the published values (-1.2 cm in Easting, 0.1 cm in Northing, and 0.7 cm in Elevation, on average).

The density of the lidar point clouds varied depending on the topographic relief and distance at which the shoreline was scanned, with higher density achieved on vertical features (e.g., bluff face) and from shorter ranges (Figure 15). When averaged across all survey sites, the mean (median) number of points per 0.5-m grid cell was 9 (7) on the beach surface and 26 (12) on the bluff face (Table 8). The highest point density obtained on a beach was at Jackson Beach on San Juan Island (41 points per 0.5-m grid cell), which was scanned at a close range (30-50 m from shore). Though it was scanned at a farther range (150-200 m from bluff), the highest point density obtained on a bluff was at Dungeness (65 points per 0.5-m grid cell), where mostly bare feeder bluff with little vegetation resulted in a high data-return surface. The lowest point density was obtained on the beach at Useless Bay (3 points per 0.5-m grid cell), where the shoreline was scanned from a distance approaching 500 m due to the wide exposed low tide terrace.

When compared to the ground-based beach topography data, the boat-based lidar data was consistently lower, exhibiting a mean offset of 10 cm, ranging from 6 to 15 cm (Table 9). The lidar point cloud was adjusted using the mean offset for a survey area, resulting in better vertical agreement of the point cloud with the ground control targets (2 cm lower, on average, after adjustment vs. 12 cm prior). Not all ground control targets produced reliable results, as this depended on the density of laser returns on the target's surface and the ability to accurately detect the center and/or corners of the target. When averaged across all survey sites, the ground control targets suggest a mean horizontal offset of 5.2 ± 19.5 cm in Easting and -7.7 ± 22.0 cm in Northing between the lidar and ground-based GPS measurements.

DEMs with 0.5 m-grid resolution were generated for the beaches and bluffs of the 16 survey sites. These DEMs serve as baseline datasets, documenting the coastal landscape at the time in which they were surveyed. The high-resolution of the DEMs makes it possible to discern detailed morphology, such as irregularities of a bluff face, shallow intertidal sand bars, and the intricacies of an armored shoreline (Figure 16). Appendix C gives more specific information about the DEMs and includes graphics for each DEM produced as part of this project.

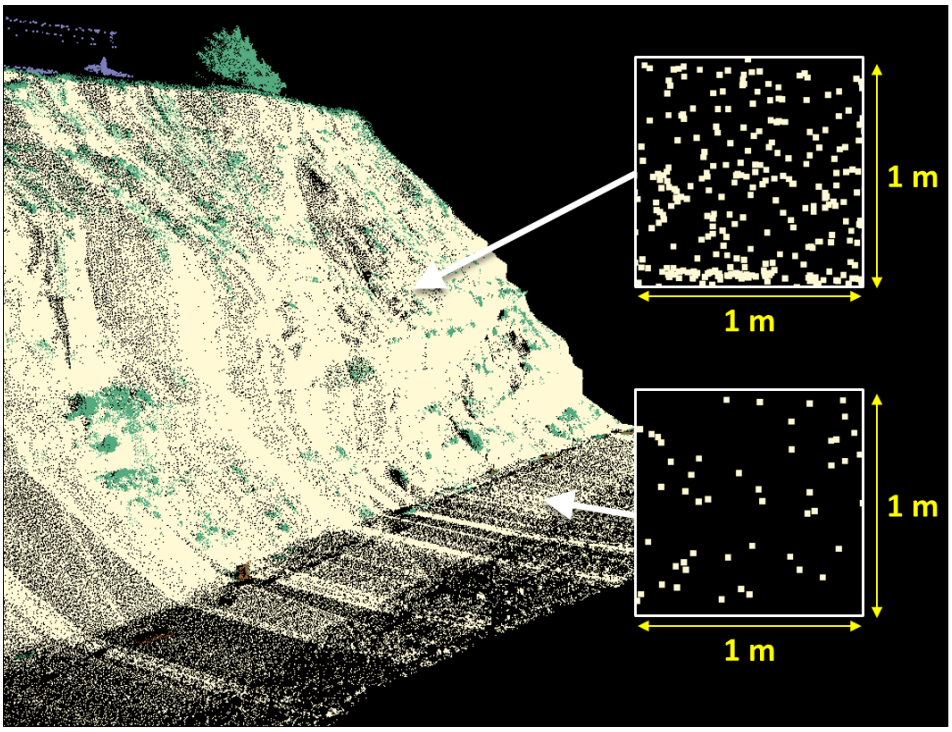

Figure 15: Illustration of point density within 1-m^2 sections of the lidar point cloud from the bluff and beach ground surface

Table 8: Lidar point cloud density (calculated as number of points per 0.5-m grid cell) for the beaches and bluffs at each survey site

Survey Site	Section	Area (m^2)	Points per 0.5-m grid cell		
			Median	Mean	St. Dev.
Agate Beach	Beach	10,494	10	12	11
	Bluff	3,245	24	38	48
Camano Island	Beach	59,165	4	6	5
	Bluff	23,359	12	30	57
Cattle Point	Beach	84,189	10	15	17
	Bluff	102,324	14	25	40
Dabob Bay	Beach	26,783	3	4	5
	Bluff	30,745	7	17	33
Dungeness	Beach	353,233	6	9	9
	Bluff	337,365	37	65	109
Edgewater Beach	Beach	178,271	8	9	7
	Bluff	52,121	7	20	46
Guemes Island	Beach	208,593	5	7	8
	Bluff	72,240	9	29	73
Jackson Beach	Beach	8,405	38	41	34
	Bluff	9,927	10	16	24
Ledgewood	Beach	146,613	4	6	8
	Bluff	14,667	16	46	121
Marrowstone Island	Beach	374,136	3	6	7
	Bluff	88,776	18	46	102
Maury Island	Beach	66,087	5	7	6
	Bluff	48,063	3	9	15
Point Roberts	Beach	228,692	3	5	6
	Bluff	32,311	5	12	25
Point Whitehorn	Beach	100,566	4	5	5
	Bluff	72,973	3	7	15
Seahurst Park	Beach	128,081	2	3	4
	Bluff	10,920	4	9	15
Useless Bay	Beach	285,568	2	3	3
	Bluff	288,734	5	11	21
Whidbey Island	Beach	704,314	5	7	9
	Bluff	877,664	17	29	50

Table 9: Summary statistics for comparison between boat-based lidar and ground-based GPS data for each survey site, as well as the vertical adjustment made to each lidar dataset

Survey site	Mean offset (cm)	Std. Dev. (cm)	N comps	Avg lidar pts/comp	Z- shift (cm)
Agate Beach	11.6	3.2	119	17	+ 12
Camano Island	10.8	4.2	808	12	+ 11
Cattle Point	9.9	2.5	3088	19	+ 10
Dabob Bay	9.4	5.1	292	11	+ 9
Dungeness	6.9	3.5	1545	14	+ 7
Edgewater Beach	13.4	6.3	5496	14	+ 13
Guemes Island	12.7	5.5	1172	9	+ 13
Jackson Beach	14.9	2.4	1168	51	+ 15
Ledgewood	6.1	5.3	1125	13	+ 6
Marrowstone Island	8.7	4.0	3420	13	+ 9
Maury Island	6.1	2.5	420	12	+ 6
Point Roberts	8.4	3.8	2289	15	+ 8
Point Whitehorn	11.0	7.5	2556	12	+ 11
Seahurst Park	10.6	5.1	59	11	+ 11
Useless Bay	12.2	4.4	98	10	+ 12
Whidbey Island	8.5	4.4	4907	14	+ 9

The alongshore distribution of sediment grain size observed in the cobble cam data for several sites confirms the delivery of sediment from feeder bluffs to nearby beaches, as illustrated by larger grain sizes near feeder bluffs and finer sediments toward the distal end of the drift cell. For example, the beaches backed by FBEs at Fort Ebey State Park on the west side of Whidbey Island contain a mix of sediments ranging from cobble to sand, while beaches to the north are characterized by sand and fine- to medium-sized gravel. Beaches dominated by large gravel, such as on the east side of Cattle Point, indicate they are sediment starved. The sandiest beach surveyed was at Useless Bay where the majority of the samples consisted of sand or very fine gravel across wide beaches exposed at low tide. The cross-shore profiles at Useless Bay show a band of larger sediment occurring within one meter of the mean tide level. Appendix D provides cobble cam data results, including plots of alongshore and cross-shore sediment grain size distributions for each survey site.

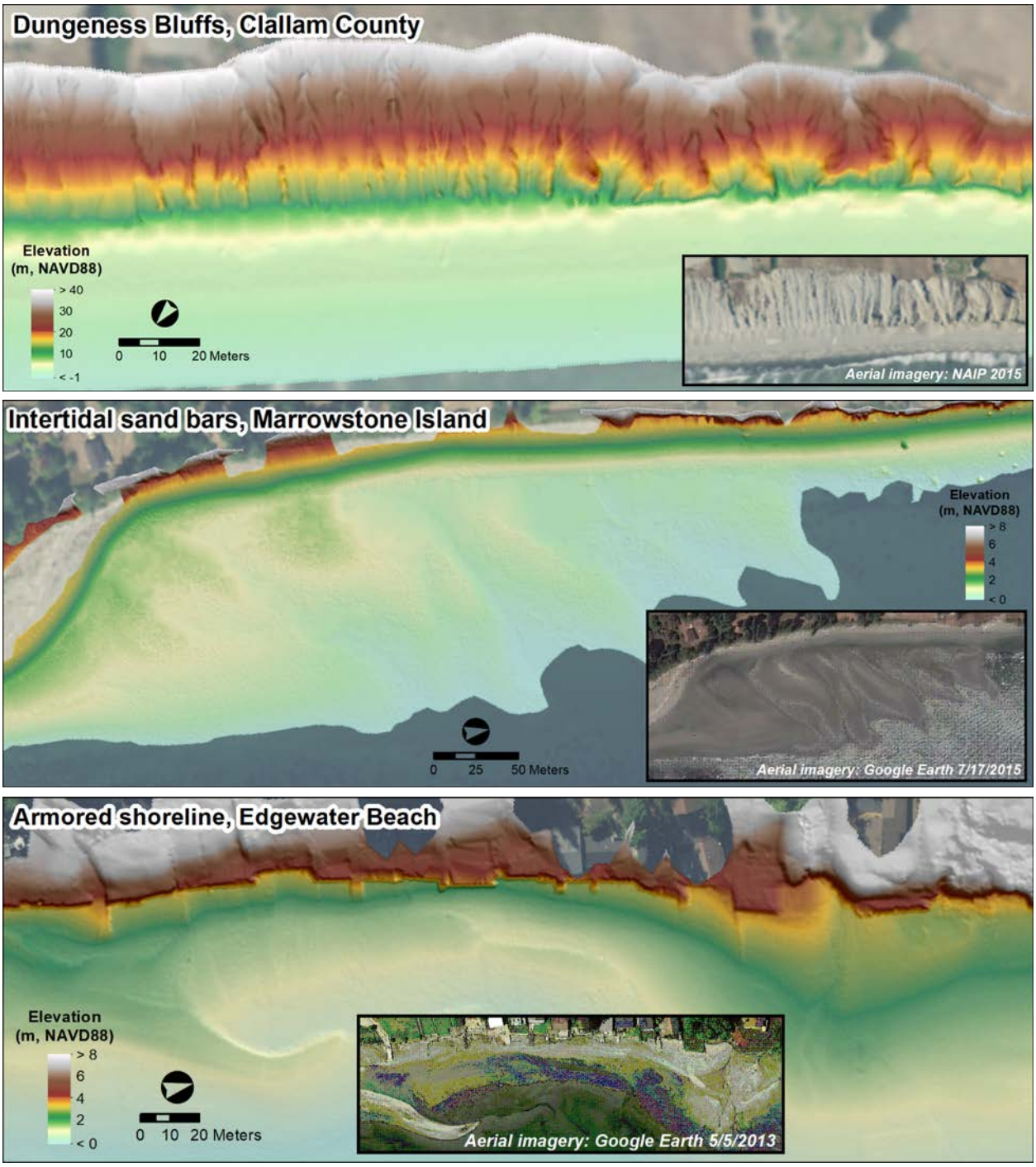

Figure 16: Close-up views of high-resolution DEMs showing details of different shoretypes

This page is purposely left blank

Discussion

This project developed an objective systematic site-selection process that harnessed existing spatial physical, ecological, and social data and made use of multiple criteria, metrics, and their relative weighting to determine high-value locations to prioritize for mapping. The criteria used in this project identified drift cells that offer the greatest potential return on ecosystem services based on currently functioning intact contiguous drift cells that can be largely protected through management measures. The approach serves as a model for determining where in the landscape to strategically invest capital and social inputs for protection and restoration efforts, with the tools and processes described here easily adapted to different priorities and weightings. Specific approaches to nearshore ecosystem management will be further informed by the baseline mapping, characterization, and future monitoring of landscape and geomorphic changes at each site.

This project provided high-resolution baseline topographic data of beaches and bluffs, shoreline photographs, and sediment grain size along 16 survey sites, comprised of over two dozen drift cells, prioritized by the site-selection process. The combined data sets serve as a physical inventory and documentation of the landscape at the time of their collection, providing a reference point for historical and future change analysis. The final DEM surfaces map decimeter- to regional-scale variability in alongshore and cross-shore beach and bluff morphology. Some data sets provide a pre-bulkhead removal condition survey (e.g., Dabob Bay, Edgewater, and Seahurst; Figure 17), enable a detailed erosion mitigation project design assessment (e.g., Agate Beach), or facilitate planned restoration projects (e.g., Jackson Beach, Marrowstone). Spatial analyses of sediment texture along West Whidbey Island and other drift cells document an alongshore gradient in sediment size from feeder bluffs to downdrift barrier beaches.

This project demonstrated that boat-based lidar can be mobilized quickly and efficiently to remotely collect topographic data on beaches and bluffs, which can be otherwise difficult to access and survey by land. The methodology provides high-resolution 3D surface elevation data that is critical to understanding the details of coastal processes at scales spanning projects to drift cells. Nevertheless, some landscapes remain difficult to obtain complete coverage due to the shadows created by the horizontal look angle of the laser (e.g., behind boulders, large woody debris, or beach ridges).

Alternatives to boat-based lidar include airborne lidar or traditional ground-based survey methods such as walking beach profiles, mounting GPS to an All-Terrain Vehicle (ATV), or using a total station. While airborne lidar can be collected over large areas with meter-scale (or greater) accuracy and can provide complete coverage over most terrain types, it is often more expensive to collect and produces poor coverage on vertical surfaces, often obscuring features like the top edge of bluffs. Traditional survey methods require significantly more effort to merely collect discrete points, which in turn requires more interpolation using less data than high-resolution lidar if producing a DEM. Unmanned aerial vehicles (UAVs) with cameras offer another approach that could be complementary to boat-based lidar, while having other limitations in terms of range, weather, vegetation, and processing time.

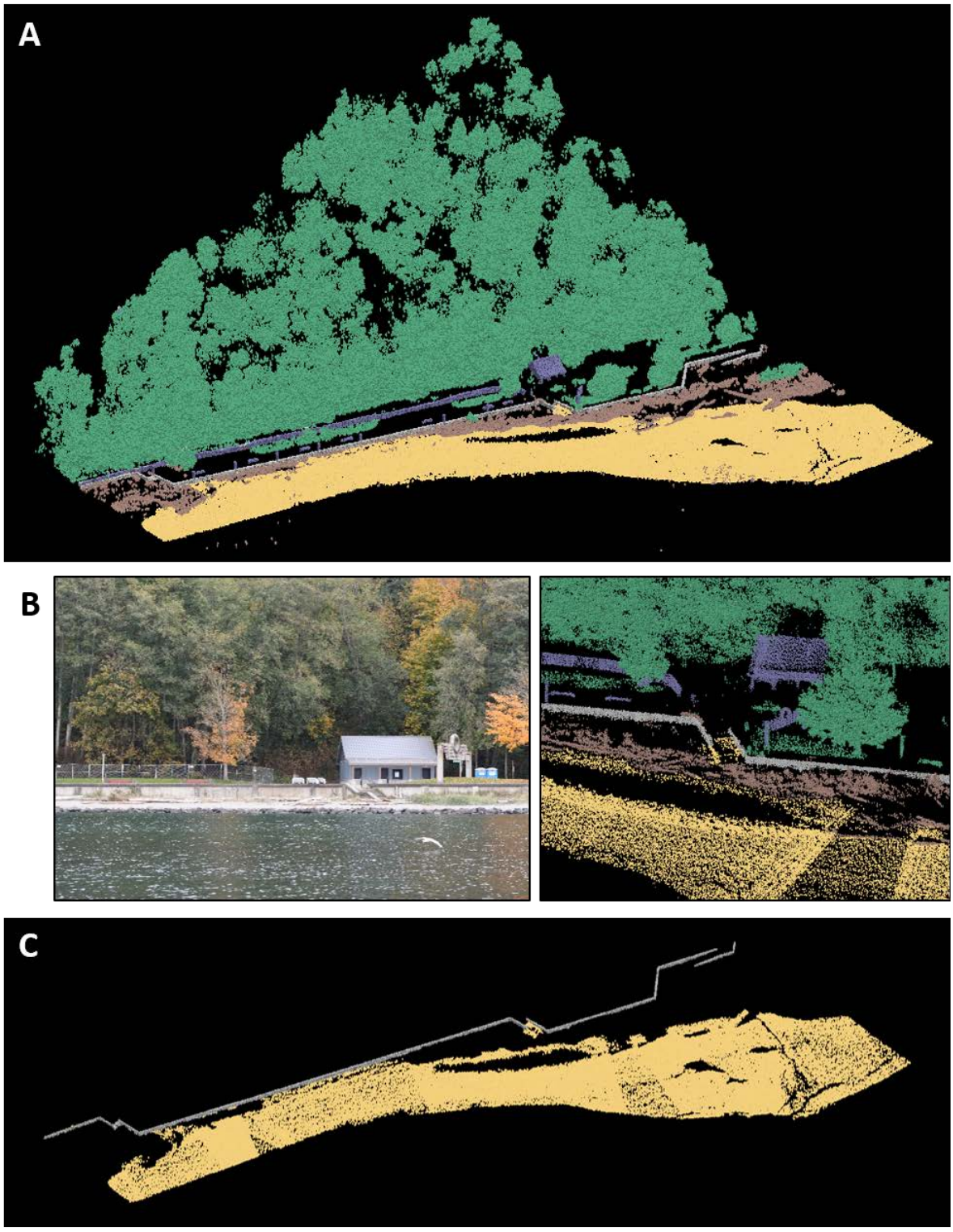

Figure 17: Subset of the laser point cloud for Seahurst Park showing data colored by feature type: beach surface (yellow), bulkhead (light gray), vegetation (green), large woody debris (brown), and other man-made structures (dark gray); (A) full point cloud, (B) close-up of the point cloud with a photo taken from the boat, for reference; (C) points used to create the final DEM with only the beach surface and bulkhead remaining

While bare-earth DEMs are the main deliverable of this project, features within the DEMs and the lidar point clouds can be extracted for a more comprehensive inventory, classification, and analyses of site conditions and variability. For example, quantitative metrics of shoreline characteristics can be derived from DEMs such as bluff crest height, bluff slope, bluff toe elevation, beach slope, and shoreline armoring elevations. These metrics can then be compiled and compared within and among drift cells to determine regional variability such as differences between updrift and downdrift beaches and the effect of fetch, orientation, and other exposure variables.

Certain features can also be correlated to characterize how the shoreline landscape may be affecting nearshore ecosystem services. For example, variability and gradients in beach slope and width may be correlated to proximity to feeder bluff activity and the position, length, and elevation of armoring relative to the shoreline and backshore. Upland development and shoreline modification may be correlated to the amount of overhanging vegetation, large woody debris, or beach wrack, and these findings can be compared to conditions at undeveloped shorelines. Details in the lidar point clouds, such as intensity values, can help identify groundwater seepage and potential bluff failure and erosion mechanisms. The complementary photos to the lidar point clouds provide additional documentation of bluff geology, stratigraphy, groundwater flow, and other characteristics to help assess relative bluff stability. Appendix E provides examples of lidar data applications and metrics that can be extracted from the DEMs.

Repeat surveys of the same sites would enable change analysis of many of the features mentioned above. The patterns and rates of bluff erosion, as well as sediment volume contributions from bluff failures to adjacent beaches, could be determined along with insights on the temporal variability of episodic landslides. Bluff and beach change over time could be analyzed by differencing 3D DEMs or comparing extracted 2D cross-shore profiles (Figure 18). Furthermore, changes in ecological characteristics such as large woody debris and overhanging vegetation could be assessed and used as an indicator of beach health over time. As a longer term and more comprehensive baseline dataset is accrued and repeat surveys are collected, additional questions can begin to be addressed. For example: Under what conditions will beaches be able to keep up with sea-level rise? How will beach ecosystem services be affected by sea-level rise and shoreline armoring? Which beach restoration projects are most viable given projections of sea-level rise, sediment supply, and shoreline armoring? Appendix E provides examples of lidar data applications related to morphology and habitat change.

The sub-aerial beach is only part of the active coastal zone. Coastal processes are also influenced by nearshore bathymetry. Multibeam sonar surveys can extend the high-resolution topographic lidar data across the nearshore zone to document longshore and cross-shore sediment distribution and habitat characteristics. By collecting boat-based lidar data at low tide and multibeam sonar data at high tide, a continuous DEM of the entire coastal zone, from bluff top to nearshore, can be produced (Figure 19). Complete coastal zone mapping enables assessment of bluff sediment supply to beaches and the dispersal of sediment through the nearshore zone, and provides insight to the importance of terrestrial sediment supply for sustaining nearshore habitats, such as for forage fish and eelgrass.

Quantifying sediment supply across a range of drift cells, beach types, geomorphic settings, and energy regimes will inform the type and scale of adaptive management measures needed to protect or restore sediment sources and barriers to sediment transport. Similarly, knowledge

gained on beach processes and dynamics provide an important context for evaluating the suitability and potential effectiveness of restoration actions. Currently, there is limited to no site-specific information on bluff erosion rates or forecasted erosion hazards, yet this is needed by local managers to establish buffer zones and setback ordinances, and shoreline property owners need to be informed about erosion processes and the consequences of shoreline armoring. Bluff sediment supply information developed from repeat surveys will assist local governments in their efforts to protect feeder bluffs, encourage alternatives to shoreline armoring, and improve policies and restoration plans.

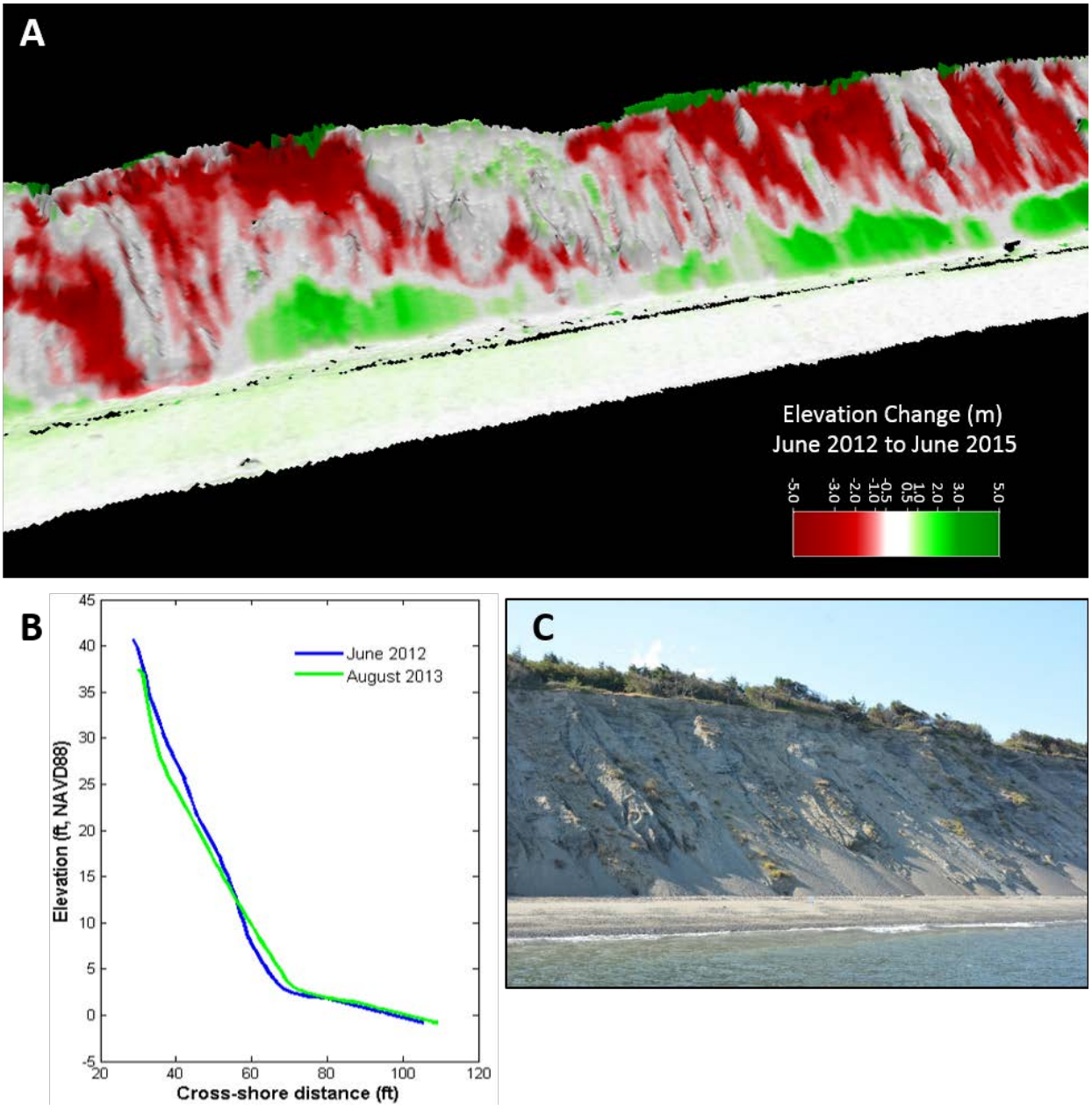

Figure 18: Example data products for a bluff change analysis project using boat-based lidar of the Dungeness Bluffs near Port Angeles; (A) 3D volume change, (B) 2D cross-shore profile change, (C) photo of the bluffs during the 2015 survey

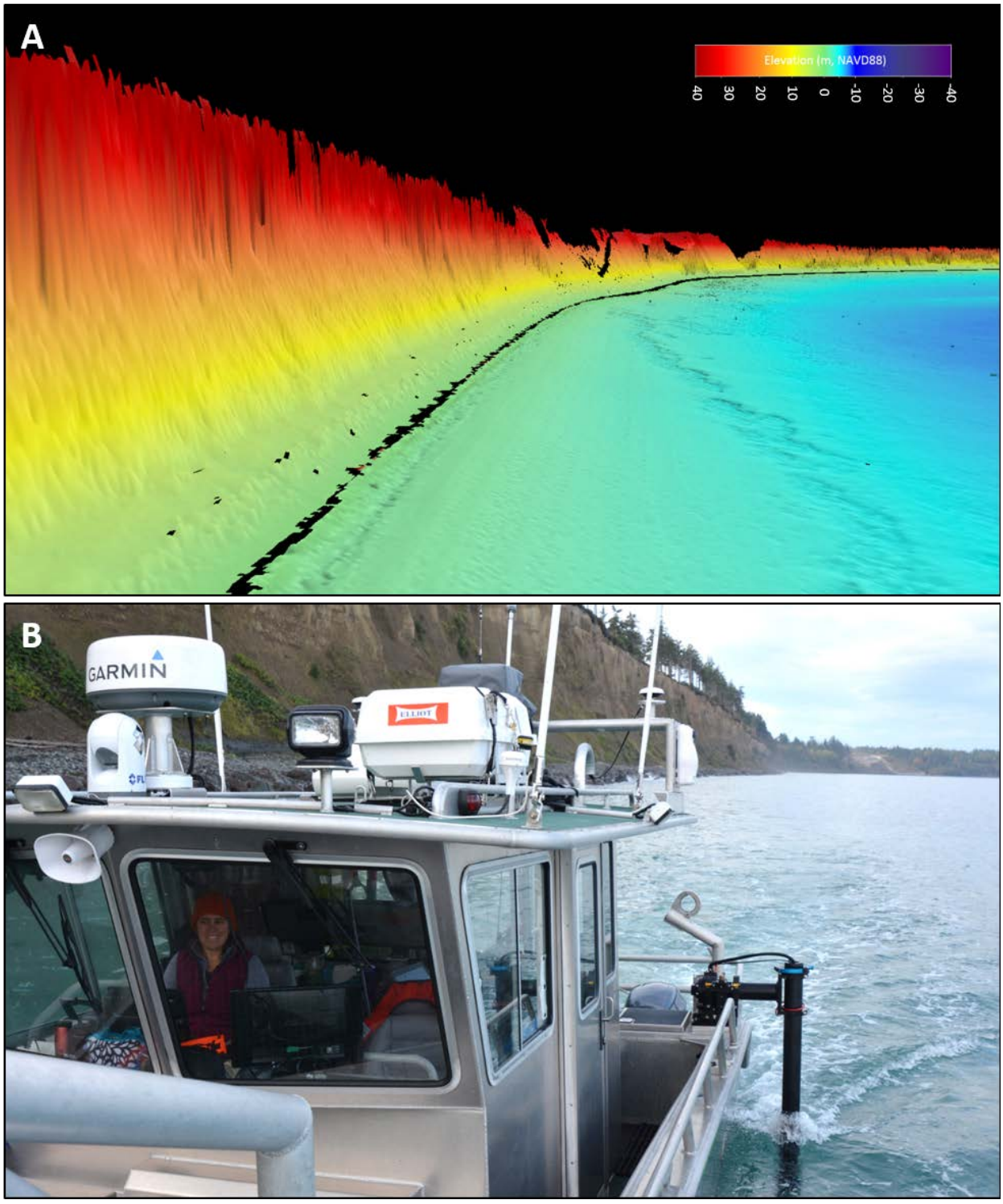

Figure 19: Example data product from high-resolution coastal zone mapping of the Elwha Bluffs near Port Angeles using boat-based lidar and multibeam sonar; (A) 3D gridded data of bluff, beach, and nearshore, (B) photo of boat and bluffs taken during 2015 survey

This page is purposely left blank

References

Byrd, K.B., J.R. Kreitler, and W.B. Labiosa, 2011. Tools and methods for evaluating and refining alternative futures for coastal ecosystem management—the Puget Sound Ecosystem Portfolio Model: U.S. Geological Survey Open-File Report 2011–1279, 47 p., available at http://pubs.usgs.gov/of/2011/1279/.

[Ecology] Washington State Department of Ecology, 2003. Washington Coastal Atlas, drift cells. Digitized by Cinde Donoghue based on work from multiple graduate students in 1980s-1990s under the direction of Dr. Maurice Schwartz at Western Washington University. Available at: https://fortress.wa.gov/ecy/coastalatlas/Default.aspx

[Ecology] Washington State Department of Ecology, 2004. Shoreline Slope Stability. Shorelands and Coastal Zone Management Program. Originally published as hard copy maps 1978-1980.

Gaeckle, J., P. Dowty, H. Berry, and L. Ferrier, 2011. Puget Sound Submerged Vegetation Monitoring Project: 2009 Report. Nearshore Habitat Program, Washington Department of Natural Resources, Olympia, Washington, 76pp. plus appendices.

Griggs, G.B., 2005. The Impacts of Coastal Armoring, *Shore and Beach*, 73, 13–22.

Macdonald, K., D. Simpson, B. Paulsen, J. Cox, and J. Gendron, 1994. Shoreline armoring effects on physical coastal processes in Puget Sound, Washington: Coastal Erosion Management Studies, Vol. 5, Shorelands Program, Washington Department of Ecology, Olympia, DOE Report 94-7.

MacLennan, A.J., J.W. Johannessen, S.A. Williams, W.J. Gerstel, J.F. Waggoner, and A. Bailey, 2013. Feeder Bluff Mapping of Puget Sound. Prepared by Coastal Geological Services, for the Washington Department of Ecology and the Washington Department of Fish and Wildlife. Bellingham, Washington, 118 pp., 42 Maps.

[NOAA] National Oceanic and Atmospheric Administration Center for Operational Oceanographic Products and Services (CO-OPS), 2013. Tides Predictions, accessed December 16, 2014, available at: https://tidesandcurrents.noaa.gov/tide_predictions.html

Pilkey, O.H., and H.L. Wright, III, 1988. Seawalls versus beaches, *Journal of Coastal Research*, Special Issue 4, 41–64.

This page is purposely left blank

Appendices

Appendix A. Lessons Learned

Site-selection process

Considerable time and resources were taken up by a rigorous site-selection process. The objective of this project was to collect baseline data on feeder bluffs in order to have a basis for comparison for future surveys to enable quantifying sediment supply to the coastal zone. While the process produced tangible benefits of a GIS database and model to objectively rank project sites according to criteria and weighting of parameters, there are also benefits that can be derived from subjectively selecting particular sites (e.g., bulkhead removal projects along feeder bluffs) that offer their own unique learning opportunities and management applications.

Moreover, while some of the Tier 1 sites did contain active feeder bluffs, the majority of coastline surveyed was comprised of low-lying beaches and vegetated bluffs in areas adjacent to active feeder bluffs. Surveying entire drift cells is important for understanding the role feeder bluffs play in supplying sediment to the adjacent shorelines; however, it may first be more important to obtain high-resolution data on feeder bluffs themselves. Once feeder bluff activity is quantified, then more extensive surveys that include the entire drift cell can be prioritized and performed to learn where the sediment is going and how long it takes to be distributed within the drift cell.

For future surveys aiming to provide baseline data on sediment supply from coastal bluffs as done in this project, improvements to the site-selection process could be made before prioritizing future sites. Many of the Tier 2 sites subjectively chosen for this project were based on the timeliness of restoration projects happening around the Puget Sound. While aligning interests with other groups was a priority for this project, the same sites may not be prioritized for future surveys. Modifications to the input criteria (sub-priorities) could include cumulative FBE in a shoreline segment rather than just considering contiguous FBE. For simplification of results spatially, the base unit for the site selection process should be standardized using complete drift cells rather than, in some cases, having a separate shoreline segment where the divergence and convergence zones of adjacent drift cells overlap.

Boat-based lidar

Because an entire year of the project was spent on site selection, nearly all surveys had to be completed during an extended survey season (spring-fall) during the 2nd year of the grant such that there was not time to develop data processing work flows and certain efficiencies until after nearly all the data was collected. As a result, there was not enough time to clean the datasets in their entirety and a decision was made to focus on Tier 1 bluff-backed beaches as a deliverable for this project. As time and resources allow, additional data will be cleaned and made available to users.

Having been able to collect boat-based lidar data along approximately 220 km of shoreline during a single year suggests that it is possible to collect much of the highest priority Tier 2 and 3 sites, along with selected repeat surveys of Tier 1 sites as warranted by actively eroding bluffs,

within the time frame of two biennium budget cycles and learn about the range of bluff erosion rates from a wide variety of settings throughout Puget Sound. Therefore, it is feasible to fill an important knowledge gap without having to survey all Puget Sound shorelines; however, this requires programmatic commitment to follow through on monitoring surveys in order to better understand the importance of feeder bluffs to beaches and nearshore ecosystems.

With the current workflow, boat-based lidar data takes upward of 1 day to clean 1 km of shoreline, especially for sections of heavily vegetated bluffs. The software used originated as hydrographic survey software that has been developing capability for boat-based lidar data; however, the automated cleaning tools used for bathymetry data do not work as well for topographic lidar data. For this project, we chose to forego classifying the lidar in another software and manually cleaned the lidar in Qimera and Fledermaus. If the data is classified and manipulated outside the QPS suite, the edits would not be retained in a way that can be transferred back to the QPS-compatible format.

Modifications to lidar data collection could be made to ease the point cloud cleaning process. When surveying shorelines with vegetation, it would be better to survey during leaf-off conditions in winter. However, daylight hours are shorter in the winter and low tides are better in spring and summer. Multiple passes of the same stretch of shoreline and a high degree of rotation while scanning complicated point cloud cleaning. While making multiple passes and rotating to scan behind large objects may increase data coverage, it also increases noise in the data and the data processor must make decisions about what data to keep and what to discard. Experience has shown that laser returns collected perpendicular to the beach, ideally at a constant heading, and at the shortest range have the best positional accuracy.

Collecting the last returned laser pulse, rather than the first (the two options given in the Optech software), has shown to be essential for lidar collection on vegetated bluffs or when environmental conditions are unfavorable for the laser scanner to have a clear sight of the shoreline (e.g., rain, fog, and moisture in the air). The first return often reflects off vegetation or ground cover resulting in few returns on the actual beach or bluff surface (Figure A-1). It can still be challenging to discern the ground surface with the last return when there is dense vegetation, but the results are much better.

1-m^2 ground control targets with engineer-grade reflective material on alternating quadrants of a checkerboard pattern were originally made for this project to best define the center using intensity differences. It was later determined that the reflective material caused too much scattering of the laser, making it difficult to distinguish the center if the point density was insufficient. To maximize returns on the target surface, the targets were painted flat white providing more high intensity returns over a larger surface area. Because the ground control targets are flat, they must be scanned perpendicularly for the best data coverage and most accurate returns.

If there are insufficient returns on the target surface, it is difficult to estimate the center of the target which is used to assess the accuracy of the point cloud. Other shapes, such as round or cylindrical targets that can be scanned from any direction, could be evaluated as the target center could be modeled more accurately even if the entire target was not scanned. A prototype spherical target was tested during the Ledgewood survey in May 2015 (Figure A-2). This inflatable beach ball covered with aluminum foil was consistently visible in the point cloud and

provided results comparable to or better than the large metal targets; however, more development effort is needed to ensure the positional stability of the target under windy conditions.

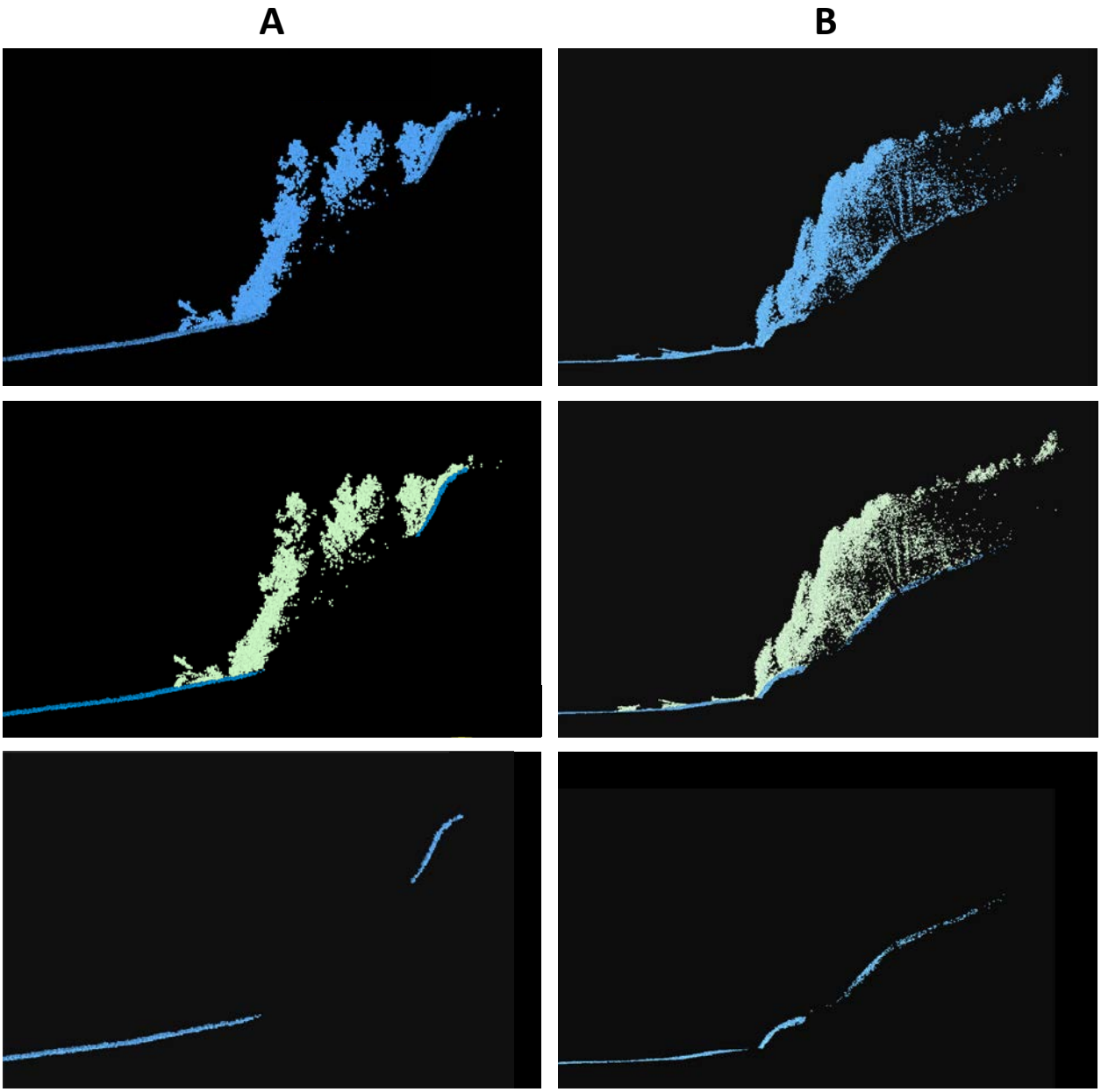

Figure A-1: Lidar point cloud cross-sections for vegetated bluffs using the first vs. last returned laser pulse. The ground surface resolution through dense bluff vegetation is lower using (A) the first than (B) the last returned laser pulse; (top) unclean point cloud, (middle) vegetation (green) and ground surface (blue), (bottom) clean point cloud with only ground surface remaining

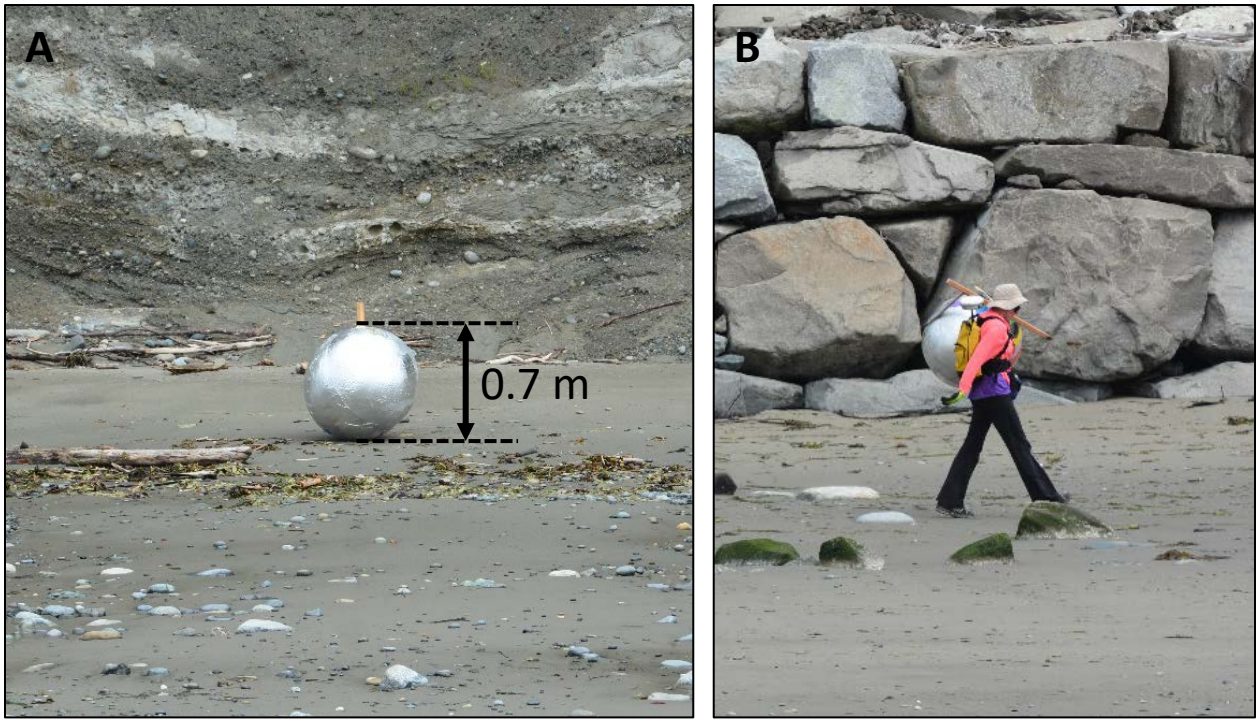

Figure A-2: Photos of prototype spherical ground control target: (A) target set up on the beach during the Ledgewood survey; (B) ground-based surveyor carrying target to another location

Augmenting boat-based lidar with other techniques would enable more complete coastal mapping, especially of barrier beaches, which would be useful for performing full-scale change analysis. Due to the look angle of the boat-based lidar scanning the beach from offshore, large gaps may be present in the point cloud data due to the morphology of the coastal landscape. The largest gaps typically occur over the backshore platform between the beach face and bluff that cannot be seen by the laser scanner. Though it was beyond the scope of this project, additional ground-based GPS data could be collected to fill these gaps by walking cross-shore profiles or alongshore contours that would enable an accurate interpolation of the beach surface where no lidar data is present.

Cobble cam

There are a variety of photogrammetric methods from which grain size information can be extracted. Initially, an automated method developed by Daniel Buscombe to extract grain size distributions from the photographs was applied (Buscombe, 2008). This method fits ellipsoids to individual grains based on the autocorrelation coefficients between pixel intensity. This automated tool was chosen because it offers a fast and efficient method to extract data from sediment photographs. The user defines the reference length in the photograph for each picture, but the rest of the process is automated and completed in MATLAB. However, it was found that this tool does not accurately calculate the grain size distribution for sediment samples with a bimodal grain size distribution or in areas where barnacles and organic matter are present (Figure A-3). For this reason, the point count tool developed by Ian Miller from Washington Sea Grant was applied to process the photographs. Miller's method requires significantly more work and time by the user, as individual grain axes must be traced manually, but it proved to be more

robust and allows the user the ability to distinguish between actual sediment and other objects common along Puget Sound beaches (barnacles, sea weed, shells, etc.).

Figure A-3: Example beach types that present challenges when using automated tools to process sediment grain size photographs; (A) occurrence of large cobbles and sand together results in bimodal grain size distribution, (B) excessive organic matter covering surficial sediments makes it difficult to distinguish individual grains

To achieve the best results when processing digital photos of sediment grain size, as little substrate as possible should be covered by the reference scale and picture label. The scale of reference should go toward the center of the photograph, as to avoid distortion, while the photo label can go toward the edge so that it does not cover as much sediment. As this was our first experience collecting photos for sediment grain size data using cobble cam techniques, the reference scale was often placed near the edge of a photograph.

Where bi-modal sediment samples are present, photographs should be taken at various distances from the substrate. As a rule of thumb, photographs should be taken from a distance that positions approximately 100 grains along the horizontal edge of the field of view. For mixed sediment samples, it is suggested that photographs be taken (1) close to the substrate, capturing a distance of 100 of the smaller grains along the horizontal edge, and (2) further away from the substrate, capturing a distance of 100 of the larger grains along the horizontal edge. This way, the smaller grains can be resolved during data processing without sacrificing a wider sample area for the larger gravels and cobbles present.

For this project, sediment grain size photos were collected along transects chosen in the field spaced roughly every kilometer or when there was a significant change in beach texture. Transects were numbered chronologically according to the order in which the photos were collected. When analyzing the data, it was difficult to draw conclusions about sediment patterns within a drift cell due to the jumbled order of the transect numbers with respect to their geographic locations. To rectify this, the transects within each survey site were re-numbered from south to north (or from west to east) so that their representation in plots and figures was more logical. It is suggested that in future studies, the transects be labeled according to their location prior to data collection in the field.

Along each cobble cam transect, sediment photographs were taken every 0.5-m change in elevation or more frequently in areas where the substrate character varied, starting with the lowest elevation exposed. In order to repeat the survey and evaluate change over time, either each individual point must be staked out using GPS equipment to take photographs in the same locations or a list of the elevations collected for each transect must be consulted to repeat photographs at the same elevations, since these varied from transect to transect.

For future surveys, it is suggested that for each survey site, samples (photos) be taken at the same, standard elevations for each transect (e.g., 0.0 m, 0.5 m, 1.0 m, 1.5 m, etc.) and more frequently in areas where the substrate varies. While the exact elevations will vary between each survey site depending on beach width and slope, standardizing the photos at every whole or half meter would make the survey more repeatable and allow for better comparison of alongshore sediment variation. This method requires accurately georeferenced positioning from the base station in real-time.

Recommended citation for Appendix A

Weiner, H.M., G.M. Kaminsky, and M. Gostic, 2018. Mapping Bluffs and Beaches of Puget Sound to Quantify Sediment Supply, Estuary and Salmon Restoration Program Learning Project Final Report, Appendix A: Lessons Learned. Shorelands and Environmental Assistance Program, Washington Department of Ecology, Olympia, Washington, Publication #18-06-008, pp. 49-55.

References

Buscombe D., 2008. Estimation of grain-size distributions and associated parameters from digital images of sediment, *Sedimentary Geology*, 210, 1-10.

This page is purposely left blank

Appendix B. Image Archive

The selected set of images provided with this report were collected during the boat-based lidar and ground-based GPS topography surveys. High-resolution digital photographs were taken of the shoreline from the boat during the laser scan of each survey site and serve as the best documentation of site condition during data collection. The photos aid in interpretation of the lidar point cloud during data processing and provide a qualitative assessment of shoreline morphology. Images that illustrate various shoretypes (e.g., bare bluff, vegetated bluff, residential-backed beaches and bluffs) observed at each survey site were selected. Table B-1 gives an overview of the photos included in the image archive.

Photomosaics were generated by joining overlapping photographs together using Autopano Giga Pro v3.0.3, an image stitching software that accounts for a moving reference point. Photomosaics generally span a few hundred meters of shoreline, depending on the quality of the successive photographs and whether distortion is introduced. A subset of the photomosaics created for each survey site has been selected for the image archive to provide examples of the various coastal landscapes surveyed.

Digital photographs of beach sediments were collected for an assessment of sediment grain size using “cobble cam” techniques. Photos were taken at several locations along kilometer-spaced transects at 0.5-m elevation intervals, aiming to have approximately 100 grains along the horizontal edge of the frame. A set of these images for selected profiles showing a variety of beach textures have been included in the image archive.

Photos of survey activities are also provided. Images showing the GPS base station, ground-based surveyors collecting beach topography data, boat-based surveyors collecting lidar data, ground control target set-up, and cobble cam data collection illustrate survey methodology and further demonstrate project conditions.

Images are provided in a single ZIP file with no internal folders using the file naming convention: location, date (MMDDYY), subject (e.g., Camano_090915_Bluff). Photomosaics are identified with the additional subject name, “panorama”. Cobble cam photos were collated by profile and labeled with the actual NAVD88 elevation in the upper left-hand corner. Note that the elevation label and the profile number listed in the file name may not correspond with the chalkboard label in the photo, as the elevations measured in the field were preliminary and the profiles were re-ordered geographically during data processing.

Table B-1: Inventory of photos included in the image archive provided with this report

Survey site	GPS Base Station	Boat	Beach	Bluff (bare)	Bluff (grassy)	Bluff (vegetated)	Ground Control Targets	Bluff-top Houses	Beach Houses	Overhanging Vegetation	GPS Topo Data Collection	Cobble Cam Photos	Shoreline Panoramas
Agate Beach						X							1
Camano Island			X			X		X	X	X	X	X	
Cattle Point			X	X		X	X		X		X		1
Dabob Bay		X	X			X	X			X			
Dungeness			X	X	X				X				2
Edgewater Beach			X						X	X		X	4
Guemes Island	X	X	X	X		X	X		X	X			1
Jackson Beach	X	X		X			X				X	X	
Ledgewood		X		X		X					X	X	
Marrowstone Island		X		X		X		X					
Maury Island						X			X			X	
Point Roberts		X	X	X		X			X				2
Point Whitehorn		X	X		X	X		X	X				
Seahurst Park								X	X	X			4
Useless Bay			X	X	X	X		X	X			X	
Whidbey Island			X	X	X		X	X	X				5

Appendix C. Digital Elevation Models

High resolution, 0.5-m digital elevation models (DEMs) of the beach and bluff ground surface were produced for each of the 16 survey sites listed in Table 5. The DEMs were derived from boat-based lidar data collected between October 2013 and May 2016, with concurrent ground-based GPS data collected to fill minor gaps or shadows in the lidar. For this project, lidar data cleaning was focused on Tier 1 bluff-backed beaches for the generation of DEMs, the extents of which are shown in Figure C-1. In most cases, additional data was collected at a survey site, usually extending to include the entire drift cell and adjacent Tier 2 or 3 areas, and will be cleaned as time and resources allow. Users are asked to contact CMAP before using the provided DEMs as a newer version may be available.

Ground-based GPS beach topography data were used to ground-truth the lidar and adjustments to the elevation of the lidar data at each site were made accordingly. The accuracy of the cleaned lidar data was assessed by comparing independently surveyed ground control targets with lidar points; when averaged across all survey sites, the lidar data were found to be within 9 cm horizontally and 2 cm vertically, after adjusting the lidar to agree with the ground-based GPS data (12 cm prior to adjustment). The mean (median) point density of the lidar on the beach surface was 9 (7) points per 0.5-m grid cell with greater density achieved on bluff faces of 26 (12) points per 0.5-m grid cell (refer back to Table 6).

The combined topography data were gridded at 0.5 m and interpolated using a Triangulated Irregular Network (TIN) in ArcGIS v10.2. A 10-m interpolation distance around the perimeter of the TIN was used for all survey sites, except for Jackson Beach and Agate Beach where 5-m interpolation was more appropriate for the relatively short scanning ranges and low topographic relief, and Useless Bay and Dabob Bay where 15-m interpolation was used to fill in gaps across the low tide terrace and vegetated bluff, respectively.

Users should be aware that due to the oblique look-angle of the laser scanner, some features may not appear in their entirety in the DEM (i.e., the laser scanner can only acquire returns off surfaces oriented toward the scanner itself and therefore cannot see the back sides of rocks, for example). Furthermore, due to the small grid size, variable terrain, and limited interpolation distance imposed around the perimeters of the data sets, the DEMs are not always continuous. Data gaps are present where no lidar was collected either because of a shadow caused by the morphology or being unable to resolve the ground surface through dense vegetation (Figure C-2).

At some survey sites, the back-beach contains a large accumulation of drift logs, which creates a highly irregular topographic surface with many localized shadows that result in gaps in the point cloud (Figure C-3). Returns on drift logs and vegetation were removed from the gridded surface and the remaining ground surface was interpolated. Further interpolation over gaps in the DEM should be done at the user's discretion. Edge effects may be present at the top of or behind the bluff due to TIN interpolation. Due to issues with gridding near-vertical surfaces, especially those with more than one elevation value such as overhanging bluff tops, the DEM may not reflect the actual topography.

DEMs are provided as a raster in ESRI ASCII grid format (.asc) in Washington State Plane North/South, NAD83 (2011), meters, with elevations relative to NAVD88 (GEOID12B), meters.

WA State Plane North (4601) is used for all survey sites except for Edgewater Beach, which is in WA State Plane South (4602). Projection information is provided as PRJ files. Figures C-4 through C-19 show the coverage and extent of the DEMs created for each survey site. These high-resolution DEMs can be used to analyze bluff recession and beach change over time as more surveys are conducted. Metadata content for each dataset is provided as internal ArcGIS metadata as well as both XML and HTML files using the Federal Geographic Data Committee's (FGDC) Content Standard for Digital Spatial Metadata (CSDGM).

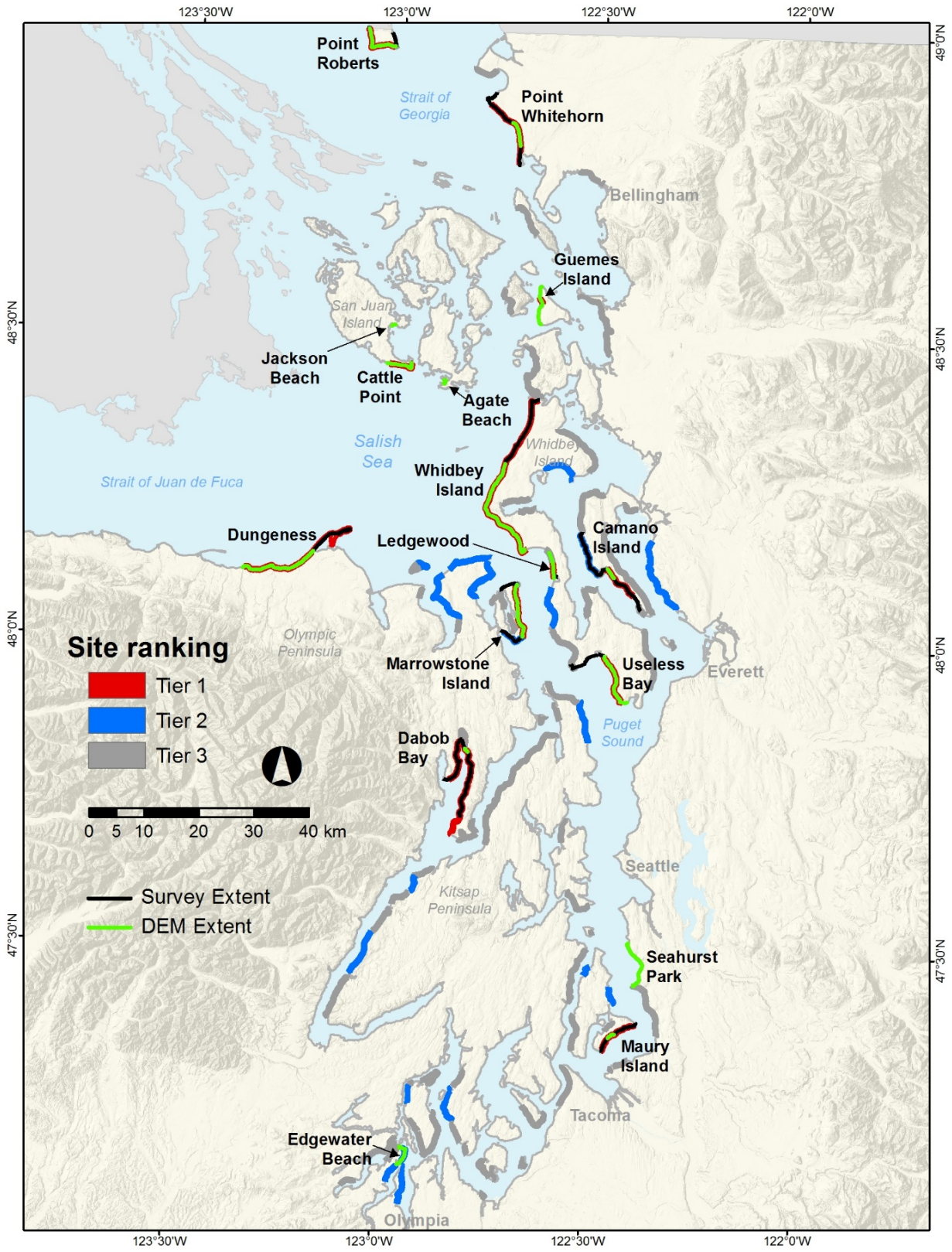

Figure C-1: Map showing location and extents of processed boat-based lidar data used to create DEMs for this project

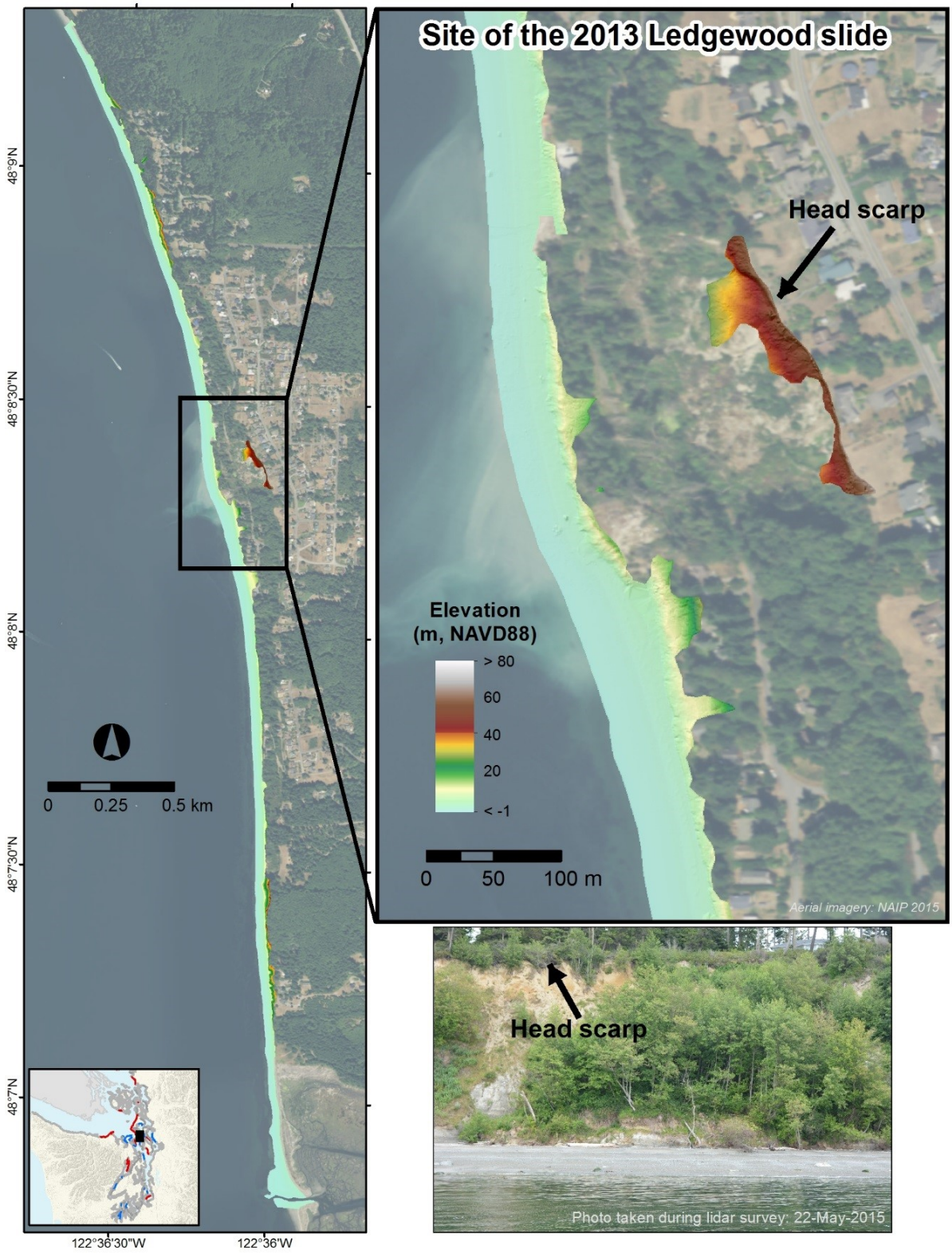

Figure C-2: Example showing where boat-based lidar DEM is not continuous due to dense vegetation and coastal morphology at the site of the Ledgewood bluff slide that occurred in April 2013; DEM resolution is 0.5 m

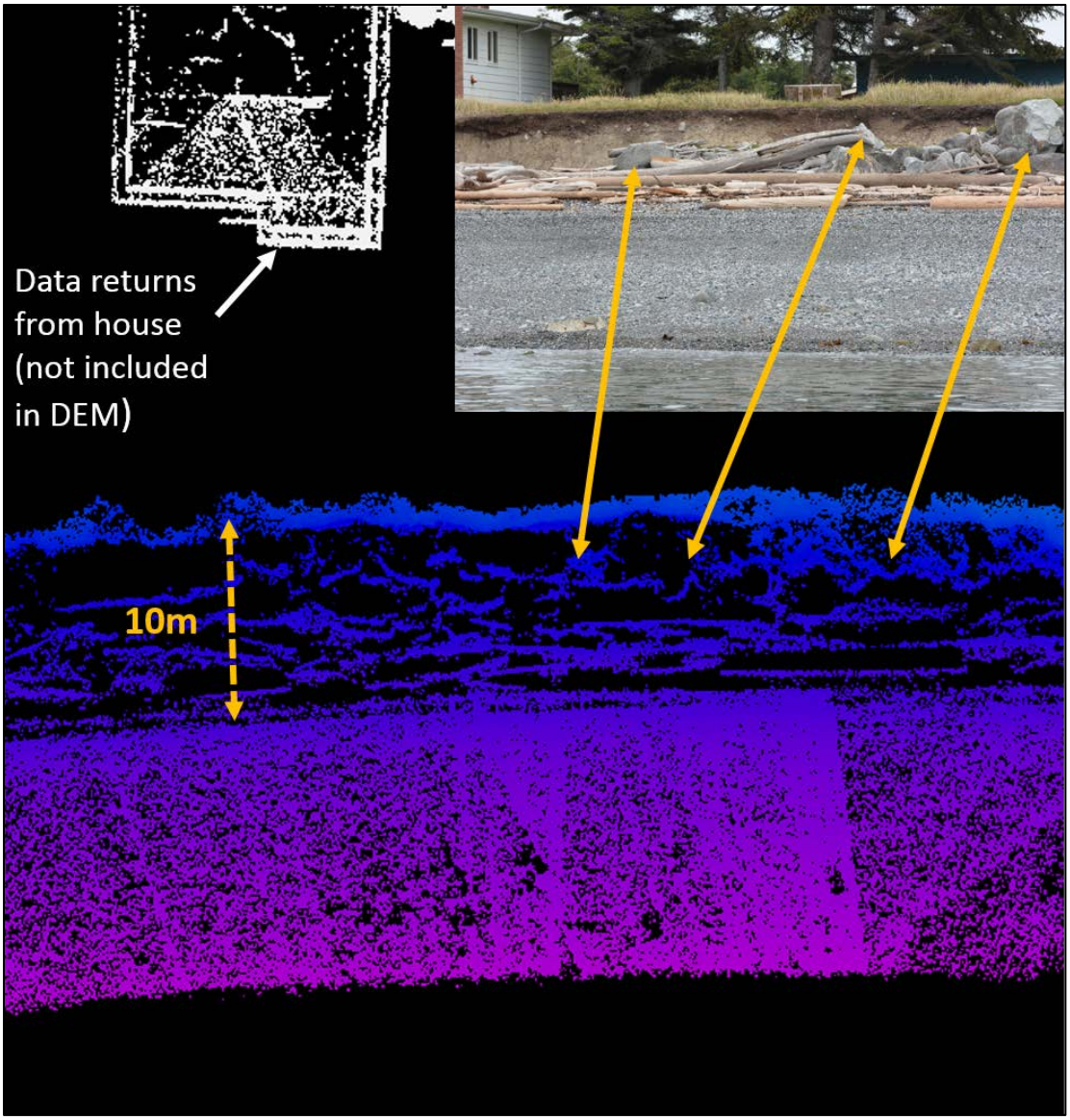

Figure C-3: Example from Agate Beach of variable point distribution due to an area of large woody debris spanning 10 m in width on the upper beach creating shadows in the lidar data; returns from drift logs were excluded from the gridded data prior to DEM generation

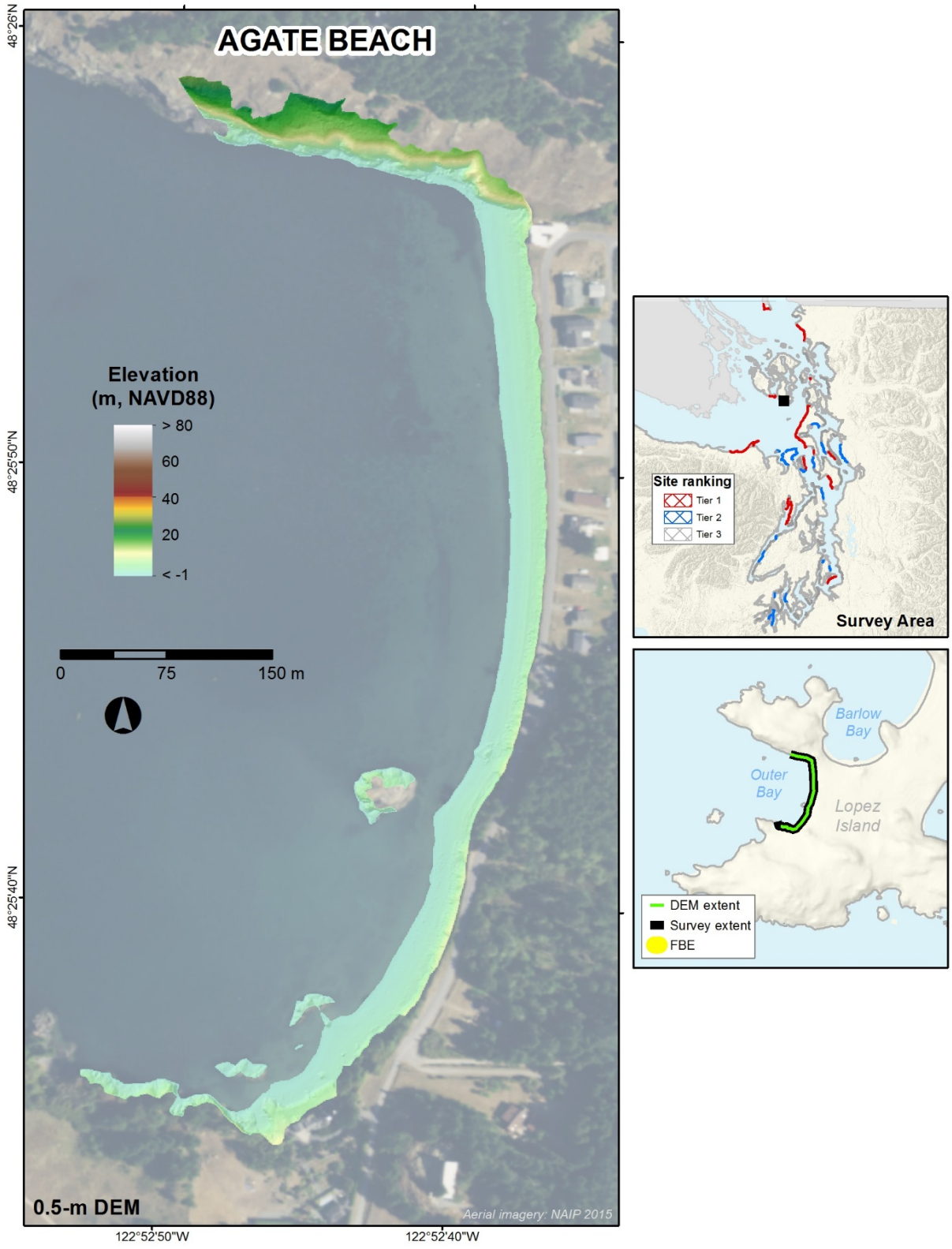

Figure C-4: Map showing boat-based lidar DEM for the Agate Beach survey site, located on Lopez Island; DEM resolution is 0.5 m

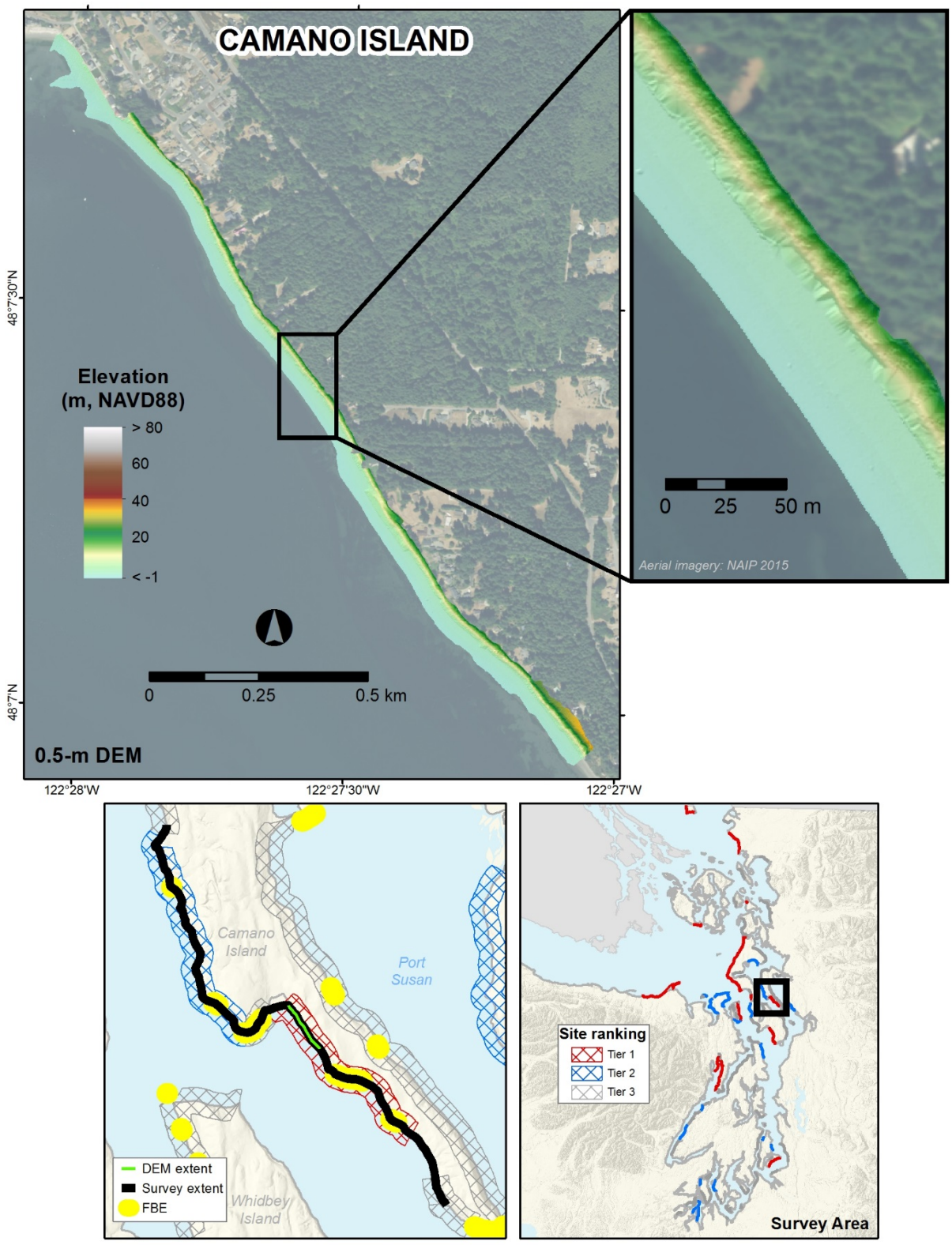

Figure C-5: Map showing boat-based lidar DEM for the Camano Island survey site; DEM resolution is 0.5 m

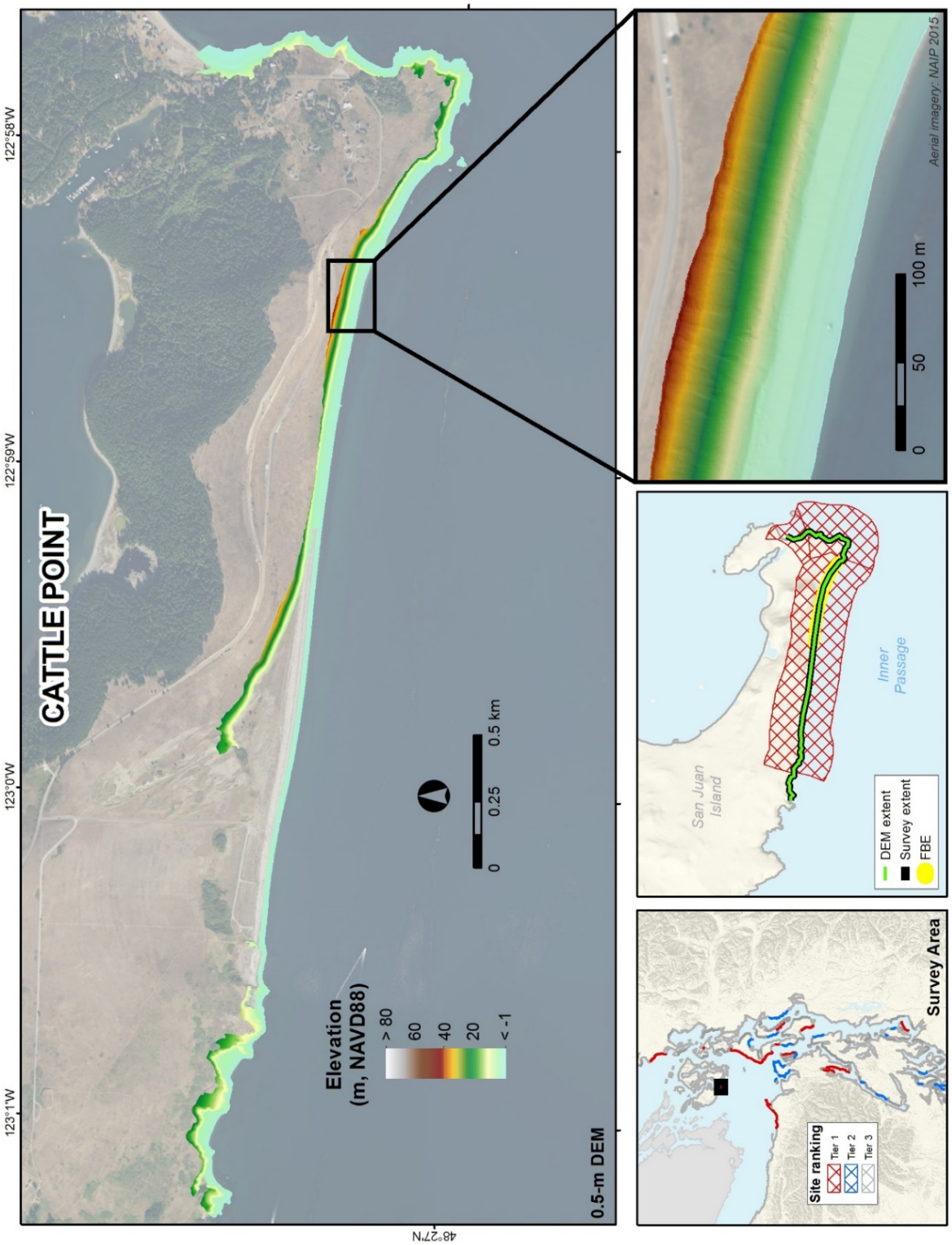

Figure C-6: Map showing boat-based lidar DEM for the Cattle Point survey site, located on San Juan Island; DEM resolution is 0.5 m

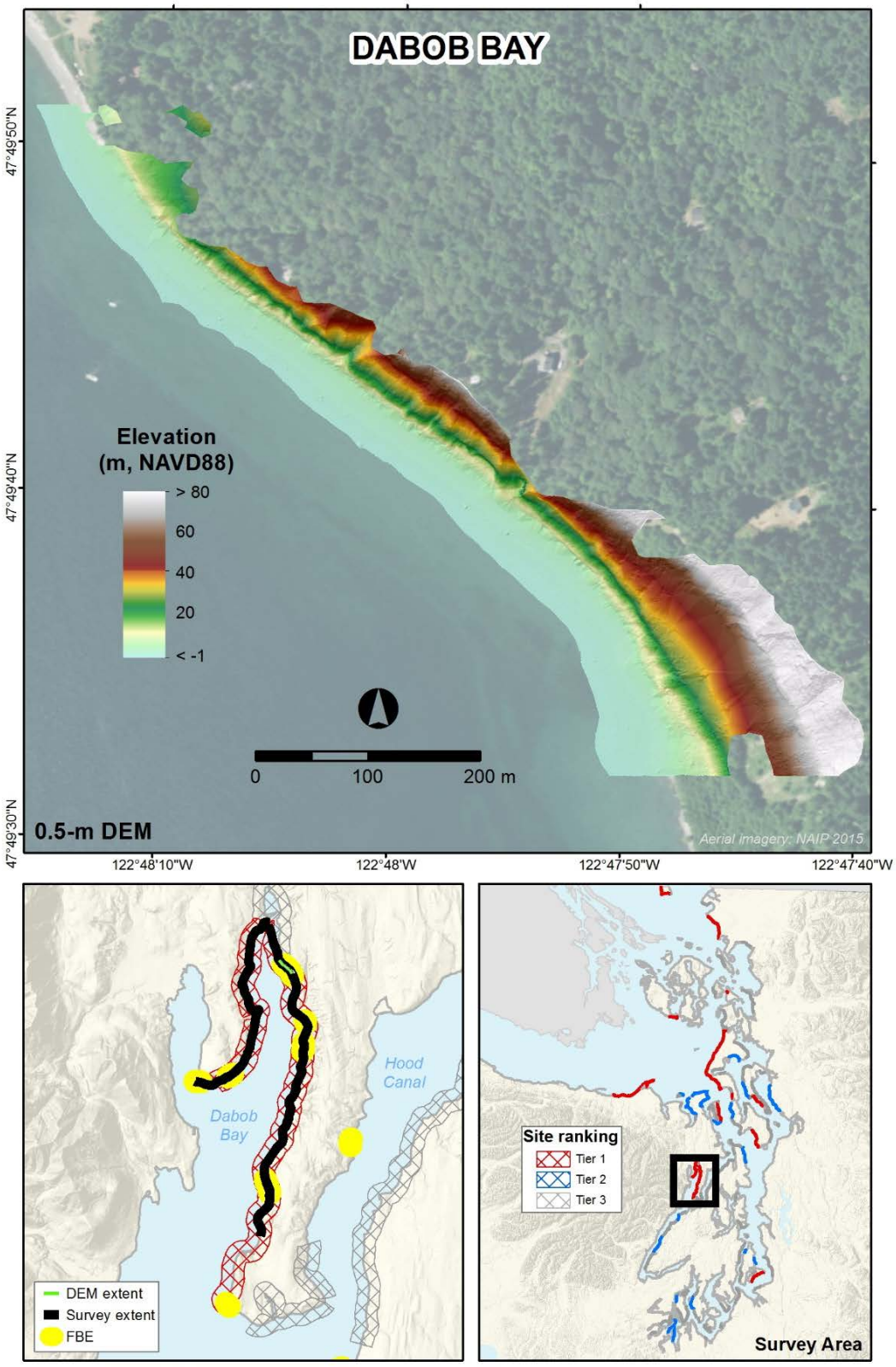

Figure C-7: Map showing boat-based lidar DEM for the Dabob Bay survey site; DEM resolution is 0.5 m

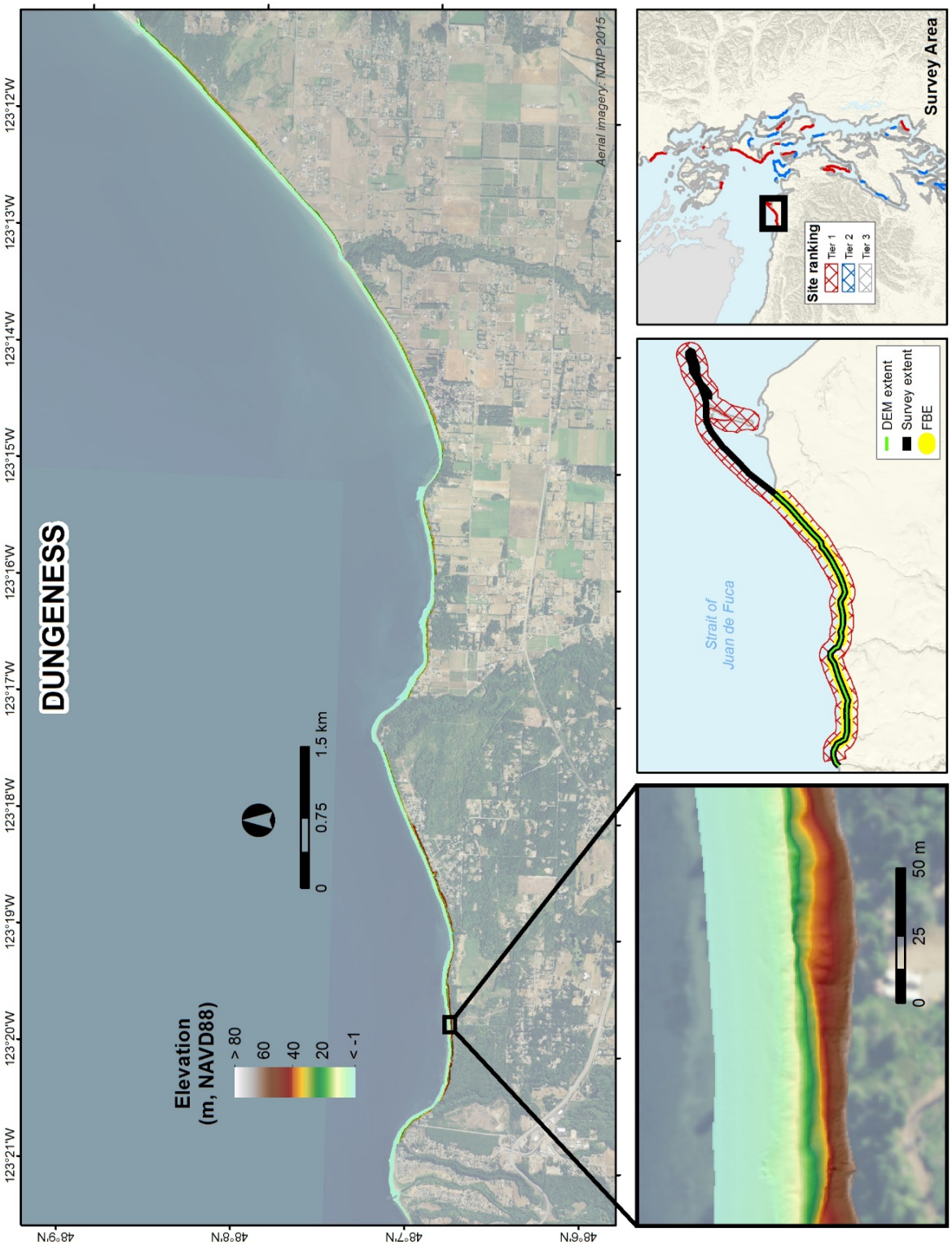

Figure C-8: Map showing boat-based lidar DEM for the Dungeness survey site; DEM resolution is 0.5 m

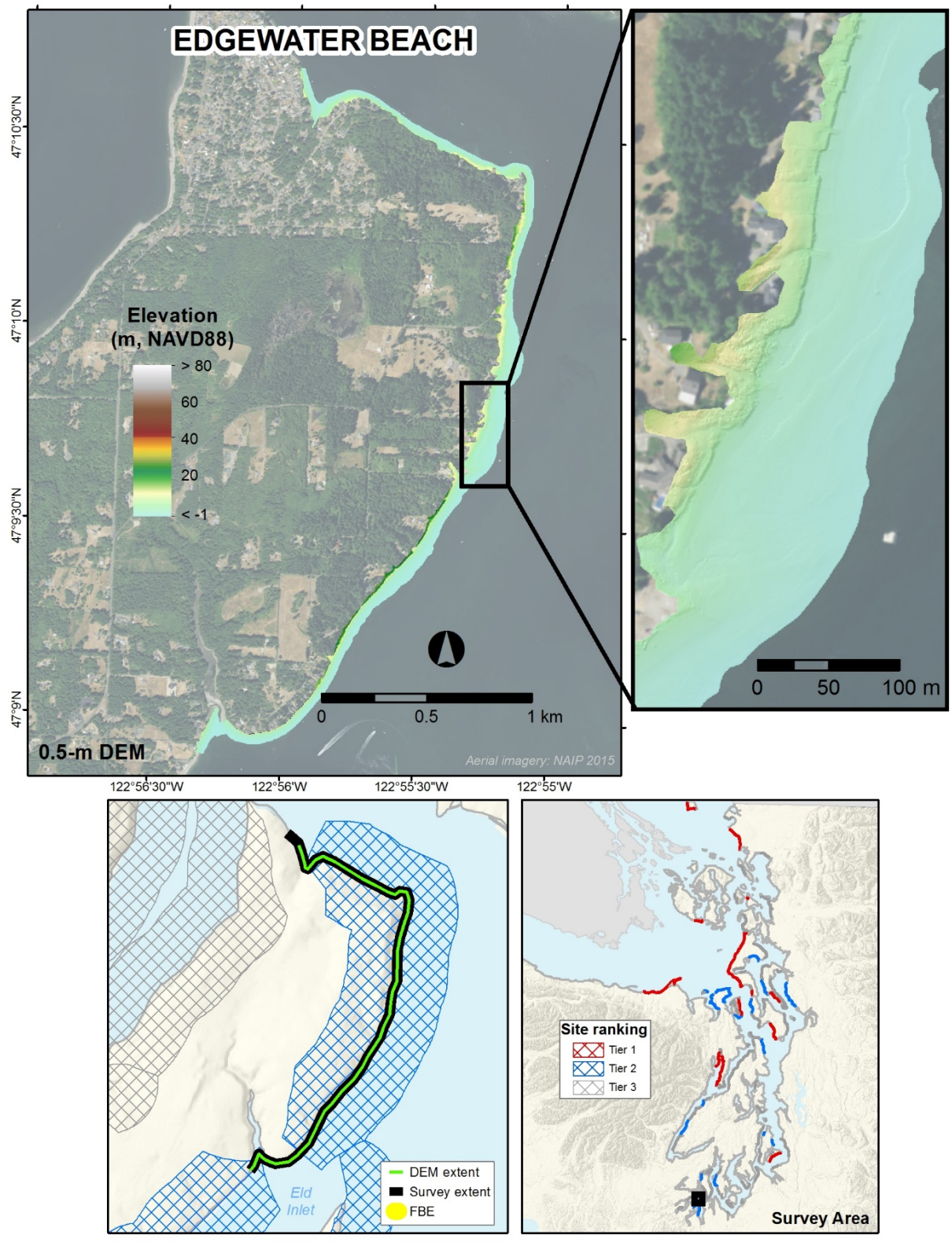

Figure C-9: Map showing boat-based lidar DEM for the Edgewater Beach survey site, located near Olympia; DEM resolution is 0.5 m

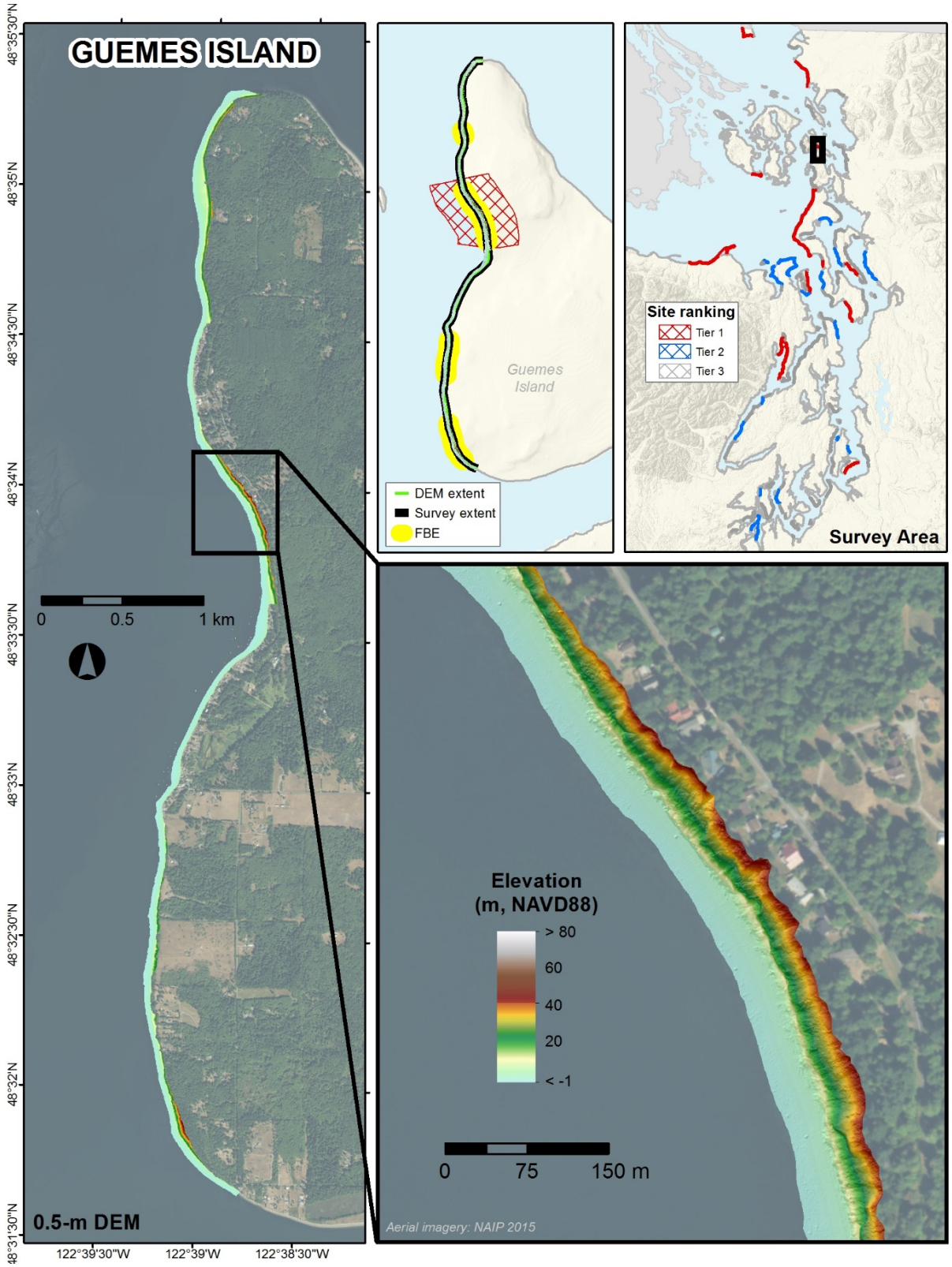

Figure C-10: Map showing boat-based lidar DEM for the Guemes Island survey site; DEM resolution is 0.5 m

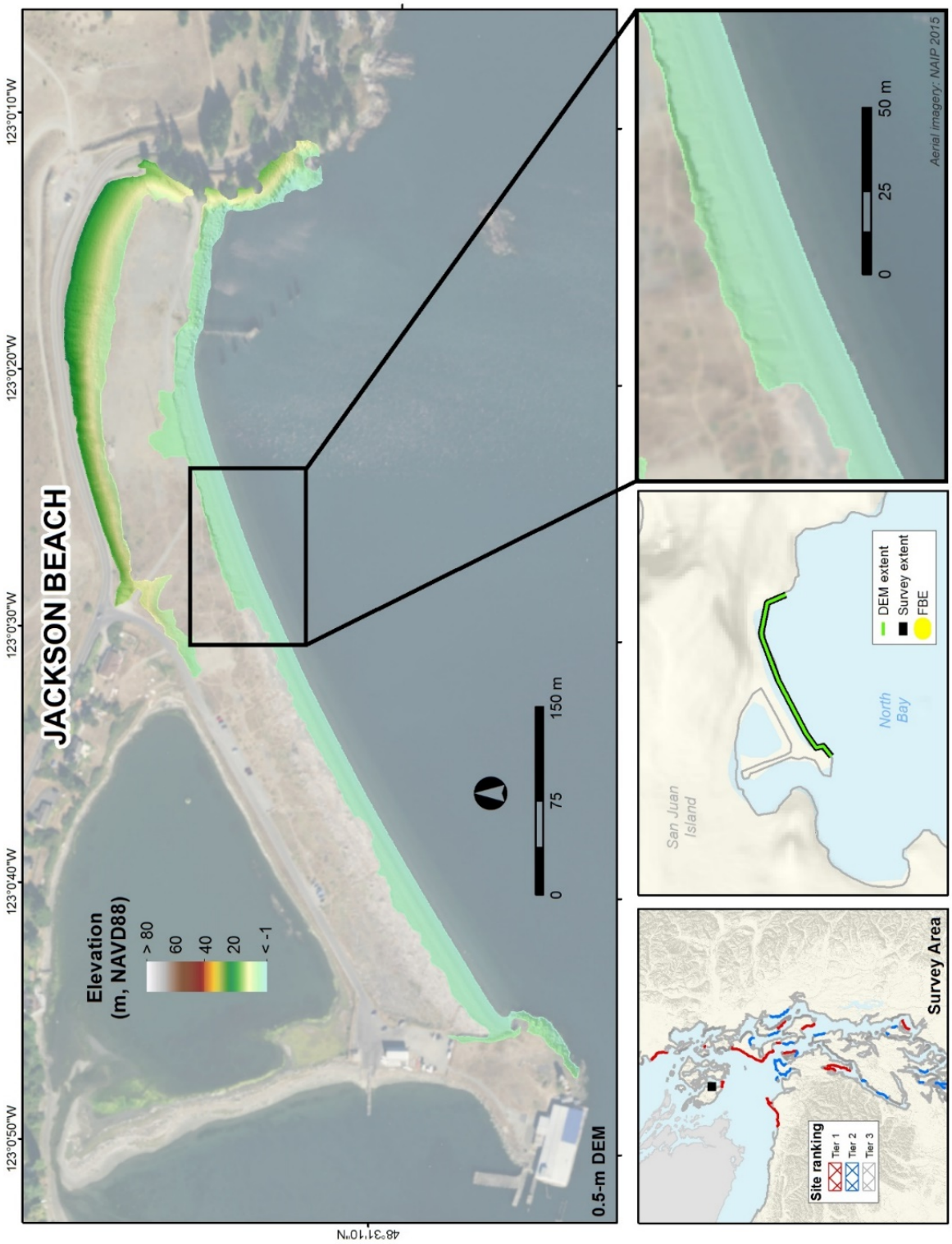

Figure C-11: Map showing boat-based lidar DEM for the for the Jackson Beach survey site, located on San Juan Island; DEM resolution is 0.5 m

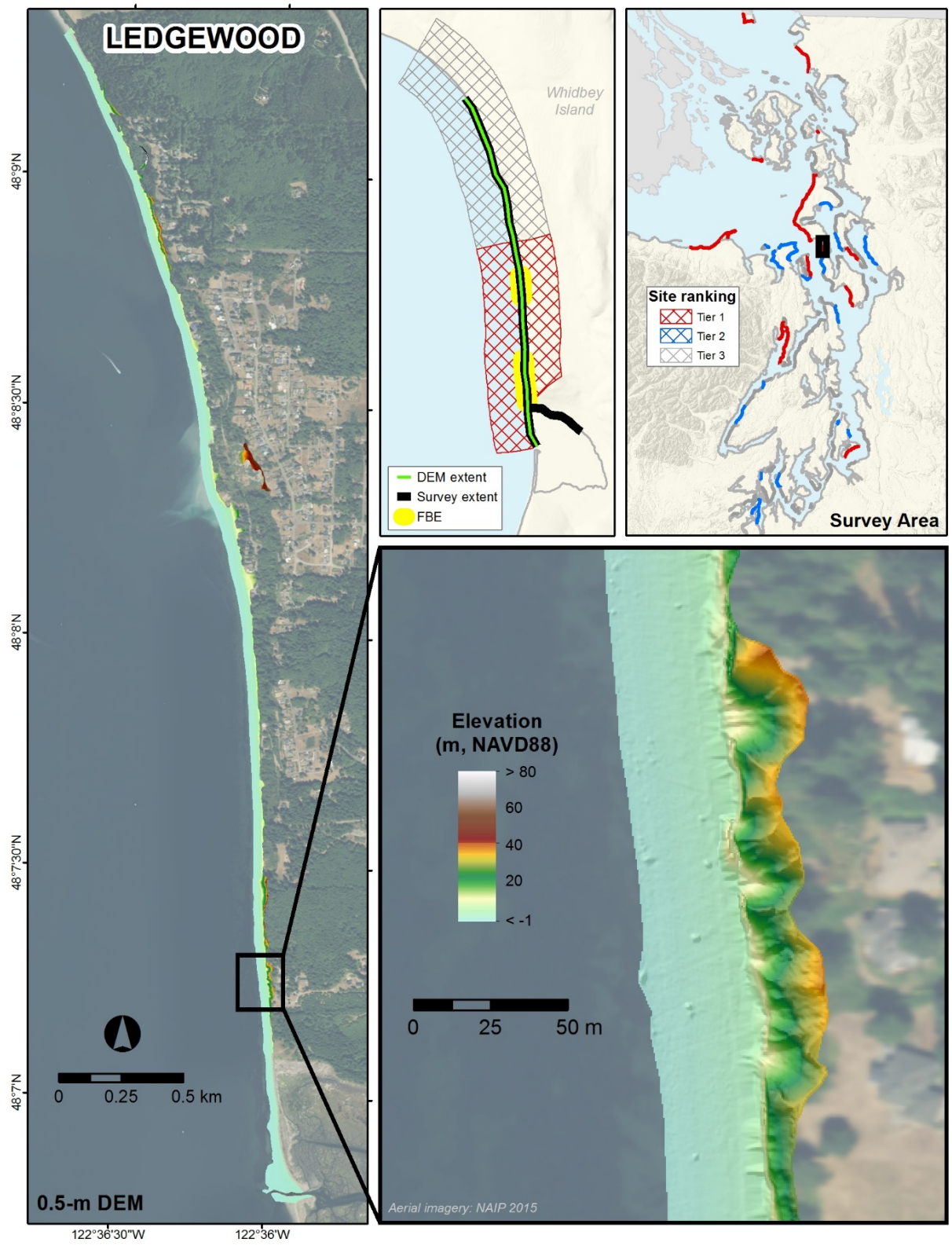

Figure C-12: Map showing boat-based lidar DEM for the Ledgewood survey site, located on Whidbey Island; DEM resolution is 0.5 m

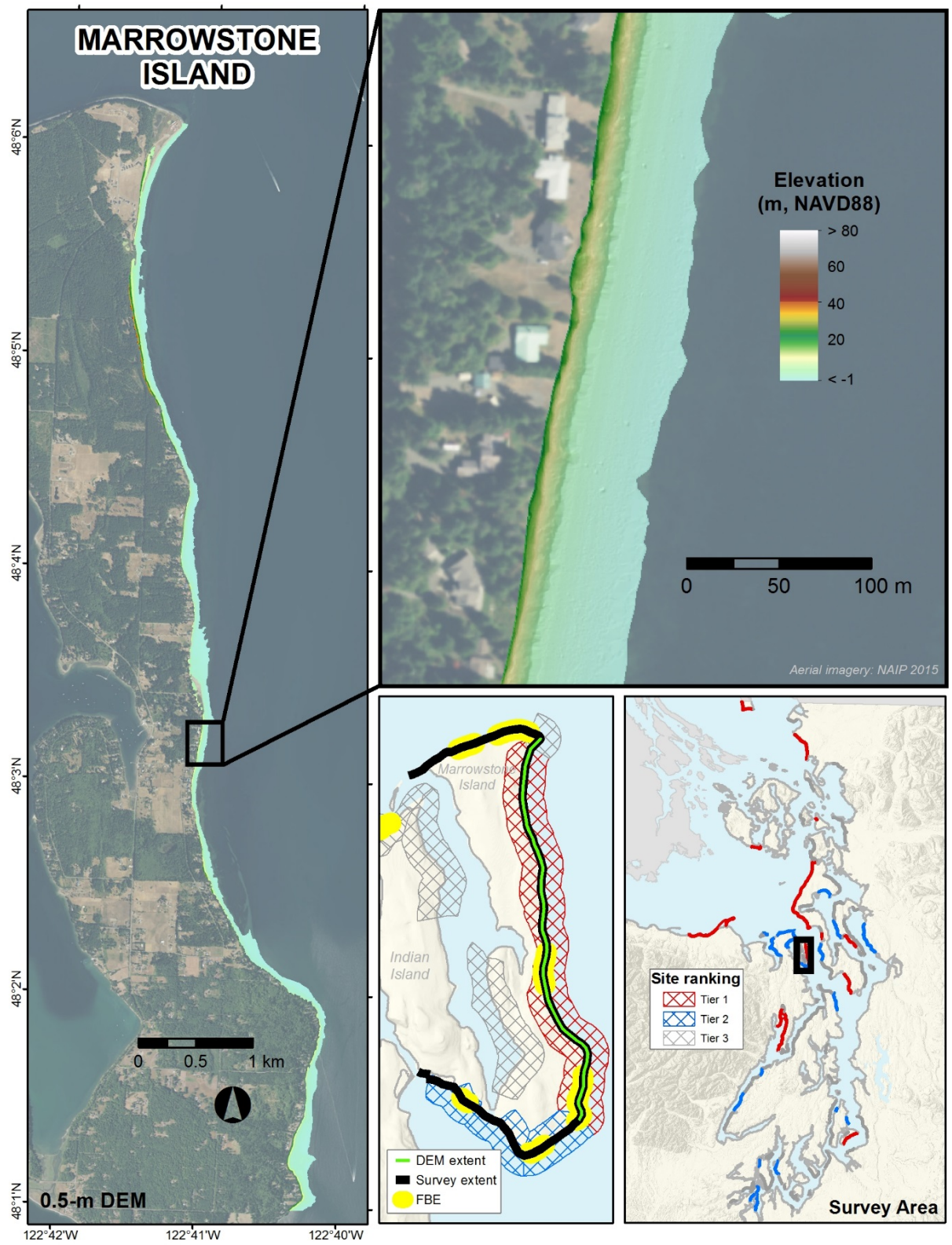

Figure C-13: Map showing boat-based lidar DEM for the Marrowstone Island survey site; DEM resolution is 0.5 m

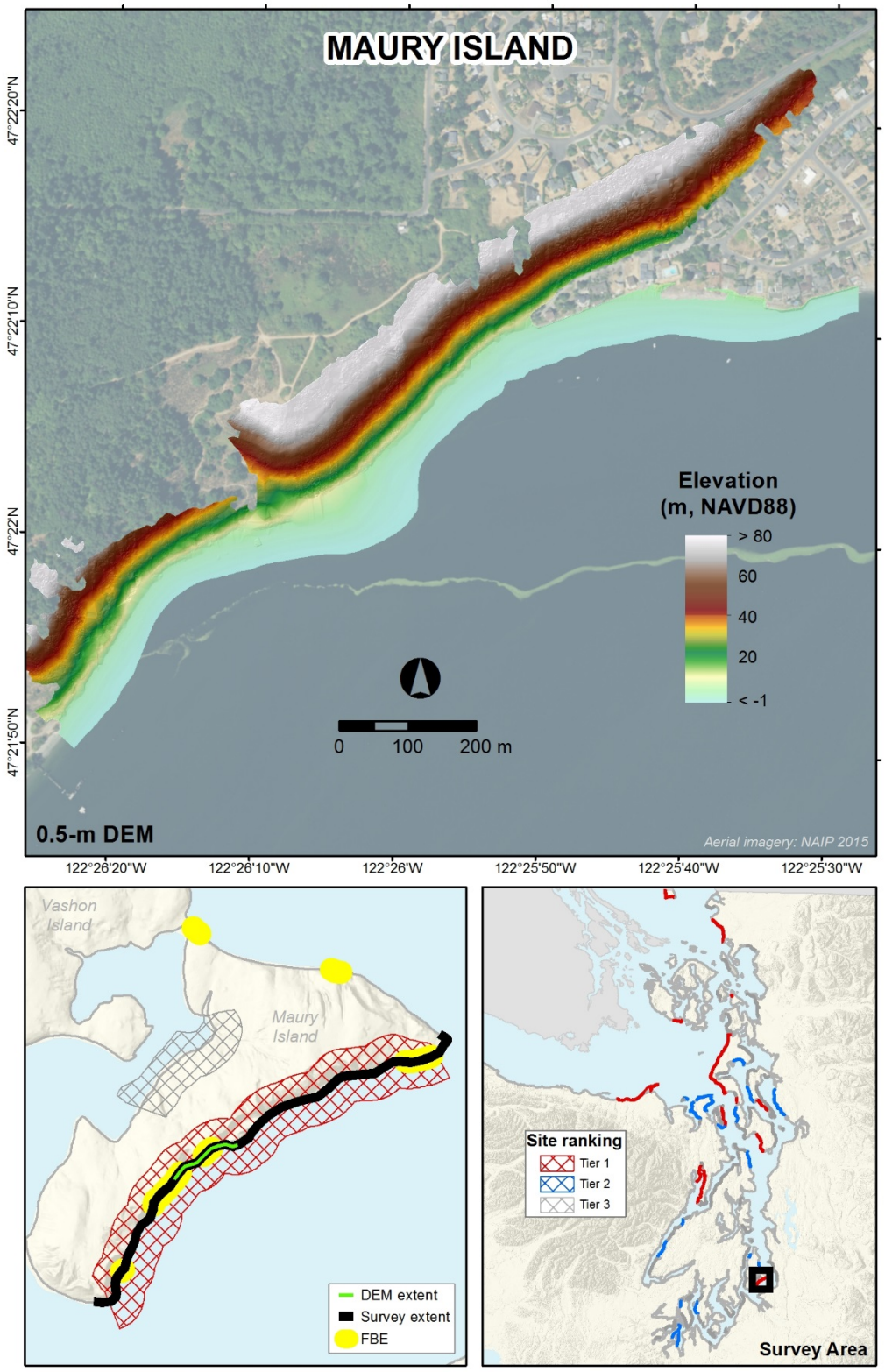

Figure C-14: Map showing boat-based lidar DEM for the Maury Island survey site; DEM resolution is 0.5 m

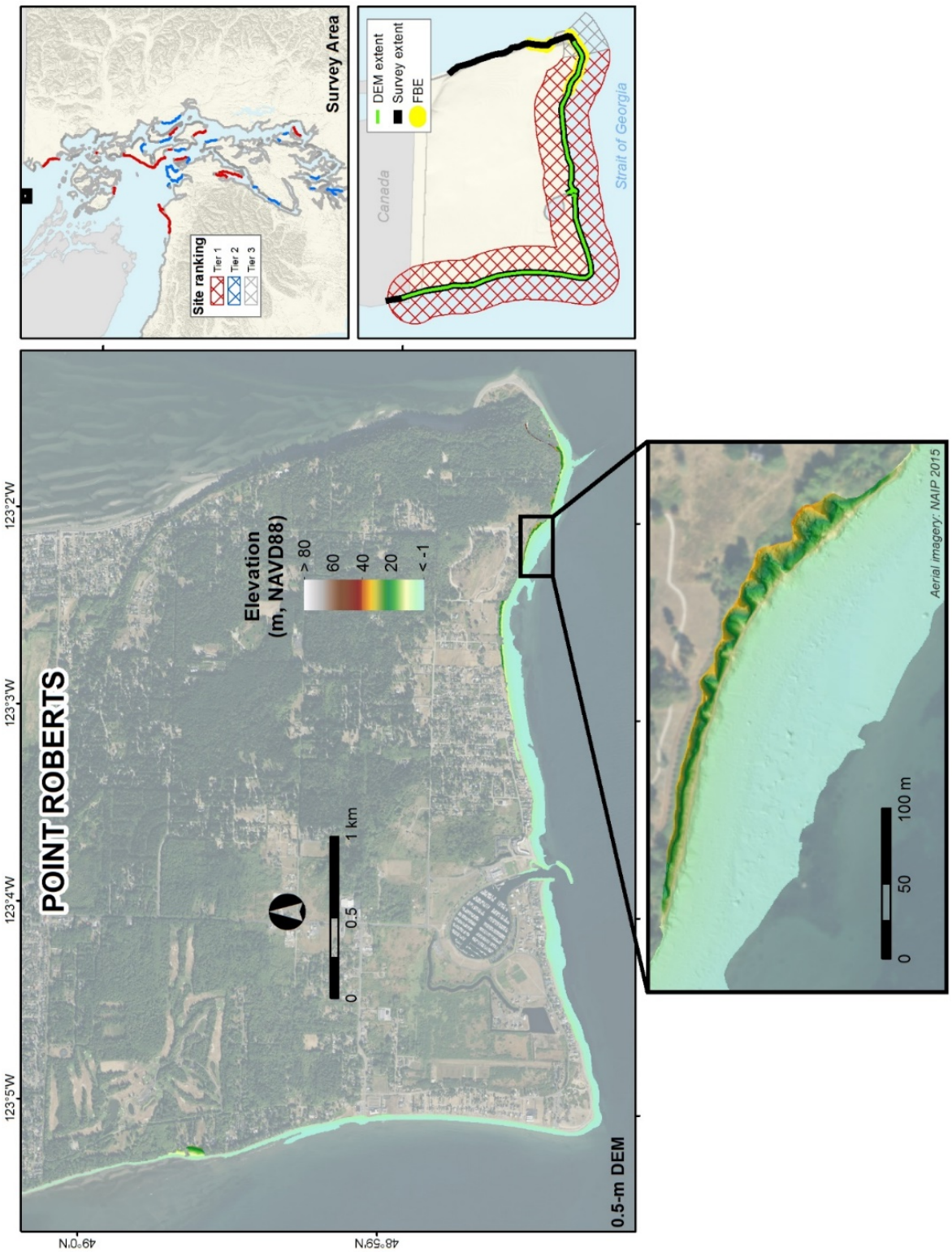

Figure C-15: Map showing boat-based lidar DEM for the Point Roberts survey site; DEM resolution is 0.5 m

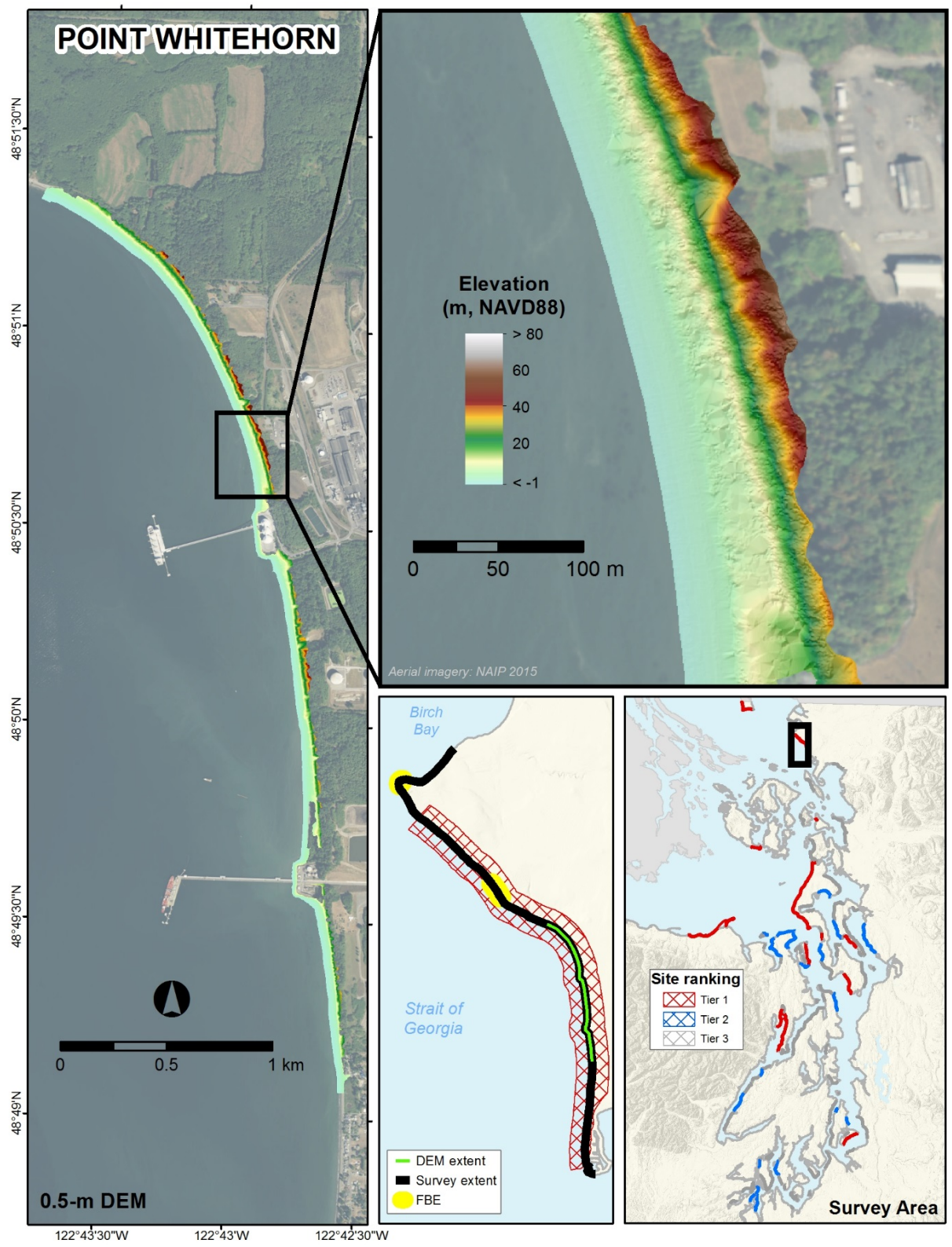

Figure C-16: Map showing boat-based lidar DEM for the Point Whitehorn survey site; DEM resolution is 0.5 m

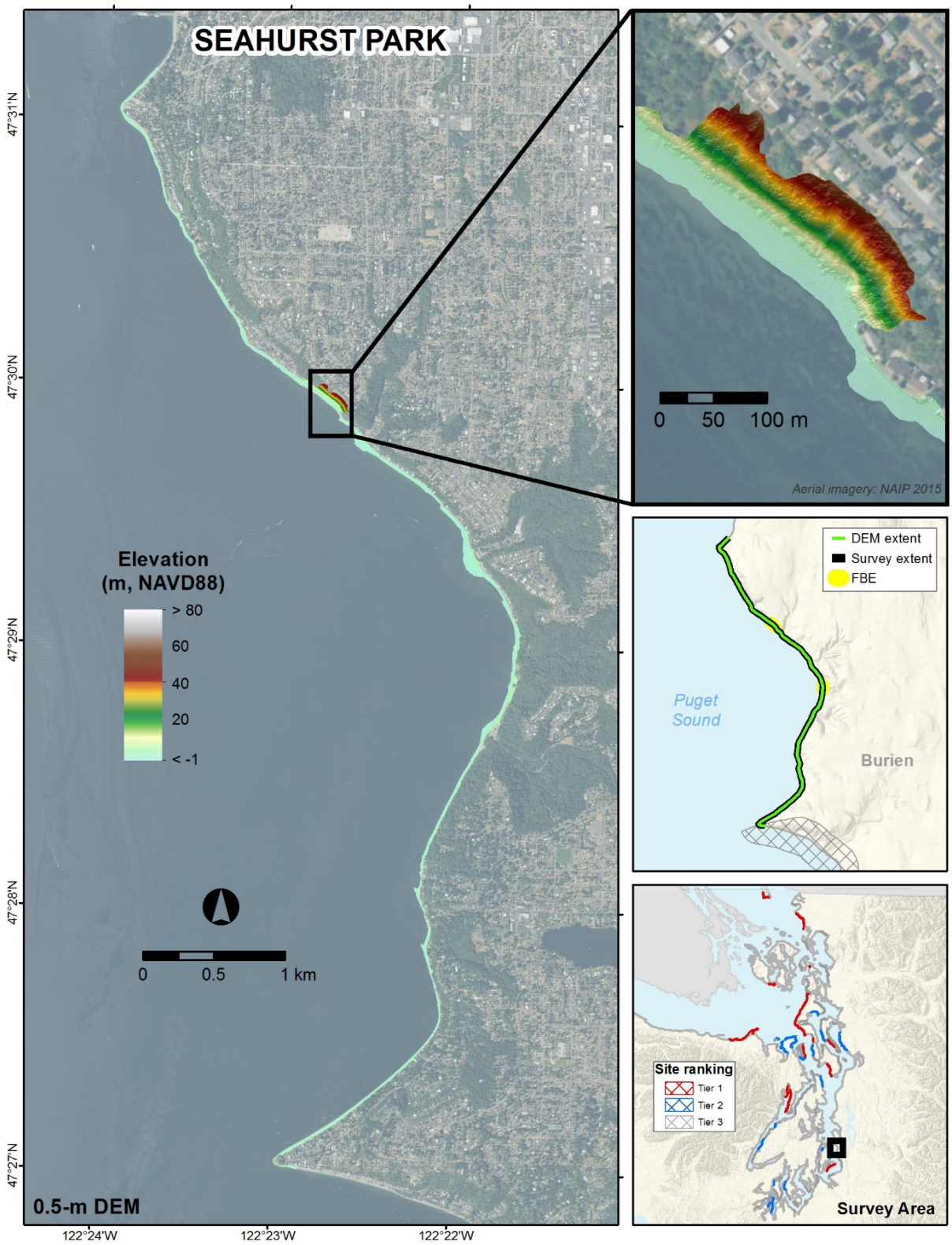

Figure C-17: Map showing boat-based lidar DEM for the Seahurst Park survey site, located near Burien; DEM resolution is 0.5 m

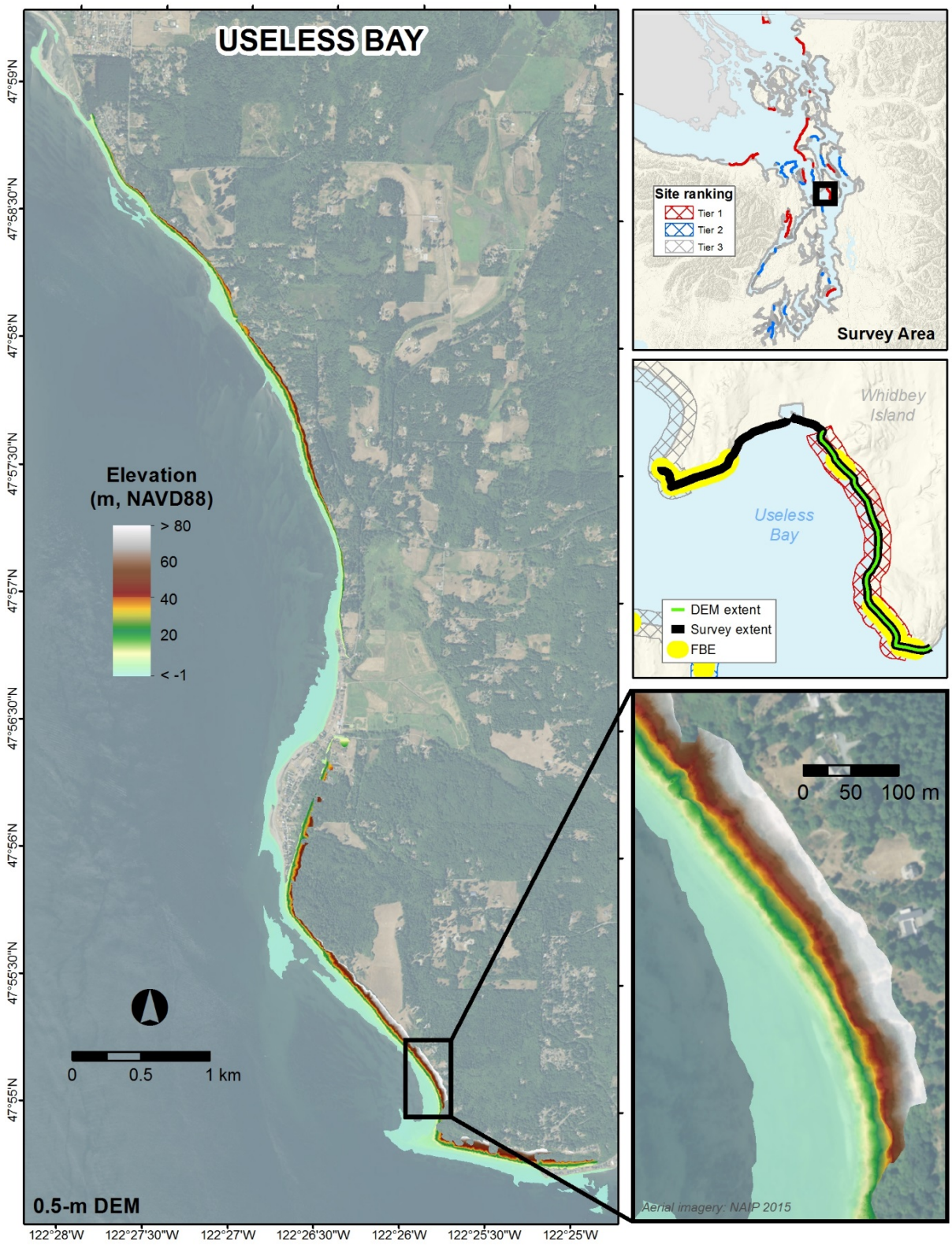

Figure C-18: Map showing boat-based lidar DEM for the Useless Bay survey site; DEM resolution is 0.5 m

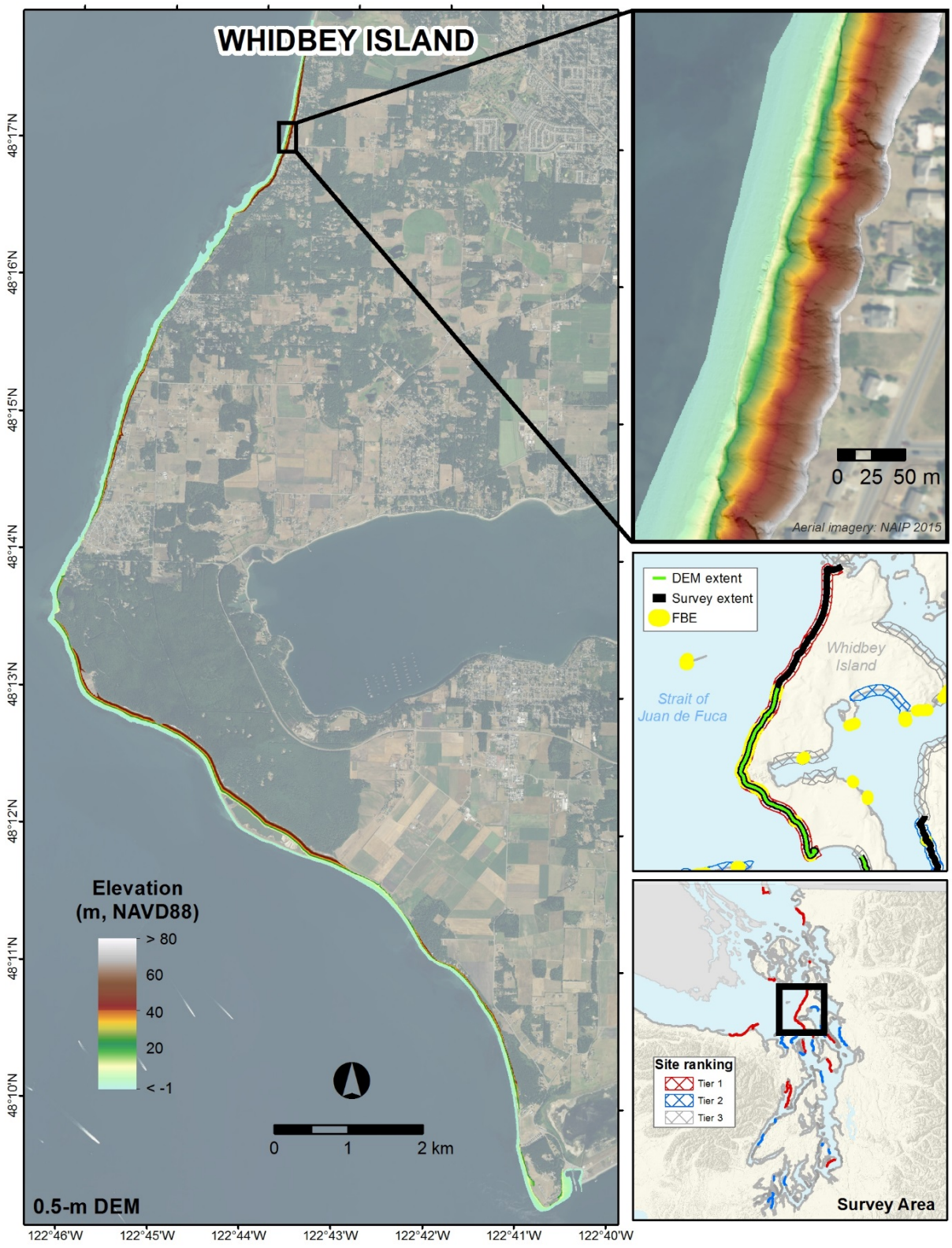

Figure C-19: Map showing boat-based lidar DEM for the Whidbey Island survey site; DEM resolution is 0.5 m

This page is purposely left blank

Appendix D. Sediment Grain Size

Sediment grain size data were collected at 13 survey sites along 108 cross-shore transects, spaced approximately 1-km apart, using the "cobble cam" technique whereby digital photographs of the beach substrate are analyzed as described in the Data Processing section of the report. Photographs were captured at 0.5-m elevation intervals along each transect or more frequently where there were significant changes in substrate (roughly 4-7 samples per transect). A MATLAB-based algorithm was used to determine the median grain size (D_{50}) of the substrate in each image and then categorized according to size class per the Wentworth classification scale shown in Figure D-1.

A summary of the sediment grain size data collected is provided as a set of figures in this appendix, ordered alphabetically by survey site (Figure D-2 through D-13). The first figure for each survey site (A) shows the locations of the cobble cam photographs collected. The second figure for each site (B) shows the alongshore distribution of the median grain size (D_{50}) for each sediment sample collected per transect. The third figure (C) shows the cross-shore distribution of median sediment grain sizes (D_{50}) for each transect. Where the elevation of a continuous cross-shore profile was collected at or nearby the cobble cam transect, it is displayed on the plot as a thick black line. In some cases, the profile may be offset from the sample locations.

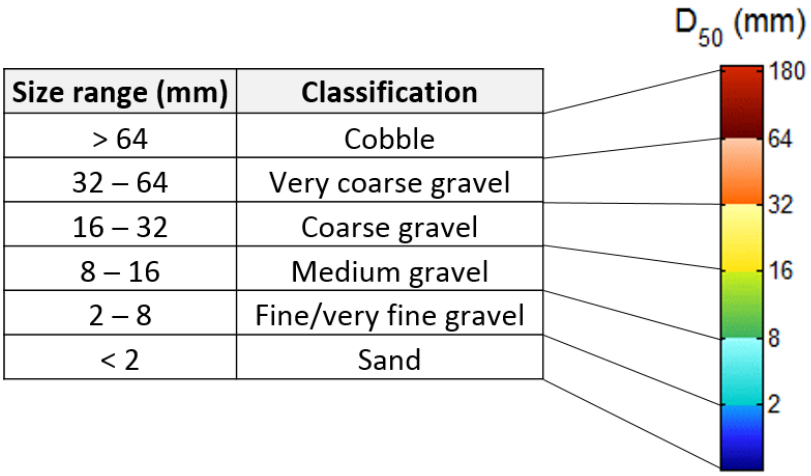

Size range (mm)	Classification
> 64	Cobble
32 – 64	Very coarse gravel
16 – 32	Coarse gravel
8 – 16	Medium gravel
2 – 8	Fine/very fine gravel
< 2	Sand

Figure D-1: Wentworth classification for sediment grain size data as it relates to the color scheme used in the cross-shore distribution plots

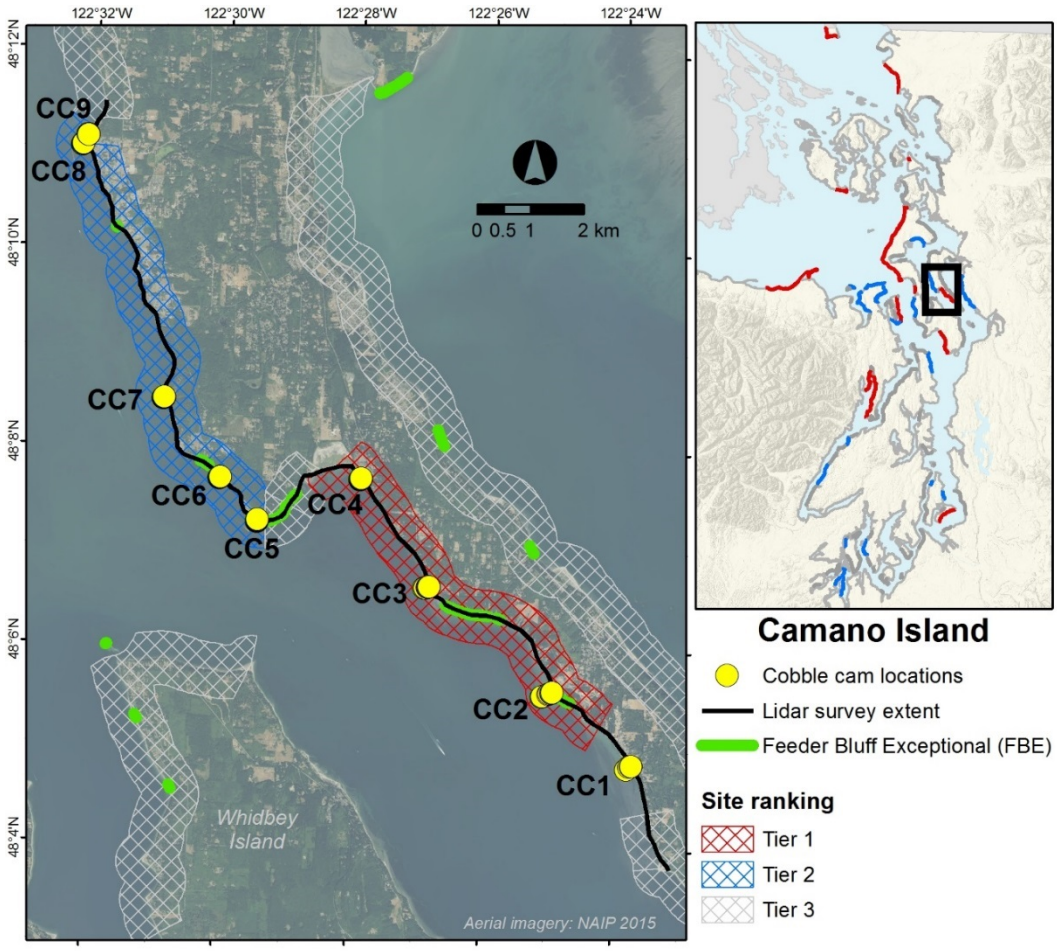

Figure D-2A: Locations of cobble cam transects for the Camano Island survey site

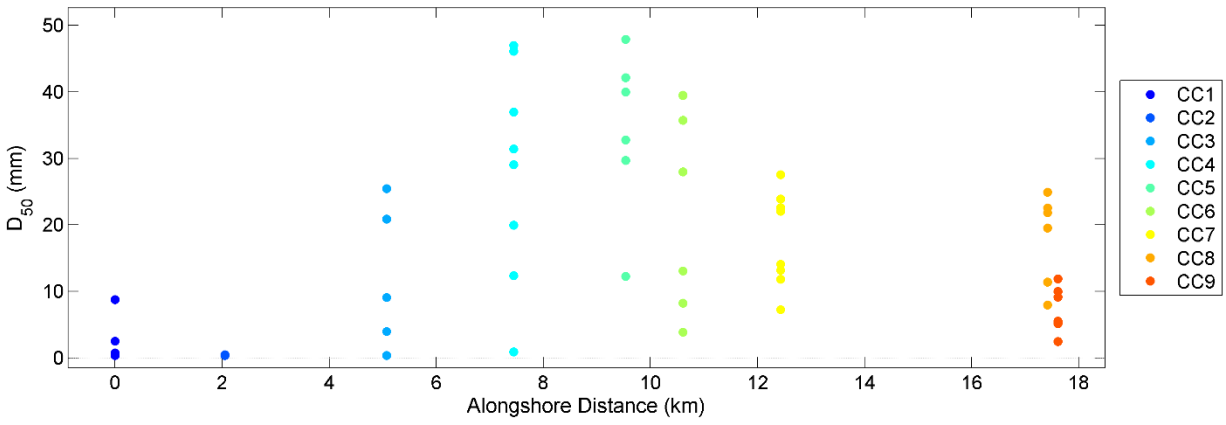

Figure D-2B: Median grain size (D_{50}) for each sediment sample collected along the cobble cam transects at the Camano Island survey site

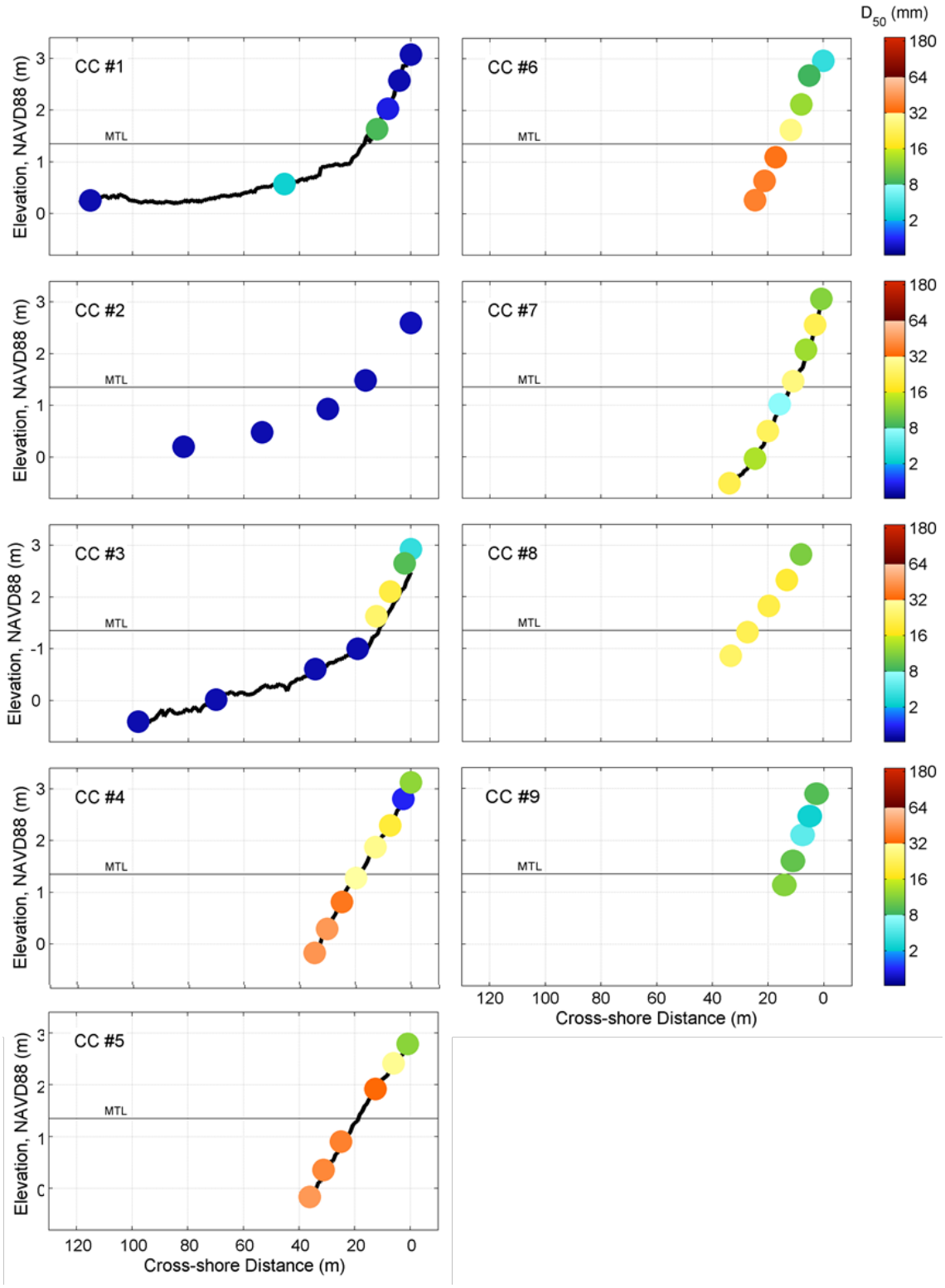

Figure D-2C: Cross-shore distribution of median grain size (D_{50}) for each cobble cam transect at the Camano Island survey site; the mean tide level (MTL) is shown for reference. The black line between samples shows the beach profile (where collected)

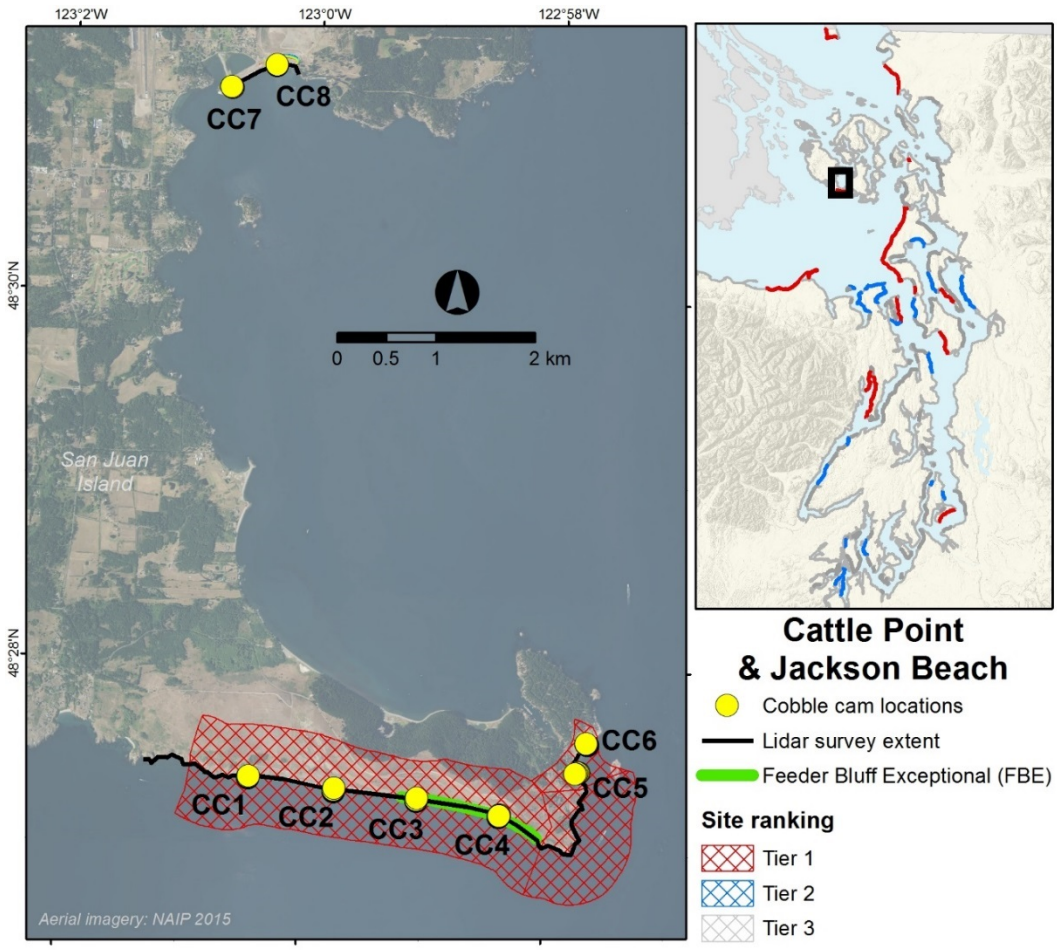

Figure D-3A: Locations of cobble cam transects for the Cattle Point (CC1-CC6) and Jackson Beach (CC7-CC8) survey sites located on San Juan Island

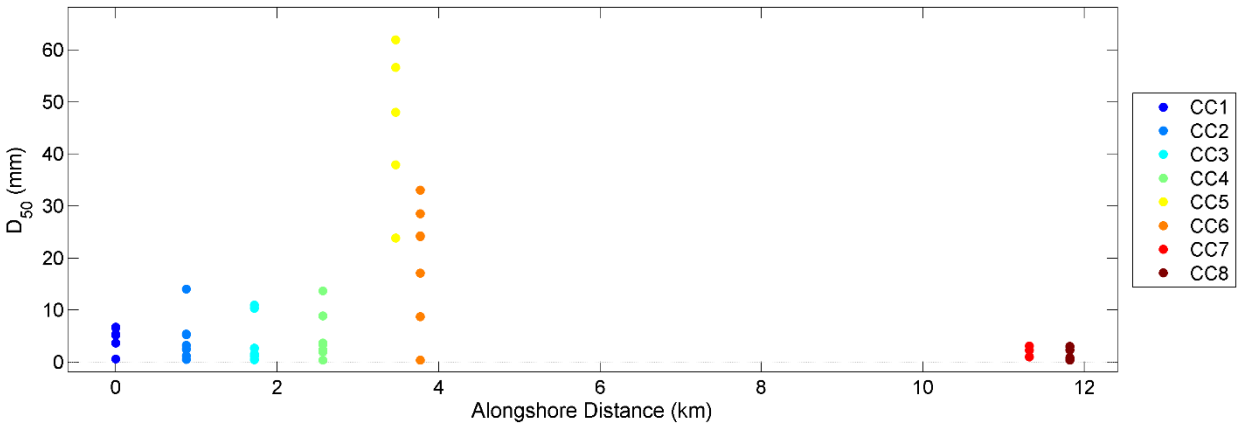

Figure D-3B: Median grain size (D_{50}) for each sediment sample collected along the cobble cam transects at the Cattle Point (CC1-CC6) and Jackson Beach (CC7-CC8) survey sites

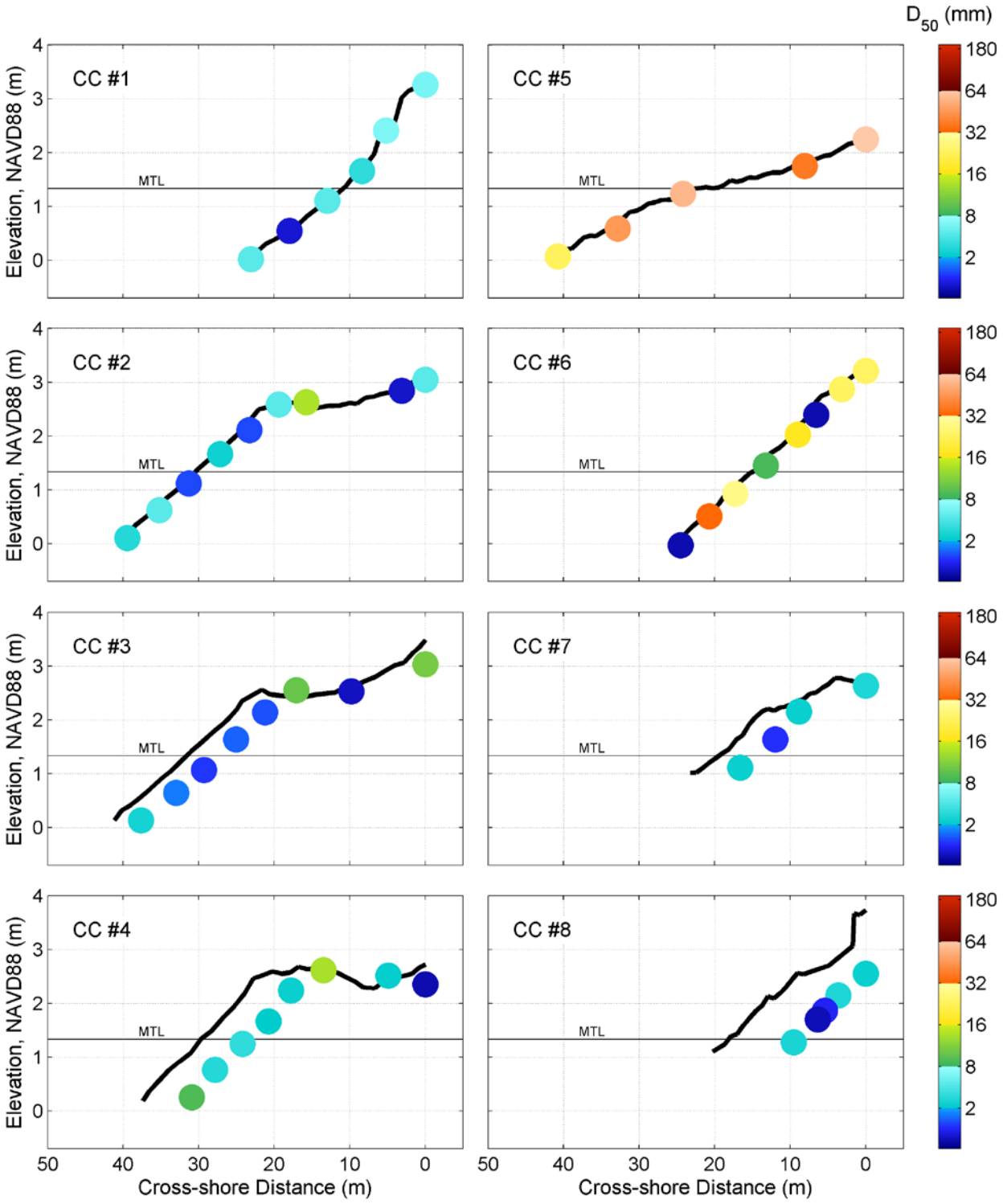

Figure D-3C: Cross-shore distribution of median grain size (D_{50}) for each cobble cam transect at the Cattle Point (CC1-CC6) and Jackson Beach (CC7-CC8) survey sites; the mean tide level (MTL) is shown for reference. The black line between samples shows the beach profile collected

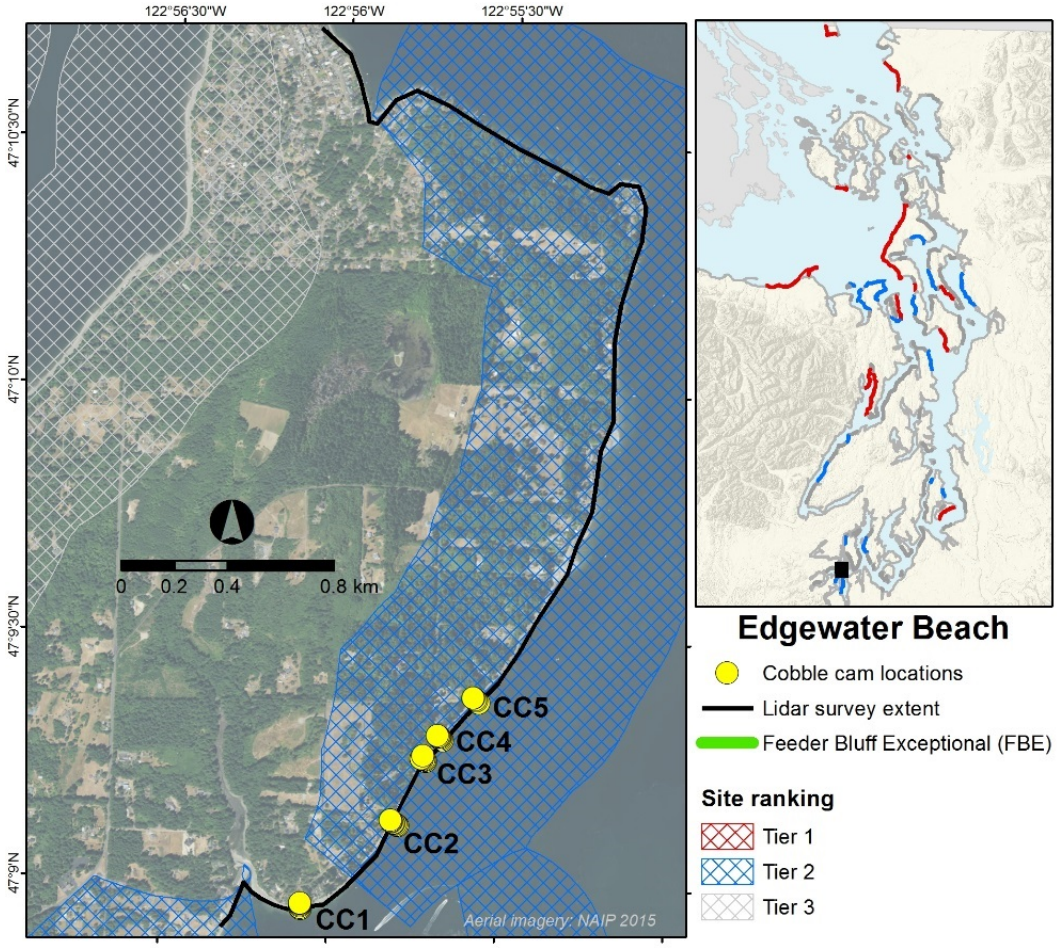

Figure D-4A: Locations of cobble cam transects for the Edgewater Beach survey site located in South Puget Sound

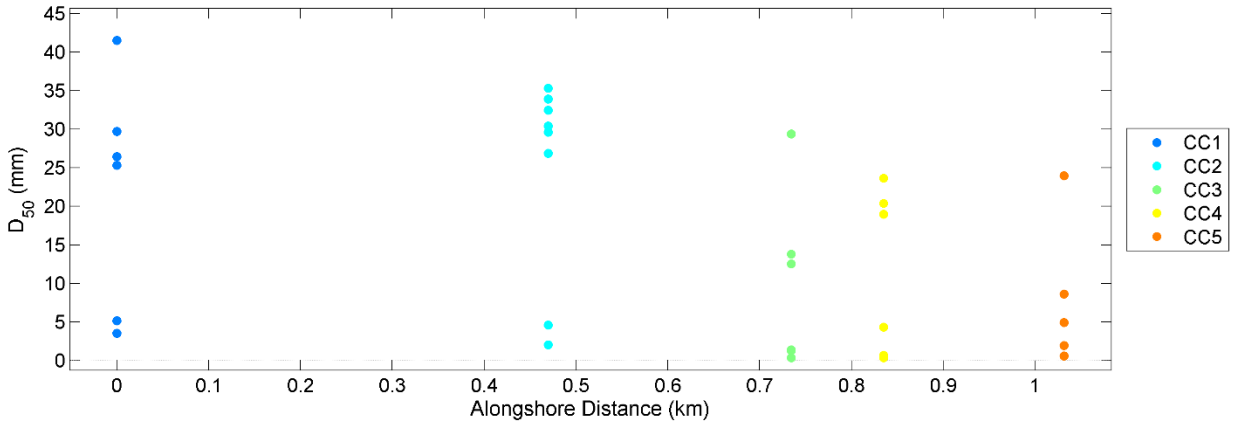

Figure D-4B: Median grain size (D_{50}) for each sediment sample collected along the cobble cam transects at the Edgewater Beach survey site

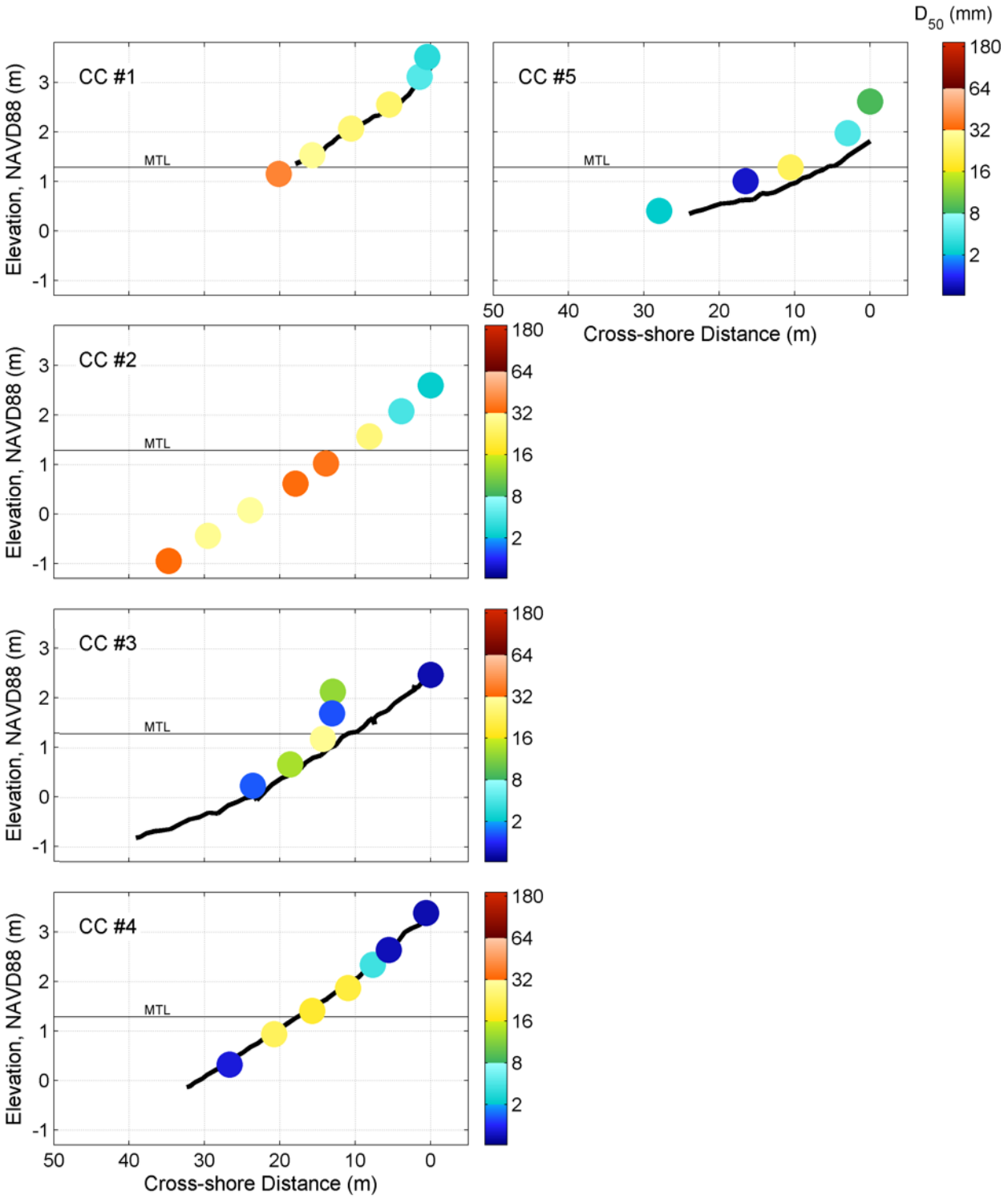

Figure D-4C: Cross-shore distribution of median grain size (D_{50}) for each cobble cam transect at the Edgewater Beach survey site; the mean tide level (MTL) is shown for reference. The black line between samples shows the beach profile (where collected)

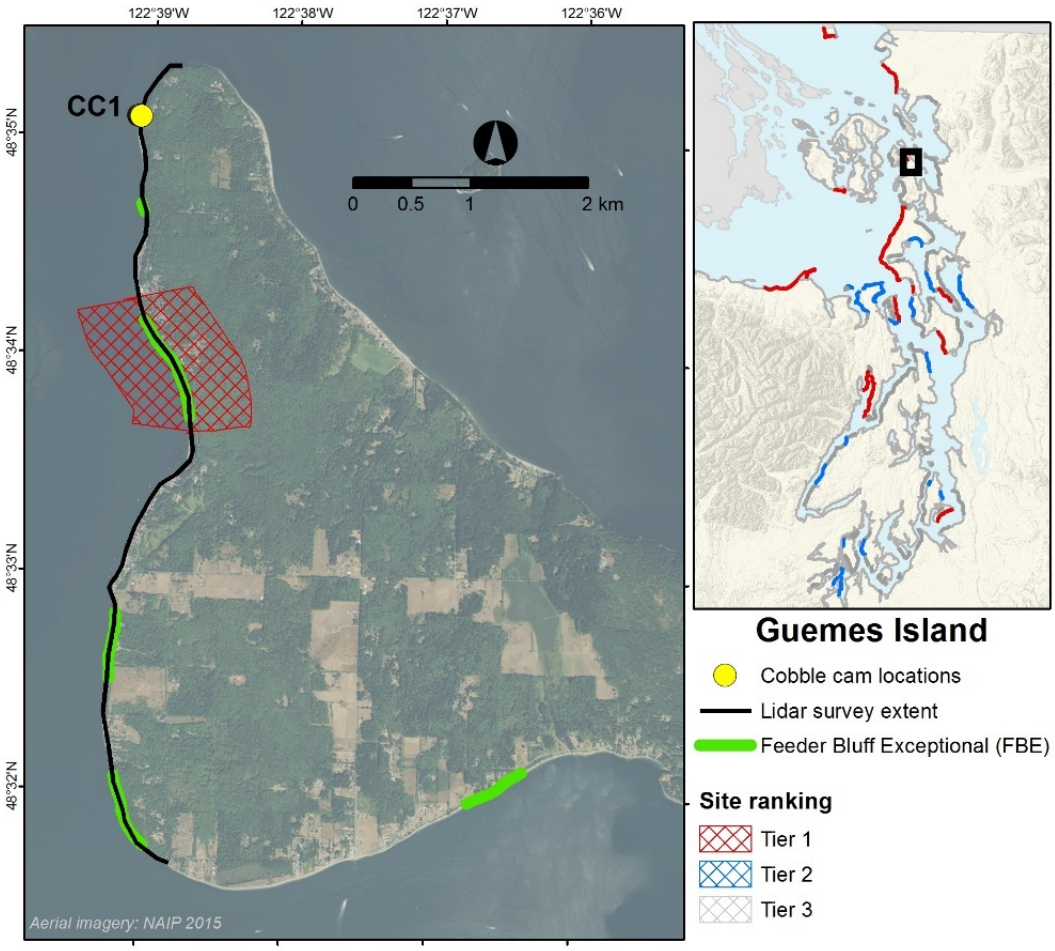

Figure D-5A: Location of the cobble cam transect for the Guemes Island survey site

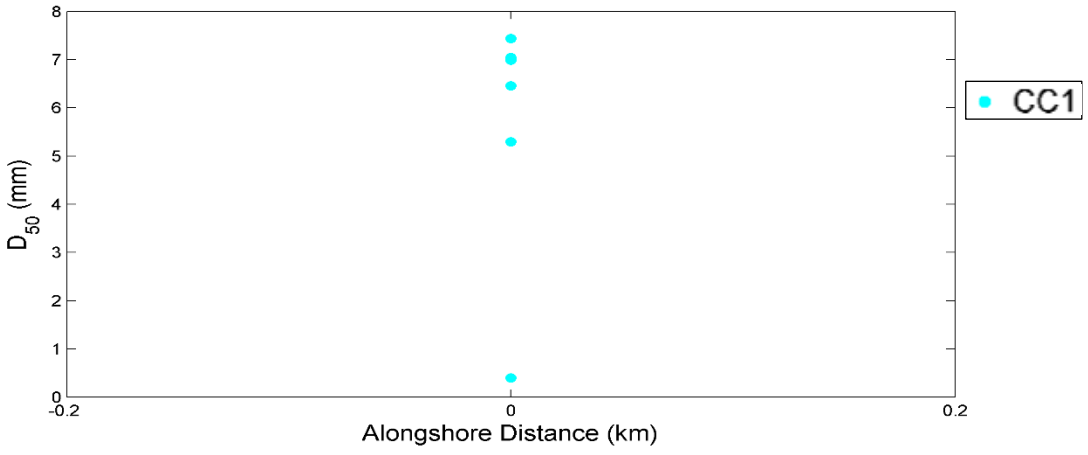

Figure D-5B: Median grain size (D_{50}) for each sediment sample collected along the cobble cam transect at the Guemes Island survey site

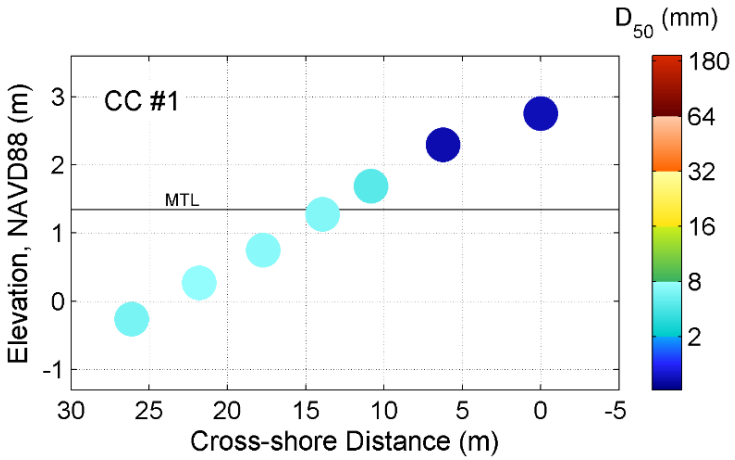

Figure D-5C: Cross-shore distribution of median grain size (D_{50}) for the cobble cam transect at the Guemes Island survey site; the mean tide level (MTL) is shown for reference

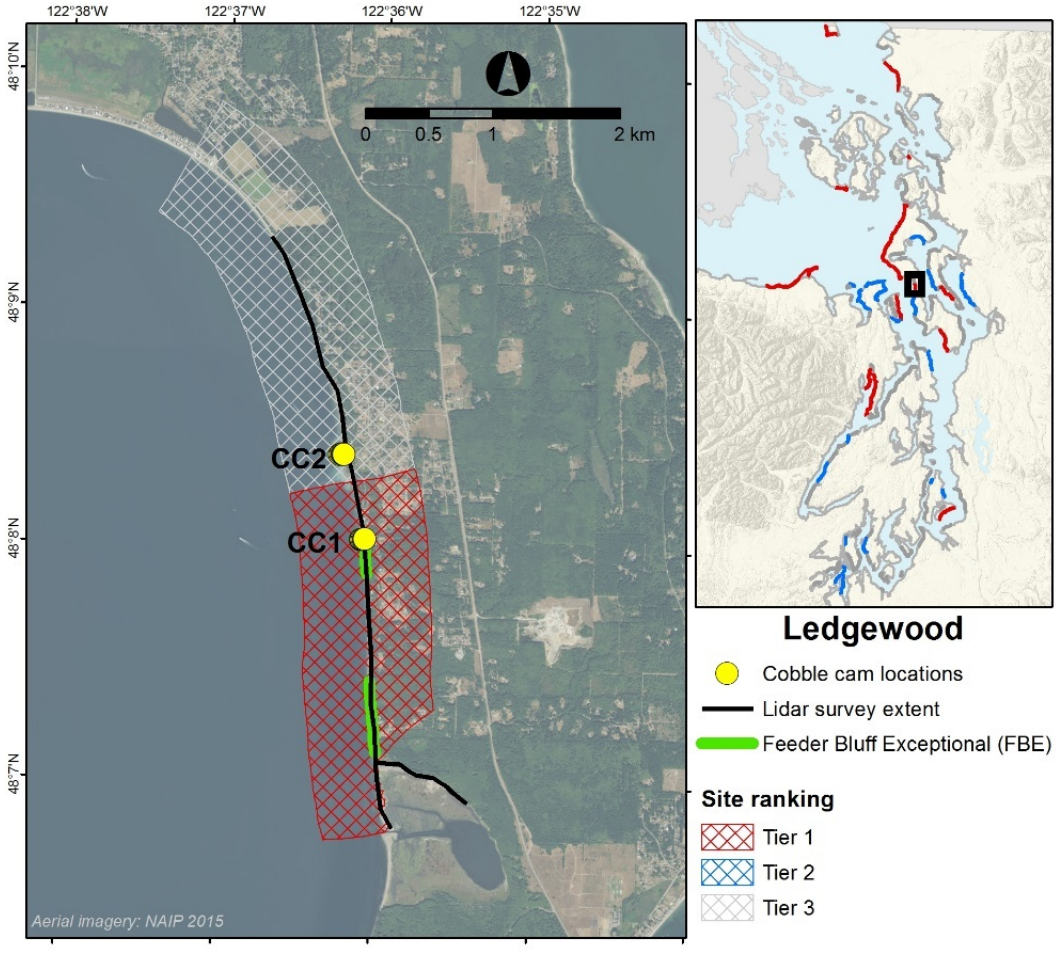

Figure D-6A: Locations of cobble cam transects for the Ledgewood survey site located on Whidbey Island

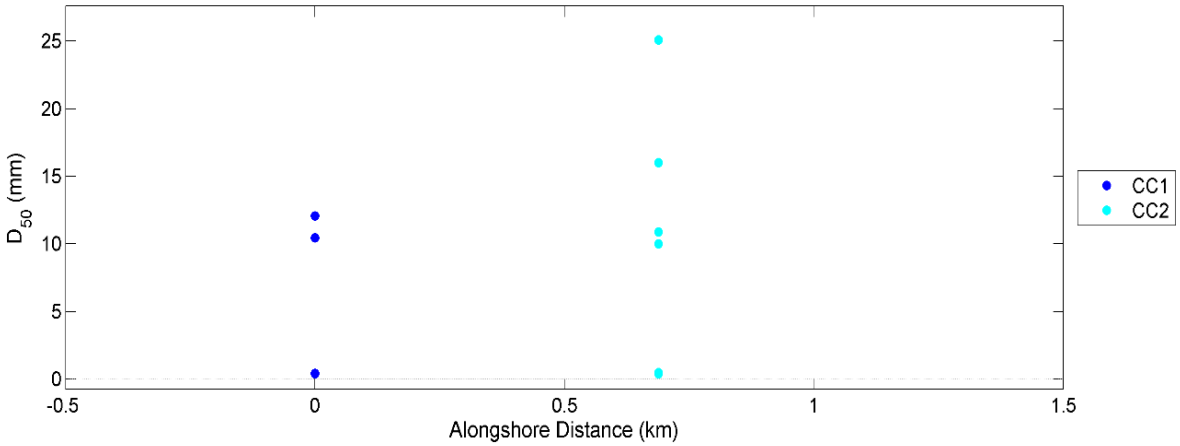

Figure D-6B: Median grain size (D_{50}) for each sediment sample collected along the cobble cam transects at the Ledgewood survey site.

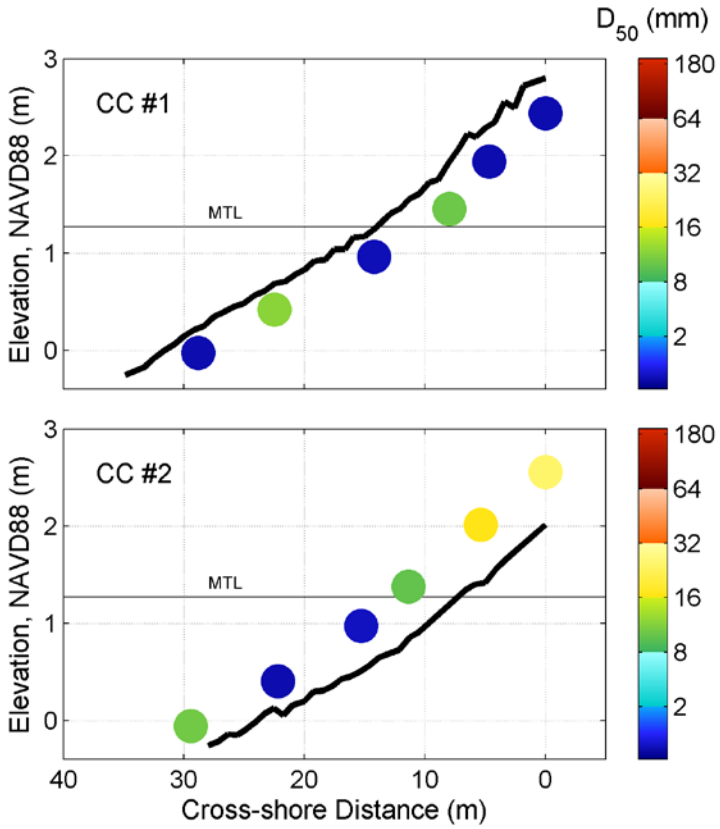

Figure D-6C: Cross-shore distribution of median grain size (D_{50}) for each cobble cam transect at the Ledgewood survey site; the mean tide level (MTL) is shown for reference. The black line between samples shows the beach profile collected

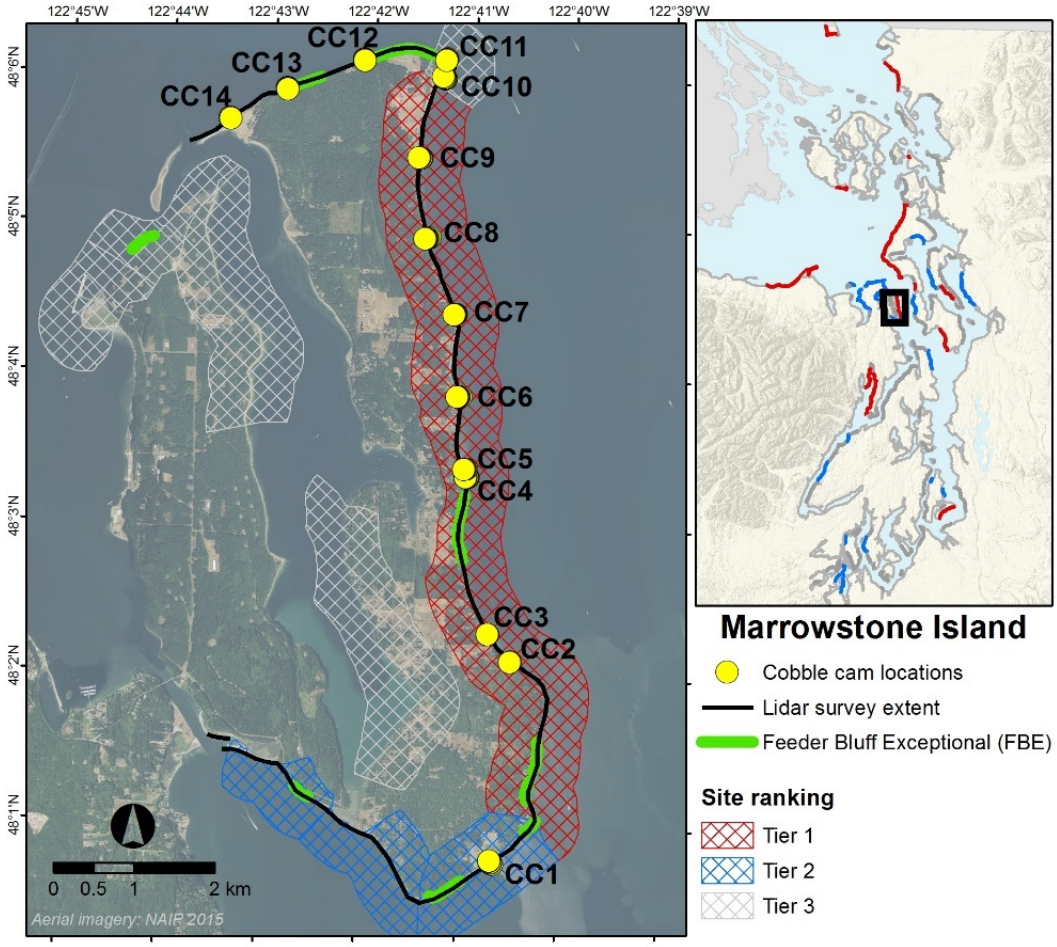

Figure D-7A: Locations of cobble cam transects for the Marrowstone Island survey site

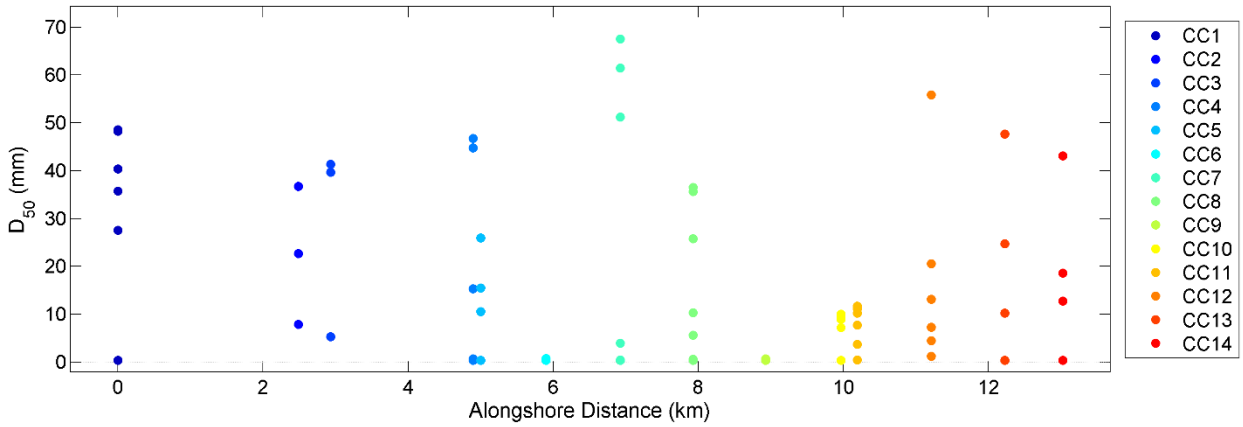

Figure D-7B: Median grain size (D_{50}) for each sediment sample collected along the cobble cam transects at the Marrowstone Island survey site

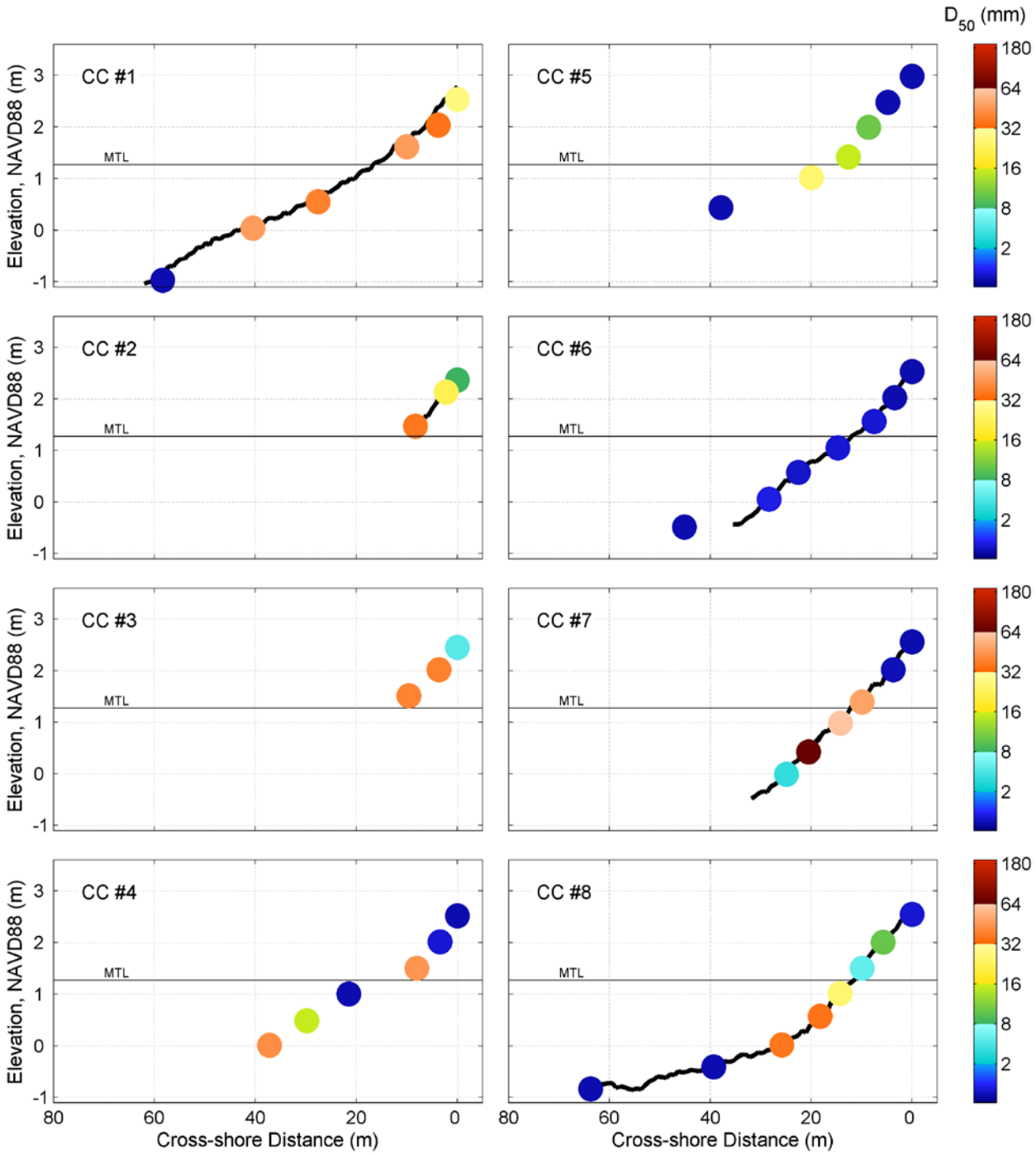

Figure D-7C: Cross-shore distribution of median grain size (D_{50}) for each cobble cam transect at the Marrowstone Island survey site; the mean tide level (MTL) is shown for reference. The black line between samples shows the beach profile (where collected) *(Continued on next page)*

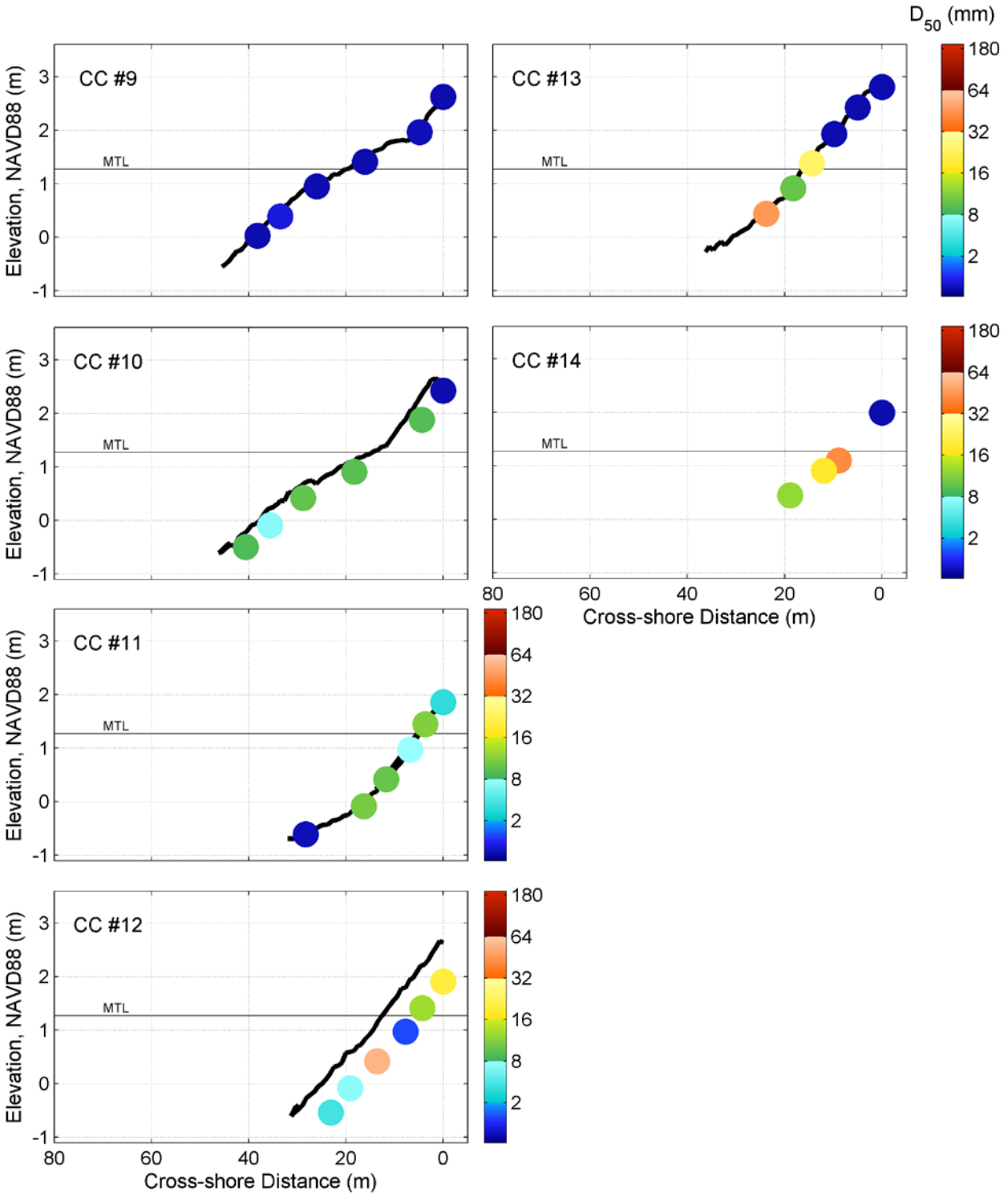

Figure D-7C: Continued from previous page

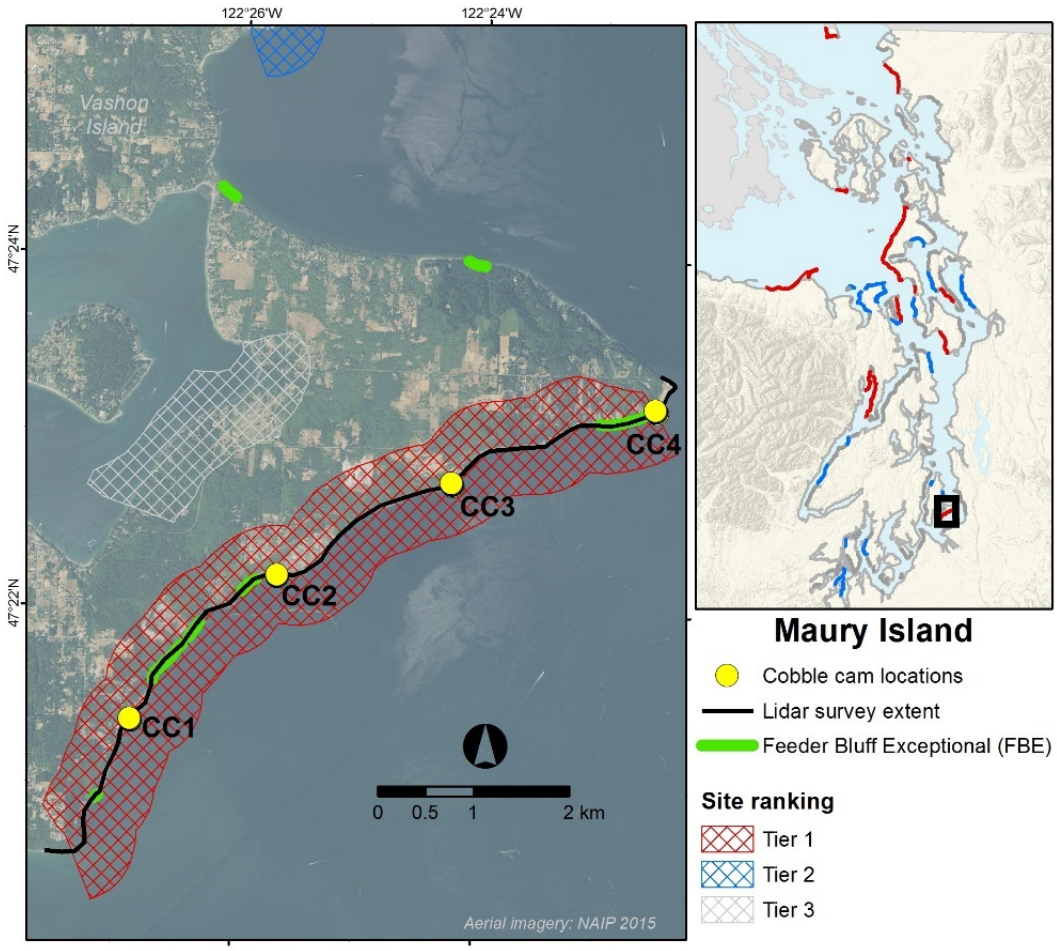

Figure D-8A: Locations of cobble cam transects for the Maury Island survey site

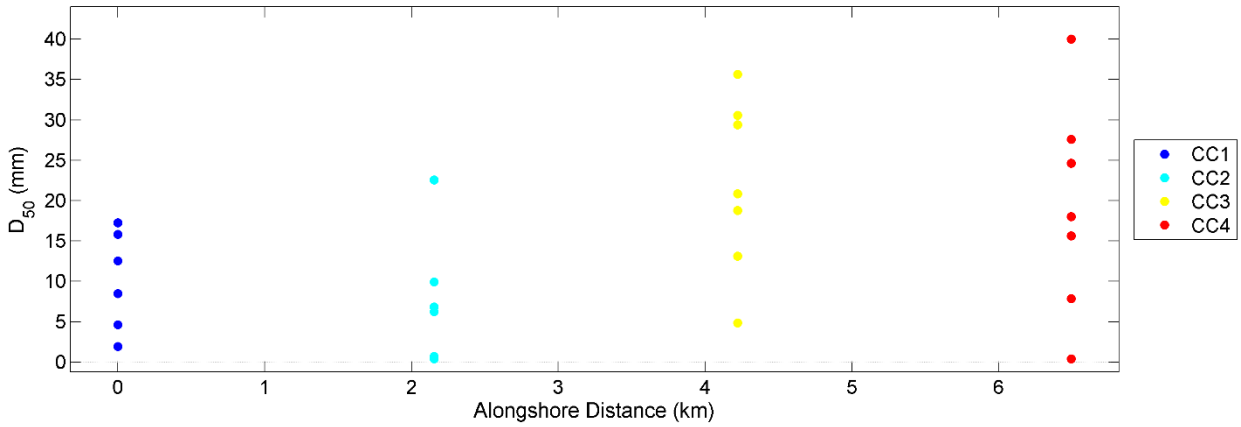

Figure D-8B: Median grain size (D_{50}) for each sediment sample collected along the cobble cam transects at the Maury Island survey site

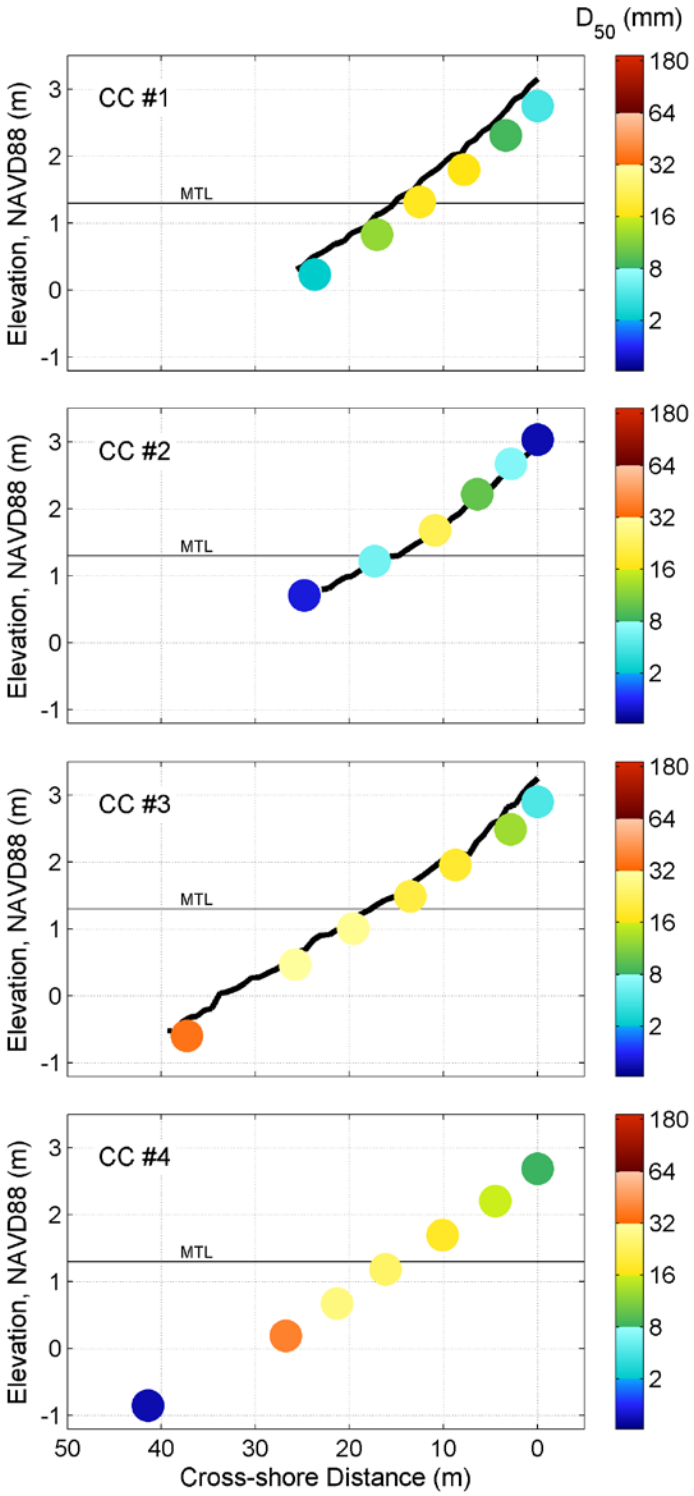

Figure D-8C: Cross-shore distribution of median grain size (D_{50}) for each cobble cam transect at the Maury Island survey site; the mean tide level (MTL) is shown for reference. The black line between samples shows the beach profile (where collected)

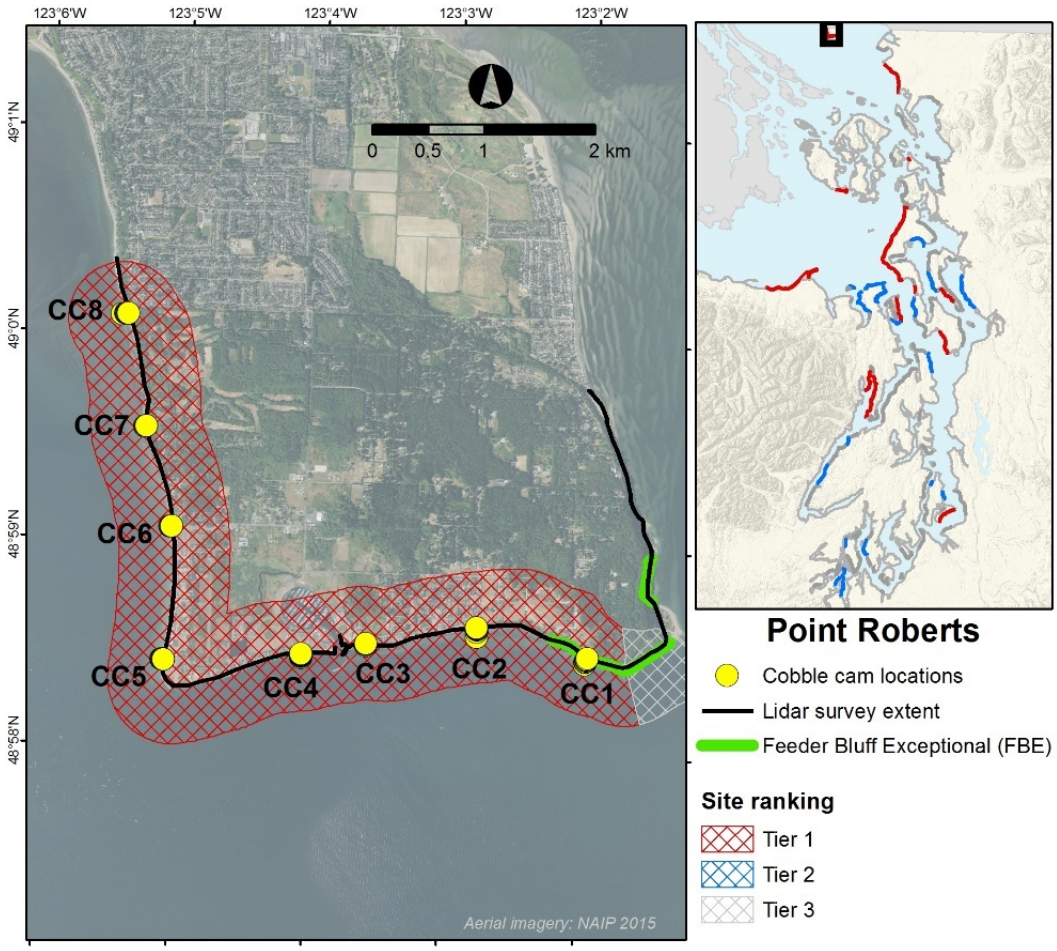

Figure D-9A: Locations of cobble cam transects for the Point Roberts survey site

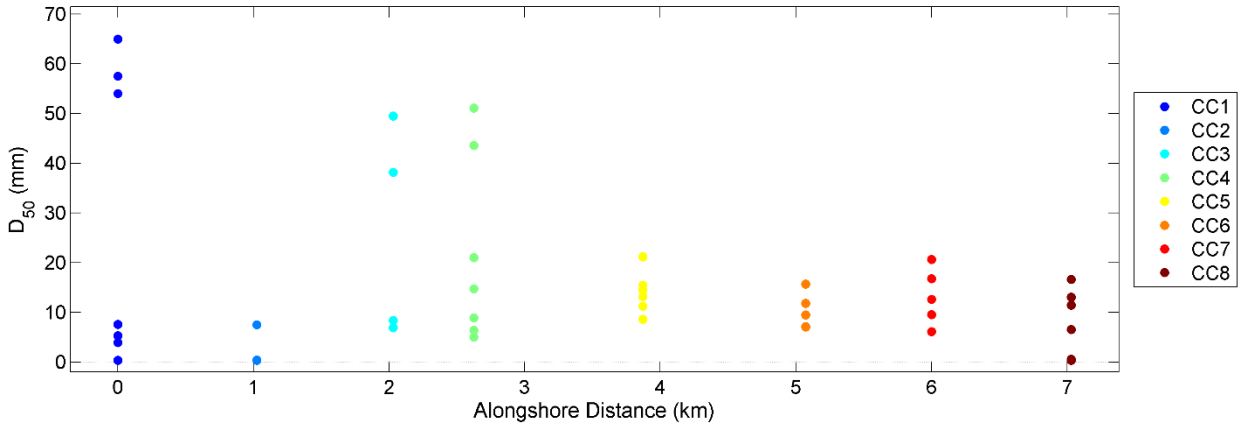

Figure D-9B: Median grain size (D_{50}) for each sediment sample collected along the cobble cam transects at the Point Roberts survey site

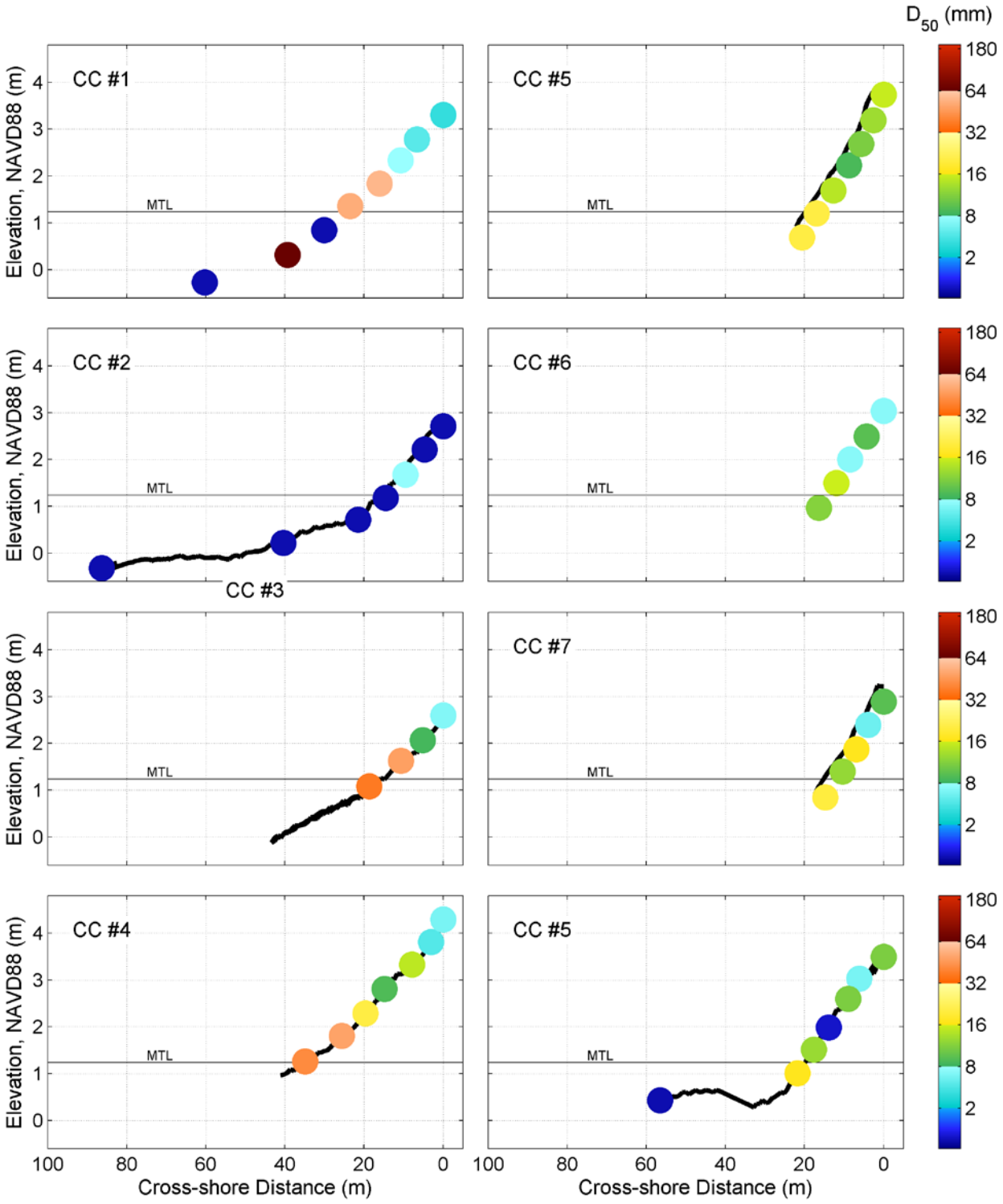

Figure D-9C: Cross-shore distribution of median grain size (D_{50}) for each cobble cam transect at the Point Roberts survey site; the mean tide level (MTL) is shown for reference. The black line between samples shows the beach profile (where collected)

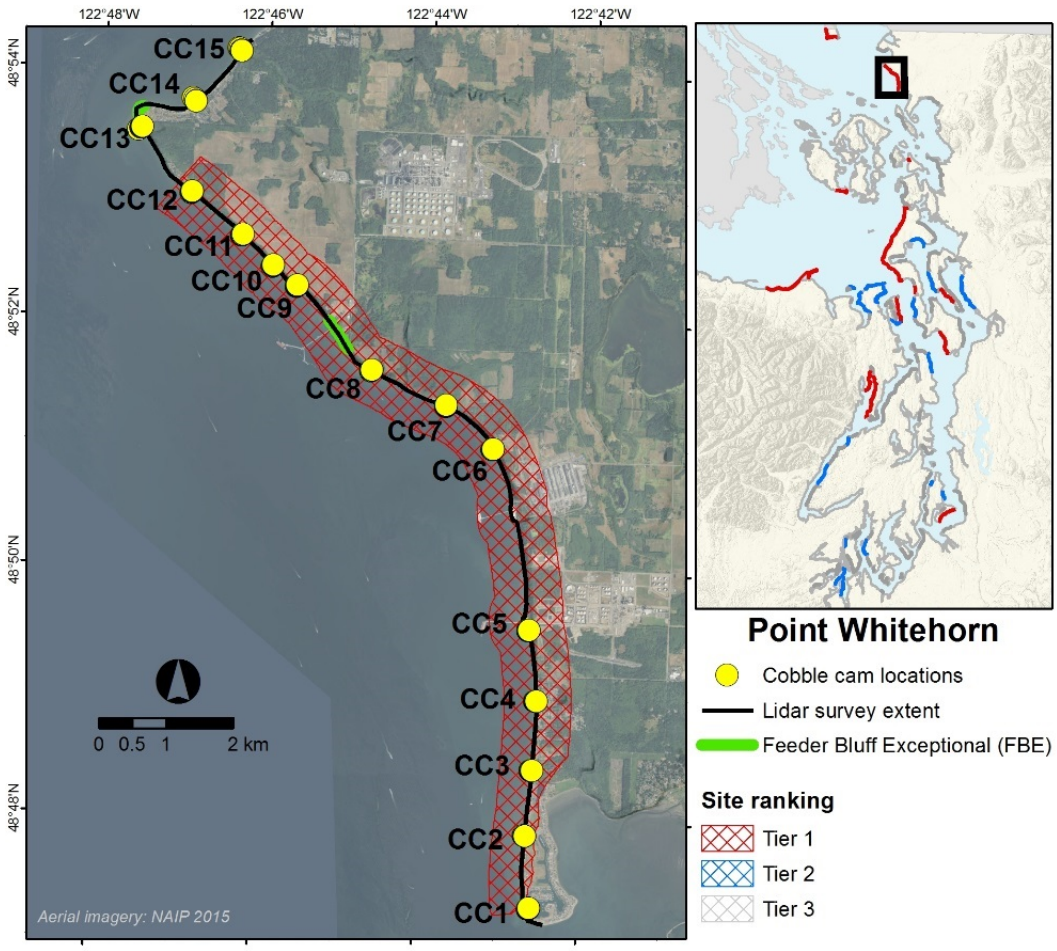

Figure D-10A: Locations of cobble cam transects for the Point Whitehorn survey site

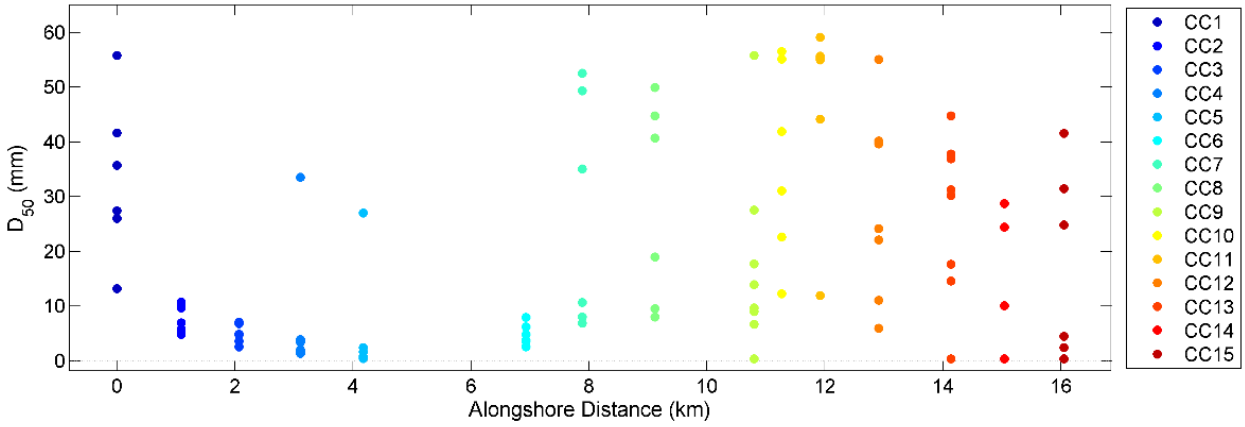

Figure D-10B: Median grain size (D_{50}) for each sediment sample collected along the cobble cam transects at the Point Whitehorn survey site

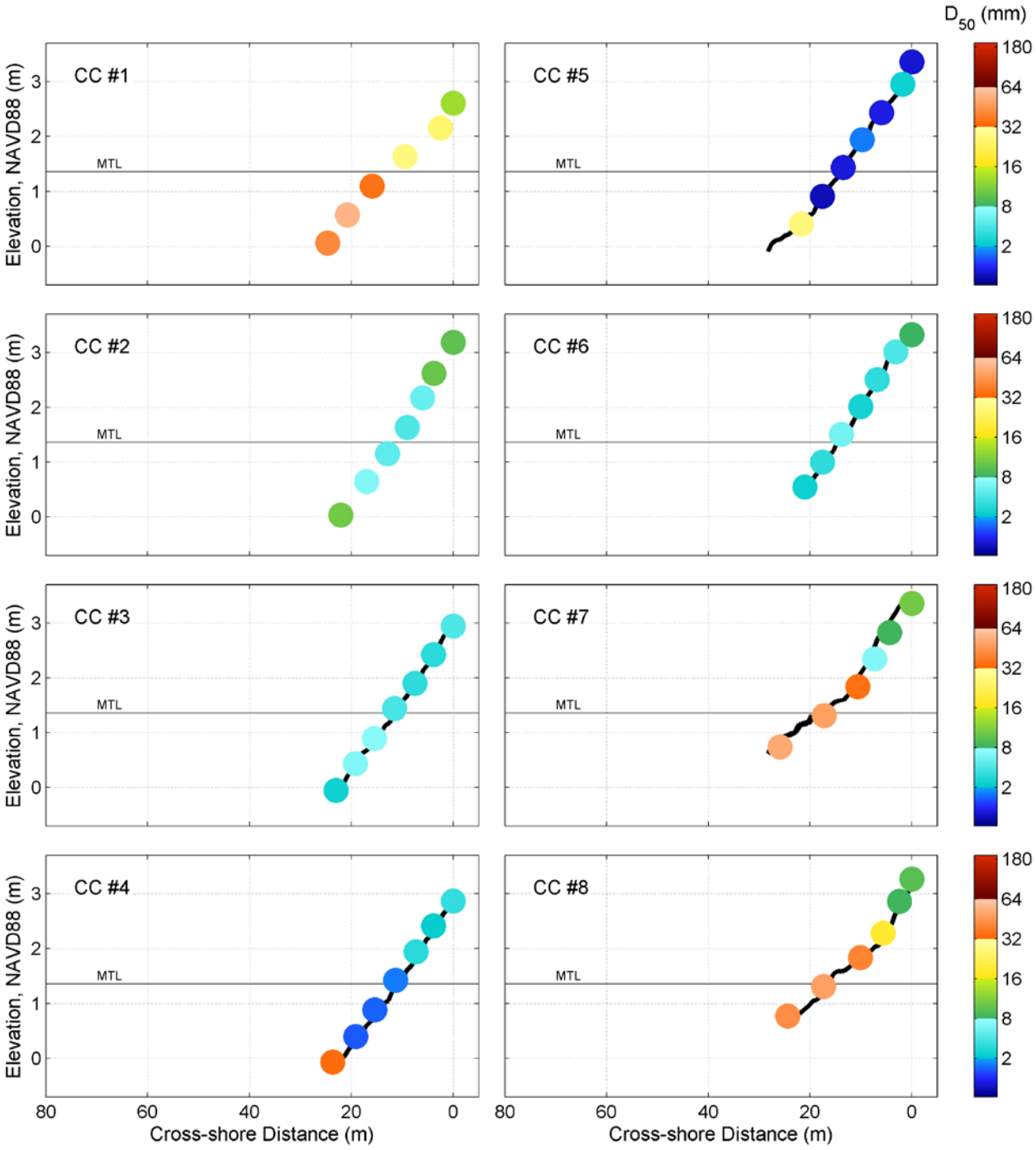

Figure D-10C: Cross-shore distribution of median grain size (D_{50}) for each cobble cam transect at the Point Whitehorn survey site; the mean tide level (MTL) is shown for reference. The black line between samples shows the beach profile (where collected) *(Continued on next page)*

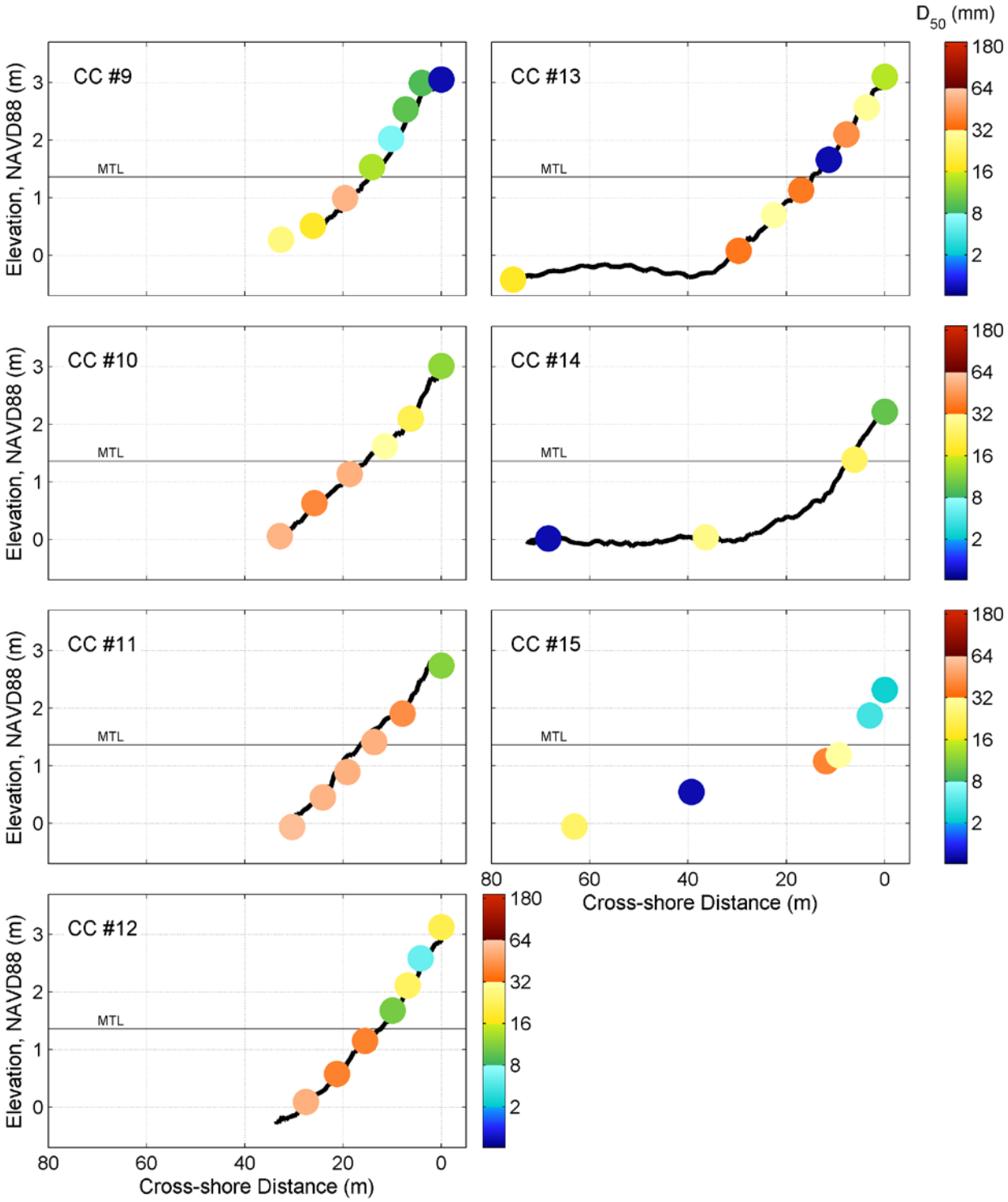

Figure D-10C: Continued from previous page

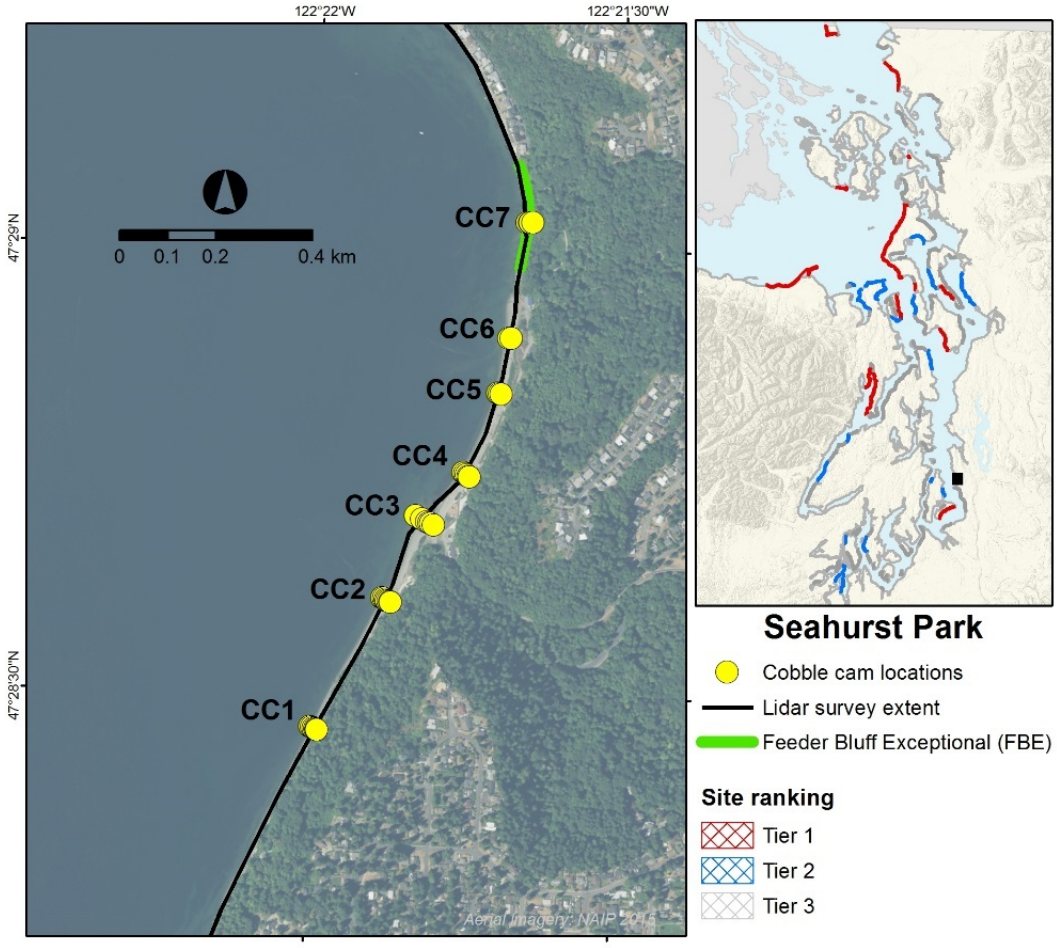

Figure D-11A: Locations of cobble cam transects for the Seahurst Park survey site in Burien

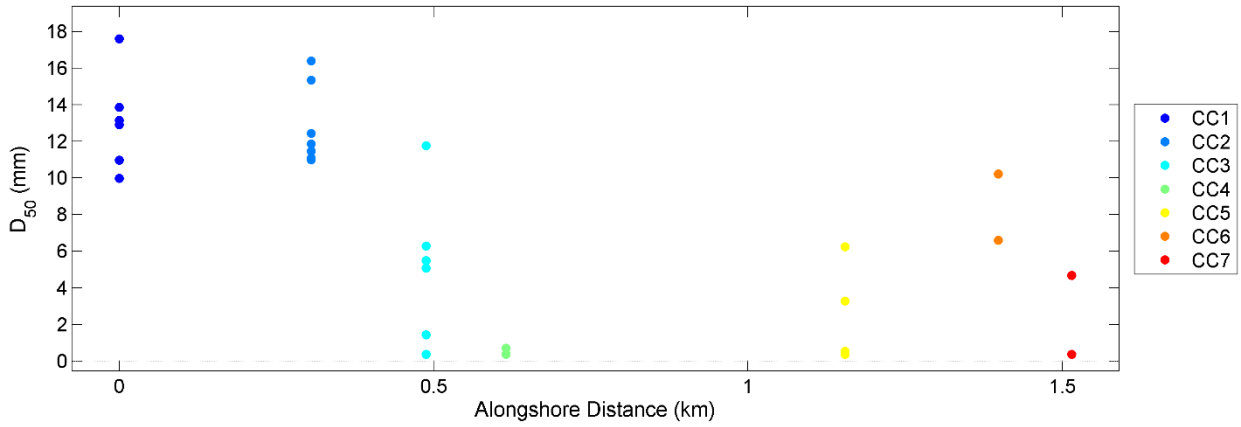

Figure D-11B: Median grain size (D_{50}) for each sediment sample collected along the cobble cam transects at the Seahurst Park survey site

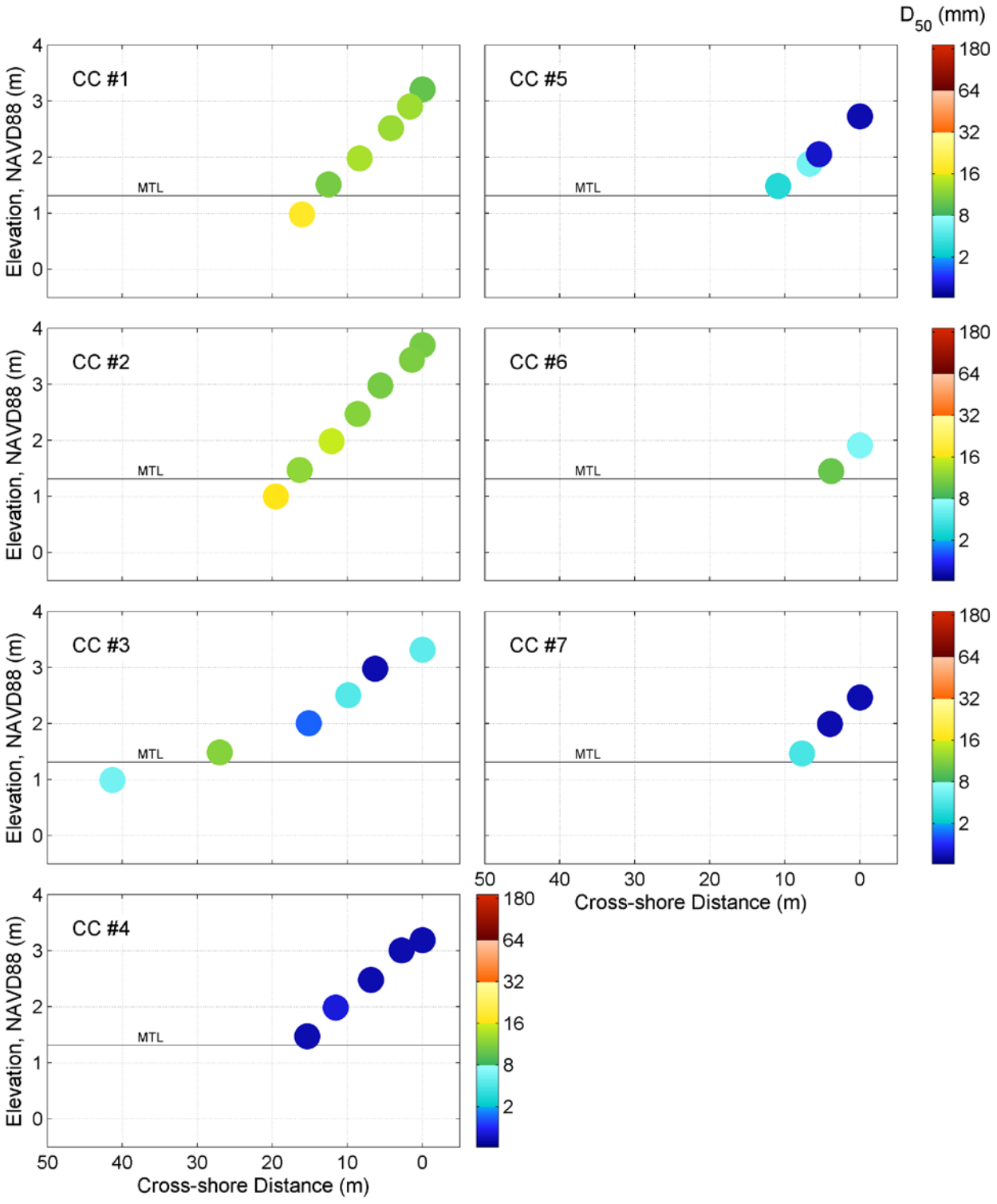

Figure D-11C: Cross-shore distribution of median grain size (D_{50}) for each cobble cam transect at the Seahurst Park survey site; the mean tide level (MTL) is shown for reference

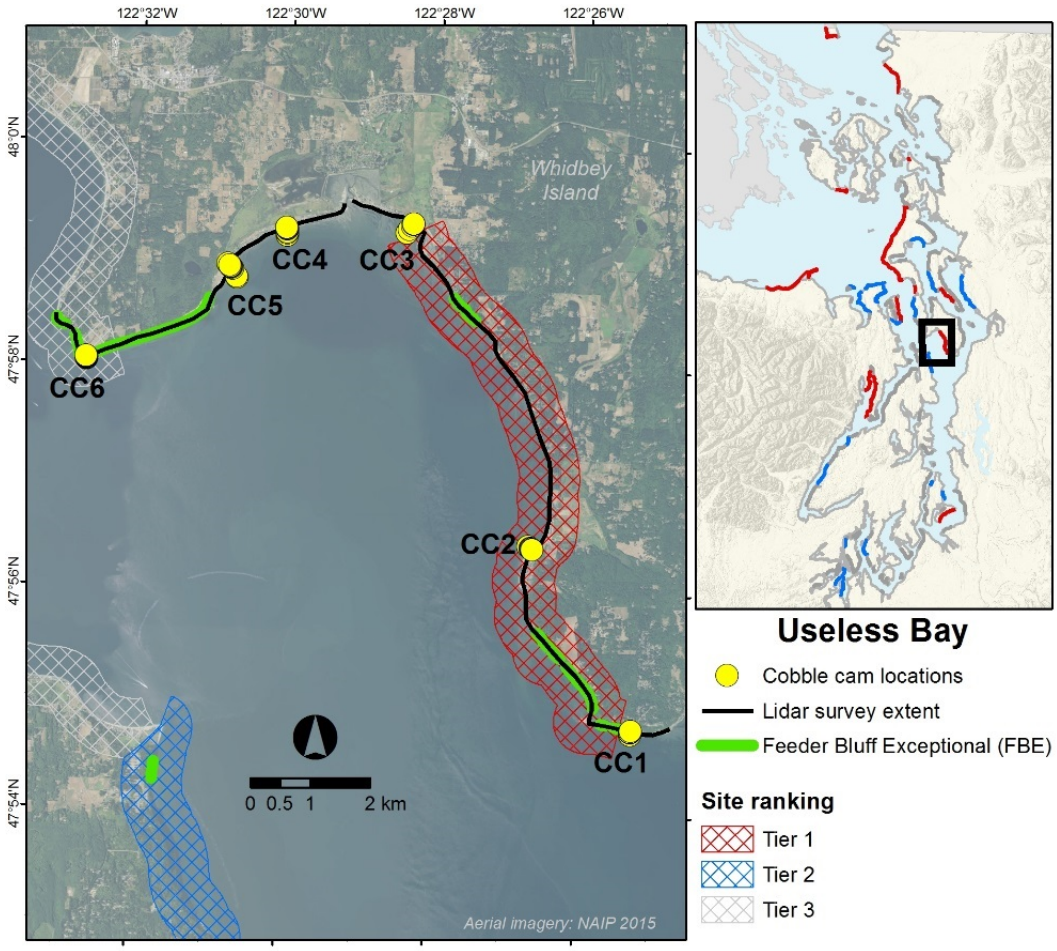

Figure D-12A: Locations of cobble cam transects for the Useless Bay survey site located on Whidbey Island

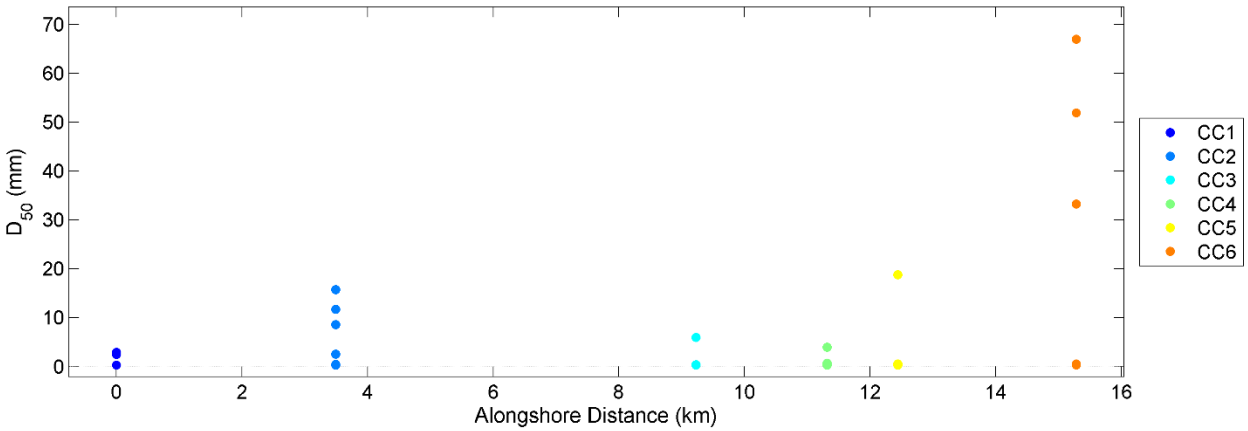

Figure D-12B: Median grain size (D_{50}) for each sediment sample collected along the cobble cam transects at the Useless Bay survey site

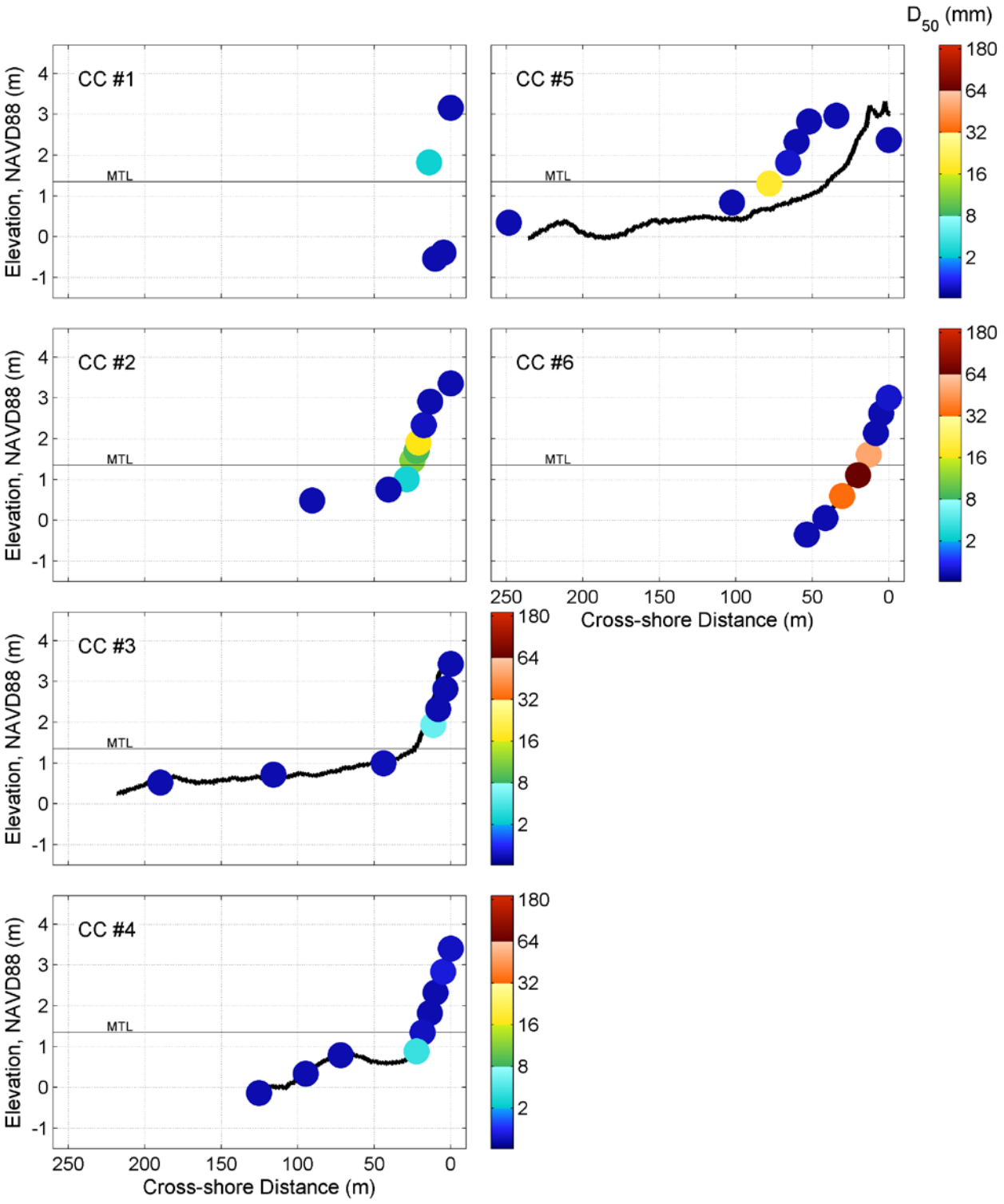

Figure D-12C: Cross-shore distribution of median grain size (D_{50}) for each cobble cam transect at the Useless Bay survey site; the mean tide level (MTL) is shown for reference. The black line between samples shows the beach profile (where collected)

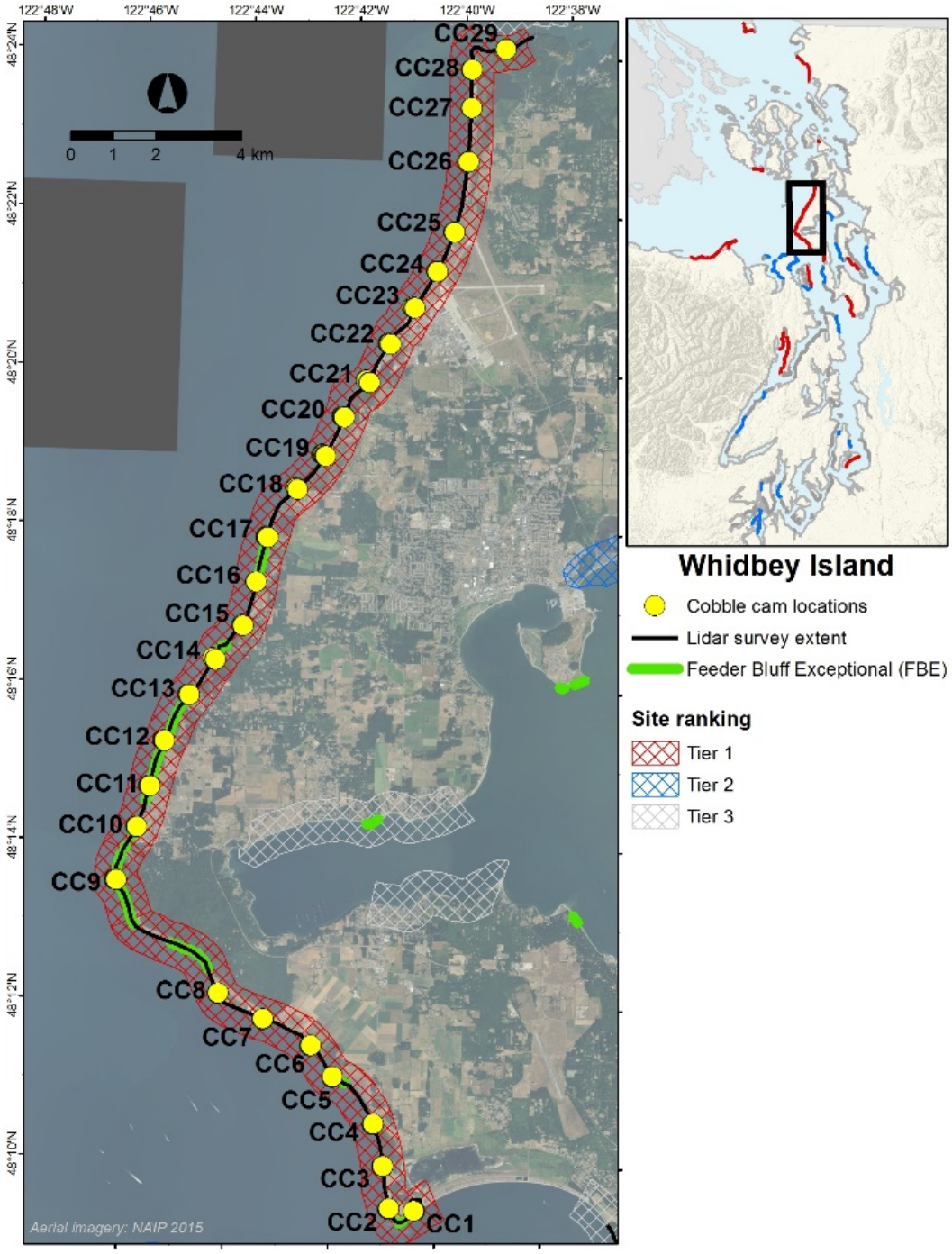

Figure D-13A: Locations of cobble cam transects for the Whidbey Island survey site

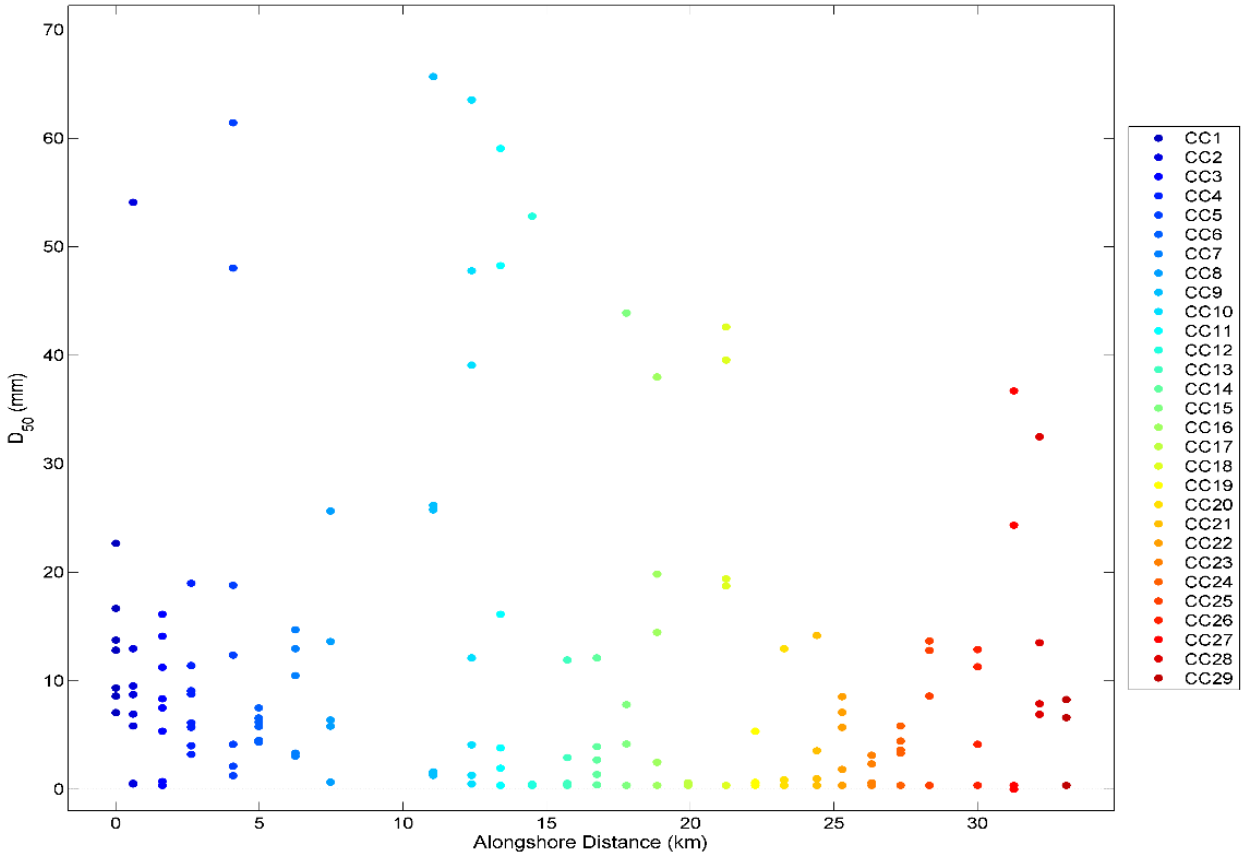

Figure D-13B: Median grain size (D_{50}) for each sediment sample collected along the cobble cam transects at the Whidbey Island survey site

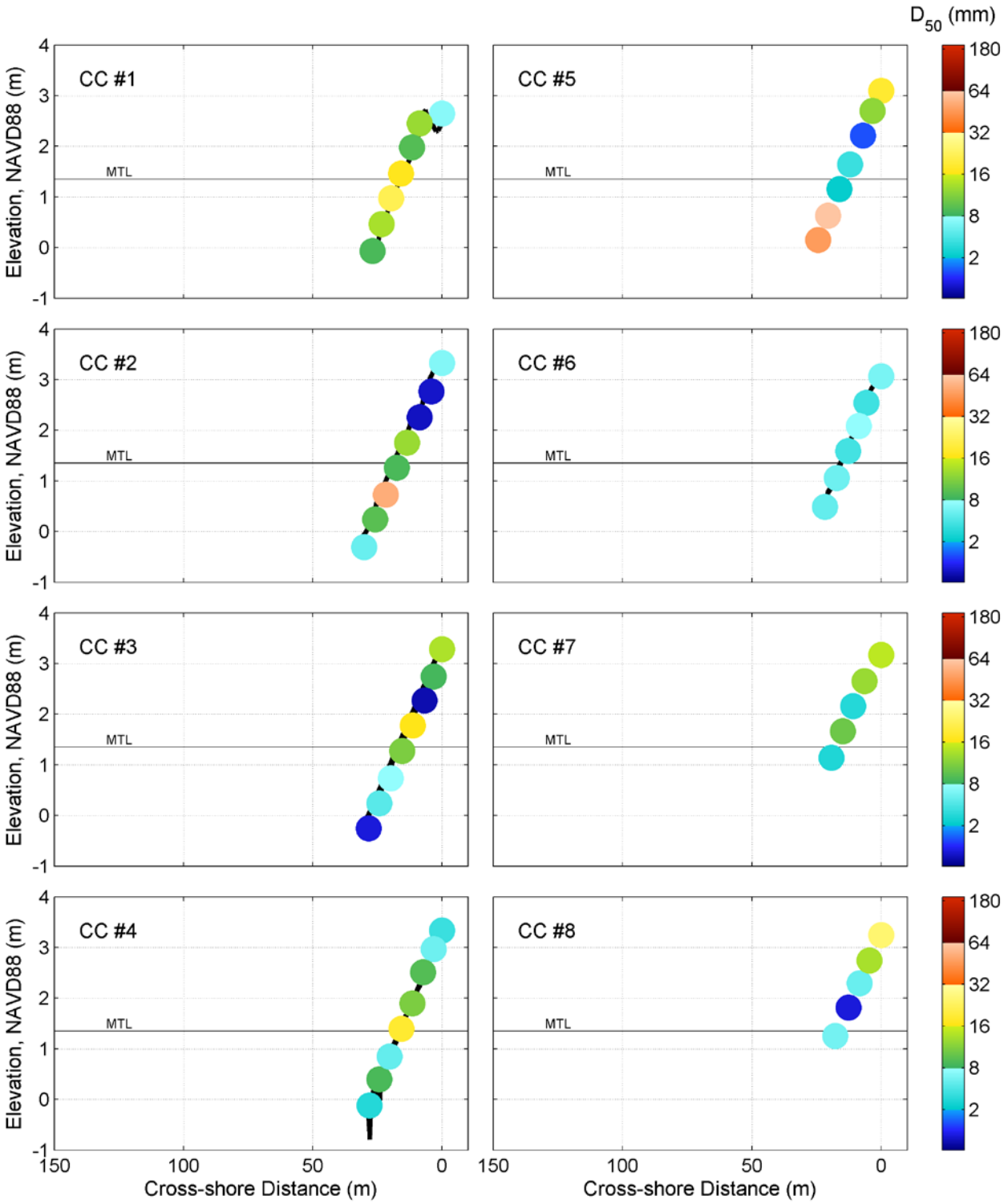

Figure D-13C: Cross-shore distribution of median grain size (D_{50}) for each cobble cam transect at the Whidbey Island survey site; the mean tide level (MTL) is shown for reference. The black line between samples shows the beach profile (where collected) *(Continued on next page)*

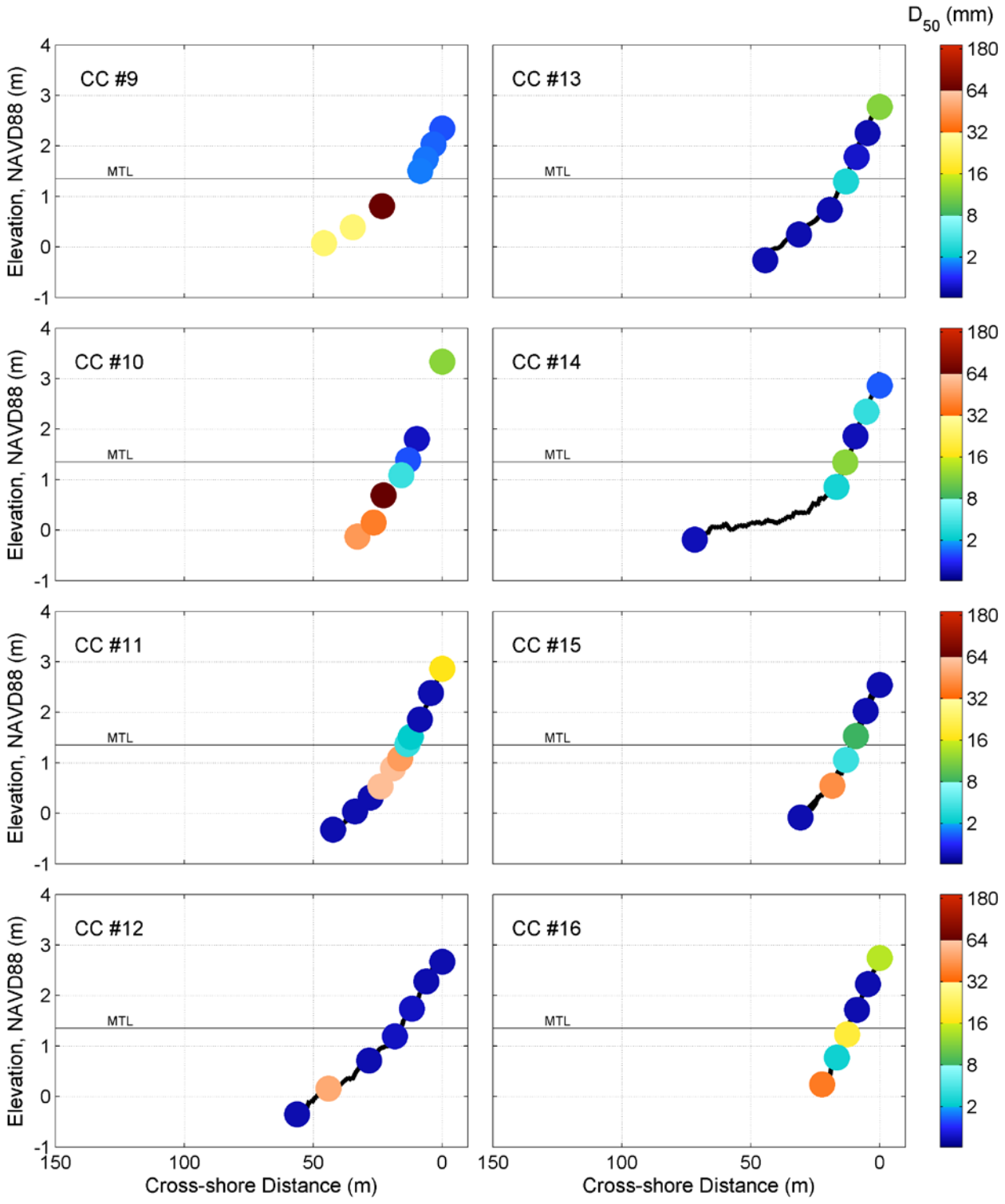

Figure D-13C: Continued from previous page

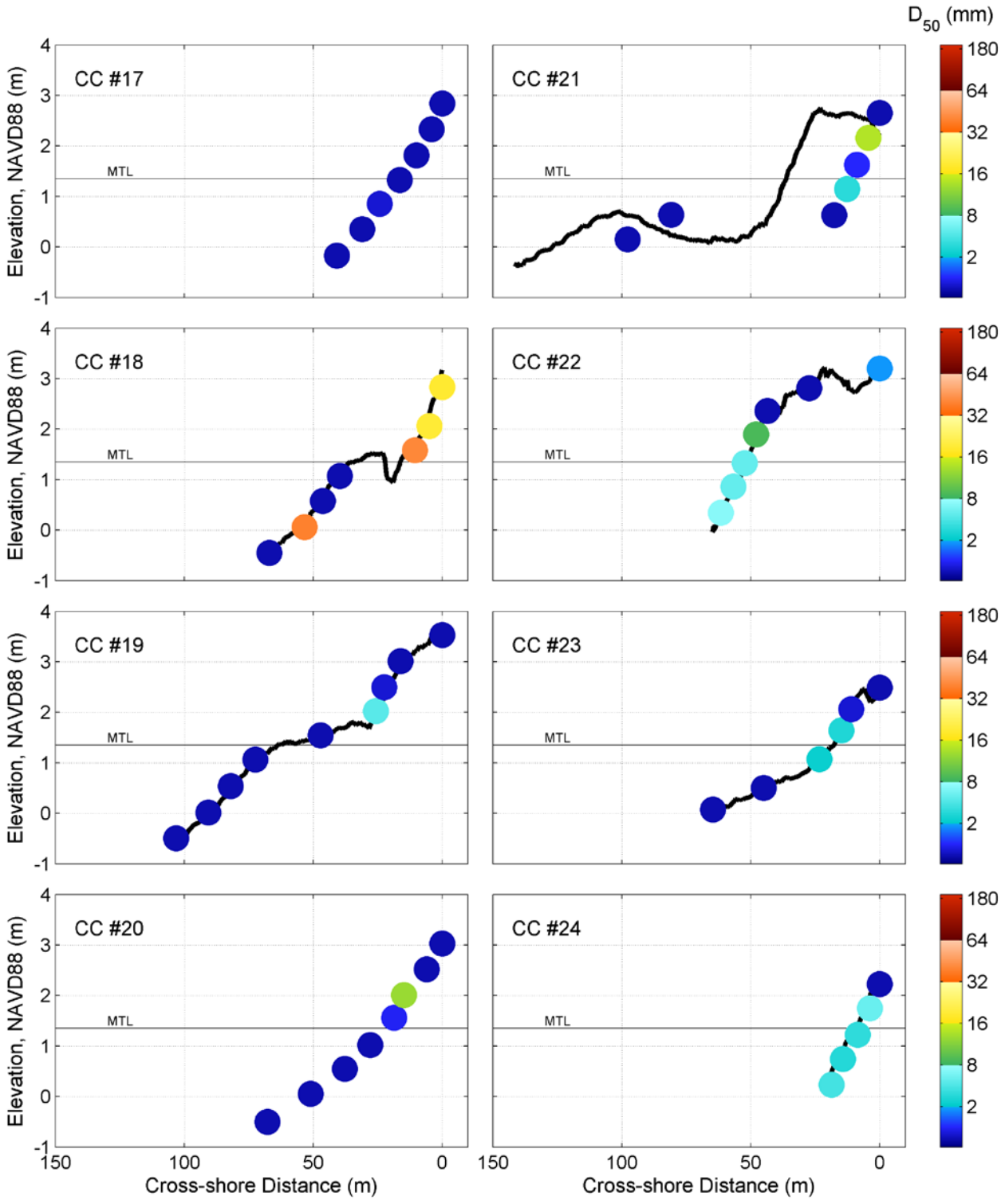

Figure D-13C: Continued from previous page

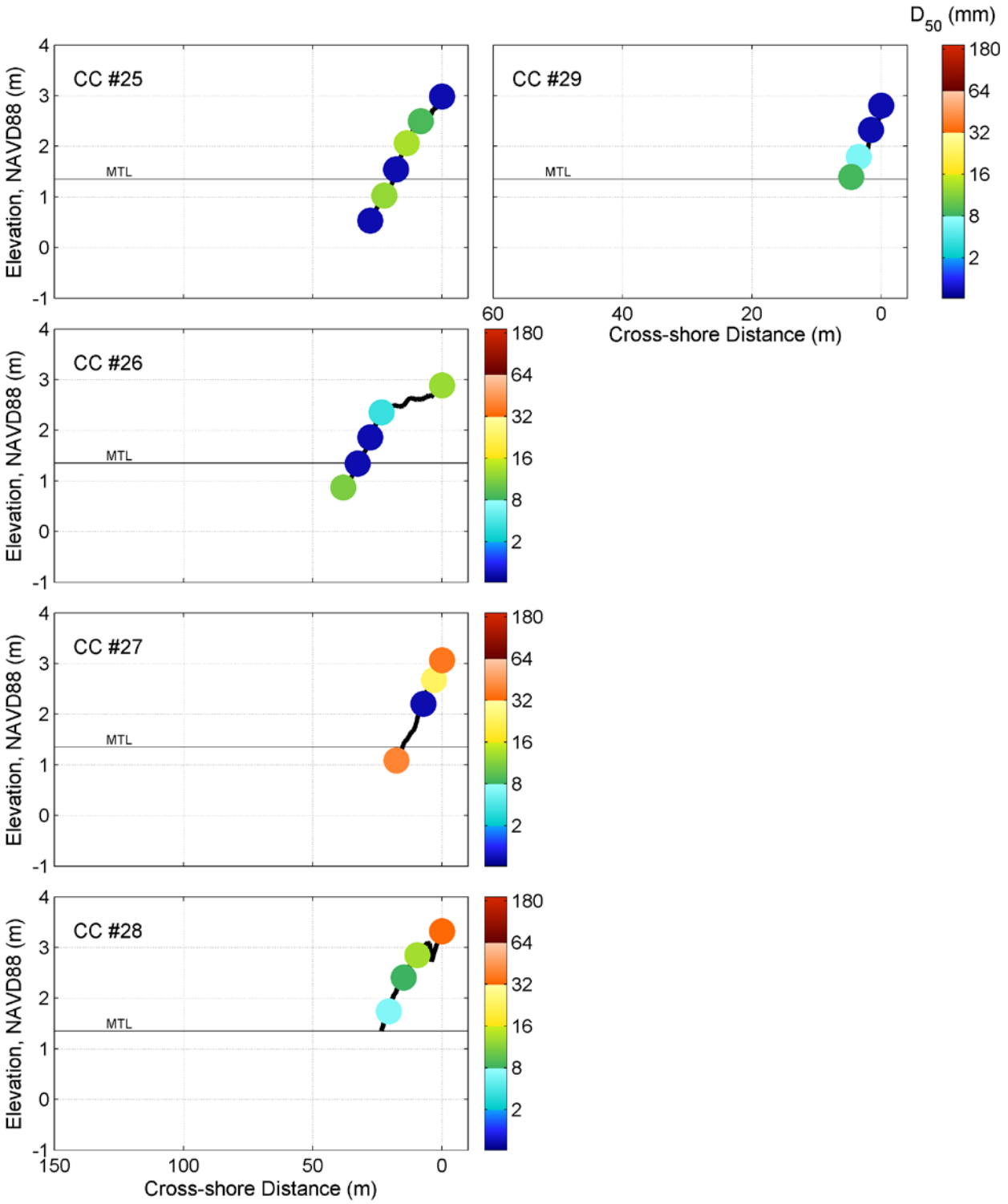

Figure D-13C: Continued from previous page

Appendix E. Example Lidar Data Applications

In addition to creating high-resolution digital elevation models (DEMs) of coastal topography, boat-based lidar data can provide detailed quantitative information about the physical and ecological landscape for a variety of applications. The high point density achieved with boat-based lidar allows for decimeter-level, detailed mapping of shoreline characteristics at a drift-cell scale. Features within the DEMs and lidar point clouds can be extracted for a more comprehensive inventory, classification, and assessment of site conditions and variability. Furthermore, features can be correlated to characterize how the shoreline landscape may be affecting nearshore ecosystem services. This appendix shows many examples of how boat-based lidar data can be used for both geomorphological and ecological applications. Unless otherwise specified, all examples shown in this appendix are derived using Ecology CMAP boat-based lidar data collected as part of this project.

Classified lidar point clouds

Lidar point clouds obtained using the boat-based laser scanner provide detailed resolution of the coastal landscape. All physical features of the shoreline visible from the laser scanner are mapped in three-dimensional space, represented by millions of data points, each with an X, Y, and Z value. The oblique look-angle of the laser scanner, which scans the shoreline from a boat offshore rather than an airplane from above, provides high-resolution data on vertical or near-vertical surfaces, such as bulkheads and bluffs that are characteristic of Puget Sound shorelines.

The points in the point cloud can be classified by the type of feature they represent (e.g., vegetation, ground, man-made structures, large woody debris, shoreline armor, beach wrack) in order to group lidar returns off similar objects and quantify various metrics about the landscape. Figure E-1 shows an example of a relatively bare bluff from the west side of Whidbey Island. There are small patches of vegetation on the bluff face, as well as some large woody debris stranded on the back beach at the base of the bluff. Because of the horizontal-look angle of the scanner from the boat, the ground on top of the bluff is not visible; however, taller trees and structures can occasionally be seen.

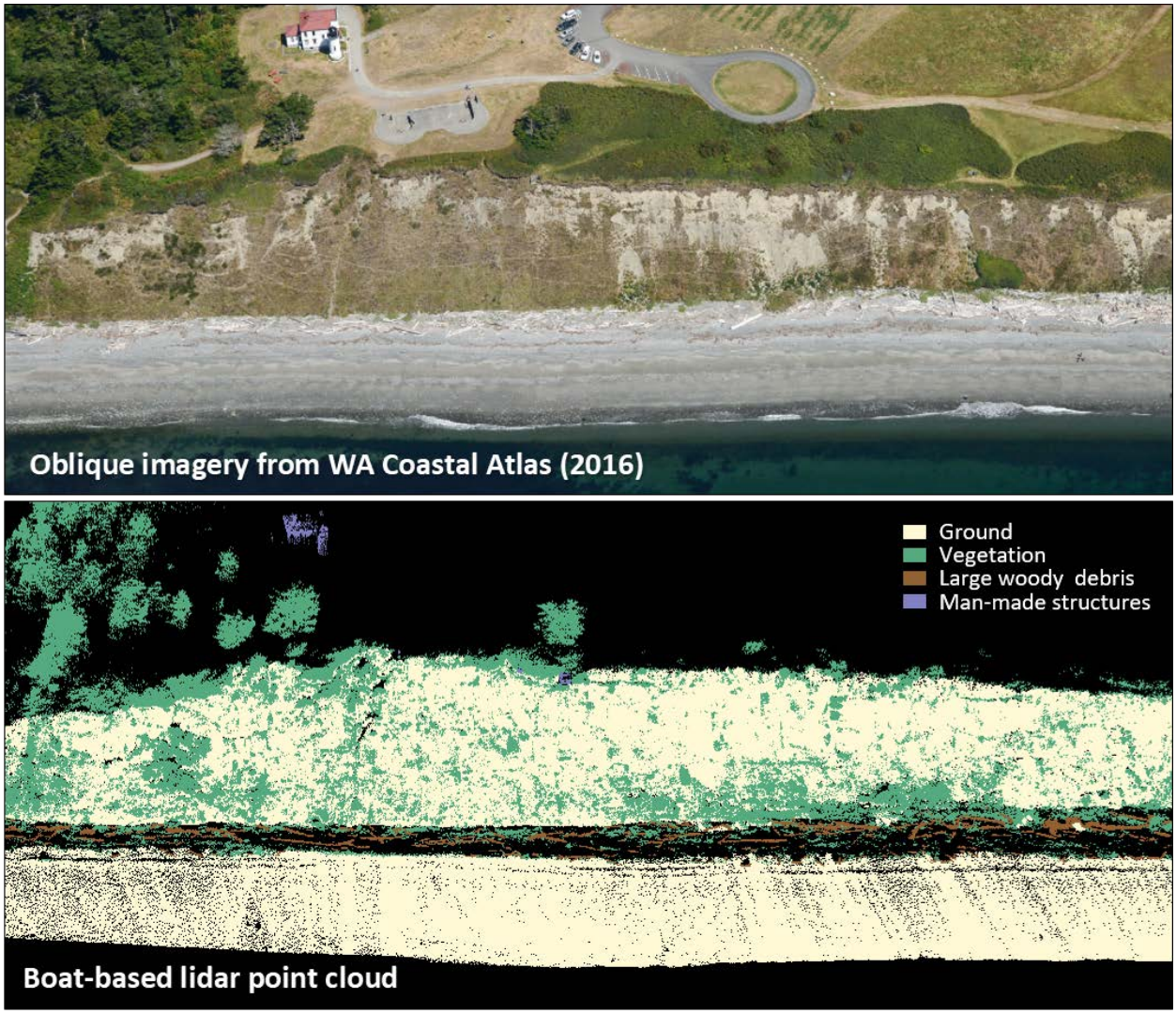

Figure E-1: Classified lidar point cloud of a bluff-backed beach on Whidbey Island

The feature classes can be isolated or temporarily removed from the point cloud for further quantification of individual classes and interpretation of the interaction of one class with another (Figure E-2). This is helpful, for example, when quantifying the amount of large woody debris on a beach, creating a map layer of shoreline armoring, or generating a DEM of the ground surface. Figure E-3 shows an example of removing vegetation to reveal the ground surface of a high bluff at Edgewater Beach in South Puget Sound. The overall point density on the bluff is lower where the vegetation was covering the ground; however, there are generally enough points to develop a high-resolution surface elevation model, which cannot be as readily achieved with other technologies.

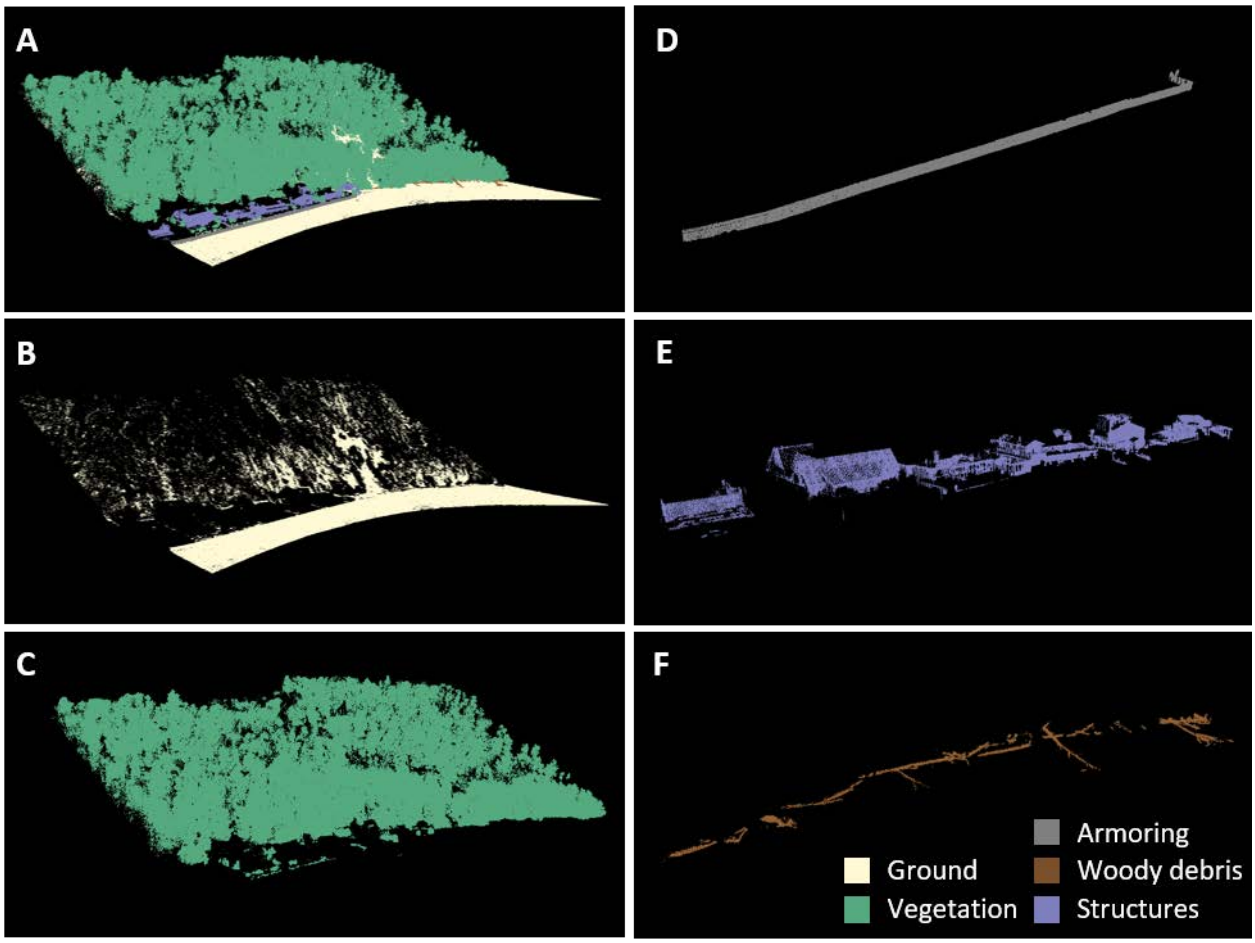

Figure E-2: Lidar point cloud of a shoreline reach with adjacent armored and bluff-backed beach, illustrating isolation of feature classes; (A) classified lidar point cloud, (B) ground surface only, (C) vegetation only, (D) shoreline armoring only, (E) man-made structures only, and (F) large woody debris only

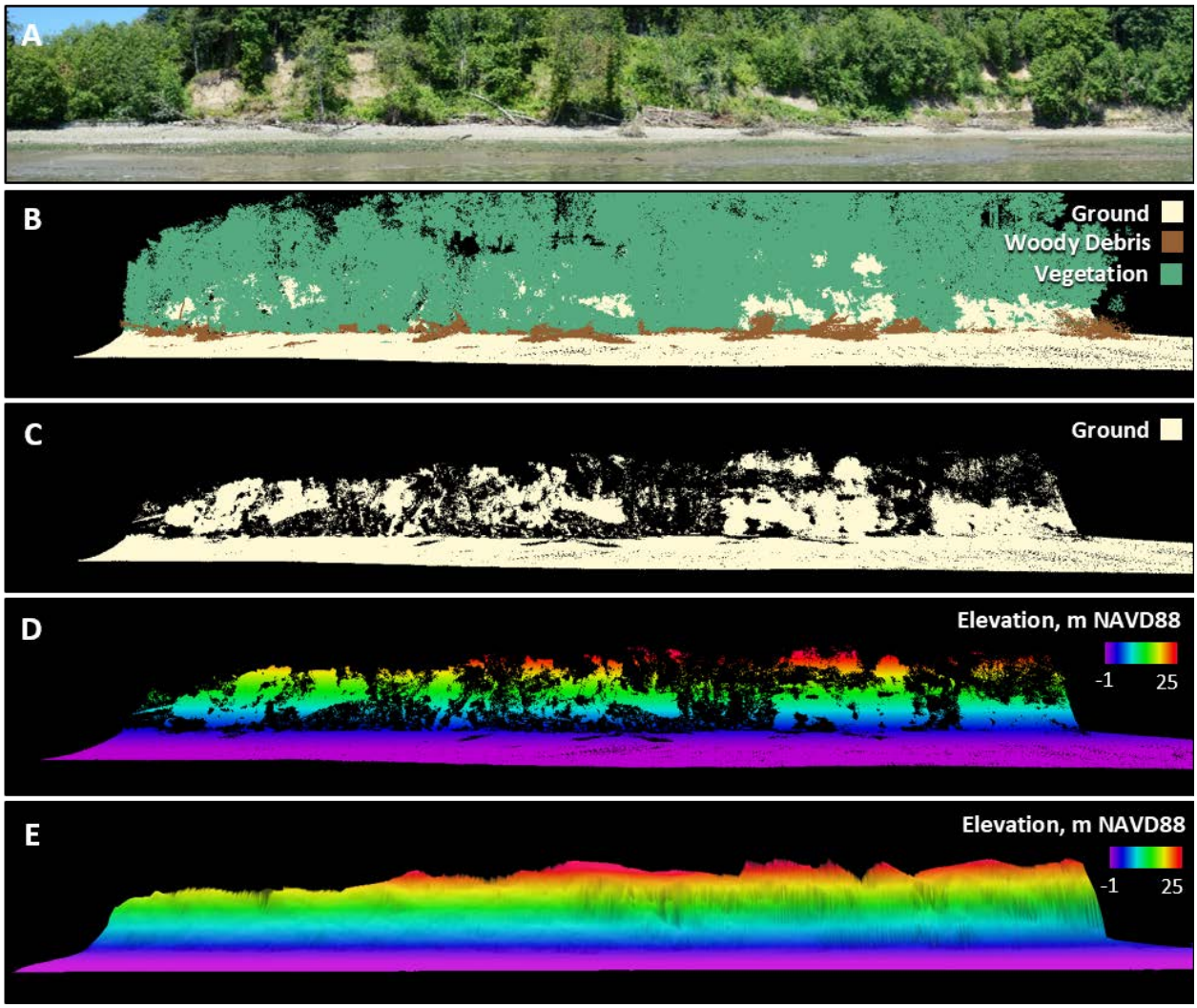

Figure E-3: Lidar point cloud of a vegetated coastal bluff; (A) shoreline photomosaic, (B) classified lidar point cloud showing vegetation, large woody debris, and ground, (C) lidar point cloud showing ground surface only, (D) lidar point cloud of ground surface colored by elevation relative to NAVD88, and (E) digital elevation model with 0.5-m resolution

For this project, with a survey objective to collect boat-based lidar data at the drift-cell scale efficiently, average point densities of 9 points per 0.5-m grid cell on the beach surface and 26 points per 0.5-m grid cell on the bluff face were obtained. The shorter the range between the boat and the shoreline, the higher the point density, with the best results achieved when the boat is 50 m or less from the shoreline. The high point density of the boat-based lidar point cloud allows for sub-decimeter details to be resolved and accurately measured to within about 10 cm or less. Figure E-4 illustrates details that can be seen on a bulkhead with the cross-beam and metal fasteners colored by intensity.

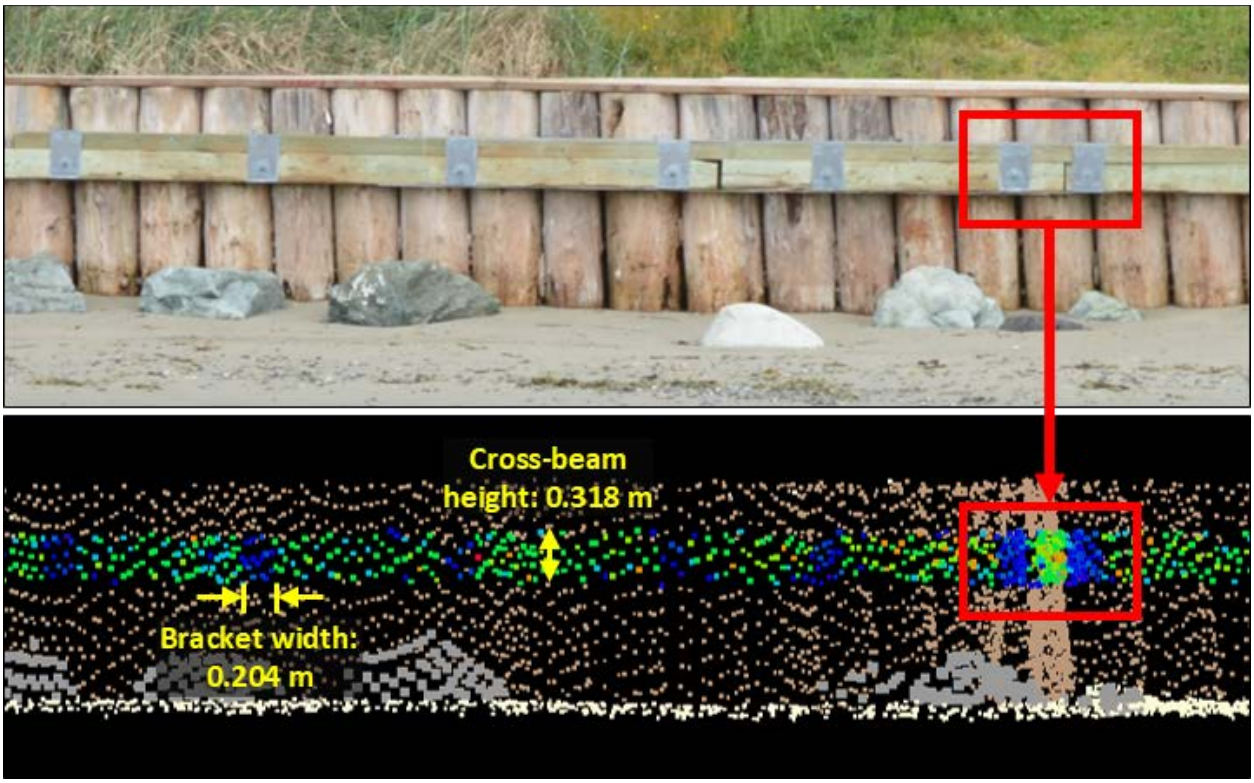

Figure E-4: Lidar point cloud of a wooden bulkhead; (A) shoreline photomosaic and (B) classified lidar point cloud with cross-beam and metal brackets colored by intensity

Beach and bluff morphometrics

Quantitative metrics of shoreline physical characteristics can be derived from DEMs or the lidar point clouds, for higher accuracy. Such metrics include: location of tidal datums, beach slope, beach width, bluff crest height, bluff slope, bluff toe elevation, and shoreline armoring elevations. These metrics can then be compiled and compared within and among drift cells to determine regional variability, such as differences between updrift and downdrift beaches and the effect of fetch, orientation, and other exposure variables.

Tidal datums

Collecting high-resolution, full coverage beach topography data enables the ability to precisely and accurately locate tidal datums on the beach face, such as Mean Lower Low Water (MLLW), Mean Tide Line (MTL), Mean Higher High Water (MHHW), and so on (Figure E-5). Because of the oblique look-angle of the laser scanner from the boat, accurate delineation of tidal datum contours beneath overhanging vegetation is possible. Knowledge about where tidal datums are located across the beach face is necessary for a variety of reasons, such as proper citing of backshore protection structures, locating jurisdictional boundaries, performing shoreline vulnerability assessments, planning sea-level rise adaptation, and standardizing beach metrics such as back beach width and shoreline armor encroachment.

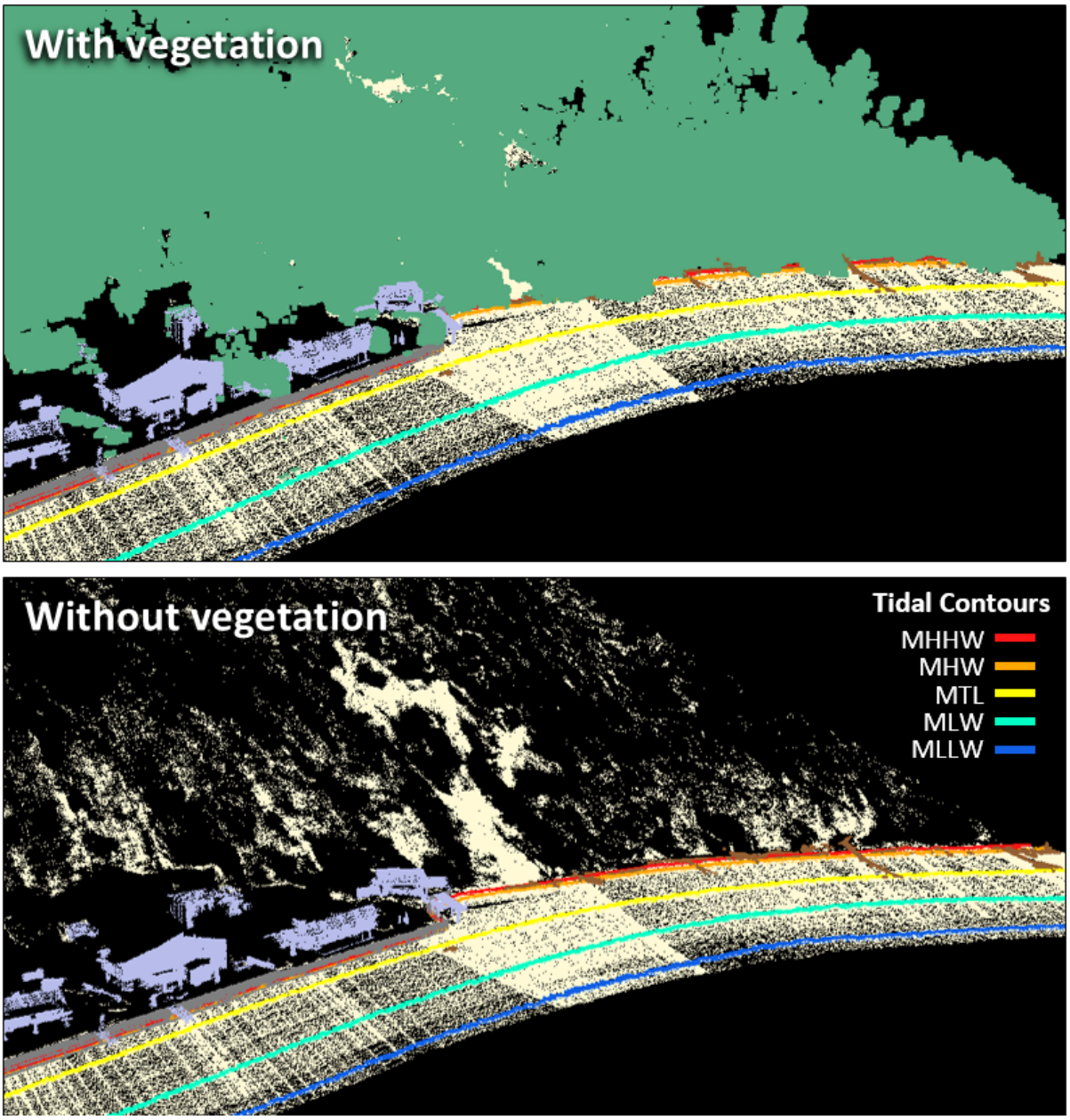

Figure E-5: Boat-based lidar allows for accurate location of tidal datum contours even when vegetation is overhanging the upper beach

Cross-shore profile extraction

An effective way to begin exploring physical features of the beach and bluff is by viewing cross-sections of the lidar point cloud and/or bare-earth DEM to identify parameters for one segment of shoreline at a time through the extraction of cross-shore profiles. Two-dimensional profiles can be extracted for any location within the lidar point cloud or DEM. In addition, because of the three-dimensional nature of the lidar data, the metrics derived from the cross-shore profiles can be applied to every location along the shoreline to provide a comprehensive view of the entire coast.

Typically, profiles are taken perpendicular to the shore for a cross-sectional view of the beach to examine morphological characteristics like beach slope, width, and the elevation of key features, such as the bluff or armor toe. Profiles can also be taken parallel to the shoreline along the bluff or beach face to examine the variability alongshore, if desired. Figure E-6 shows an example of two cross-shore coastal profiles extracted from the lidar point cloud north of Sandy Point near Bellingham of a bluff-backed beach where vegetation is partly obscuring the bluff face, though the ground surface can still be discerned.

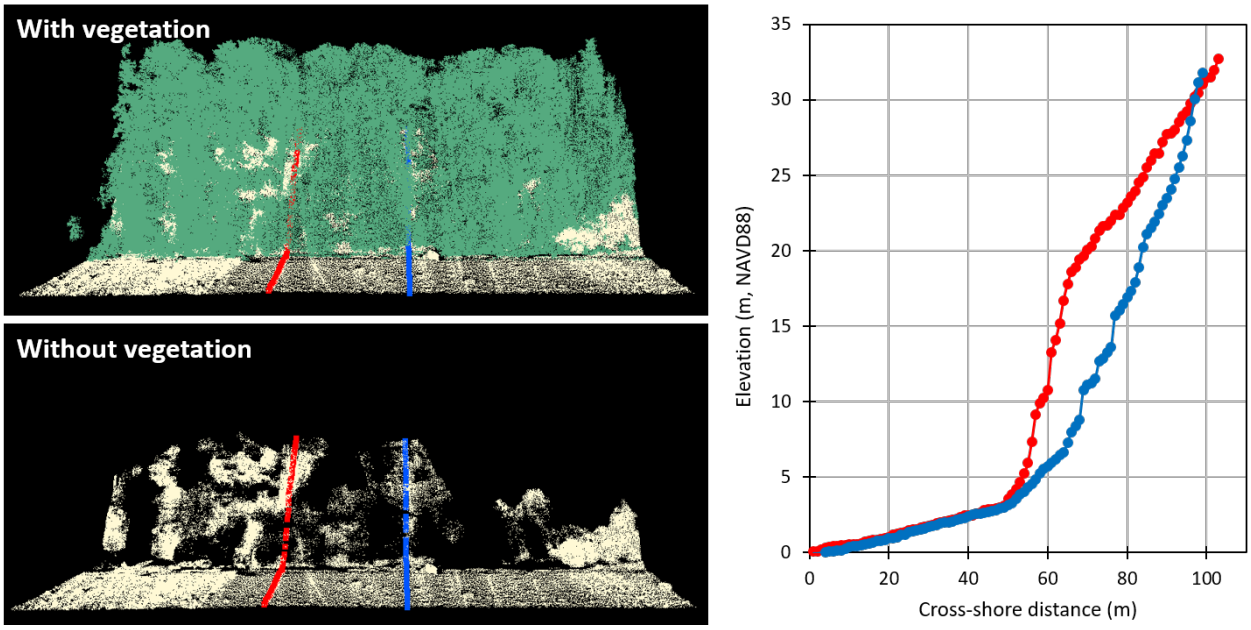

Figure E-6: Cross-shore profiles extracted from lidar point cloud of beach and bluff through dense vegetation (green)

Cross-shore profiles are an effective way to examine how beach elevation, slope, and width can change alongshore. Figure E-7 shows an example from the west side of Whidbey Island of how a shore-perpendicular structure can influence sediment accumulation on the beach face. The beach on the updrift (south) side of the approximately 3 m-wide by 65 m-long concrete outfall pipe is more gently sloping than the beach on the downdrift (north) side (7% vs. 11%) and extends further seaward by about 10 m.

A set of pre-defined transects can be established for a reach of shoreline that are extracted each time a new dataset is collected to compare change over time. The profiles from the boat-based lidar data can also be compared to an airborne dataset or other coastal profiles collected for any numbers of reasons. Automated methods for extracting morphometric parameters (e.g., bluff toe, bluff crest, beach slope, beach width) from cross-shore profiles can be developed in order to efficiently identify features and characterize beaches and bluffs at a drift-cell scale.

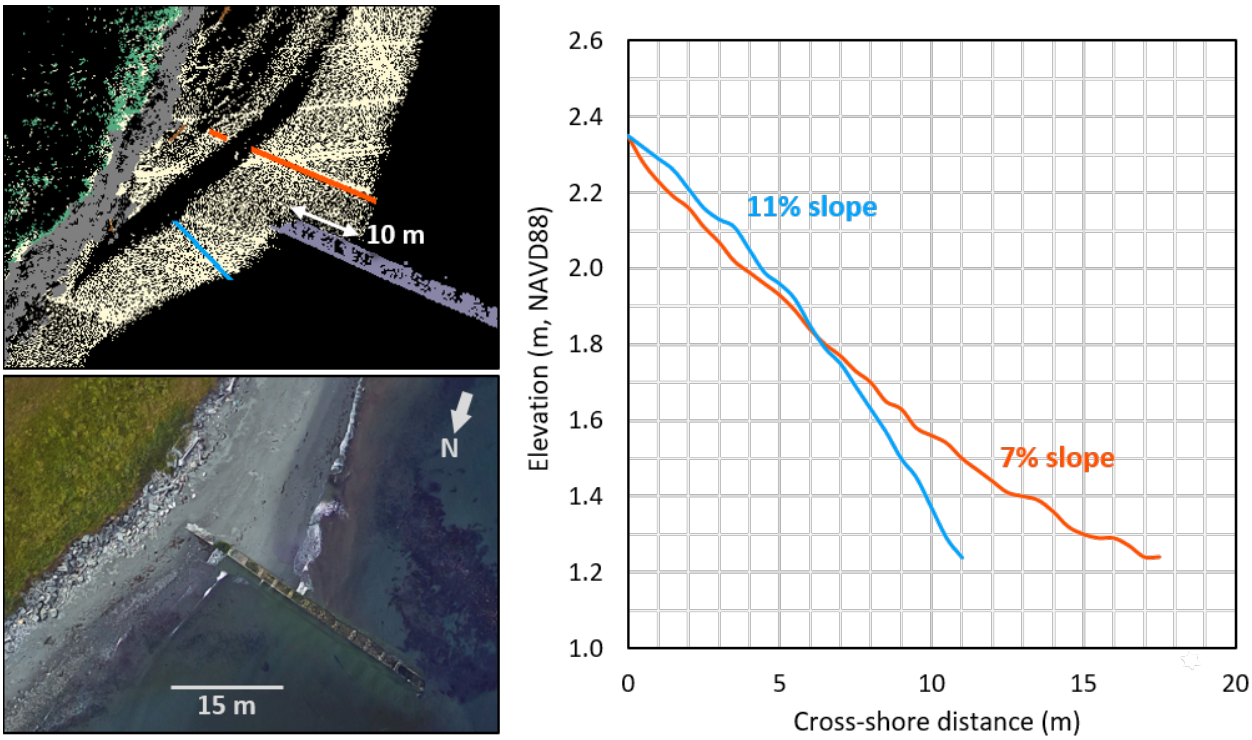

Figure E-7: Cross-shore profiles extracted from lidar point cloud of beach face from either side of a concrete outfall pipe

Beach and bluff slope and width

The slope of the beach and bluff are important indicators of condition and relative stability. A steep beach may indicate an erosional condition, a sediment budget deficit, or a divergence in sediment transport while a mild beach slope may suggest an accretional condition, an abundance of sediment, or a convergence in sediment transport. Bluff slope is typically controlled by local geology and the variability in slope across the bluff face can reveal distinct geologic units and differences in composition and erodibility. The reported slope and width of a beach depends on the cross-shore limits across which they are measured. Typically, the lower beach face is wider and flatter than the mid or upper beach. The measurement of beach slope and width must be standardized to compare beaches from different locations around Puget Sound. Here, we define beach slope and width between MTL and MHHW or between MTL and the bluff or armor toe, if MHHW is higher than the toe feature.

The slope of a beach or bluff can be measured from individual cross-shore profiles. In Figure E-8, an example from the west side of Whidbey Island, the average slope of the bluff is much steeper than the slope of the beach (53% vs. 5%). Moreover, the bluff slope varies along its face, ranging from 42-87% slope. A three-dimensional surface of the slope can be made from the bare-earth DEM to examine how the slope varies across the beach or bluff per grid cell rather than along one cross-shore location (Figure E-8, lower right). Here, the 0.5-m bare-earth DEM was used to create a slope surface in ArcGIS where every 0.5-m grid cell has a calculated slope value. The slopes were binned into three categories (low, medium, and high) to highlight low-sloping and steeply-sloped areas on the beach and bluff surface.

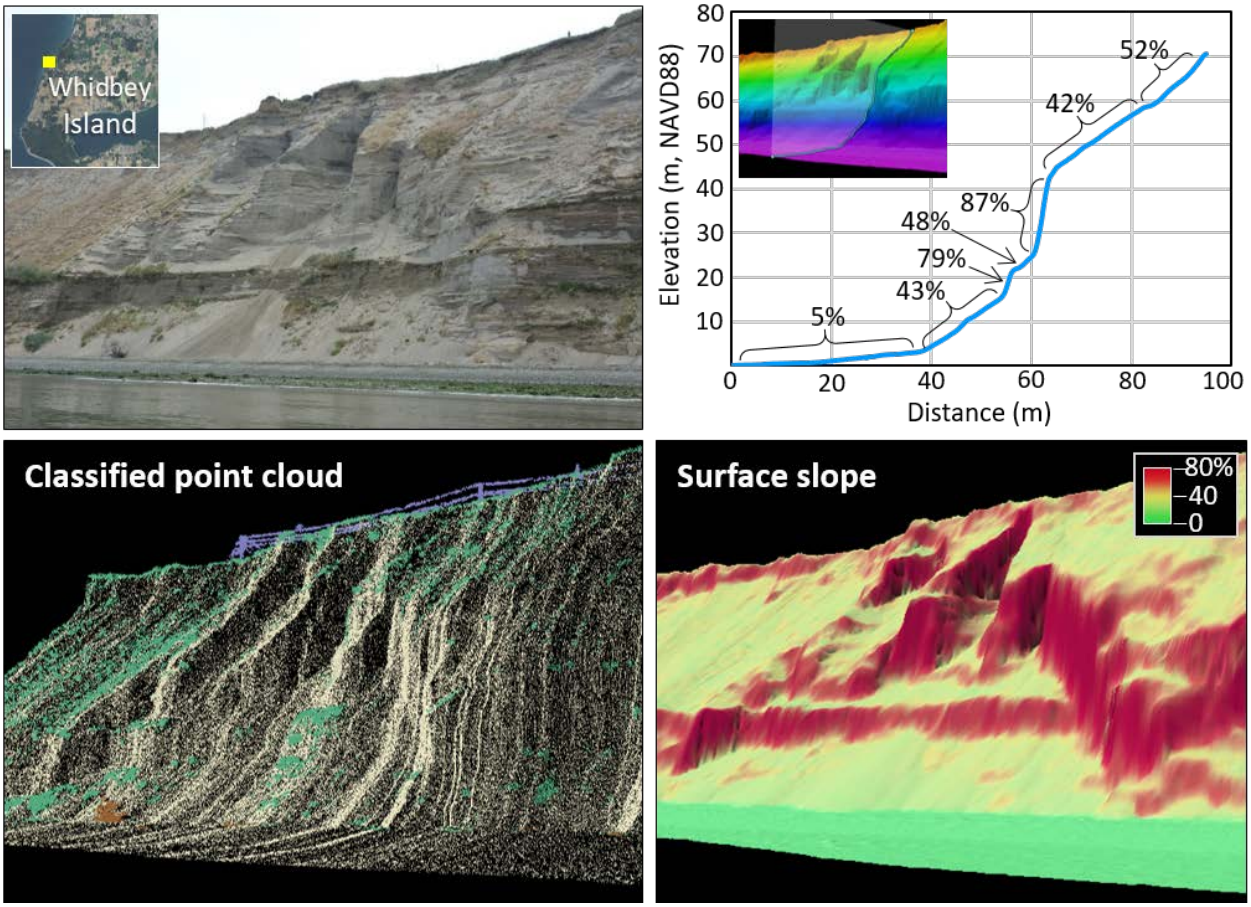

Figure E-8: Beach and bluff slope illustrated using a slope surface created from the DEM and a cross-shore profile extracted from the lidar point cloud

Using the same elevation contours as for slope, the horizontal width of the beach can also be calculated and compared within and among drift cells. In Figure E-9, an example near Ledgewood Beach on Whidbey Island, the relationship between beach slope and width within a drift cell are shown as the shoreline progresses from a bluff-backed beach at the north end of the drift cell to a low-lying spit at the south end of the drift cell, terminating at the entrance to a coastal lagoon. At the north end, the bluff backing the beach acts as a source of sediment to the drift cell. Here the beach is more steeply sloped and composed of coarser material (as seen in digital photos collected at the time of that boat-based lidar survey). Here, the sediment transport direction is to the south and a spit has formed at the south end of the drift cell. The southward end of the spit is more gently sloping than the northward end, with a wider beach face consisting of slightly finer material.

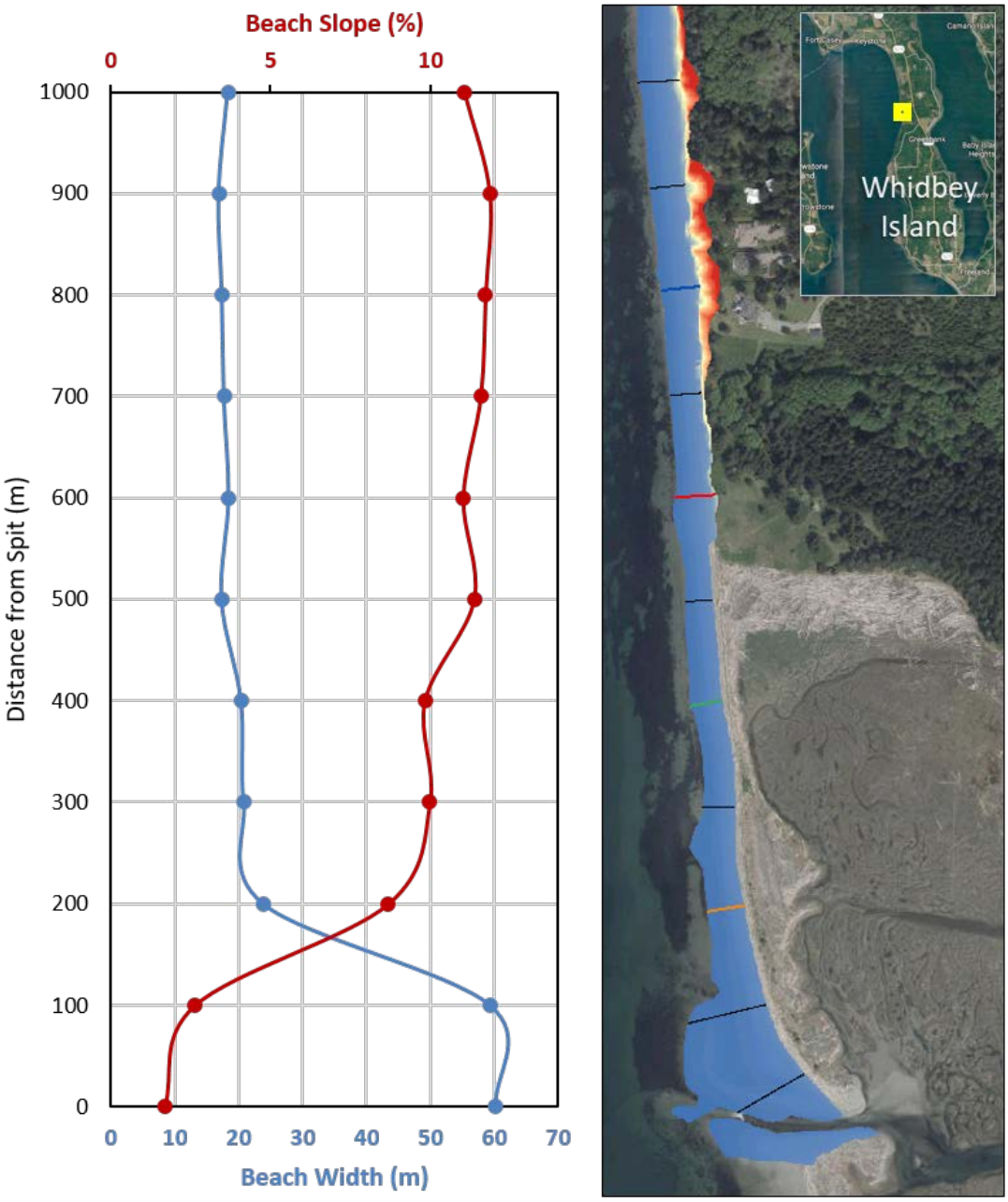

Figure E-9: Beach slope and width alongshore variability from a bluff-backed beach (sediment source) to a spit (sediment sink) backed by a lagoon south of Ledgewood Beach on Whidbey Island

Back-beach width

The back beach, or backshore, is the section of the beach extending landward from mean higher high water (MHHW) to the point where there is an abrupt change in slope or material (e.g., bluff, dense vegetation, salt marsh, or lagoon). It is typically a horizontal platform which may slope gently landward, and is divided from the foreshore by the crest of the highest beach berm. While stable enough to support vegetation, the back beach usually has only sparse coverage or pioneer

species, as it is regularly disturbed by wave run-up during severe storms or exceptionally high tides. The back beach is ecologically important and serves as a refuge for invertebrates, shorebirds, and other species to use for foraging, spawning, roosting, and nesting. It is an area in which large woody debris, wrack, and sediment accumulates. The back beach buffers the upland from erosion and provides nutrients, microhabitats, and ecosystem services.

Boat-based lidar efficiently maps the variability in back-beach width along natural and armored shorelines. The back beach can be measured for single cross-shore locations on the point cloud or from a profile extracted from the point cloud (Figure E-10). It can also be identified by using a slope surface of the DEM, looking for flat or gently sloping area between MHHW and the upper edge of the beach (Figure E-10, far right). Once delineated, the back beach area can be quantified and compared between and among drift cells.

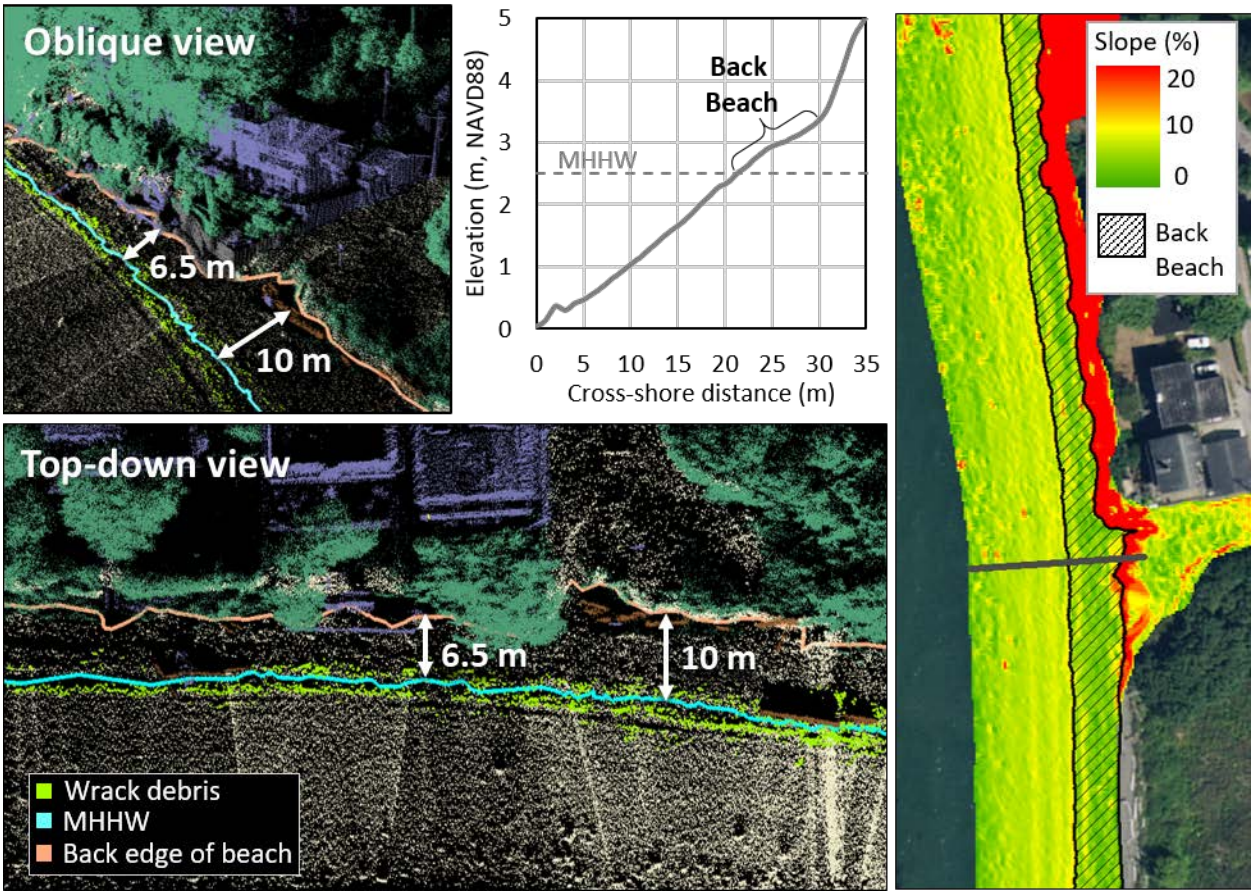

Figure E-10: Example showing variation in back beach width and delineation of a back beach polygon using slope surface for a segment of shoreline at Neptune Beach, north of Sandy Point

Depending on shoreline morphology and water level during the time of the survey, the back beach may be shadowed by the berm crest. If an upper boundary can be distinguished, such as the toe of a bluff, the back beach can still be measured in the lidar point cloud even if there is a zone without direct ground returns from the laser scanner (Figure E-11).

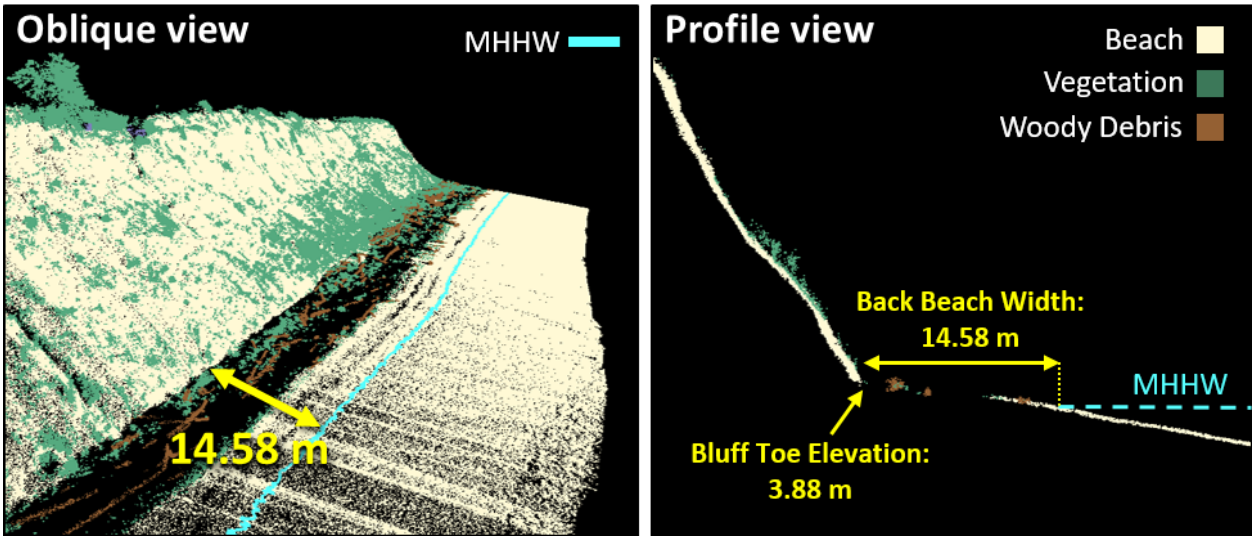

Figure E-11: Back beach shadowed in the lidar data by the berm crest, but is still identifiable between Mean Higher High Water (MHHW) and the bluff toe

As with beach slope and width, the back beach can vary within and among drift cells. Shoreline armoring has been shown to adversely affect whether a back beach is present either directly, through encroachment of the armor on the beach, or indirectly, by disrupting downdrift sediment supply. It is important to maintain sediment supply within a drift cell in order to sustain the back beach environment.

Coastal morphology inventory

With standardized methods for quantifying coastal morphology, a comprehensive inventory can be developed for all Puget Sound beaches. This inventory would allow for comparisons between and among drift cells, which would enhance our understanding of coastal processes and enable prioritization of resources for restoring Puget Sound shorelines.

As an example, Table E-1 provides a list of four morphological parameters (beach width, beach slope, bluff or armor toe elevation, and the vertical difference between the bluff or armor toe and MHHW) that were extracted from 16 cross-shore profiles taken from two boat-based lidar point clouds of the Edgewater Beach drift cell. In fall 2016, 800 ft of shoreline armor was removed from this drift cell and boat-based lidar surveys were conducted before and after shoreline armor removal in 2015 and 2017. A map of the cross-shore profiles from the drift cell is shown in Figure E-12 for reference.

Table E-1 lists morphometrics for several cross-shore profiles within one drift cell to compare and contrast alongshore differences. Once information about other drift cells is tabulated, comparisons between and among drift cells around Salish Sea can be made of the same morphological features and shoreline characteristics.

Table E-1: Morphometrics extracted from cross-shore profiles of the boat-based lidar point clouds collected at Edgewater Beach in 2015 and 2017 [excerpted from Weiner and Kaminsky (2018)]

Profile	Beach width (m) MTL-to-MHHW		Beach slope (%) MTL-to-MHHW		Toe elevation and type (m, NAVD88)				Vert. difference (m) Toe-to-MHHW	
	2015	2017	2015	2017	2015		2017		2015	2017
1.00	18.57	18.37	6.4	6.4	3.34	bluff	3.46	bluff	-0.28	-0.31
1.03	12.41	12.21	8.2	7.7	2.89	armor	2.77	armor	0.25	0.38
1.07	15.41	15.59	7.7	7.6	3.38	bluff	3.49	bluff	-0.24	-0.34
1.09	11.96	11.69	9.0	8.3	2.98	armor	2.81	armor	0.16	0.33
1.18	7.95	8.81	9.0	8.5	2.41	armor	2.46	armor	0.74	0.69
2.00	12.36	13.33	9.0	8.6	3.05	armor	3.08	armor	0.10	0.06
2.04	12.92	13.23	9.1	8.6	3.17	bluff	3.08	bluff	-0.03	0.06
2.06	8.60	11.03	8.2	9.0	2.39	armor	2.86	bluff	0.75	0.29
2.10	6.60	11.51	10.3	10.2	2.36	armor	3.49	bluff	0.79	-0.34
2.11	9.21	14.96	8.5	7.9	2.52	armor	3.99	bluff	0.63	-0.85
3.00	11.68	13.05	6.9	8.1	2.56	armor	2.96	bluff	0.59	0.19
3.01	8.98	14.01	9.3	8.4	2.60	armor	3.60	bluff	0.55	-0.45
3.02	12.86	15.02	7.9	7.9	2.88	armor	3.16	bluff	0.26	-0.01
4.00	14.73	14.59	8.0	8.1	3.50	bluff	3.70	bluff	-0.35	-0.56
4.04	15.37	15.68	7.7	7.3	3.38	bluff	3.08	bluff	-0.23	0.06
4.06	13.83	15.89	8.5	7.2	3.49	bluff	3.08	bluff	-0.34	0.06

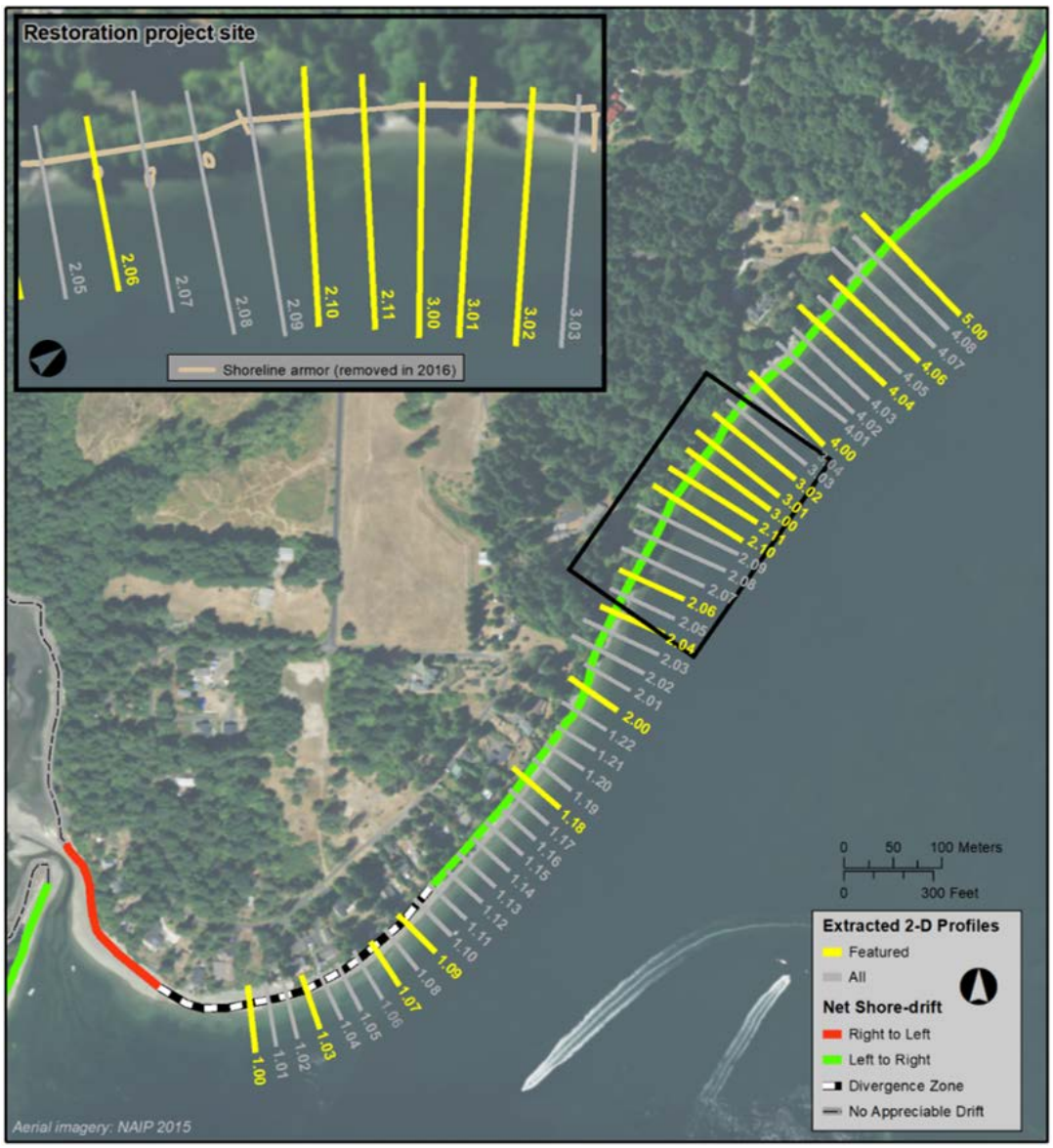

Figure E-12: Map showing the location of cross-shore profiles extracted from the boat-based lidar point clouds collected at Edgewater Beach in 2015 and 2017 [excerpted from Weiner and Kaminsky (2018)]

Armored shoreline inventory and characteristics

Shoreline armor varies in size, shape, location, and impact. Shoreline armoring can lead to coarsening of the beach sediments and steepening of the beach slope. In some cases, shoreline armor is linked to negative downdrift effects such as a decrease in sediment supply and localized scour due to end effects. It can also be associated with reductions in riparian vegetation, large woody debris, wrack, and back beach width, all of which provide critical habitat and nearshore ecosystem functions.

Accurate quantification and inventory of Puget Sound shoreline armor is crucial for assessment of impact and restoration opportunities. High-resolution point clouds from boat-based lidar allow

for detailed mapping of shoreline armor attributes such as type, length, elevation, height, slope, and condition within the context of shoreform and beach morphology. The point cloud inventory of armor attributes allows for precise measurement and change detection that is accurately georeferenced in 3D map space.

Shoreline armor encroachment

The lower shoreline armor is located on the beach profile, the more impact is has on nearshore processes, beach access, as well as the accumulation of beach wrack and large woody debris that have high ecological importance. The relative encroachment of shoreline armor can be quantified by the difference in elevation between the toe of the armoring and mean higher high water (MHHW). Following the convention of Dethier et al. (2016), positive vertical differences indicate the toe is lower than MHHW, exhibiting encroachment, while negative differences indicate the toe is higher than MHHW, which is conducive for a back beach to develop. Dethier et al. (2016) found that where relative encroachment exceeds +1.44 ft (i.e., the toe of shoreline armor was more than 1.44 ft below MHHW, vertically), there is a decline of logs, wrack, and invertebrates on the beach.

Through the collection of 3D point cloud data, boat-based lidar provides this metric, as well as the ability to quantify the horizontal encroachment of shoreline armor measured to the upper edge of the beach (intersection with a bluff or upland area) *or* to the location of MHHW as projected along the beach slope without armor. Figure E-13 illustrates both vertical and horizontal encroachment of shoreline armor measured from the lidar point cloud collected from Maury Island. Because the armor toe is 0.9 m (2.95 ft) lower than MHHW, this bulkhead exhibits encroachment on the upper beach; furthermore, +2.95 ft is greater than the +1.44 ft-threshold and, in fact, this beach is devoid of logs and wrack in front of the shoreline armor.

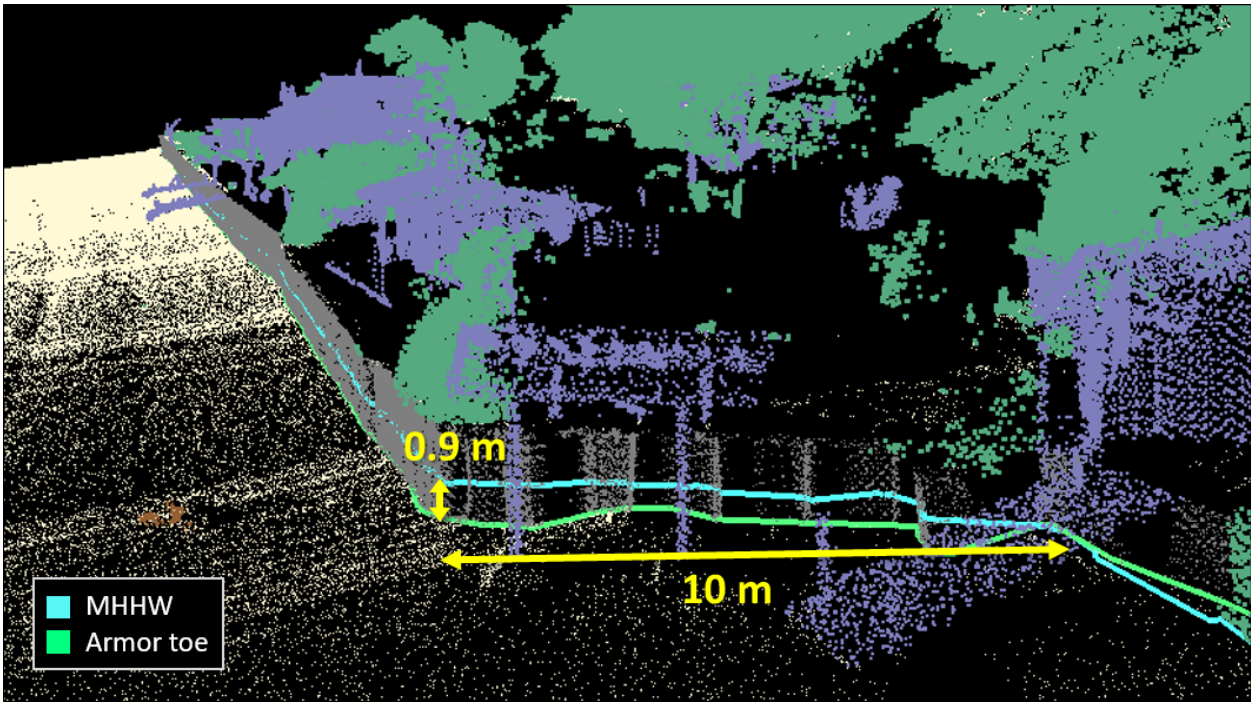

Figure E-13: Shoreline armor encroachment on the upper beach, measured as both a vertical distance below MHHW and a horizontal distance from the upper edge of the beach

Figure E-14 demonstrates the variability in relative encroachment via cross-shore profiles extracted from the lidar point cloud at three locations along Three Tree Point near Burien. For the profile on the left of the graphic (colored green), the toe of the armoring is 2.2 m below MHHW. Therefore, it has a relative encroachment value of +2.2 m (+7.2 ft). The profile in the center of the graphic (colored red) shows the armor toe is 0.7 m below MHHW, for a relative encroachment of +0.7 m (+2.3 ft). The profile on the right (colored blue) is taken across a stretch where the upper beach has accumulated large woody debris. The toe of the large woody debris is approximately 0.1 m above MHHW, for a relative encroachment value of -0.1 m (-0.3 ft).

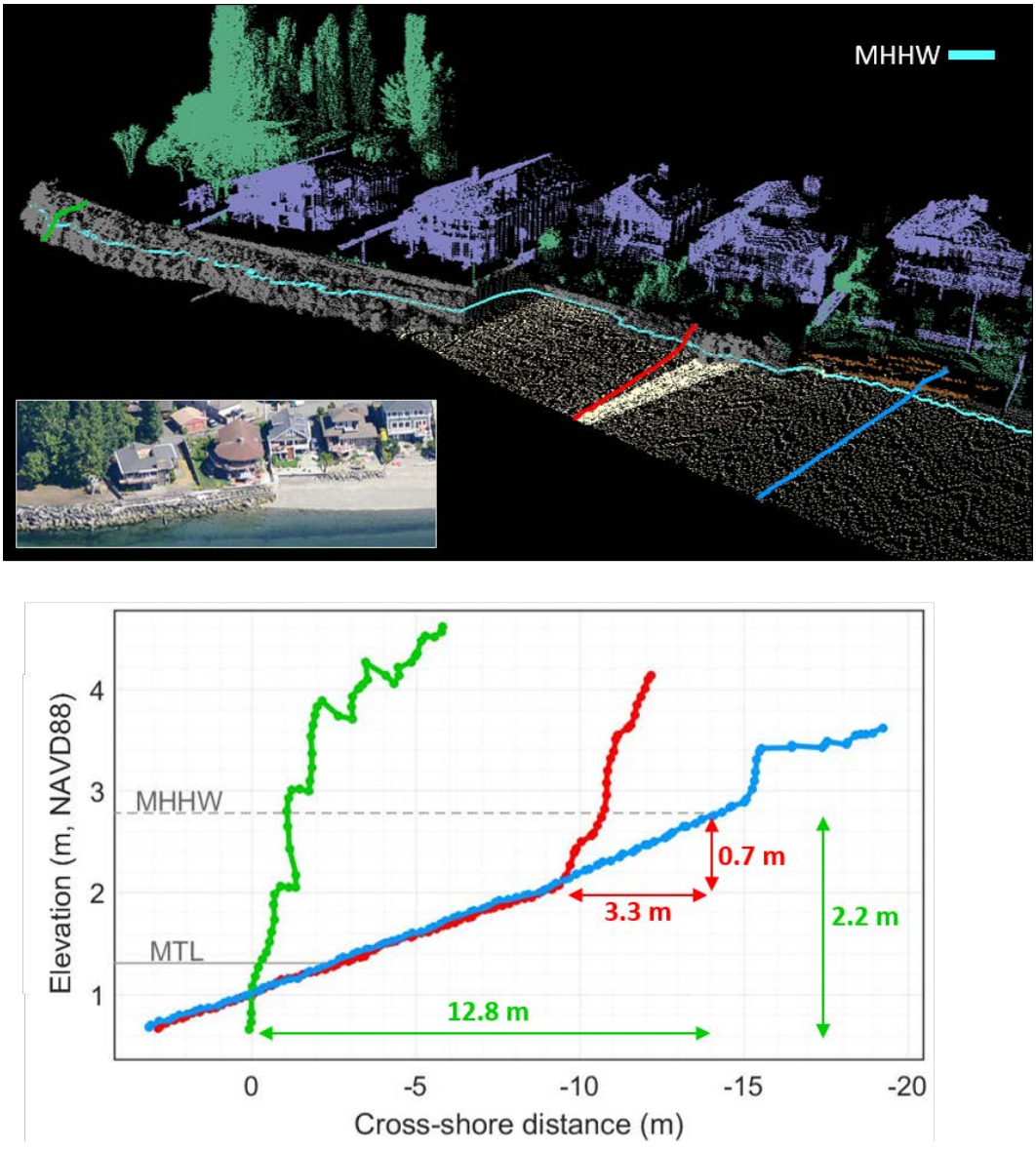

Figure E-14: Cross-shore profiles extracted from the lidar point cloud of Three Tree Point to compare relative encroachment of armor onto the beach profile compared to the adjacent armored vs. unarmored shoreline with LWD accumulation along the back beach

Documenting shoreline armor position and attributes

The combination of high-resolution point clouds and photos from field surveys enables the identification and measurement of a wide variety of shoreline modifications. The type of armoring, structure dimensions (e.g., length, height, slope), and position in horizontal and vertical space can all be accurately determined. Figure E-15 shows a sampling of shoreline armor structures and their individual components that have been mapped and quantified from the lidar point cloud. Comprehensive and precise geospatial mapping of shoreline armor attributes enables tracking of structure condition and modifications. Accurate quantification and inventory of Puget Sound shoreline armor is crucial for assessment of impact and restoration opportunities.

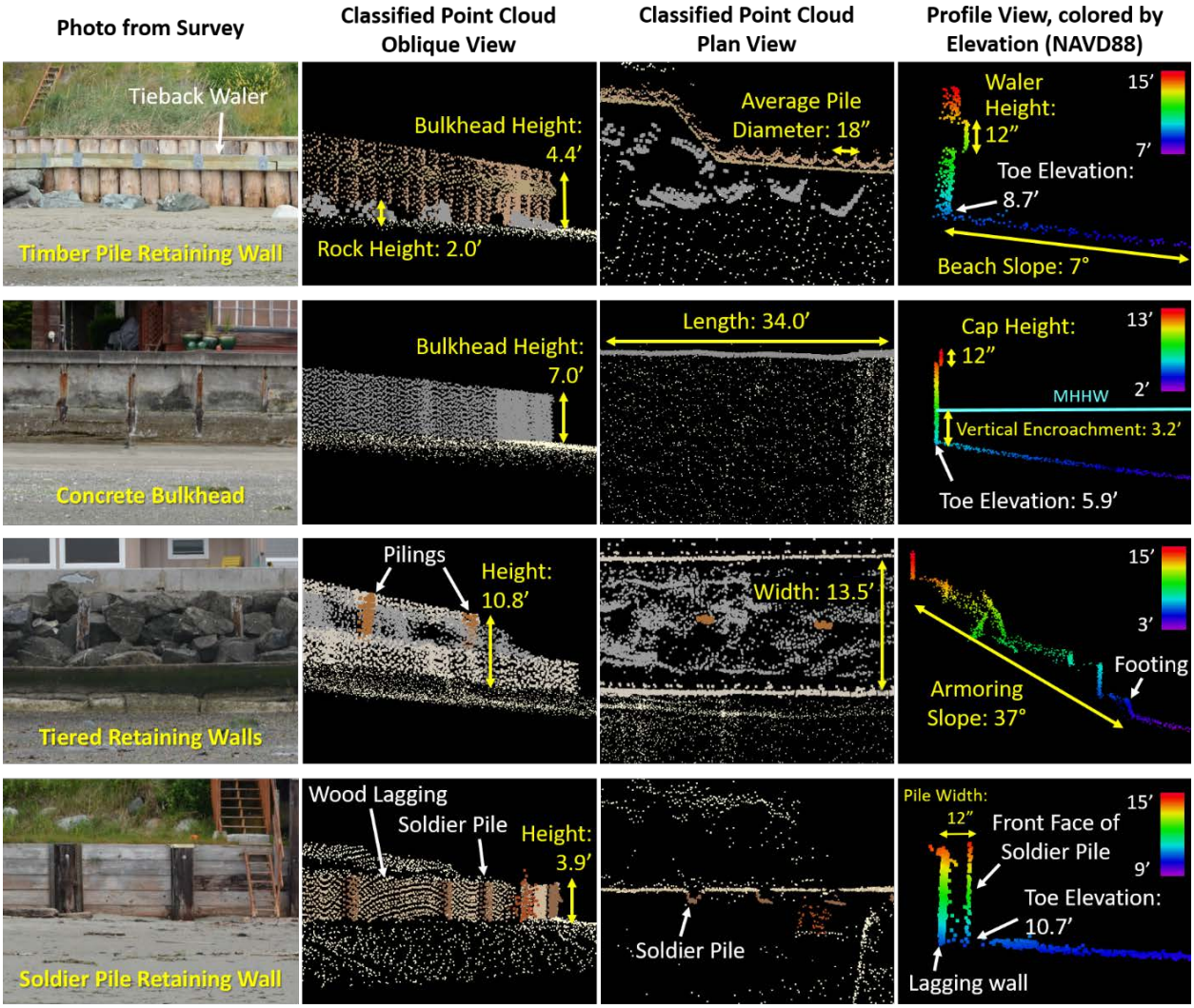

Figure E-15: Examples of shoreline armoring and the quantitative metrics that can be determined from boat-based lidar data to characterize the armoring in 3D space

Once shoreline armor has been identified in the lidar point cloud, parameters that quantify these shoreline modifications can be tabulated in ArcGIS as an attribute table associated with a map layer. Figure E-16 shows an example where adjacent installations of shoreline armor has been

classified and quantified at Three Tree Point near Burien, documenting the average length, width, toe elevation, height, slope, and vertical encroachment of the armor along with shoreline habitat features: large woody debris and overhanging vegetation.

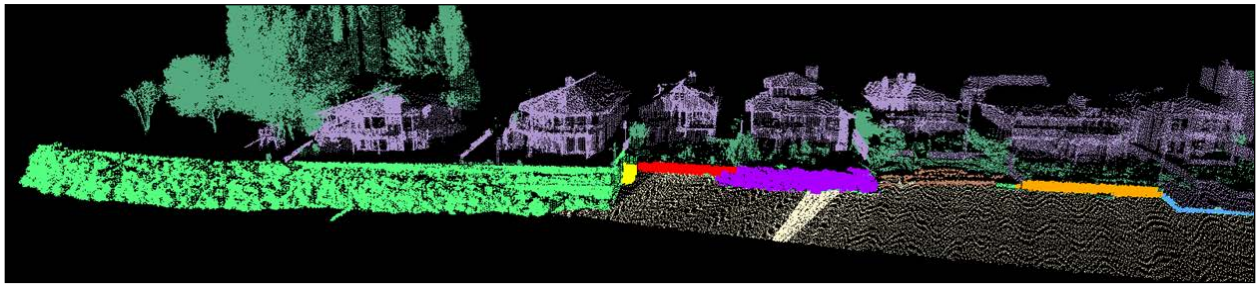

FID	Type	Length (ft)	Width (ft)	Toe Elev. (ft)	Height (ft)	Vertical Encroachment rel. to MHHW (ft)	Slope (deg)	Area of LWD (ft^2)	Area of Overhang Veg. (ft^2)
1	rip-rap	246.8	18.7	2.6	12.8	6.6	37	0	0
2	stairs	3.8	9.2	6.7	5.7	2.4	35	0	0
3	bulkhead	39.4	---	8.6	3.6	0.5	90	0	0
4	rip-rap	58.4	7.5	7.0	5.9	2.1	43	0	0
5	drift logs	46.2	13.5	10.1	---	-1.0	---	20	0
6	bulkhead	43.0	---	9.7	3.3	-0.6	78	0	0
7	bulkhead	37.7	---	8.7	2.3	0.5	90	0	0

Figure E-16: Example shoreline armor inventory for stretch of beach along Three Tree Point, showing various physical measurements extracted from boat-based lidar data

Physical habitat features

Boat-based lidar also detects measurable physical quantities related to ecological environment and nearshore habitat. These physical habitat features include the amount of overhanging vegetation, large woody debris, or beach wrack present on the beach. Upland development and shoreline modification may be correlated to these habitat features, and these findings can be compared to conditions at undeveloped shorelines.

Overhanging vegetation

Shade provided by the overhanging canopies of trees adjacent to the shoreline is important for moderating summer temperatures and moisture of the upper intertidal zone important for the spawning of surf smelt, a common forage fish in Puget Sound (Penttila, 2002). Overhanging vegetation is also important for detritus input and invertebrate habitat on the upper beach.

Traditional methods for assessing overhanging vegetation involve qualitatively approximating the alongshore length of upper beach that is shaded vs. unshaded or the use of a tape measure to quantify distance. In contrast, boat-based lidar makes it possible to readily quantify the extent of overhanging vegetation without having to make physical measurements in the field. Figure E-17 shows example cross-sections of a lidar point from Maury Island, where the cross-shore distance of overhanging vegetation varies from no overhang (Profile C) to a distance of 8.5 m (Profile B). The height of the overhanging vegetation above the beach also varies and can be easily quantified in the lidar point cloud. Vegetation width and height above the beach can be used to calculate solar incidence.

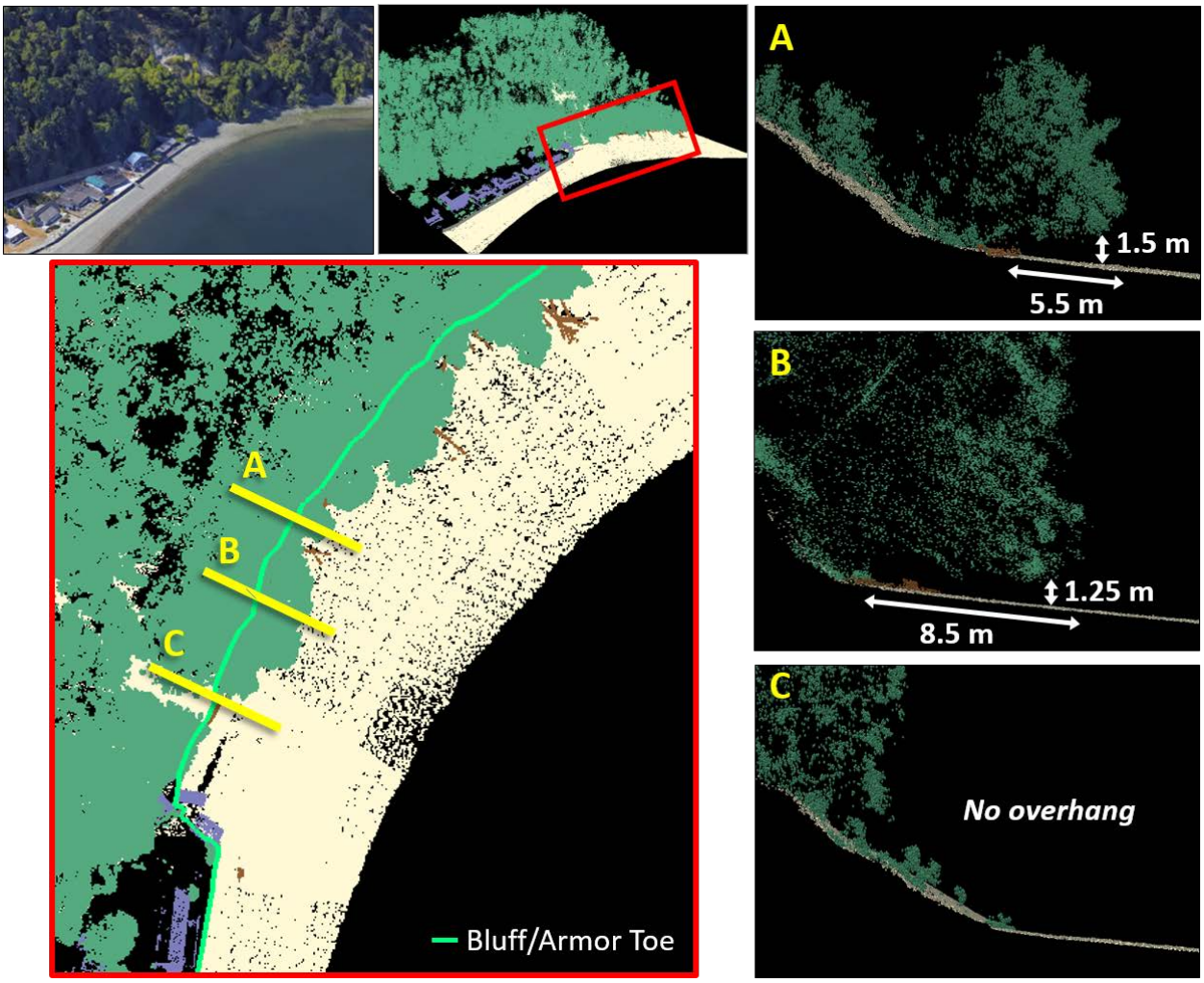

Figure E-17: Three cross-sections of the lidar point cloud from Maury Island, showing how dimensions of overhanging vegetation can be quantified (A and B) and a location with no overhanging vegetation (C)

The overhanging tree canopy can be delineated where it is landward of the upper edge of the beach, extracted from the rest of the vegetation, and intersected with the ground surface DEM to quantify how much of the beach is covered in 2D space (area), as well as the elevation of the beach under the vegetation (Figure E-18). In the example shown in Figure E-18, 86% of the unarmored, bluff-backed shoreline has overhanging vegetation present on the upper beach, whereas none of the armored shoreline has any overhanging vegetation present. The area of the upper beach covered by vegetation is 905.5 m^2, and the average elevation of the beach underneath the vegetation is 2.6 m, ranging from 1.4 to 3.6 m NAVD88.

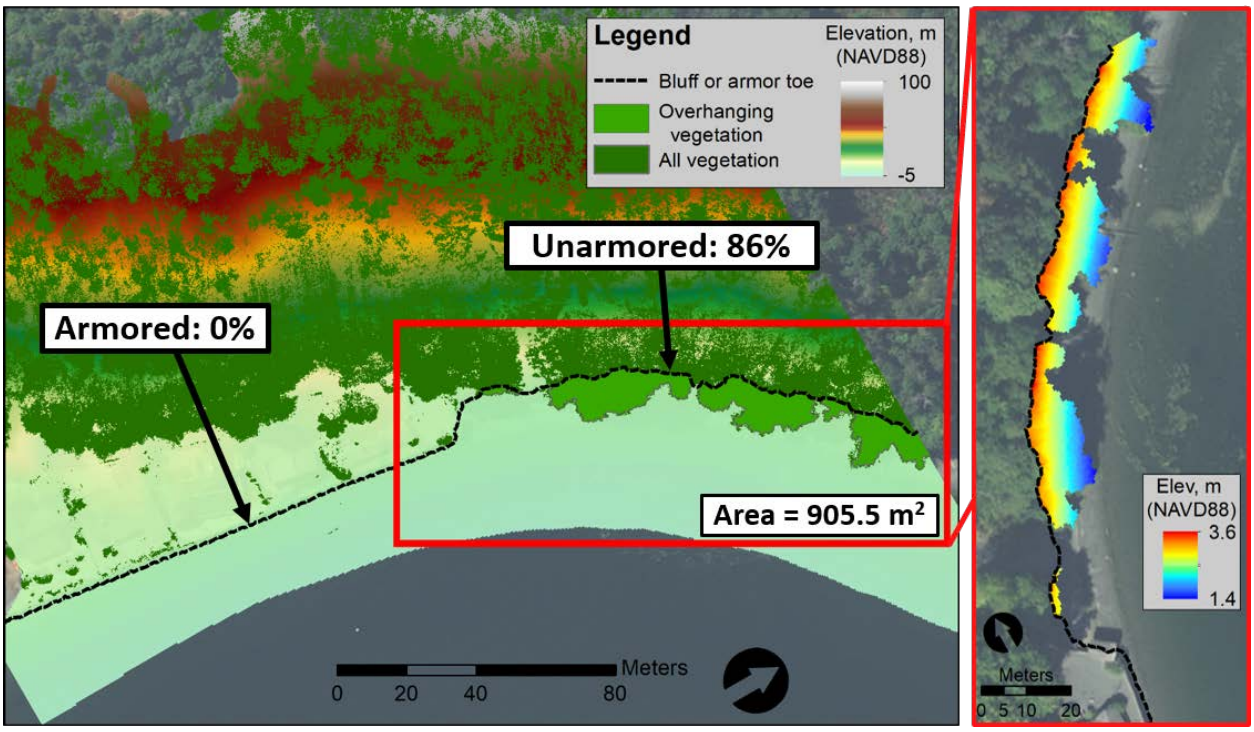

Figure E-18: Percent of shoreline with overhanging vegetation along an armored vs. unarmored reach (left); beach surface elevation under the vegetation (right)

Large woody debris

Large logs and downed trees that accumulate on the upper beach are an important part of the beach morphology and ecosystem. Large woody debris has been shown to increase the abundance and diversity of invertebrates that are important to juvenile salmon and the food web (Dethier et al., 2016; Sobocinski et al., 2010; Toft et al., 2007). In addition to providing habitat to invertebrates, large woody debris can also dissipate wave energy, enhance local sediment deposition, and help to stabilize shorelines.

After the point cloud is classified and the large woody debris is identified, it can be isolated from the point cloud and the area of the beach covered by large woody debris can be quantified (Figure E-19). In the example from Maury Island in Figure E-19, the large woody debris encompasses an area of 128.3 m^2 on the upper beach.

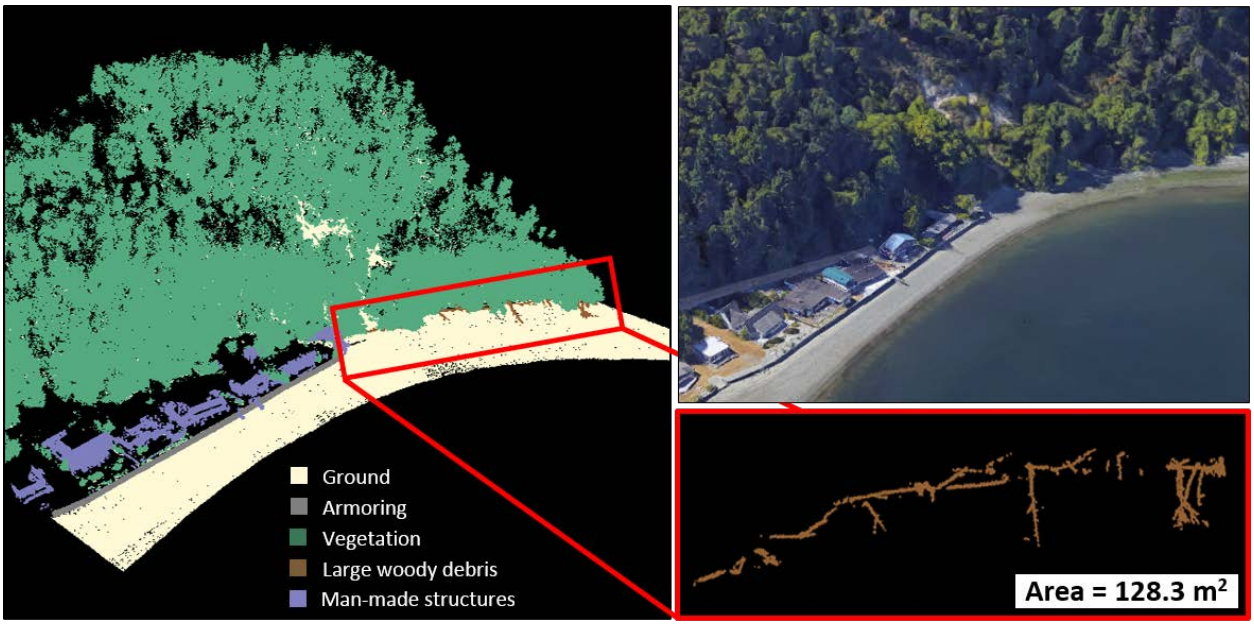

Figure E-19: Isolating and quantifying amount of large woody debris present on upper beach beneath overhanging vegetation

In addition to quantifying the total amount of large woody debris present, the size and quantity of individual logs and their location across the beach can also be determined (Figure E-20). This is possible as long as there is not too much overlap between the logs. Figure E-20 shows an example from Whidbey Island where the logs are sufficiently dispersed to discern individual logs, allowing them to be counted and measured, both in length and width. However, when logs are overlapping or shadowed by other logs, their actual size may be masked by adjacent logs, causing the true volume of large woody debris present to be potentially underestimated.

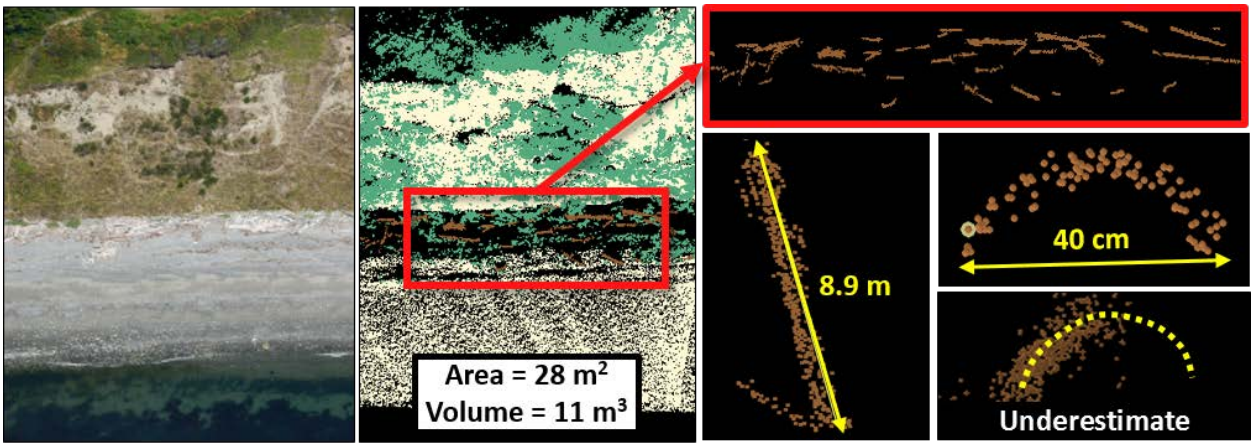

Figure E-20: Measurements of individual logs present on the upper beach

Not only can the amount of large woody debris present on a beach be compared within one site to see, for example, how it varies with the presence of shoreline armoring, but the amount of large woody debris can also be compared across many sites throughout Puget Sound (Figure

E-21). Figure E-21 shows there is a higher concentration of large woody debris per 1-m of shoreline along a spit at the north end of Dabob Bay than the other four sites investigated (2.6 m^2/m). This metric for assessing the amount of large woody debris along a shoreline could potentially be used to relate the regional variability in geomorphology and shoreline modifications to preferable beach habitat and biodiversity. The quantification of the physical habitat features of undeveloped shorelines could be used to establish objective reference criteria for evaluating restoration actions.

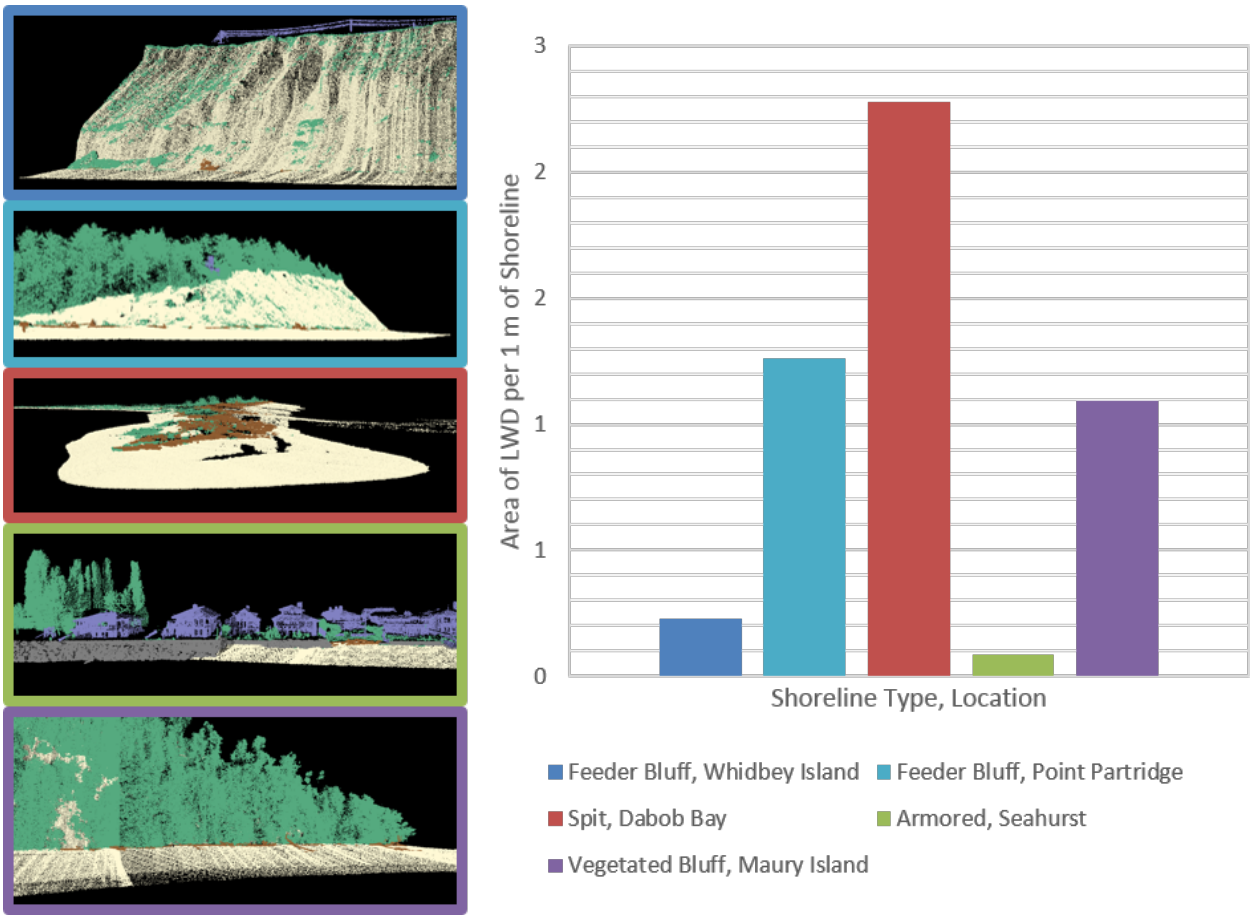

Figure E-21: Comparison showing area of large woody debris per meter of shoreline across multiple locations and shoreline types

Beach wrack

Beach wrack is stranded algae, seagrass, and terrestrial debris that accumulates on the beach surface, marking the previous high tide. Wrack can be mapped and quantified where it accumulates sufficiently on the beach surface using boat-based lidar. Quantities can be compared, for example, to back beach width and the relative encroachment of armor. Beach wrack provides habitat and a food source to invertebrates on the beach, but can only accumulate where the beach is wide enough and not backed by encroaching shoreline armoring.

In the example shown in Figure E-22 from a reach of shoreline north of Sandy Point near Bellingham, two wrack lines can be distinguished in the boat-based lidar from the previous high

tides. After classifying the lidar point cloud, the surface area of each line of wrack debris can be quantified individually: the upper wrack line has an area of 123 m^2 and the lower wrack line has an area of 187 m^2, for a total of 310 m^2 of beach covered by wrack debris in this shoreline reach. The mean elevation of the wrack debris can also be determined based on where it intersects the beach surface. In this example, the mean elevation for all of the wracked material is 2.53 m NAVD88.

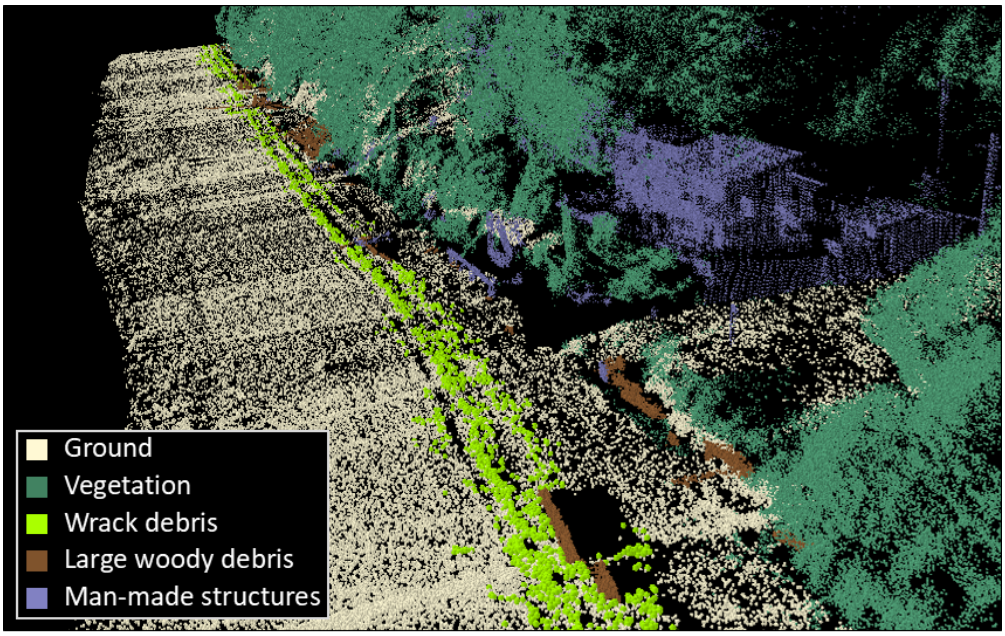

Wrack debris Measurements	Mean Elev. (m, NAVD88)	Surface Area (m^2)
Upper Line	2.72	123
Lower Line	2.41	187
All Wrack	2.53	310

Figure E-22: Example of classifying and quantifying beach wrack debris from the lidar point cloud of Point Whitehorn

By classifying and quantifying wrack debris on beaches in Puget Sound, relationships between various parameters can be explored, such as how the presence or amount of vegetation overhanging the upper beach or the relative shoreline armor encroachment coincides with the amount of wrack debris on a beach.

Habitat inventory

In addition to creating an inventory of geomorphic parameters for Puget Sound beaches, habitat features can also be quantified and inventoried in order to perform drift cell-scale assessments of

physical habitat features, such as the amount of large woody debris present on a beach or the cross-shore distance of the upper beach covered by overhanging vegetation.

Figure E-23 shows an example from Maury Island where characteristics of both the habitat (represented by overhanging vegetation and large woody debris) and beach morphology (beach width and back-beach width) of the shoreline are quantified every 20 m along the shore using a stacked bar chart. In this example, the section of unarmored shoreline with a back beach present has the largest amount of large woody debris and overhanging vegetation. In contrast, there is no large woody debris, overhanging vegetation, or back beach where the shoreline is armored in front of the residential area.

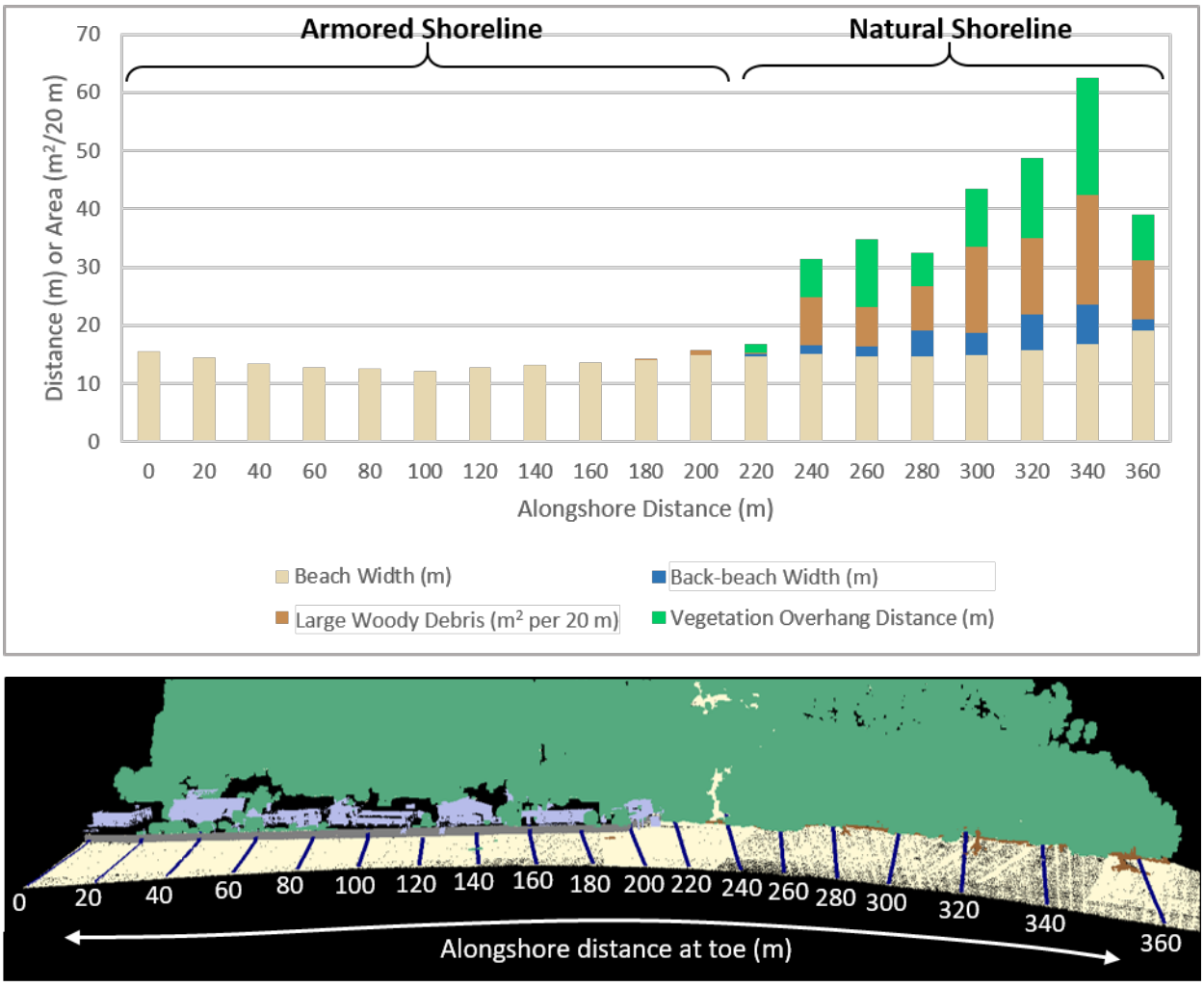

Figure E-23: Bar graph illustrating relationship between different physical and ecological parameters for adjacent armored and unarmored shoreline reaches on Maury Island

Figure E-24 shows another example of how the alongshore variability in beach morphology and habitat features can be quantified at a reach or drift-cell scale for the same section of shoreline on Maury Island. This graphic uses individual graphs to show how each variable changes per 20-m interval along the shore, with additional physical features including beach slope between 0-m

and 1.5-m elevation (relative to NAVD88), the elevation of the back edge of the beach (or uppermost point on the beach profile at the base of the bluff or shoreline armor), and the relative encroachment of shoreline armoring on the upper beach, as measured by the vertical distance between the toe and MHHW.

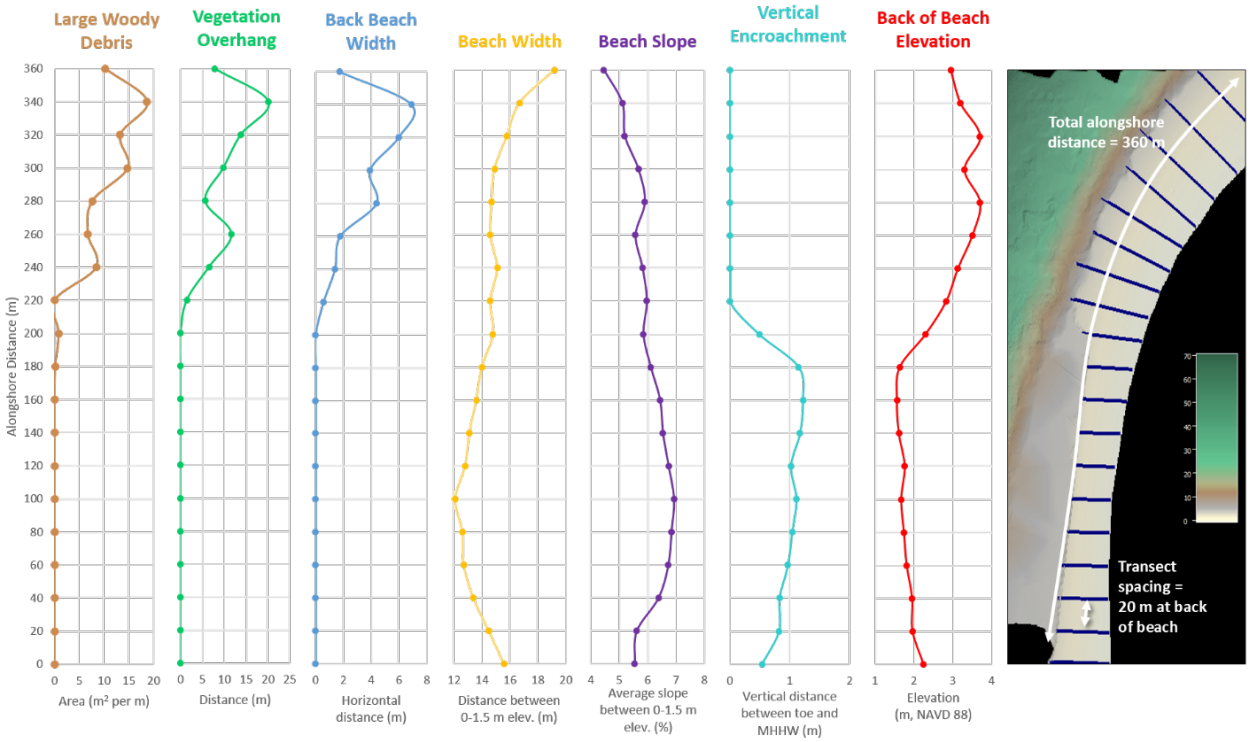

Figure E-24: Alongshore variability of various habitat and geomorphic features on a reach with armoring adjacent to natural shoreline

The data in Figure E-24 indicate there is more large woody debris and overhanging vegetation along the unarmored section of shoreline backed by a vegetated bluff as compared to the armored shoreline with the concrete bulkhead encroaching on the upper beach. The unarmored shoreline also has a wider, more gently sloping beach with a wider back beach and higher back edge of beach elevation. This comparison could be extended to different sites across Puget Sound to do an assessment of how shoreline armoring may be impacting shoreline habitat.

Beach texture/sediment grain size

Knowing the sediment grain size of a beach can be important for understanding the dissipation of wave energy, such as with a cobble berm on the upper beach, and habitat for marine organisms, such as pea gravel for fish spawning and sandy substrate for eelgrass. Preliminary results suggest it is possible to detect differences in beach texture with boat-based lidar using either intensity of the lidar returns or the surface roughness.

If the range at which the shoreline is scanned is held constant, the relative intensity of lidar returns from the beach can be used to differentiate large changes in sediment grain size. Higher intensity returns are expected where there are cobbles on the beach, while lower intensity returns are expected where the beach has finer grain silt or mud. Figure E-25, an example from Point

Roberts, shows how the intensity of lidar returns from a cross-section of the beach compares to digital photos of sediment grain size collected during the lidar survey. Relatively higher intensity of the returns occur where there is cobble present on the beach, especially at 1.84-m elevation (relative to NAVD88).

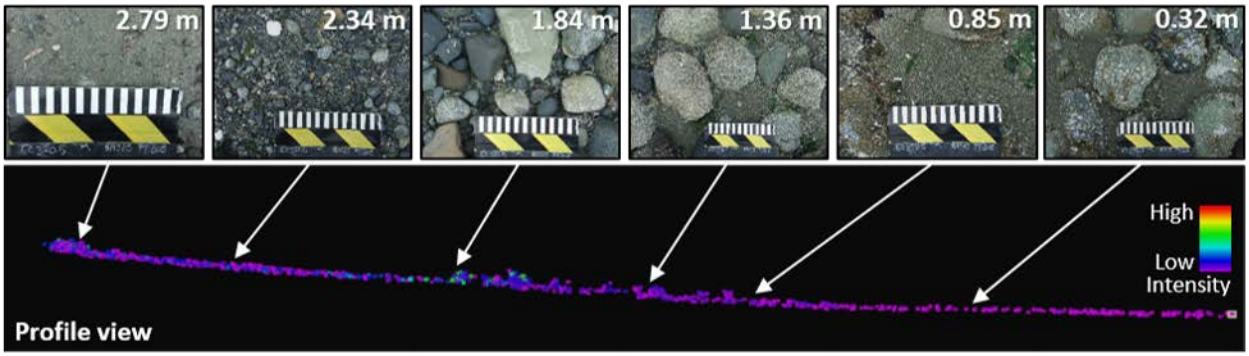

Figure E-25: Profile view of lidar point cloud, with points colored by intensity, in relation to digital photos collected of sediment grain size on the beach

The roughness of a surface is indicative of the overall sediment grain size found on a beach. Surface roughness can be calculated from the DEM as the standard deviation of the slope surface over a specified gridding window (Brubaker et al., 2013). Based on comparisons with cobble cam data collected for this project, a higher roughness value generally corresponds to a larger median grain size (i.e., coarser material, such as gravel or cobble), except where there is a large median grain size but low standard deviation (e.g., well-sorted cobble or gravel) in which case the roughness value may be lower than expected. The contrary is also true: an area with a small median grain size that is poorly sorted (i.e., mostly sand or fine silt with gravel mixed in) may have a higher than expected roughness value though the overall sediment size is relatively fine. Nevertheless, roughness can be used to identify changes in grain size across the beach surface, as shown in Figure E-26, where a higher roughness value corresponds to larger grain sizes.

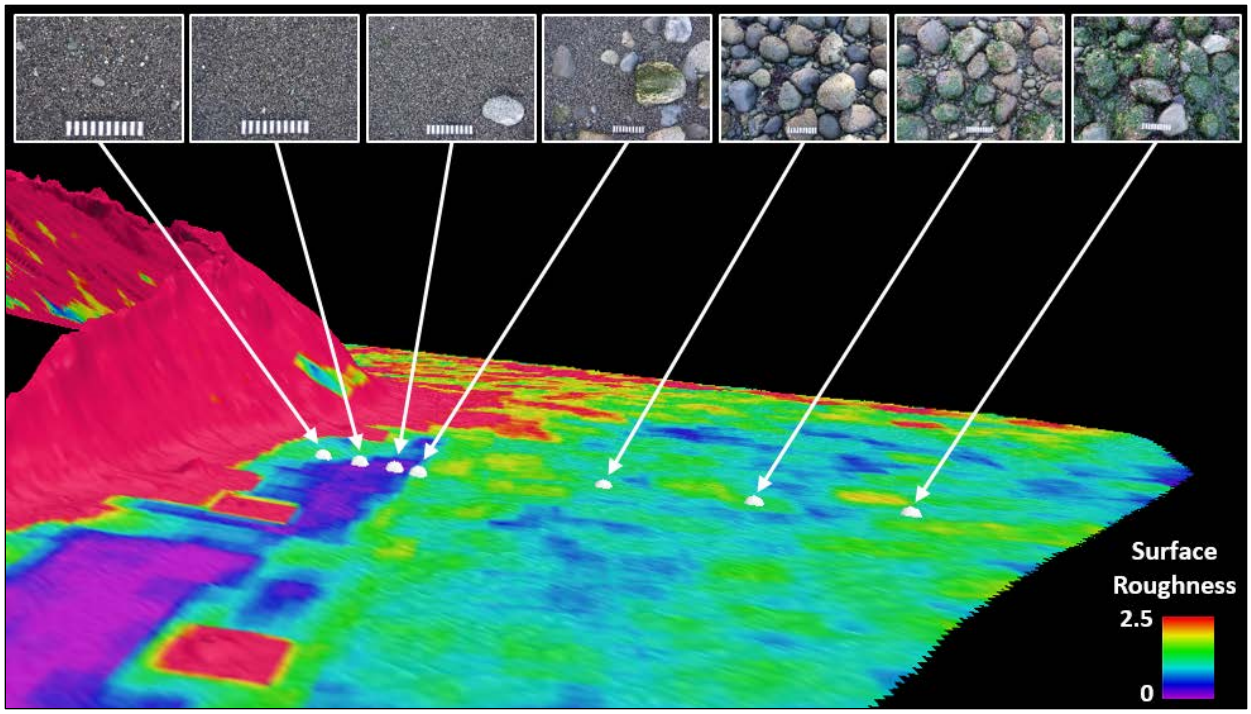

Figure E-26: Surface roughness of lidar DEM compared to digital photos collected of sediment grain size on the beach

Figure E-27 shows an example from Point Partridge on the west side of Whidbey Island of the classified lidar points and their associated intensities, as well as the bare-earth DEM created from the points and slope and surface roughness calculated from the DEM. The surface roughness and intensity of individual lidar returns can be used concurrently to differentiate the texture of the beach: the lower beach on the south side of Point Partridge is coarser in texture with larger cobbles than found to the north. With more study sites and further analysis, it may be possible to relate certain values of intensity, roughness, or a combination of both, with a corresponding sediment grain size.

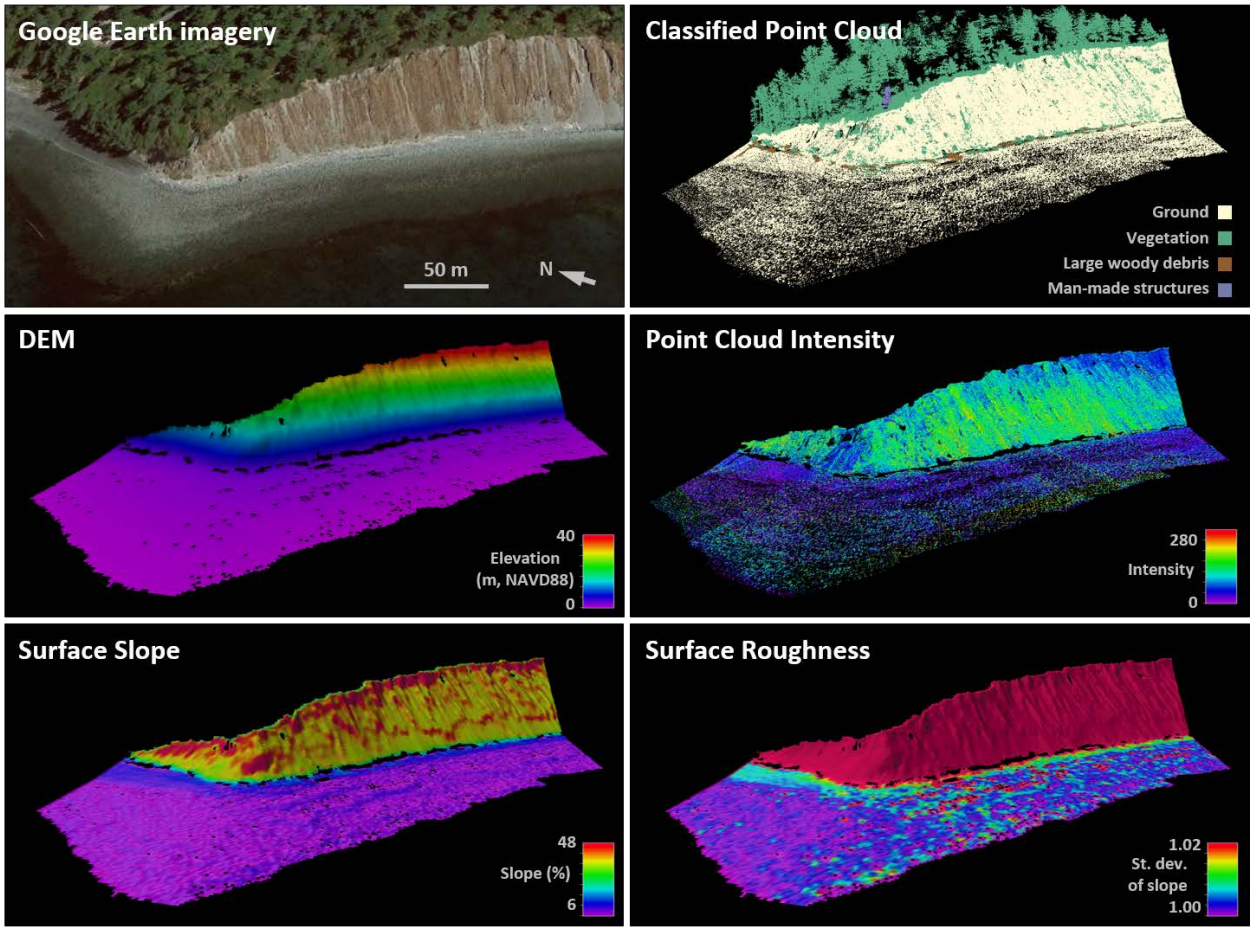

Figure E-27: Classified lidar point cloud, DEM, and derivative products used to differentiate beach texture at Point Partridge on Whidbey Island

Change detection and analysis

When more than one dataset has been collected, the bare-earth DEMs or point clouds can be compared in order to assess changes in the physical environment over time. Depending on the frequency of recurring surveys, seasonal changes or long-term trends in coastal morphology can be quantified. Changes can be viewed in two-dimensions along cross-shore profiles extracted from each dataset, as changes in elevation contours to examine alongshore variation in beach change, or as three-dimensional volume change found by differencing subsequent DEMs. Furthermore, changes in ecological characteristics such as large woody debris and overhanging vegetation can be assessed and used as an indicator of beach health over time. As a longer term and more comprehensive baseline dataset is accrued and repeat surveys are collected, additional questions can begin to be addressed. For example: Under what conditions will beaches be able to keep up with sea-level rise? How will beach ecosystem services be affected by sea-level rise and shoreline armoring? Which beach restoration projects are most viable given projections of sea-level rise, sediment supply, and shoreline armoring?

During this ESRP project, each study site was surveyed one time only and serves as baseline data for future studies. As part of another ESRP-funded project by the South Puget Sound Salmon

Enhancement Group, Ecology CMAP conducted a second boat-based lidar survey of the Edgewater Beach drift cell, located in South Puget Sound near Olympia, following the removal of 800 ft of shoreline armoring that occurred in fall 2016. The second survey was performed in June 2017, almost eight months following shoreline armor removal, and 1.5 years since the first survey in September 2015. These surveys allowed for a comparison of how the morphology and physical habitat changed after the shoreline armor was removed (Weiner and Kaminsky, 2018). Examples from the 2018 project report are included here.

Morphology change

Cross-shore profile change

When multiple datasets are collected for a shoreline reach, two-dimensional profiles can be extracted at the exact same location, allowing for change between the two profiles to be quantified. For the Edgewater project, multiple cross-shore profiles were extracted at approximately 20-m intervals along the shoreline (Figure E-12) and analyzed for change.

Figure E-28 gives an example of the profile data from 2015 and 2017 extracted for Transect 2.10 across a bluff-backed beach within the site where the bulkhead was removed. In the 2015 data, the vertical bulkhead can be seen around a cross-shore distance of 18 m. In 2017, the profile shows erosion landward of the bulkhead and accretion on the upper beach where the bulkhead toe previously existed. The 2D change area can be multiplied by a 1 m-width, resulting in 12.34 m^3 of sediment lost from the bluff and 7.19 m^3 of sediment gained on the upper beach at this 1 m-wide profile.

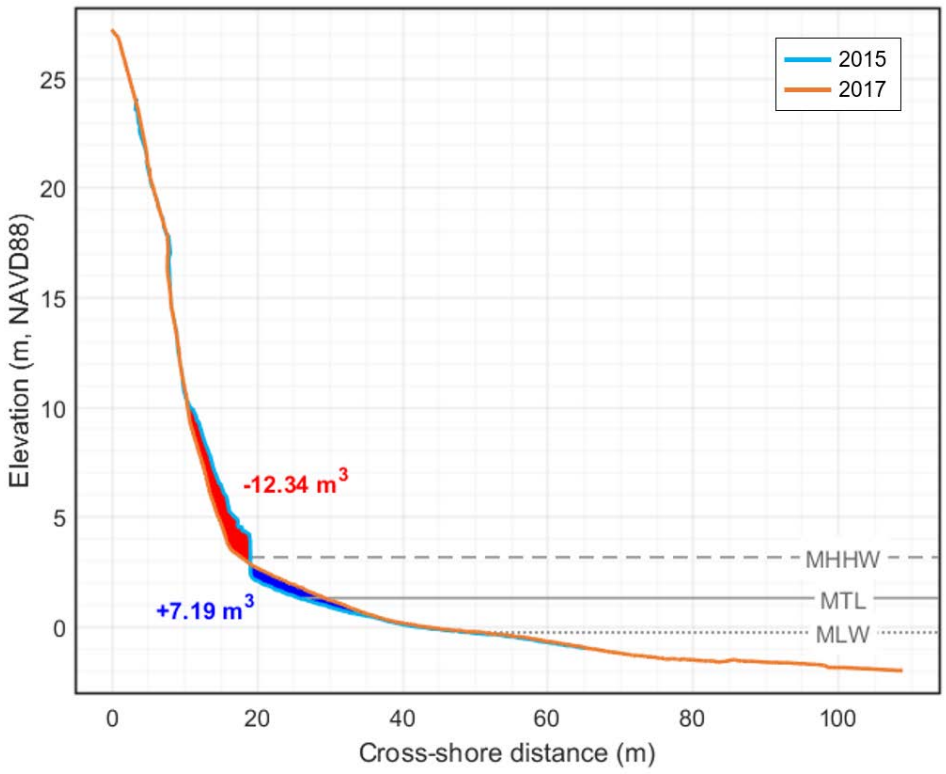

Figure E-28: Cross-shore profile change between 2015 and 2017 at Edgewater Beach Transect 2.10, showing volume of sediment lost (red) and gained (blue) as a 2D area × 1 m-wide profile

Contour change

Another way to document coastal change is based on the movement of elevation contours. Because contours are continuous in the alongshore, they provide more context for cross-shore profiles by showing the alongshore variability or change in a parameter. Figure E-29 shows an example from Edgewater Beach where the landward movement of the MHHW contour and seaward movement of the MTL following bulkhead removal resulted in an increase in beach width of almost 3.5 m in one location and by variable widths alongshore.

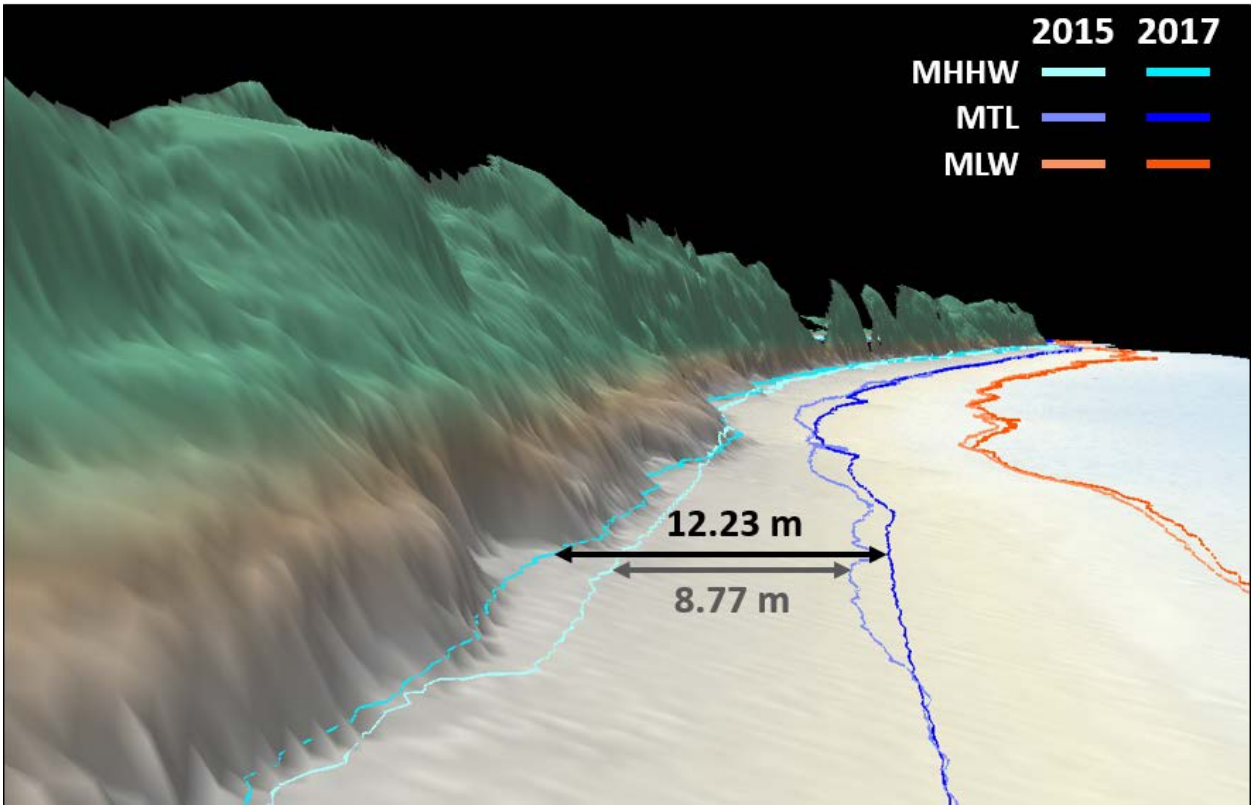

Figure E-29: Change in beach width from 2015 to 2017 as measured by the distance between MHHW and MTL contours at Edgewater Beach

Volume change

To visualize changes in both the cross-shore and alongshore simultaneously, bare-earth DEMs created from the boat-based lidar data from repeat surveys can be subtracted from one another to determine the change in elevation per grid cell between the two surveys. The resultant difference surface can be used to calculate the volume change between the surveys in order to accurately quantify erosion and deposition of sediment in three-dimensional space.

Figure E-30 shows an example of 3D beach change from the Edgewater Beach drift cell. DEMs from the two boat-based lidar surveys collected in 2015 and 2017 are shown on the left with the difference between the surveys shown on the right. Blue areas in the difference surface indicate places were the beach was higher in 2017 than 2015 (accretion), while red areas show places where the beach was lower (erosion). The morphology of the area and the pattern of this change

suggests the migration of intertidal sand bars that migrated onshore by about 8-10 m to the northwest, with bar crests filling in landward troughs and leeward troughs developing in the area of the prior crests. The volume of accretion in this area is similar to the volume of erosion (1,845 m^3 vs. 1,550 m^3) for a net gain of sediment of 295 m^3.

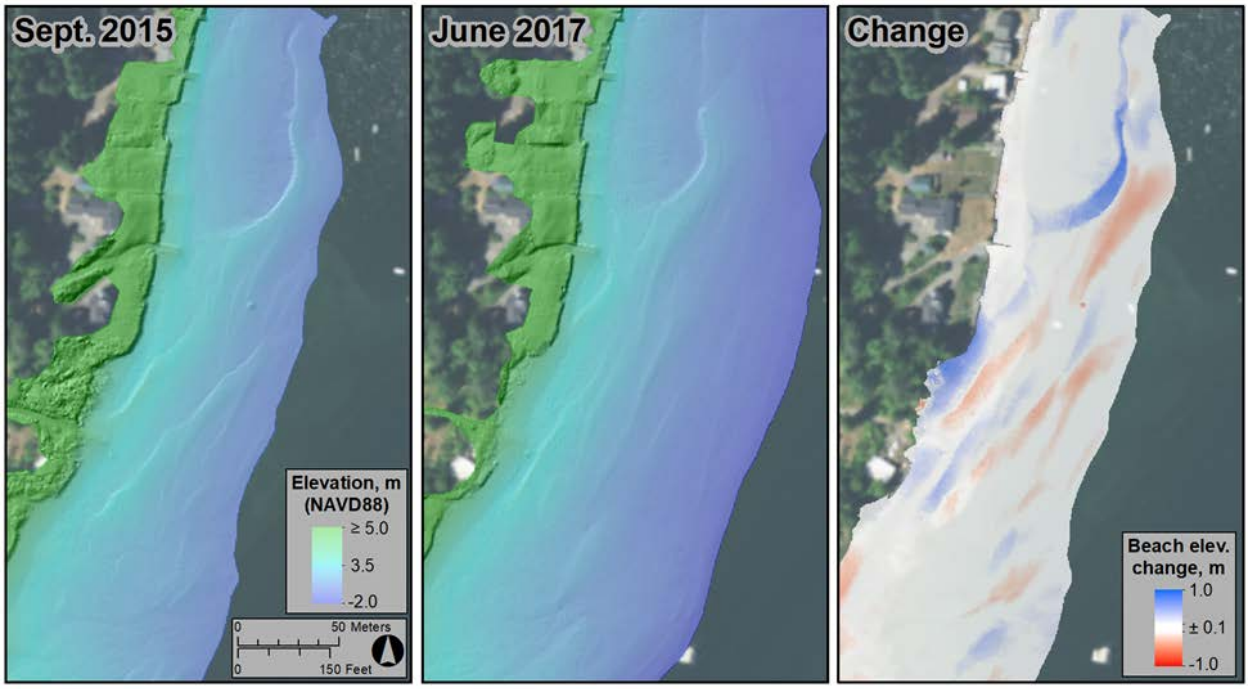

Figure E-30: Migration of shallow intertidal sand bars from September 2015 to June 2017 at Edgewater Beach [excerpted from Weiner and Kaminsky (2018)]

Quantifying landslide deposits

With data collected before and after a landslide occurs, the volume of material lost from a bluff can be quantified by finding the difference in elevation per grid cell between the DEMs of both surveys. In lieu of having a pre- and post-landslide survey, the volume of material lost from the bluff can be approximated by comparing the bluff face at the location of the slide with an area adjacent to it with similar morphology.

Figure E-31 shows an example from Useless Bay where a landslide occurred before the shoreline was surveyed. The landslide talus has been identified and classified as a separate feature in the lidar point cloud. By extracting a cross-shore profile at the location of the slide and 50 m to the south of the slide where the bluff morphology is similar, the difference between the two profiles suggests about 200 m^3 of material was lost from the bluff, estimated to be between 18 m and 54 m NAVD88. The talus extended about 12 m onto the upper beach seaward of the former bluff toe. With additional surveys, the rates at which the landslide material is distributed alongshore by coastal processes can be studied.

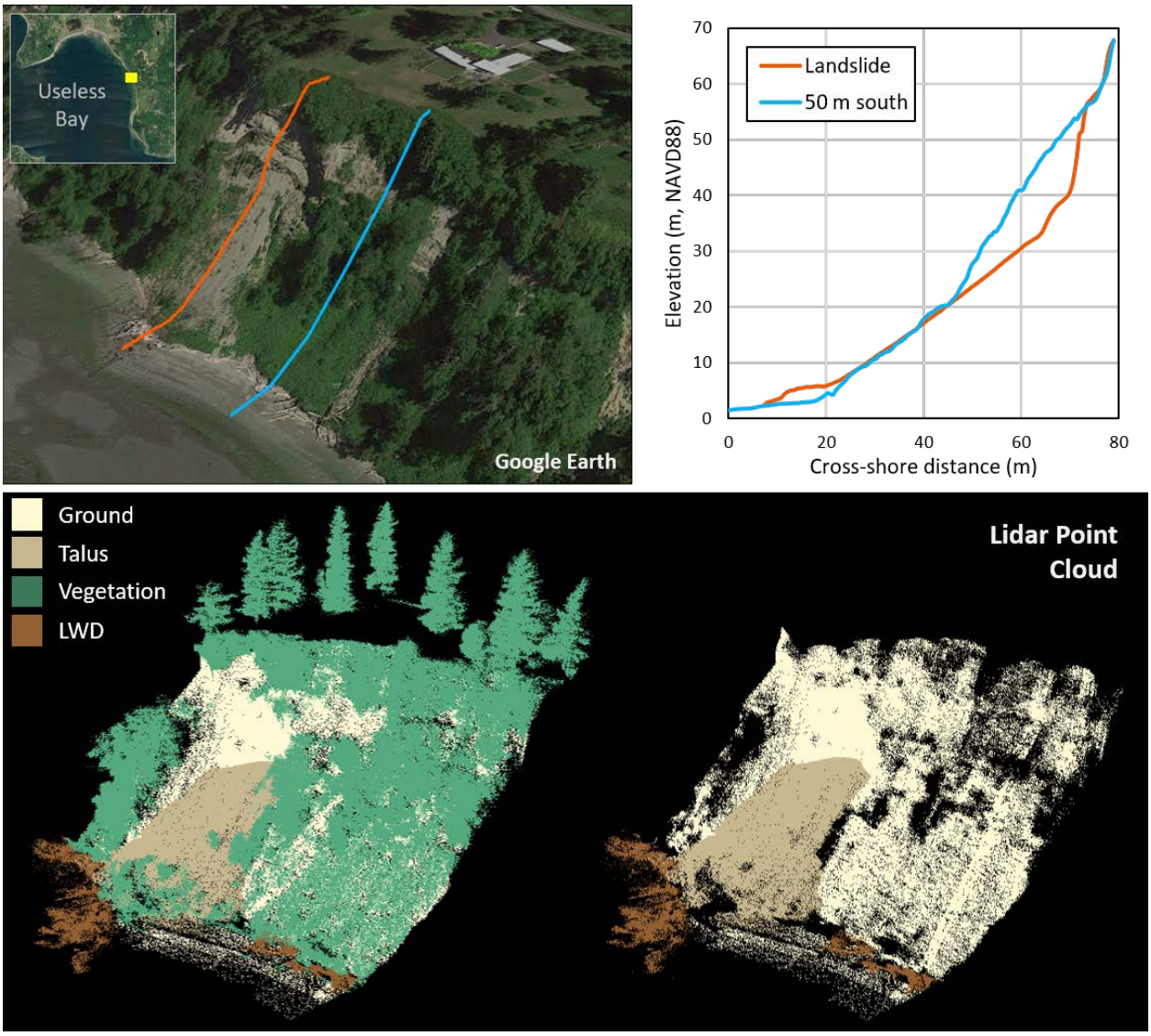

Figure E-31: Cross-shore profiles from the lidar point cloud taken across the bluff face at the site of a slope failure and 50 m south to estimate landslide volume; bottom—classified point cloud with landslide talus, both with and without vegetation

Habitat change

Large woody debris

Similar to calculating changes in morphology that determine whether there is more or less material on the beach, change in the amount of large woody debris can also be calculated once it is identified, classified, and quantified in the lidar point cloud. In the example shown in Figure E-32 from Edgewater Beach, the area of the beach covered by large woody debris almost doubled after removal of the bulkhead: there was an 81% increase in the amount of large woody debris found on the upper beach between the first and second survey.

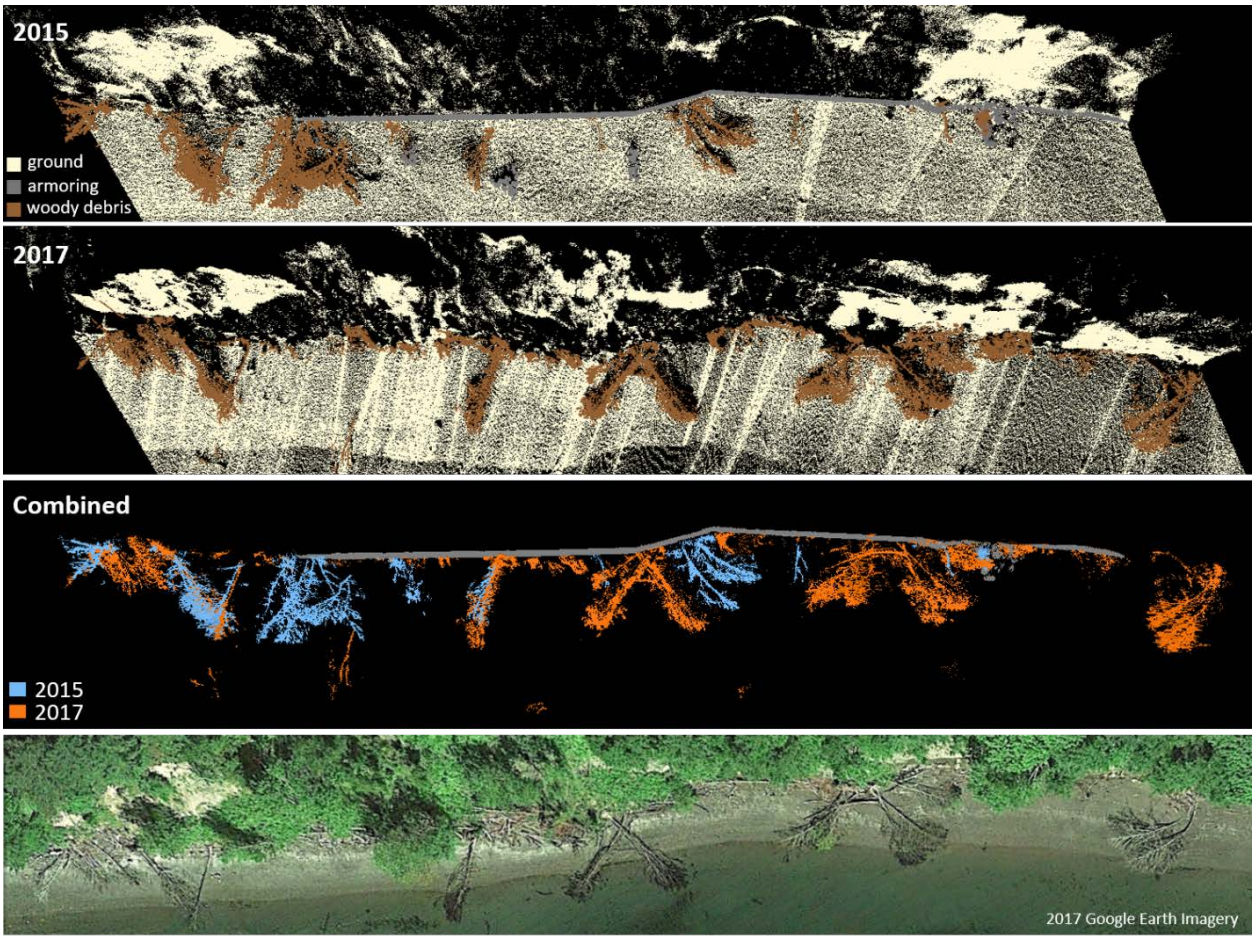

Figure E-32: Increase in large woody debris between September 2015 and June 2017 at the Edgewater Beach restoration project site after shoreline armor removal [excerpted from Weiner and Kaminsky (2018)]

Overhanging vegetation

With multiple surveys performed, the change in overhanging vegetation can also be quantified. Figure E-33 illustrates how a change in the amount of overhanging vegetation between one survey to the next may be measured. In lieu of actual data, the Maury Island dataset was modified to show a loss in overhanging vegetation. The second (modified) dataset shows 301.9 m^2 less beach area covered by overhanging vegetation, the difference of which is shown, spatially, in the bottom panel of Figure E-33.

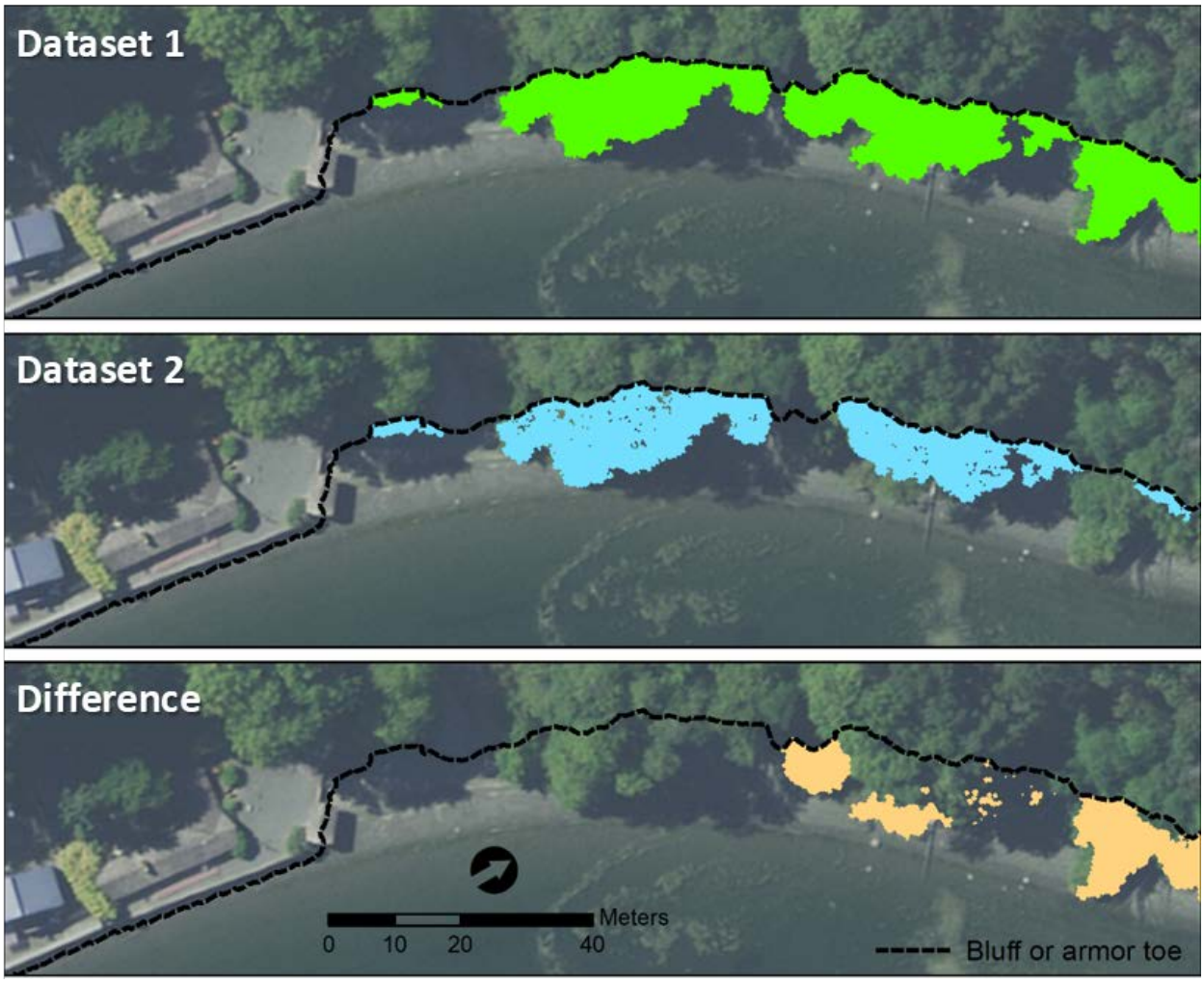

Figure E-33: Difference in upper beach area covered by overhanging vegetation between two datasets to illustrate change over time

Beach restoration monitoring and assessment

By surveying the shoreline before and after a restoration project, boat-based lidar can accurately and efficiently document changes in both morphology and habitat. In contrast to other field methods, scanning a shoreline with boat-based lidar will document the entire landscape, resulting in comprehensive, high-resolution 3D elevation data on all ground, vegetation, structures, and other physical features that are visible from the vessel. Furthermore, boat-based lidar can achieve high-resolution ground returns through moderate vegetation and see under overhanging vegetation, which may not be possible with other airborne techniques.

As previously mentioned, another ESRP-funded project by the South Puget Sound Salmon Enhancement Group funded Ecology CMAP to conduct a second boat-based lidar survey of the Edgewater Beach drift cell to document beach restoration following the removal of an 800 ft-long section of shoreline armoring in fall 2016 (Weiner and Kaminsky, 2018). Figure E-34 shows the change in elevation following beach restoration between the 2015 and 2017 surveys.

The beach elevation change is shown using a color ramp of red (erosion) to blue (accretion), while the bluff elevation change is shown as yellow (erosion) to green (accretion). Including the shoreline armor, about 1,760 m^3 of material was lost from the base of the bluff. Directly in front of the shoreline armor that was removed in 2016, an increase in sediment volume of 785 m^3 was measured on the upper beach in 2017. The remaining sediment that eroded from the bluff is expected to have been dispersed to the nearshore or transported northward within the drift cell.

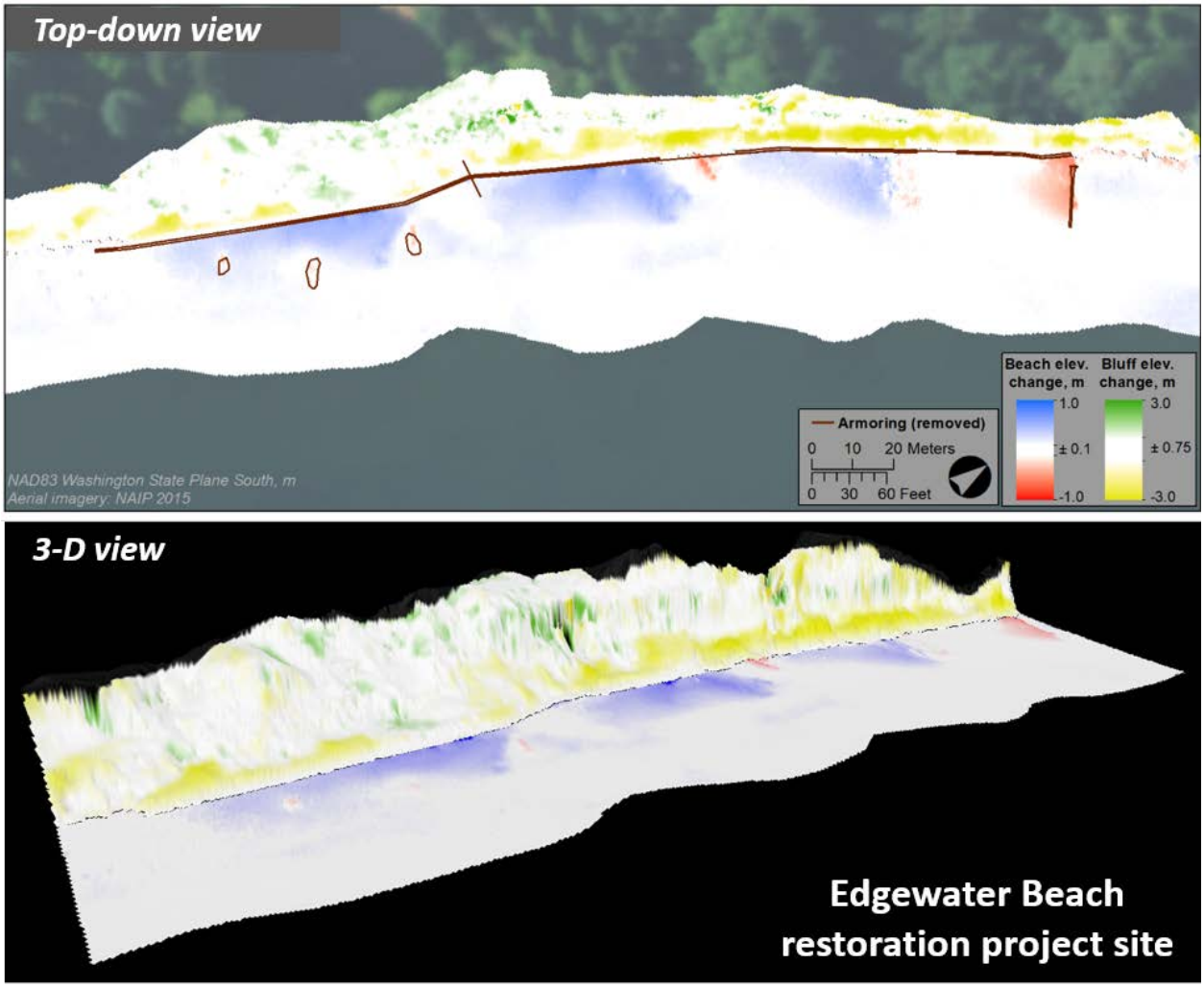

Figure E-34: 3D beach and bluff elevation change measured using boat-based lidar between September 2015 and June 2017 at Edgewater Beach [excerpted from Weiner and Kaminsky (2018)]

The removal of the bulkhead was also associated with a flattening and widening of the beach at the restoration site, which may facilitate the development of a back beach (Figure E-29). The drift cell-scale survey enabled downdrift sediment deposition to be tracked and resulted in the development of a preliminary sediment budget. In addition to mapping the changes in morphology that occurred post-restoration, physical changes to the habitat were also documented, showing an influx in large woody debris (Figure E-32) and changes in sediment grain size on the surface of the beach (Weiner and Kaminsky, 2018).

Boat-based lidar vs. airborne lidar

Collecting lidar of Puget Sound shorelines from a boat provides an advantageous perspective of vertical features, such as shoreline armor and bluff faces, which is not as readily achieved with airborne lidar. However, because of the horizontal look-angle of the boat-based laser scanner to the shoreline, some flat or landward-sloping surfaces may be shadowed and void of data whereas these surfaces are perpendicular and conducive to data collection by airborne lidar systems.

A comparison of Ecology's boat-based lidar data to airborne topo-bathy lidar data collected by the Joint Airborne Lidar Bathymetry Technical Center of Expertise (JALBTCX) at Port Gamble Bay, Washington, was funded by the National Oceanographic and Atmospheric Administration (NOAA) in 2017 (Hacking et al., 2018). The two datasets were collected in 2014, within six months of one another. The results showed that both airborne and boat-based lidar can detect objects on the scale of individual wood pilings. Airborne lidar has a significant advantage on horizontal surfaces that cannot be seen from a boat, such as upland plateaus. However, the point density and horizontal look-angle of the boat-based lidar allows for easier object detection, identification, and analysis of both vertical surfaces and objects under overland structures such as piers. As shown in Figure E-35, while the airborne topo-bathy lidar is able to acquire data on upland regions landward of the bluff, the boat-based lidar obtains more complete coverage on the bluff face itself, which appears as a gap in the topo-bathy lidar. Together, aerial and boat-based lidar could produce seamless, high quality DEMs of the coastal zone and upland areas with fewer data gaps than may be present with one system individually.

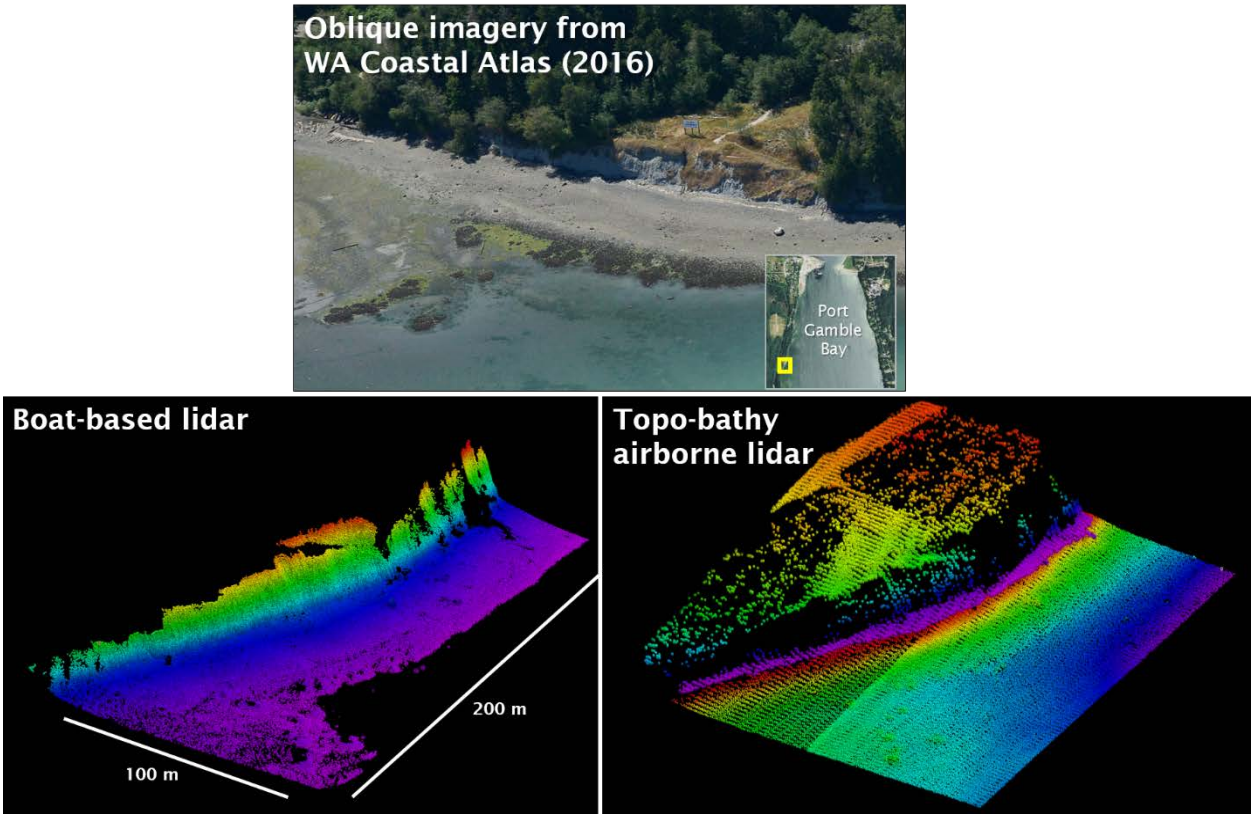

Figure E-35: Comparison between Ecology CMAP boat-based lidar and JALBTCX topo-bathy airborne lidar of a bluff-backed beach in Port Gamble Bay

Recommended citation for Appendix E

Weiner, H.M., H. Drummond, G.M. Kaminsky, and A. Henderson, 2018. Mapping Bluffs and Beaches of Puget Sound to Quantify Sediment Supply, Estuary and Salmon Restoration Program Learning Project Final Report, Appendix E: Example Lidar Data Applications. Shorelands and Environmental Assistance Program, Washington Department of Ecology, Olympia, Washington, Publication #18-06-008, pp. 111-147.

References

Brubaker, K.M., W.L. Myers, P.J. Drohan, D.A. Miller, and E.W. Boyer, 2013. The use of LiDAR terrain data in characterizing surface roughness and microtopography. Applied and Environmental Soil Science, 13, 891534, doi: 10.1155/2013/891534.

Dethier, M.N., W.W. Raymond, A.N. McBride, J.D. Toft, J.F. Cordell, A.S. Ogston, S.M. Heerhartz, and H.D. Berry, 2016. Multiscale impacts of armoring on Salish Sea shorelines: Evidence for cumulative and threshold effects. Estuarine, Coastal and Shelf Science, 175: 106-117.

Hacking, A., D. McCandless, G.M. Kaminsky, and H.M. Weiner, 2018. Evaluating methods to obtain high-resolution nearshore bathymetry and coastal topography of Puget Sound. Salish Sea Ecosystem Conference Poster, SSE101-663.

Penttila, D., 2002. Effects of shading upland vegetation on egg survival for summer-spawning surf smelt on upper intertidal beaches in Puget Sound. *In* Puget Sound Research 2001 Conference Proceedings, Puget Sound Water Quality Action Team, Olympia, Washington, 9 p.

Sobocinski, K.L., J.R. Cordell, and C.A. Simenstad, 2010. Effects of shoreline modifications on supratidal macroinvertebrate fauna on Puget Sound, Washington beaches, Estuaries and Coasts, 33: 699-711.

Toft, J.D., J.R. Cordell, C.A. Simenstad, and L.A. Stamatiou, 2007. Fish distribution, abundance, and behavior along city shoreline types in Puget Sound, North American Journal of Fisheries Management, 27: 465-480.

Weiner, H.M. and G.M. Kaminsky, 2018. Coastal morphology change in response to bulkhead removal at Edgewater Beach, South Puget Sound. Shorelands and Environmental Assistance Program, Washington State Department of Ecology, Olympia, WA. Publication #18-06-002. https://fortress.wa.gov/ecy/publications/summarypages/1806002.html